UNIVERSITY OF SHEFFIELD

Department of Civil and Structural Engineering

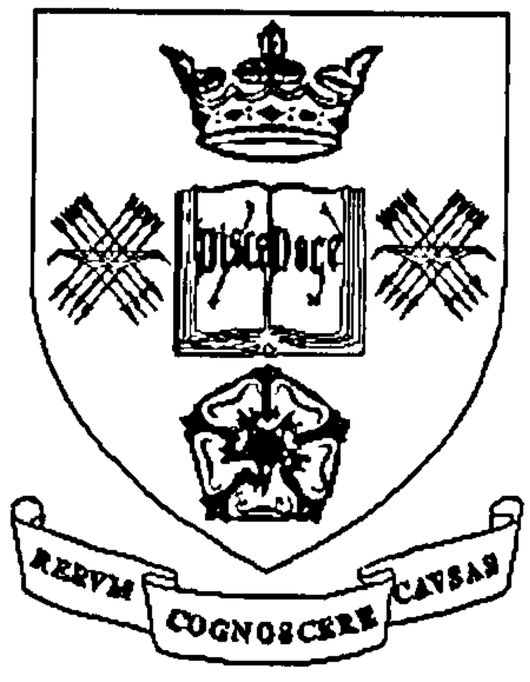

The Structural Response of Industrial Portal Frame Structures in Fire

By

Shao Young Wong

A thesis submitted in partial fulfilment of the requirements for the Degree of Doctor of Philosophy

May 2001

ABSTRACT

A number of recent fires in single-storey warehouses have drawn attention to a current lack of understanding about the structural response of industrial portal frame structures to elevated temperatures. This research project has investigated the subject by conducting fire tests on a scaled model and by computer modelling using the non-linear finite element program VULCAN. This program has been developed in-house by the University of Sheffield and is capable of modelling the behaviour of three-dimensional steel and composite frames at elevated temperatures. It has been validated throughout its development. An initial investigation was conducted to validate the program for analysing inclined members, which form part of a pitched-roof portal frame, but for which it was not initially developed. Additional features were implemented into the program where necessary.

A series of indicative fire tests was conducted at the Health and Safety Laboratories, Buxton. A scaled portal frame model was designed and built, and three major fire tests were conducted in this structure. In the third of these tests the heated rafters experienced a snap-through failure mechanism, in which fire hinges could clearly be identified. The experimental results were then used for validating the numerical results produced by VULCAN analyses. The correlations were relatively close, both for predictions of displacements and failure temperatures. This gave increased confidence in using VULCAN to conduct a series of parametric studies. The parametric studies included two- and three-dimensional analyses, and a number of parameters were investigated, including the effects of vertical and horizontal load, frame geometry, heating profiles and base rotational stiffness. The influence of secondary members was investigated in the three-dimensional studies using different fire scenarios.

A simplified calculation method has been developed for estimating the critical temperatures of portal frames in fire. The results compare well with predictions from VULCAN. The current guidance document for portal frames in boundary conditions has been reviewed, and the concept of performance-based design for portal frame structures has been discussed.

CONTENTS

LIST OF FIGURES

LIST OF TABLES

Notation

(Only the general notations used during this thesis are presented here. Symbols which have only been used once and are of a more specific nature have been clearly explained where they arise in the text.)

δ_j	Displacement
ε	Strain
η	Strength reduction factor at elevated temperature
σ	Stress
ϕ, θ	Rotation
ϕ_c	Column base rotation
A_t, B_t, N_t	Temperature dependent Ramberg-Osgood parameters
A	Cross section area
E	Young Modulus
H_p	Perimeter of section exposed to fire
I_{xx},I_{yy}	Second moment area about major/minor axis
M_i	Internal moment
M_p	Plastic moment resistance
W_j	External Load

ACKNOWLEDGEMENT

The author is greatly indebted to Prof. Ian Burgess and Prof. Roger Plank for their excellent supervision and support during this research project. The financial assistance from Health and Safety Laboratories, Buxton and Overseas Research Scholarship is gratefully acknowledged.

I would also like to thank Graham Atkinson of HSL, Buxton for the kind assistance and discussions throughout the fire tests. Intellectual support from my colleagues of the Steel Fire research group is very much appreciated and acknowledged.

Finally, I would like to thank my parents, brother and sister for the endless support from Malaysia, and Winsome who often inspires and motivates me during the work.

DECLARATION

Except where specific reference has been made to the work of others, this thesis is the result of my own work. No part of it has been submitted to any University for a degree, diploma, or other qualification.

Shao Young Wong

1 Introduction

Over half of the total market share of the constructional steelwork fabricated in the United Kingdom is used in single-storey buildings. Portal frame construction is the most common form of these single-storey buildings found on any modern industrial estate, due to the fact that it is simple and cost-efficient. A steel portal frame structure is a rigid plane frame with assumed full continuity at the intersections of the column and rafter members. In the United Kingdom it is usual to design such structures plastically. However, steel is very vulnerable in fire due to its high thermal conductivity, losing strength and stiffness rapidly compared to other materials. The steel industry has invested much research in finding better solutions this major disadvantage, such as alternative design methods, new protective materials, improvement to steel properties etc. A number of recent fires in single-storey warehouses[1-7] have drawn attention to a current lack of understanding about the structural response of industrial portal frame structures to elevated temperatures.

Regulatory requirements state that all buildings require a minimum degree of fire resistance to fulfil two main objectives:

- To ensure life safety, which includes allowing the occupants to leave and fire fighting personnel to enter if necessary.
- To minimise property or financial losses, and delay the spread of fire to adjoining property.

Structures designed using ambient-temperature steel properties are usually required to be insulated so that their temperatures remain sufficiently low in the event of fire. This is the most common method at present, but is a prescriptive method. Alternatively, high-temperature properties of steel can be taken into account in design, considering the load ratio, temperature gradient, dimensions and stress distribution.

The fire safety of all buildings in England and Wales is governed by the provisions of Approved Document B[8]. The regulations in the document apply only to structural elements used in:

- Buildings, or parts of buildings, of more than one storey;
- Single-storey buildings built close to a property boundary.

Therefore, there may be no need for fire resistance for portal frame structures. In fact, it is stated in the document that:

> "It is considered technically and economically feasible to design the foundation and its connection to the portal frame so that it would transmit the overturning moment caused by the collapse, in a fire, of unprotected rafters, purlins and some roof cladding while allowing the external wall to continue to perform its structural function."

The Steel Construction Institute has therefore published a document[9] which gives guidance on designing the column bases to resist rafter collapse. The basis of the method is a plastic collapse model of the rafter in fire, and will be elaborated later in this chapter.

1.1 Fire Concepts

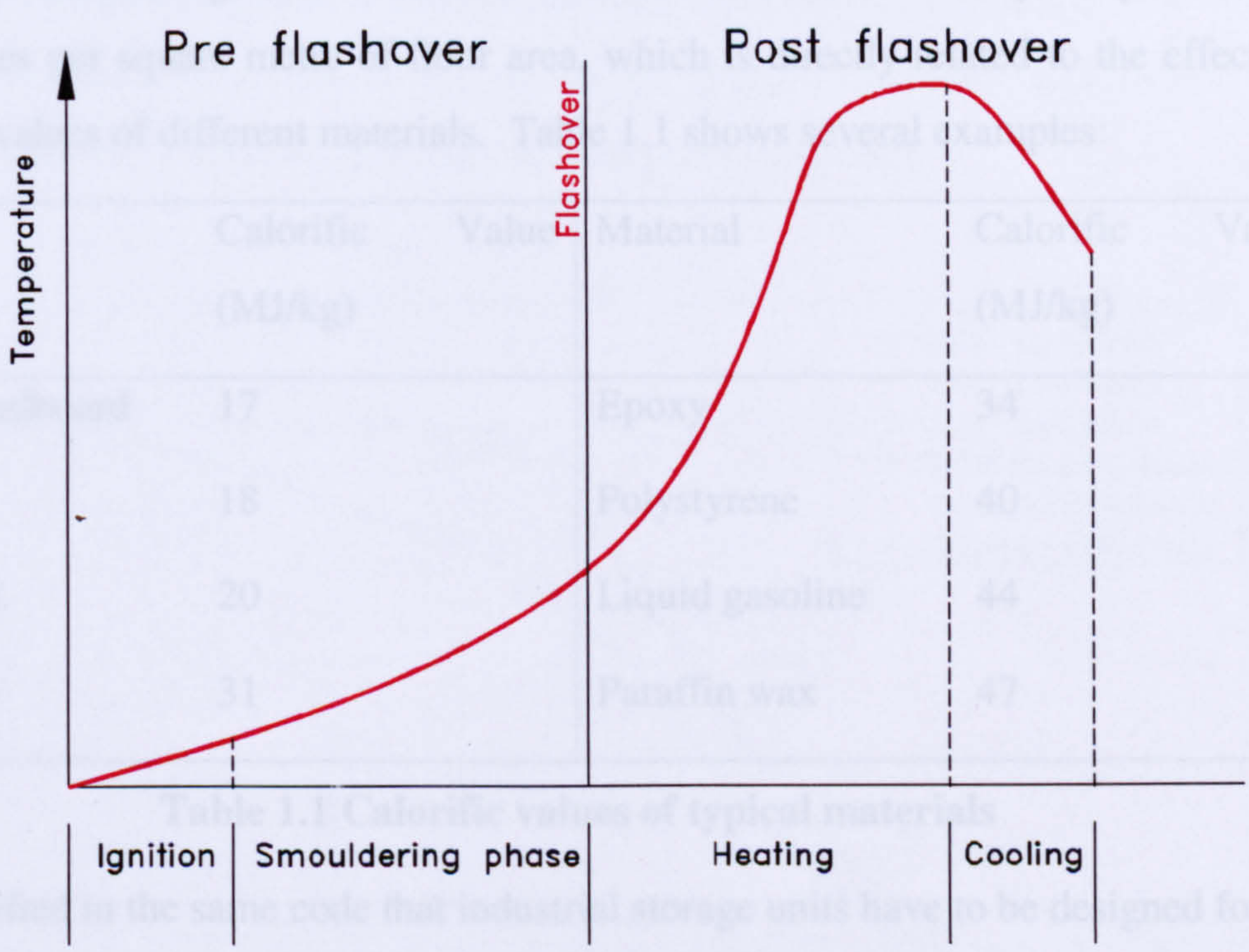

Figure 1.1 Development of a natural fire

In considering the occurrence of a typical fire, Figure 1.1 shows the diagram of a natural fire curve, where four stages are defined. The first (ignition) stage is most important to allow early detection and suppression, whereas the risk to life or property is not very high in this phase. When the fire develops into the second

(smouldering) stage, there will be progressive smoke production from combustible materials, causing danger to the occupants. The structural damage is still small at this phase until a critical point, known as flashover, is reached depending on the fire load density and ventilation. This indicates that the fire is out of control, and the post-flashover temperatures typically rise to between 600°C and 1000°C. At this point, it is no longer possible for fire fighting to be effective, except to protect the neighbourhood. When the combustible materials finish burning, the temperature will begin to decrease, and this is hence defined as the cooling stage.

Fire in a portal frame warehouse can be different from natural fires in commercial buildings, depending on the material stored in the warehouse, which subsequently becomes the fuel for the fire. Provided there is sufficient ventilation, the fire growth rate and the ultimate temperature achieved are solely dependent of the type of material available for burning. DD240 Part 1, *Application of Fire Safety Engineering Principles to Fire Safety in Buildings (1997)* [11], published by British Standards Institute gives values of effective fire load density, expressed in megajoules per square metre of floor area, which is directly related to the effective calorific values of different materials. Table 1.1 shows several examples:

Material	Calorific Value (MJ/kg)	Material	Calorific Value (MJ/kg)
Paper, cardboard	17	Epoxy	34
Cotton	18	Polystyrene	40
Methanol	20	Liquid gasoline	44
Polyester	31	Paraffin wax	47

Table 1.1 Calorific values of typical materials

It is specified in the same code that industrial storage units have to be designed for an ultra-fast fire growth rate, where 1000 kW will be produced in 75 seconds (compared to 300 seconds for the medium fire growth rate required for offices and dwelling).

However, the concept of flashover applies most clearly to fires in relatively small enclosures, whereas a portal frame warehouse will normally occupy a larger space without many compartments. It will require a longer time for flashover to take place, and this only happens after a substantial local fire has developed. A.J. O'Meagher[12]

(1992) has introduced a "developing fire" concept, where a fire begins at a particular location over a finite time period, and then spreads outwards to other parts of the building. The portal frames are therefore heated locally and the affected area will increase as the fire develops, causing an increased length or number of portals to be heated.

The concept implies that parts of a structural frame which are near to the fire will become very hot, and hence the local material strength will decrease substantially; whereas the rest of frame remains cooler and the strength is not affected. The validity of this concept is inferred from post-fire observations of single-storey buildings and from knowledge of how structures behave under elevated temperature.

1.2 Steel Properties at Elevated Temperature

One of the major advantages of using steel for structural applications is its good strength-to-weight ratio. However, steel begins to lose strength at about 200°C and continues to lose strength at a much faster rate from 400°C to 750°C. Above this temperature, the degradation of the remaining strength continues at a slower rate until approximately 1500°C, at which melting point is reached.

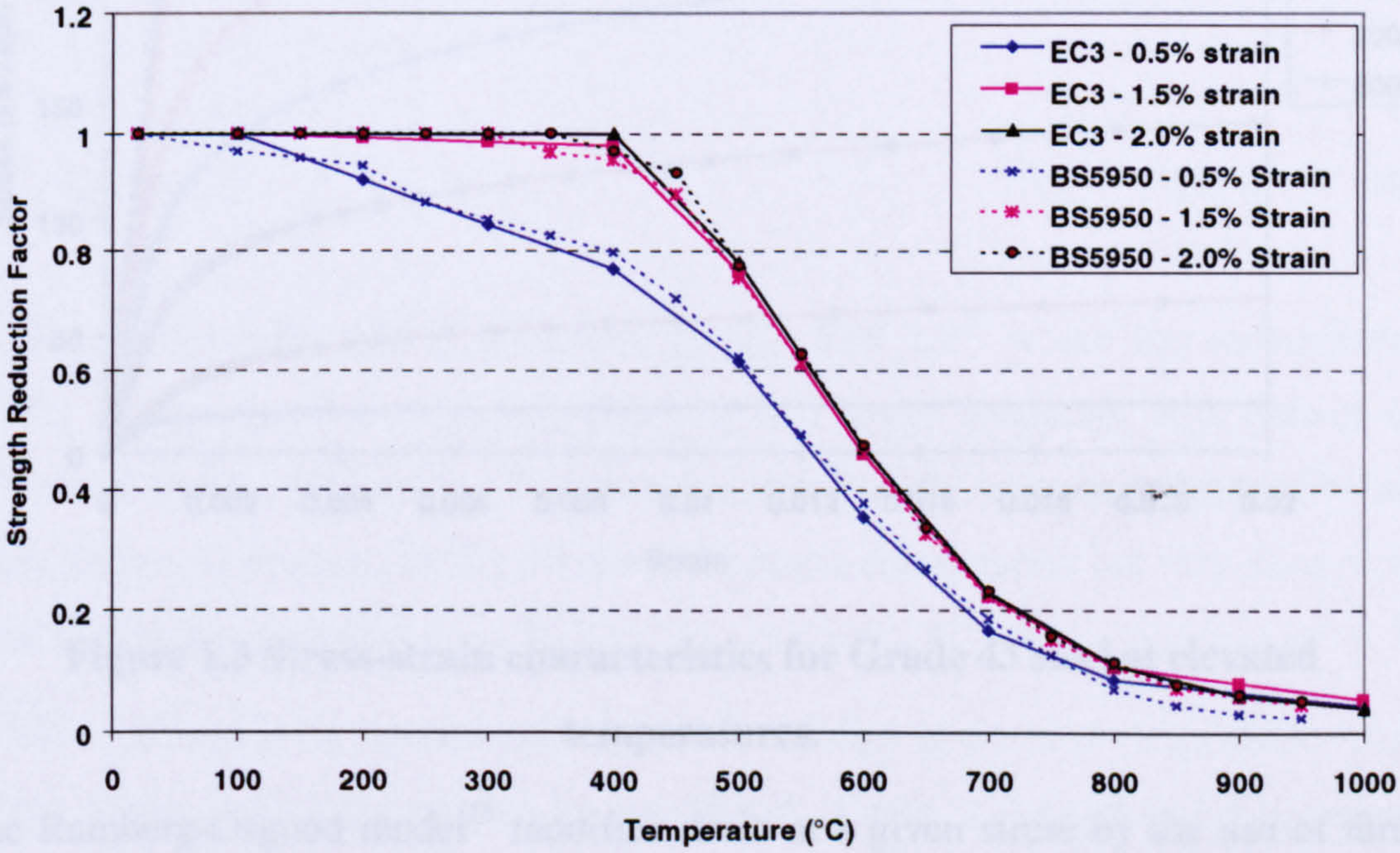

Figure 1.2 Strength reduction factors for structural steel at elevated temperatures

Recent design codes BS5950 Part 8[13] and EC3 Part 1.2[15] have published strength reduction factors of steel at different strain levels. The reduction factors are defined as the residual strength of steel at a certain temperature, relative to its strength at ambient temperature. They vary at different strain limits because there is a gradual increase in strength with strain at elevated temperature after yielding, unlike at ambient temperature where a yield stress plateau is obtained. Figure 1.2 shows a comparison of the strength reduction factors between the codes for Grade 43 steel.

The actual stress-strain data of steel published in BS5950 and EC3 are based on the high temperature stress-strain tests conducted by Kirby and Preston[17] (1988). A Ramberg-Osgood[16] type of equation has been used as one of mathematical models to represent this stress-strain behaviour, and most of the computer analyse performed in this research adopt this model for calculation. The curves for Grade 43 steel are shown in Figure 1.3.

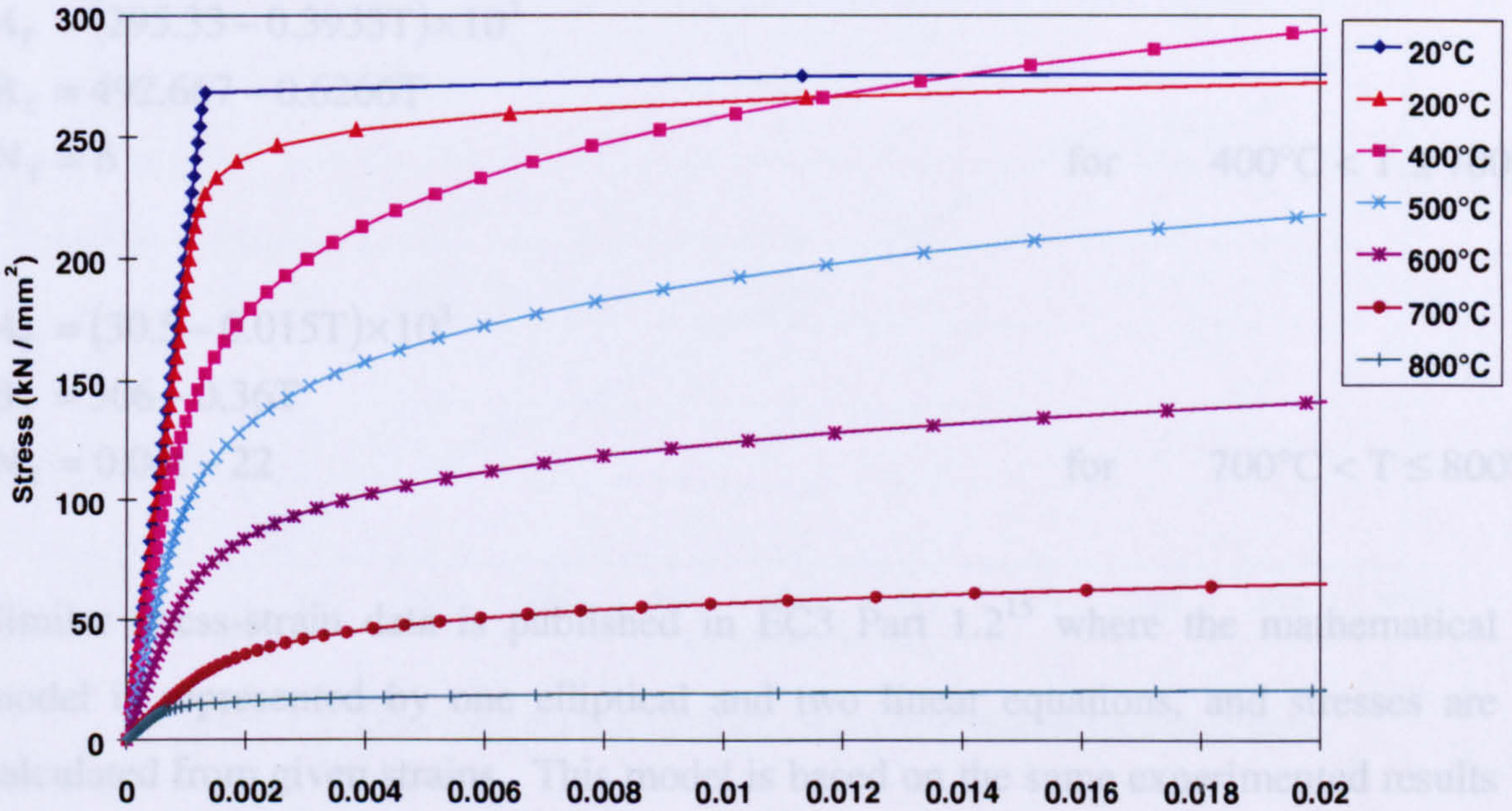

Figure 1.3 Stress-strain characteristics for Grade 43 steel at elevated temperatures.

The Ramberg-Osgood model[16] modifies strain at a given stress by the use of three temperature-dependent parameters – A_T, B_T and N_T. The equation is as follows:

$$\varepsilon_T = \left(\frac{\sigma_T}{aA_T}\right) + 0.01\left(\frac{\sigma_T}{bB_T}\right)^{N_T} \qquad (1.01)$$

Where ε_t and σ_t represent strain and stress respectively at temperature t, and

$$a = \frac{E}{180\times10^3}$$

$$b = \frac{\sigma_y}{250}$$

and

$$A_T = 180\times10^3$$
$$B_T = 0.00134T^2 - 0.26T + 254.67$$
$$N_T = 237 - 1.58T \qquad \text{for} \qquad 20°C \le T \le 100°C$$

$$A_T = (194 - 0.14t)\times10^3$$
$$B_T = 242$$
$$N_T = 15.3\times10^{-7}(400 - T)^{3.1} + 6 \qquad \text{for} \qquad 100°C < T \le 400°C$$

$$A_T = (295.33 - 0.3933T)\times10^3$$
$$B_T = 492.667 - 0.6266T$$
$$N_T = 6 \qquad \text{for} \qquad 400°C < T \le 700°C$$

$$A_T = (30.5 - 0.015T)\times10^3$$
$$B_T = 306 - 0.36T$$
$$N_T = 0.04t - 22 \qquad \text{for} \qquad 700°C < T \le 800°C$$

Similar stress-strain data is published in EC3 Part 1.2[15] where the mathematical model is represented by one elliptical and two linear equations, and stresses are calculated from given strains. This model is based on the same experimented results from Kirby and Preston (1988); therefore the stress-strain curves are very close to the Ramberg-Osgood model.

While considering the stress-strain behaviour of steel at elevated temperature, creep is one of the factors that need to be considered. Creep is defined as a visco-elastic strain which occurs with the passage of time under a constant stress state, at a rate which in controlled by the temperature. Research has been conducted into the effect of creep and at the different heating rates likely to be encountered in actual building fires. Witteveen[18] (1977) concluded from his earlier test results that with heating

rates ranging from 5° to 50°C per minute, and at temperatures not exceeding 600°C, no significant effect of creep was found. Aribert and Abdel Aziz[19] (1987) reported creep effect becomes significant at temperatures in excess of 545°C. The stress-strain data shown in Figure 1.3 is obtained with a consistent heating rate of 10°C per minute, which is believed to a good representation of real fires in average buildings.

Thermal elongation of steel in fire is critical to structural behaviour. Its main effects are thermal bowing and induced internal compression. The rate of thermal expansion increases almost linearly as temperature increases until about 720°C at which the microstructure undergoes a phase-change. As the steel absorbs energy and adopts a denser internal structure, thermal elongation stays constant up to 860°C and then starts increasing again. The variation of thermal expansion with temperature published in EC3 Part 1.2 is shown in Figure 1.4.

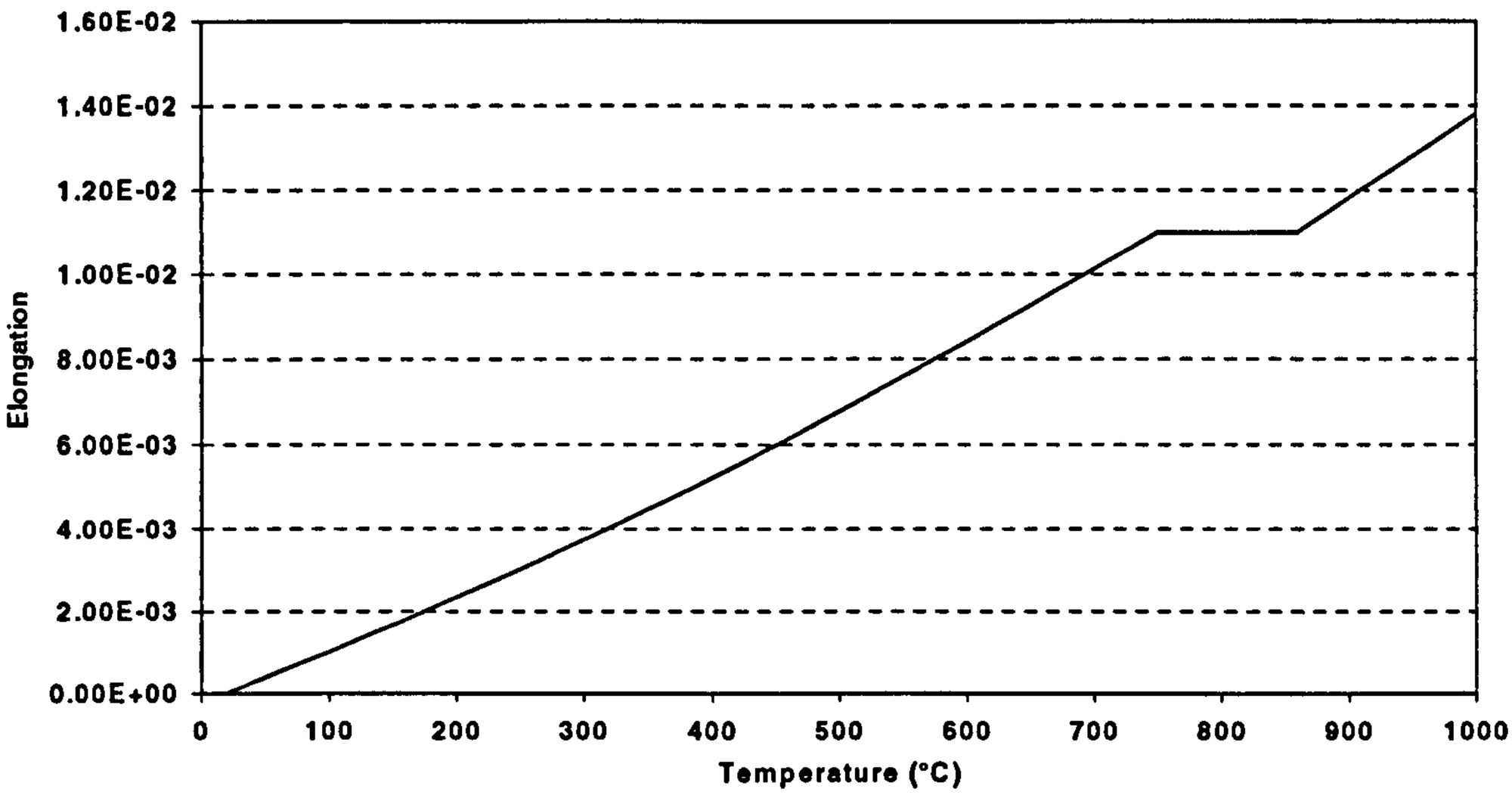

Figure 1.4 Thermal elongation of steel at elevated temperature.

The thermal elongation used throughout this research follows the EC3 data as shown below:

$$\frac{\Delta l}{l} = -2.416\times10^{-4} + 1.2\times10^{-5}T + 0.4\times10^{-8}T^2 \qquad \text{for} \qquad 20°C \le T \le 750°C$$

$$\frac{\Delta l}{l} = 1.1\times10^{-2} \qquad \text{for} \qquad 750°C < T \le 860°C$$

$$\frac{\Delta l}{l} = -6.2\times10^{-3} + 2.0\times10^{-5}T \qquad \text{for} \qquad 860°C < T \leq 1200°C$$

(1.02)

where,

l = original length at 20°C

Δl = the thermal induced expansion

T = temperature of steel

The specific heat of steel may be defined as the heat stored in a unit mass of steel for a unit temperature rise in °K. It increases slowly as temperature rises up to 700°C, when the steel's internal lattice structure changes and causes the specific heat to increase rapidly around 735°C, and reduces to almost the original level after that. The model of specific heat published by EC3 is shown below:

$$C_s = 425 + 7.73\times10^{-1}T - 1.69\times10^{-3}T^3 + 2.22\times10^{-6}T^3 \quad \text{J/kgK} \qquad \text{for } 20°C \leq T \leq 600°C$$

$$C_s = 666 + \frac{13002}{738 - T} \quad \text{J/kgK} \qquad \text{for } 600°C < T \leq 735°C$$

$$C_s = 545 + \frac{17820}{T - 731} \quad \text{J/kgK} \qquad \text{for } 735°C < T \leq 900°C$$

$$C_s = 650 \quad \text{J/kgK} \qquad \text{for } 900°C < T \leq 1200°C$$

(1.03)

where

C_s = thermal conductivity

T = steel temperature

Thermal conductivity of steel reduces as temperature increases up to 800°C, beyond which it stays unchanged. It is measured by the amount of heat in unit time passing

through a unit cross-sectional area of steel subject to a unit temperature gradient, EC3 part 1.2 gives the values as:

$$\lambda_s = 54 - 3.33\times10^{-2}T \text{ W/mK} \qquad \text{for } 20° \le T \le 800°C$$

$$\lambda_s = 27.3 \text{ W/mK} \qquad \text{for } 800°C < T \le 1200°C \qquad (1.04)$$

where

λ_s = specific heat

t = steel temperature

The density of steel is almost independent of temperature, and is given by EC3 part 1.2 as 7850 kg/m^3. Similarly, Poisson's ratio is taken as 0.3.

1.3 Steel Portal Frame Design and Construction

Single-storey portal frames can be constructed in many different shapes, Figure 1.5 illustrates various types that are used as main frames. They can be designed with elastic or plastic methods. Either way the connections between the columns and rafters must be capable of transmitting moments between the members.

If an elastic analysis is chosen, then computer software is normally used to help in solving a series of analyses with multiple load cases. Once individual member forces have been calculated, where both the column and rafters will normally be subject to a combination of moment and compression, they should be designed as normal beam-columns according to BS5950 Part 1[14]. Special considerations are given to lateral-torsional buckling, where allowance is made for the restraining effects of purlins, sheeting rails and cladding attached to the outer flanges of the main frame members.

However, since the mid 1950s, portal frame construction in the U.K. has been widely based on the principles of plastic design. Often the frames are the basic pitched-roof variety shown in Figs. 1.05 (b) and (c), of which the pinned base is more popular with designer as it avoids high foundation cost, as well as the complexity of forming a rigid connection.

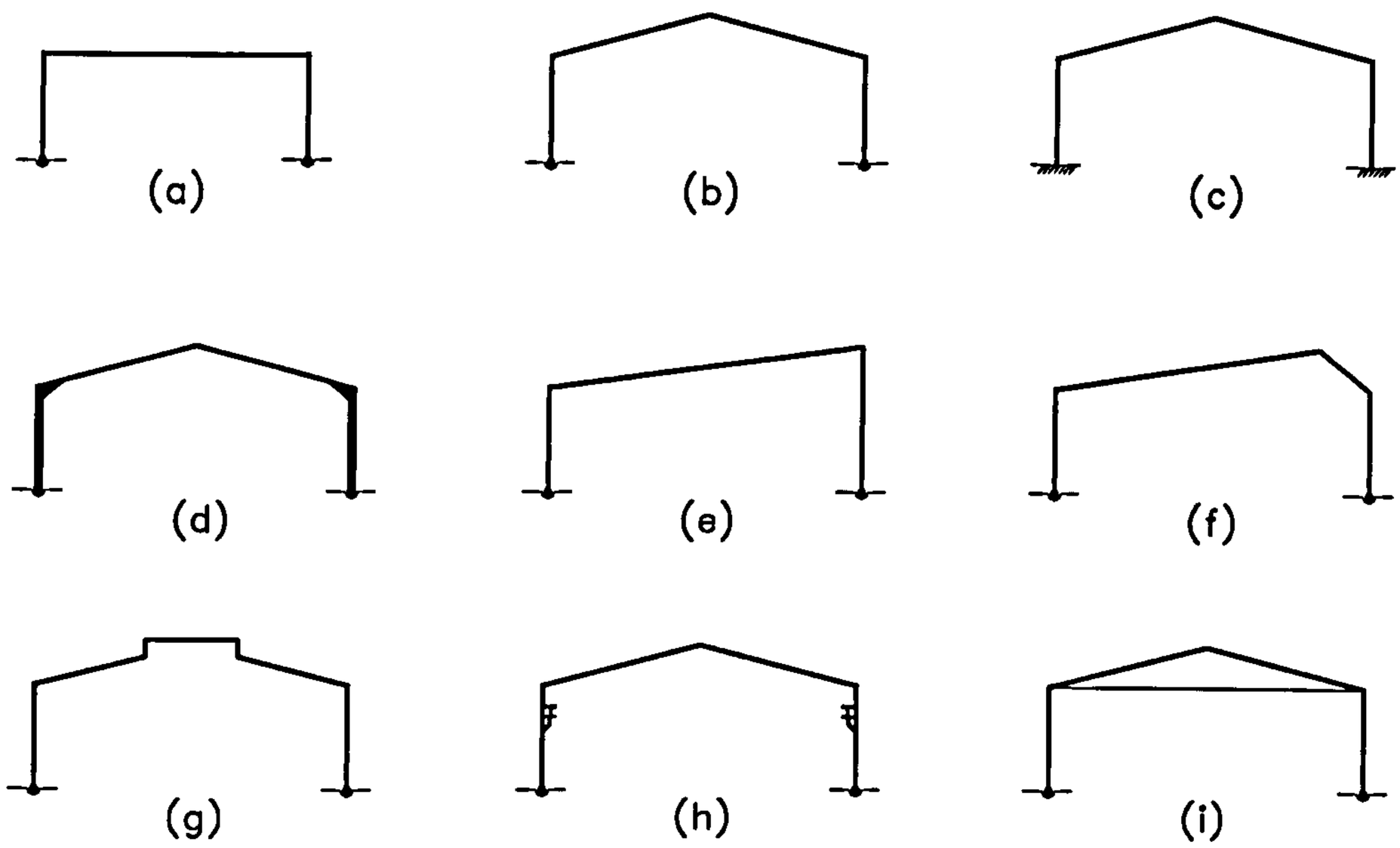

Figure 1.5 Different types of portal frames. (a) flat roof; (b) pinned base; (c) fixed base; (d) different sections with haunches; (e) lean-to frame; (f)north light; (g) monitor roof; (h) portal with crane; (i) tied portal

Plastic analyses involve identifying all possible collapse mechanisms of the portal frames and consider the lowest value of the collapse load when suitable sections are chosen. Further checks are performed to ensure that no other form of failure prevents the attainment of this collapse mechanism. Several publications[20,24] which deal with the detail design of portals by this method can be found, due to the popularity of this form of construction.

In this research, initial studies were conducted on flat-roof portal frames (Figure 1.5 (a)) and further studies were concentrated on basic pitched-roof portal frames with pinned and fixed bases (Figure 1.5 (b) and (c)).

1.3.1 Portal Frames in Fire

When fire starts in a single-storey portal frame structure, the rafter will be heated and expand, causing outward deflection of the eaves. As the fire develops further, the strength of the rafter will decrease substantially, and the rafter has to support only dead load from its self-weight, purlins, cladding and insulation. Rafter collapse will eventually take place, associated with some torsional instability due to the loss of purlins. The rafter, at this stage, is acting partially as a catenary with tensile force

pulling the tops of columns inwards. Total collapse happens when sufficient hinges form in the portal frames, either on columns or rafters, to create a mechanism.

There has been limited research done on portal frames in fire[9,12]. Current fire resistance design concentrates almost entirely on the prevention of fire spread beyond the building of origin by ensuring that column base connections retain sufficient rigidity to prevent collapse of the boundary wall. The U.K. regulatory authorities require the designer either to provide fire protection for the rafters, or to ensure that the base of the column would resist the forces caused by the rafter collapse in fire.

The only guide for designers in the U.K. to follow when considering portal frames in fire is the publication from The Steel Construction Institute*: The Behaviour of Steel Portal Frames in Boundary Conditions (1990)*[9]. The main purpose of this publication is to satisfy the U.K. authorities' concern that fires may spread to another building. Several assumptions was made in the document in order to derive the simplified equations given:

- Both columns will lean inwards by one degree.
- The rafter elongation is 2%, which includes thermal expansion and various deformations.
- The steel yield strength at failure caused by fire is equal 0.065 of the normal strength.
- The haunch length is equal to 10% of the span.

Although some of these assumptions are arguable, the method is believed to produce conservative results and is widely accepted. The equations are given as follows:

$$\text{Vertical reaction} = 0.5W_f SL + \text{dead weight of wall} \tag{1.05}$$

$$\text{Horizontal Reaction} = K\left(W_f SGA - \frac{CM_p}{G}\right) \tag{1.06}$$

$$\text{Overturning moment} = K\left[W_f SGY\left(A + \frac{B}{Y}\right) - M_p\left(\frac{CY}{G} - 0.06\right)\right] \tag{1.07}$$

Where,

G, Y and L are the dimensions shown in Figure 1.6.

W_f = load at time of collapse

S = distance between frame centres (m)

M_p = plastic moment of resistance

K = Modification factor

$\theta = \cos^{-1}(0.97\cos\theta_0)$ = original rafter pitch

θ_0 = final rafter pitch

$$A = \frac{1}{4\tan\theta} + \frac{1}{96}$$

$$B = \frac{L^2 - G^2}{8G}$$

$$C = \frac{0.255\cos\theta_0}{\sin\theta}$$

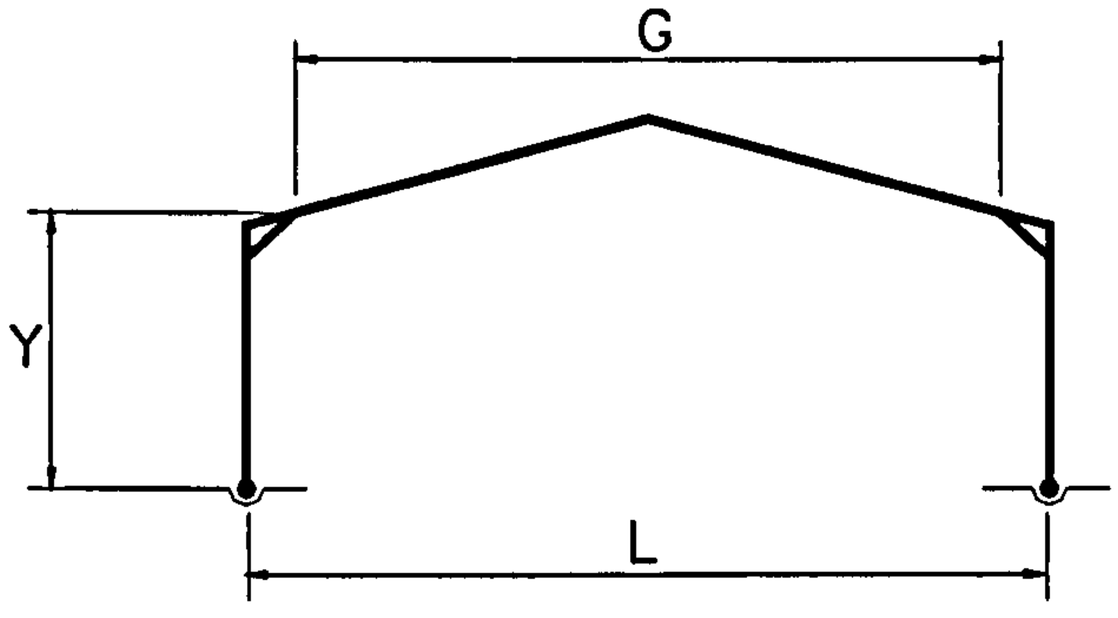

Figure 1.6 Frame dimensions

Some of the parameters in the equation are created to simplify the original formulas so that the result from the simplified method is near to the real solution. The parameters are calibrated against frames with spans greater than 12m. In calculating the required base overturning moment, it is also suggested that a minimum positive 10% of the plastic moment resistance of the column should always be considered, if the values calculated from the equation are less.

O'Meagher et al (1992)[12] has conducted research into single-storey industrial buildings in fire for the Australian Institute of Steel Construction, as a supplement to the Building Code of Australia (BCA). They concluded that the application of fire-protection to the columns of the steel portal frames would have no influence on the deformation mode or their fire resistance. There is also no need to fire-protect the roofs of the supporting steelwork when designed according to BCA. Parametric studies were conducted using a finite element program ABAQUS [26,27] on 20 portal frames with different spans, load and heating profile. It was found the most of these failed with an acceptable failure mode.

1.4 Structural Computer Modelling

Modelling of structural behaviour using the finite element method by computer has been very popular in recent years. The main reasons is the relatively high cost of conducting real structural tests. Once computer modelling has been showed to be capable of analysing real structures with acceptable accuracy, large-scale parametric studies can be performed to investigate the influences of particular factors on structural behaviour. The method has become particularly feasible due to the improved performance, in terms of speed and storage, of modern desktop computers.

VULCAN, a non-linear finite element program developed at the University of Sheffield, was used throughout this research for the purposes of computer modelling for validation and parametric studies.

1.4.1 VULCAN

The development of VULCAN is based on another program, INSTAF, which was written by El-Zanaty and Murray at the University of Alberta in 1980[28]. INSTAF is capable of analysing two-dimensional steel frames at ambient temperature, incorporating the geometrical non-linearity, penetration of material yielding into the cross section and spread of inelastic zones along member lengths. The code was written in the FORTRAN programming language. By 1990, El-Rimawi and Saab[29,30] from the University of Sheffield had successfully included the effect of thermal distribution due to fire into INSTAF, and a Ramberg-Osgood representation was used for the stress-strain data. After that, Najjar[19] further developed the program to allow three-dimensional behaviour be analysed. Bailey[31] added the capability to include semi-rigid connections introduced as spring elements, continuous concrete slab represented by shell elements, strain reversal in cooling and flexural shear forces to allow lateral-torsional buckling. Most recently, Huang[33,36] further extended the shell elements into a layered formulation which gives a better representation of concrete cracking. As the program can only analyse I-shaped symmetric cross sections, Cai[39] has included the capability to analyse asymmetric beams. Validation of the program has been carried out at each stage of development.

In the VULCAN model, beam-column elements are represented by two-noded line elements. The basic finite element model presented by El-Zanaty and Murray in the original INSTAF adopted the non-linear large displacement-strain equation as:

$$\varepsilon_z = u_o' + \frac{1}{2}\left[(u_o')^2 + (v_o')^2\right] - yv_o''\left[1 + u_o' + \frac{(v_o')^2}{\sqrt{1-(v_o')^2}}\right] + \frac{1}{2}y^2(v_o'')^2\left[1 + \frac{(v_o')^2}{(1-(v_o')^2)}\right] \tag{1.08}$$

where,

ε_z = strain in z direction

u_o', v_o', v_o'' are the first and second derivatives of the deflection components shown in Figure 1.7.

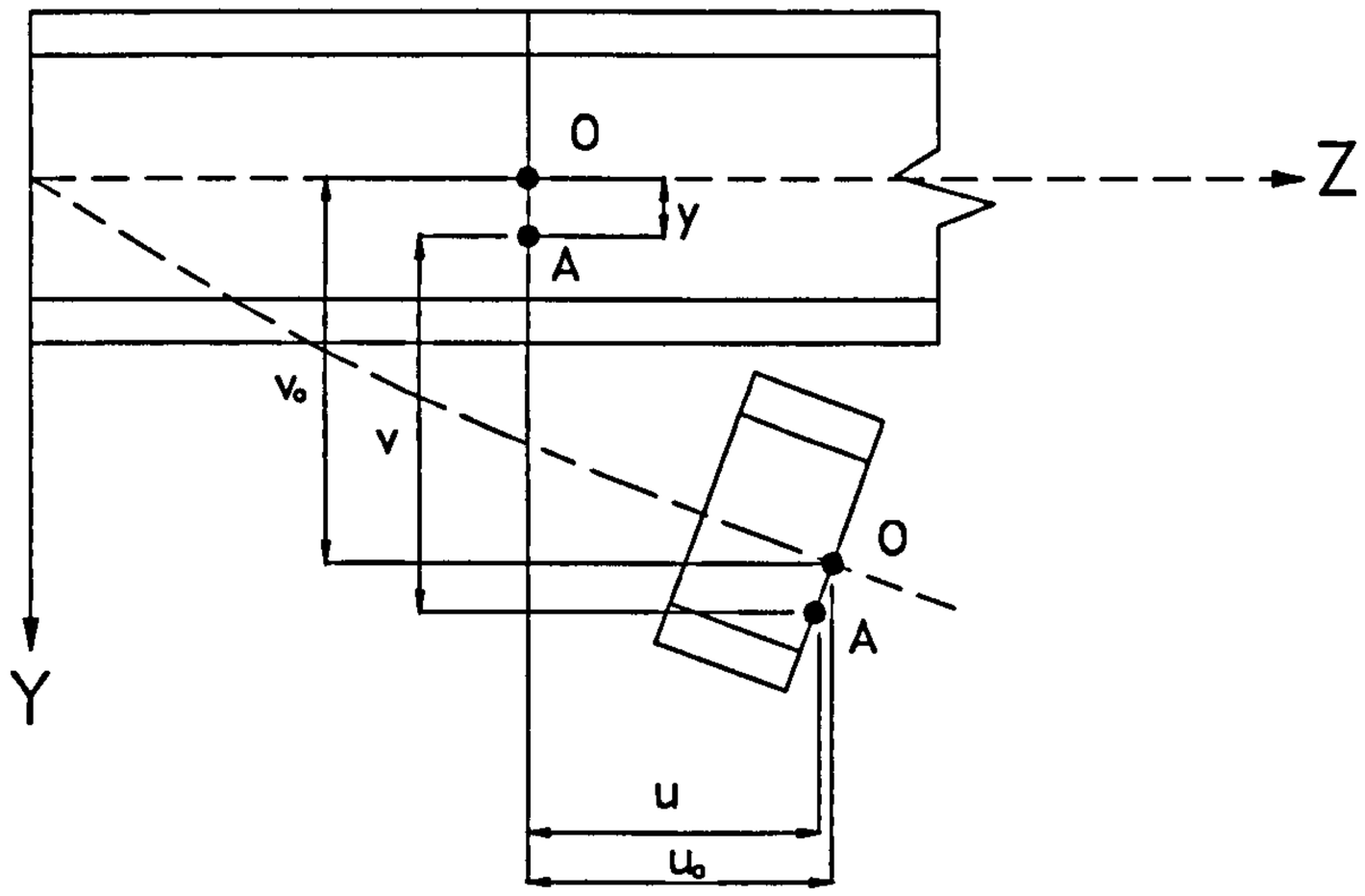

Figure 1.7 Notation for strain displacement equation

Within this model, each node has five degrees of freedom. When Najjar extended the capability into three-dimensional analysis an extra term *w'* was added, associated with three additional degrees of freedom in the local coordinates. This gives a total of eleven degrees of freedom per node in global coordinates. Every effort was made to retain the higher-order terms to enable geometrical non-linearity to be represented properly.

A physical beam-column member is separated into a number of finite elements, interconnected at nodal points. The displacements of these nodal points are to be

solved within the structural analysis. Shape functions are then used to define the displacements within an element bounded by nodal points. Displacements at any point along the element can therefore be defined, and the state of strain can be found by using the large-displacement equation (1.08).

As is typical in finite element analysis, equilibrium is enforced between boundary stresses and the external loads. The Principle of Virtual Work is applied, and the equation is shown as:

$$\partial W = \int_V \sigma_z \partial \varepsilon_z dV - \langle Q \rangle \{\partial q\} = 0 \qquad (1.09)$$

where,

σ_z = axial stress

$\delta\varepsilon_z$ = virtual axial strain (derivation from equation 1.08)

$\langle Q \rangle$ = row vector of external loads

$\{\partial q\}$ = column vector of imposed virtual displacements

The standard stiffness relationship given by a typical finite element procedure is shown as:

$$[K]\{q\} = \{Q\} \qquad (1.10)$$

where,

[K] = tangent stiffness matrix

{q} = vector of nodal displacement

{Q} = vector of nodal forces

In VULCAN, Gaussian integration[42] is applied to evaluate terms in equation 1.09. An iterative method of solution is required due to the non-linearities, and therefore the Newton-Raphson solution procedure was adopted.

The spring elements introduced by Bailey fit within the same finite element theory used for beam-column elements, except that their rotational stiffness properties are

modified in the analysis to simulate the behaviour of moment connections. Shell elements have only five degrees of freedom at each node in local-coordinates, representing displacements in three dimensions and rotations about two bending axes. Shell elements are not used within this project and the details can be found in relevant publications.

At present, extensive research is in progress to improve the modelling of connections, conducted by Al-Jabri[40,41] and Spyrou. Geometrical nonlinearity of shell elements is under development by Allam[37,38] and Huang[34,35].

1.4.2 The Application of VULCAN

Since there is no user-interface for VULCAN, a textual input file needs to be created to define a structural problem. The input file will specify the structure as a series of nodes connected by a number of beam-column, spring and shell elements with different material properties, together with heating criteria. Most recently, Shepherd[32] has reformulated the input format, using blocks of data with labels so that the measuring of each of the numerical values can be identified easily.

VULCAN will read the input file and perform the structural analysis, recording the results in a separate output file. Similarly, output results are written into blocks, and the user can select the required results on particular nodes to be written into different files so that a speadsheet program can process the results efficiently. Shepherd[43] has created an interactive graphical software tool called SHOWGRID, which can read the input and output files and displayed the arrangement and results graphically. The option to display the deflected shapes from output files as series of animations is available.

1.5 Layout and Scope of Research

This research was conducted in conjunction with the Health and Safety Laboratories at Buxton. The main objective of the research was to investigate the behaviour of steel portal frames in fire. Previous research concentrated mostly on the boundary conditions, and it was believed that other aspects of the behaviour might control the way in which the fire develops, the modes of failures and the probability of its control by fire fighters. Necessary investigations were also conducted onto the

capabilities of VULCAN as a computer modelling tool and some changes were made to improve its performance.

A general introduction to steel properties, portal frame behaviour in fire and the finite element program VULCAN have been presented in this chapter. Particular attention has been given to the widely accepted portal frame document published by SCI, which was produced to satisfy the U.K. authorities.

In the next chapter, the feasibility of using VULCAN to analyse portal frames is investigated, concentrating particularly on the analysis of sloping members since pitched roofs are necessary. Modifications done to the VULCAN are also presented.

As part of the research project, experiments were conducted at Buxton in which a scale model of a steel portal frame was constructed and tested under fire. Chapter 3 describes in detail the indicative tests and three major fire tests performed, along with the test results. The following chapter compares the test results with computer analyses performed by VULCAN. The test results obtained are discussed, as are the significance of the comparison as well as the physical observations. VULCAN analysis is also validated against the test results.

Once the validation of VULCAN has been done, the software is used to perform a series of parametric studies, investigating various factors. Chapter 5 describes the first series of parametric studies in which two-dimensional frames are investigated. The parameters concerned are the load ratios, frame geometries, heating profiles, effect of horizontal load and rotational stiffness. The next series of parametric studies involve analyses on three dimensional full scale frame, where the effects of the secondary elements are included with different fire scenarios. The three dimensional parametric studies are presented in Chapter 6. Discussions on the studies are given at the ends of these two chapters respectively.

In Chapter 7 a simplified method to estimate the critical temperatures of portal frames in fire is proposed. Its purpose is to enable practising engineers to perform quick hand calculations to obtain the failure temperature, with acceptable accuracy. Examples of calculation are also presented.

Further discussions on other aspects of the research are presented in Chapter 8. These include looking at aspects required by the original research proposal and

review of the current guide for portal frame with boundary conditions. A more general view on performance based design approach is also briefly discussed.

Finally, general conclusions are drawn in the final chapter, along with recommendations for future research.

2 Preliminary Studies on VULCAN and Portal Frames in Fire

A preliminary investigation into the use of VULCAN has been conducted, giving priority to rationalising the finite element code for use in analysing structural elements not aligned with the primary axes. The study was necessary because the most common form of portal frame is constructed with a sloping roof. Such applications had not been addressed in any previous studies.

These studies also investigate the Ramberg-Osgood stress-strain curve adopted in VULCAN and the modelling of semi-rigid connections at elevated temperatures. The solution procedure adopted by VULCAN and its significance is also briefly discussed. Some initial studies of the behaviour of goal-post (flat-roof) portal frames using VULCAN followed at the end of the chapter.

2.1 Rationalisation of VULCAN

When a VULCAN analysis is conducted, the structure is divided into a finite number of elements prior to the actual calculation, and each element is connected between two nodal points. Each node is associated with 11 degrees of freedom, namely displacements (u ,v and w), rotations ($\frac{\delta v}{\delta z}, \frac{\delta w}{\delta y} and \frac{\delta w}{\delta x}$), strains ($\frac{\delta u}{\delta z}, \frac{\delta v}{\delta y} and \frac{\delta w}{\delta x}$), as well as twisting and warping. The nine basic degrees of freedom (omitting twisting and warping) are shown in Figure 2.1.

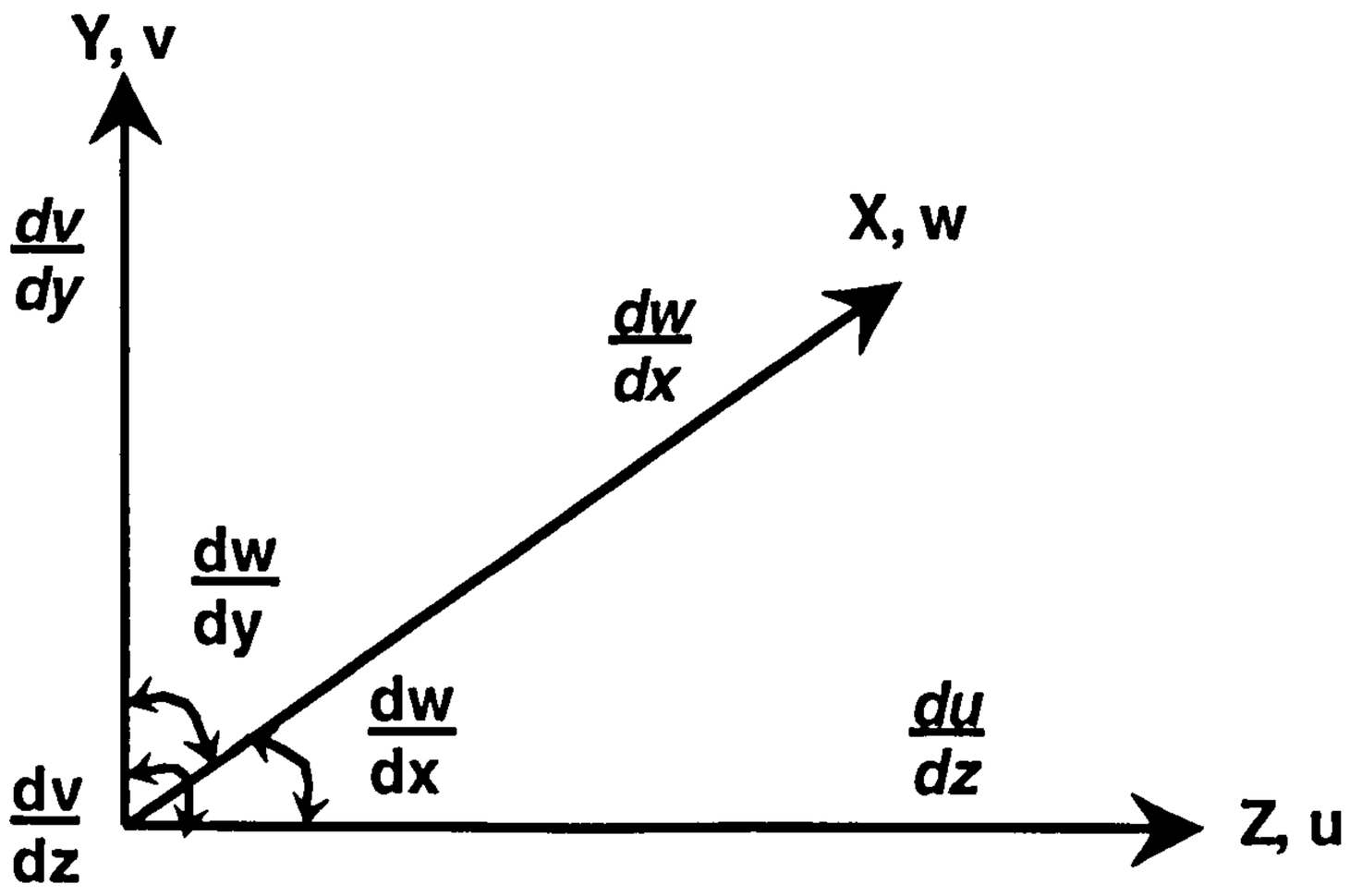

Figure 2.1 Nodal degrees of freedom in VULCAN

The strain degrees of freedom are retained so that the effect of geometrical non-linearity and large displacement behaviour of structures can be modelled more accurately by the development of plastic hinges through spread of yield. These strains are defined in local co-ordinates, and then transformed to the global directions. Therefore, the global strain degrees of freedom can be fixed or freed in the input file when setting up finite element analysis. However, if a structural member is not placed parallel to a global axis (e.g. an inclined member), the logic of whether to free or to fix the global strain degrees of freedom is rather uncertain.

2.1.1 The Effect of Strain Degrees of Freedom

In order to investigate the effect of the strain degrees of freedom, a simple cantilever beam has been set up to compare the behaviour under large displacement. The yield stress of the beam has been artificially changed to an infinite value so that the large-displacement criteria can be met. This is a load-deflection analysis which does not involve elevated temperature. The results of the analyses are shown in Figure 2.2.

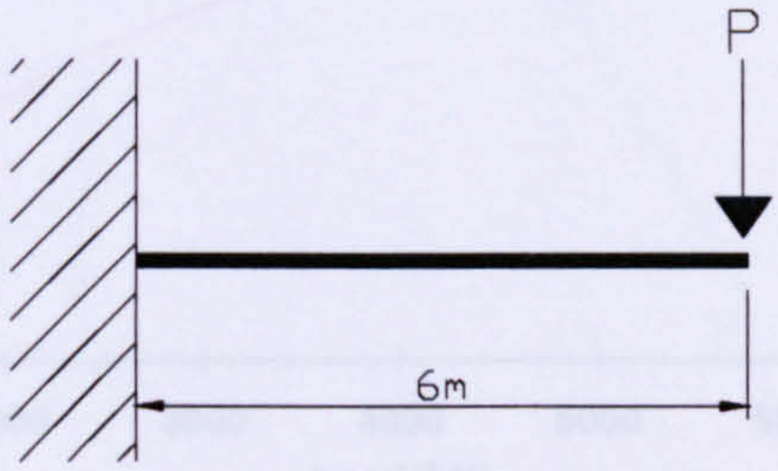

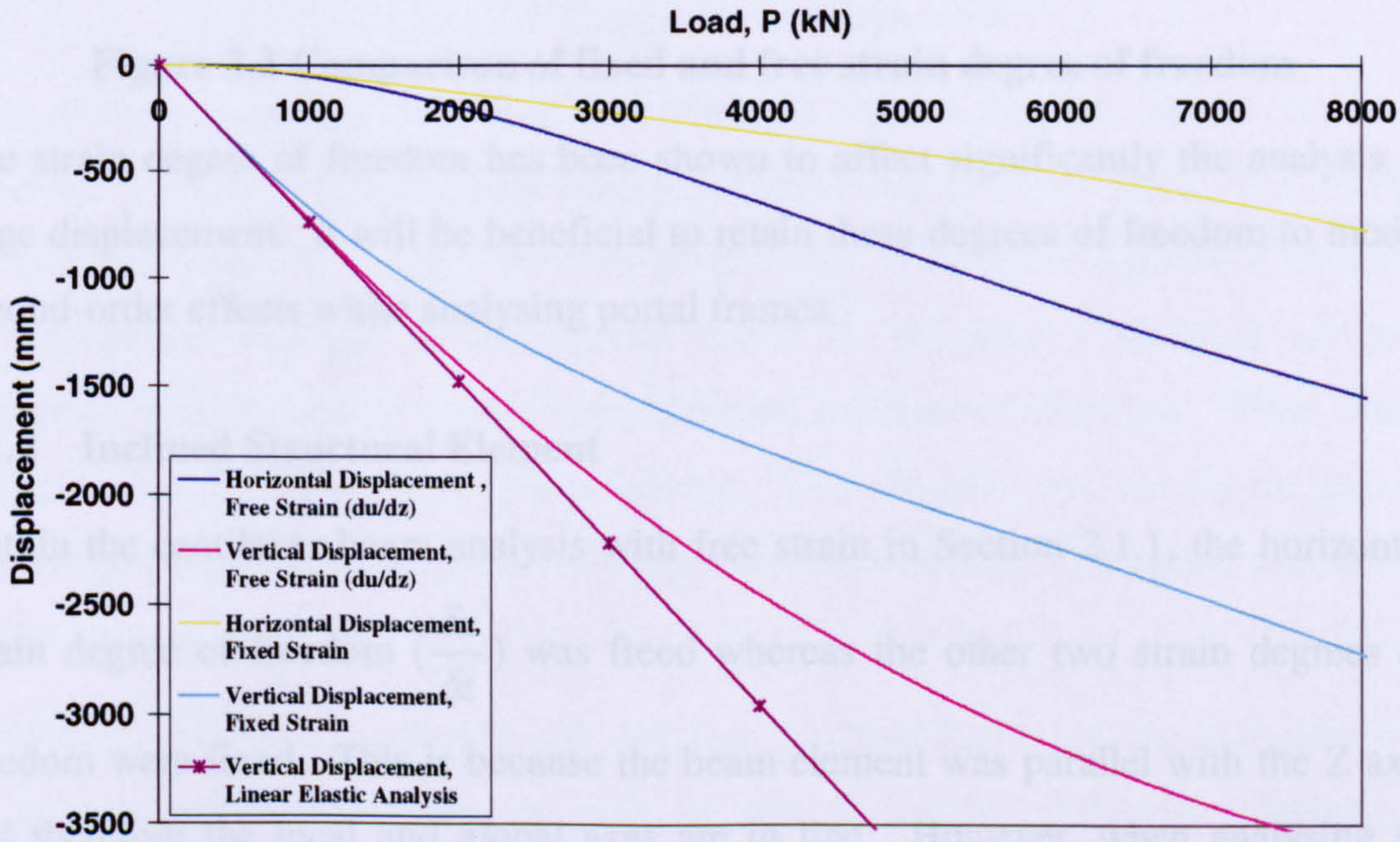

Figure 2.2 Cantilever beam - large displacement test

It can be seen that the difference in displacement between the free- and fixed-strain cases is not significant until the vertical displacements exceed 500mm, which is equivalent to span/12. The failure criterion of a single structural element under fire test is often taken as span/30, although inspections from full-scale fire tests on real buildings such as the Cardington composite frame have suggested that a real structure can sustain displacement well beyond the span/30.

Figure 2.3 shows the difference in percentage terms between the free- and fixed-strain cases. The difference between horizontal displacements is more than 50% at 6000kN, where the vertical displacement reaches approximately span/2.

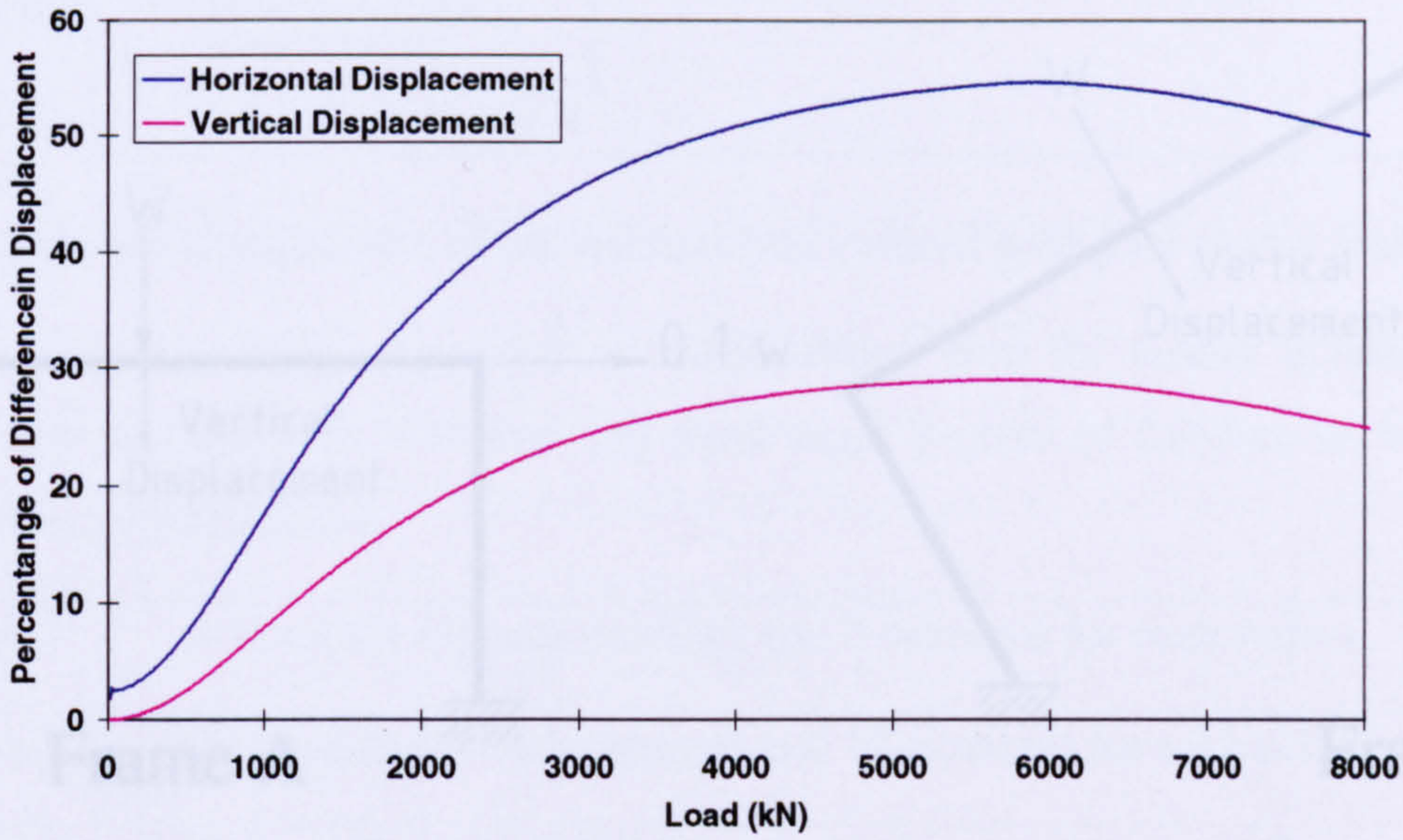

Figure 2.3 Comparison of fixed and free strain degree of freedom

The strain degree of freedom has been shown to affect significantly the analysis at large displacement. It will be beneficial to retain these degrees of freedom to model second-order effects while analysing portal frames.

2.1.2 Inclined Structural Element

Within the cantilever beam analysis with free strain in Section 2.1.1, the horizontal strain degree of freedom ($\frac{\delta u}{\delta z}$) was freed whereas the other two strain degrees of freedom were fixed. This is because the beam element was parallel with the Z axis and therefore the local and global axes are in line. However, when analysing an

inclined member, the global strain degrees of freedom have either to be free or fixed before the local stiffness matrix is assembled.

A simple test was carried out to investigate the issue. A two-dimensional goal-post portal frame was set up and modelled using VULCAN. The same frame was then rotated by 30° so that all the members were inclined to the global axes. Both layouts are shown in Figure 2.4. If VULCAN can handle the transformation correctly, it is expected that both the normal and rotated portal frames should demonstrate the same behaviour and give the same amount of vertical displacement.

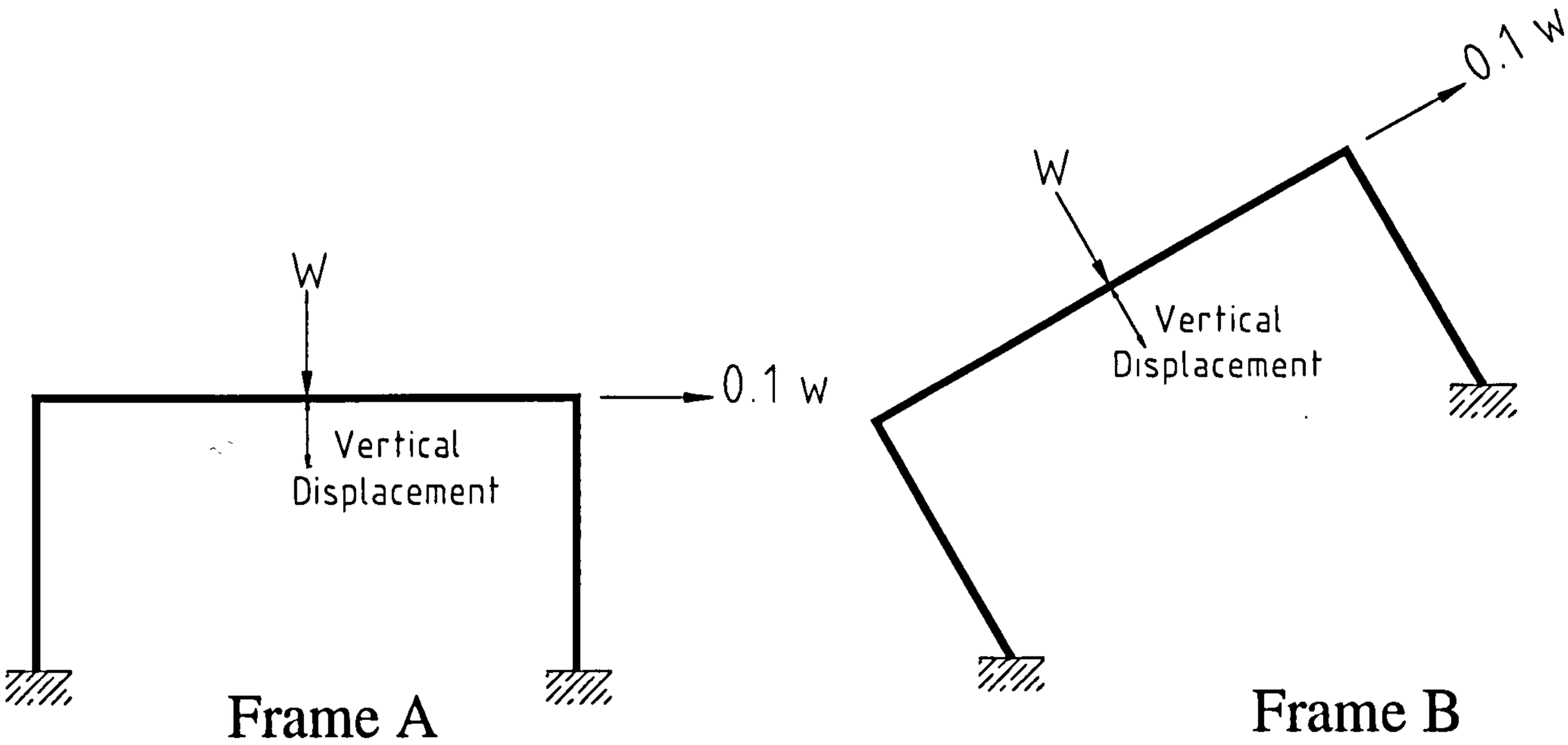

Figure 2.4 The layout of the models

Each of the frames was modelled in 2 different ways, using 14 and 28 elements respectively. This enables a more complete comparison between them. The results are shown in Figure 2.5. It is seen from the plot that, if the strain degrees of freedom are introduced into the inclined portal frame B, the results obtained are not consistent, even between the cases using different numbers of elements. When strain effects are fixed, all the results are consistent. This indicates that having the global strain degree of freedom free does not represent the boundary conditions accurately for the inclined member.

Further analyses were conducted with different combinations of numbers of elements for the rafters and columns, as well as testing various boundary conditions, particularly at the connections.

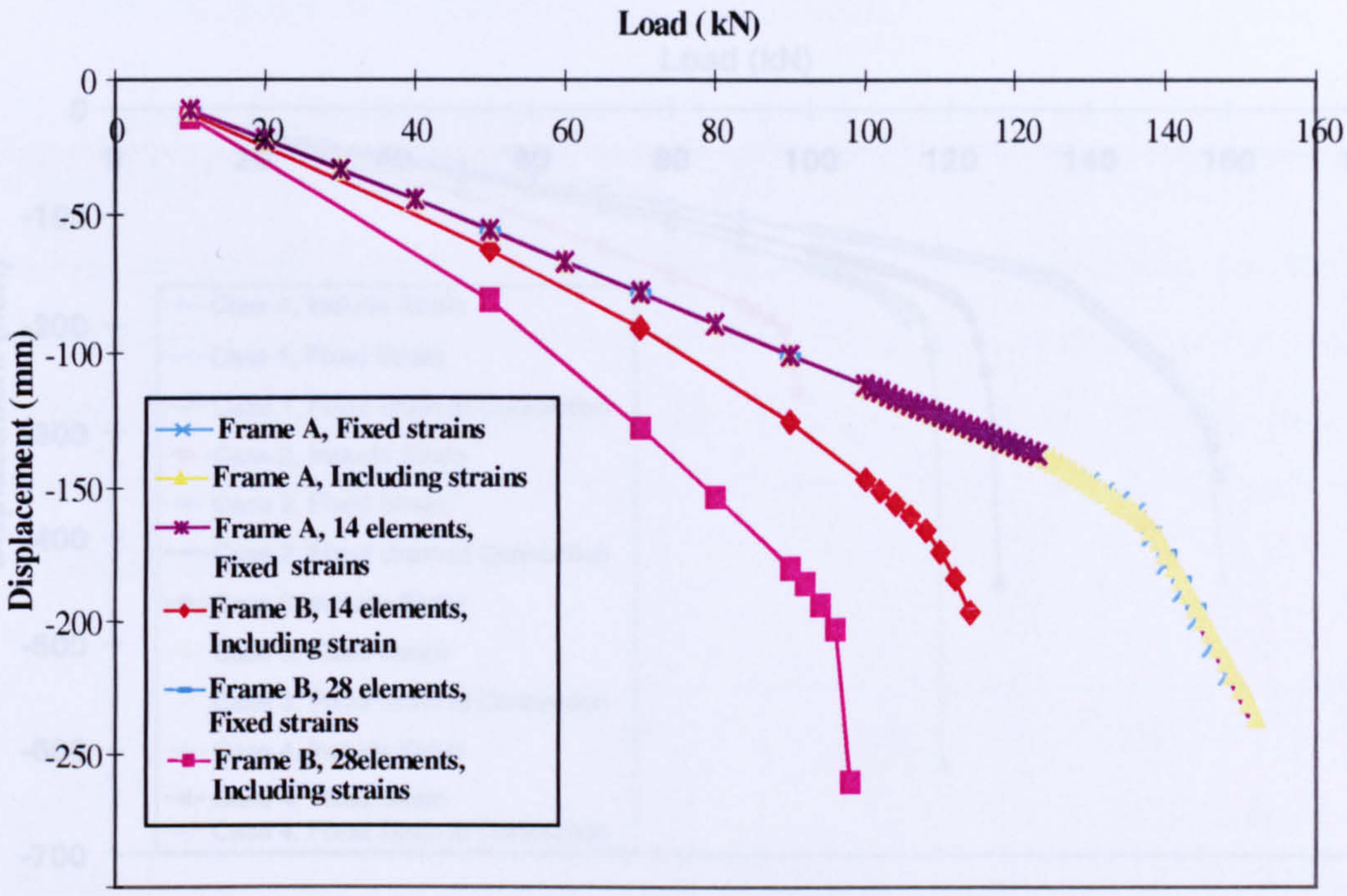

Figure 2.5 Comparison of the normal and rotated goal-post portal frames

Table 2.1 below shows the cases of combinations used for further investigation. Each case was analysed with free and fixed strain degrees of freedom on both the normal and rotated frame.

Case 1	4 elements for each columns and 6 elements for each rafters.
Case 2	8 elements for each columns and 12 elements for each rafters.
Case 3	1 elements for each columns and 6 elements for each rafters.
Case 4	1 elements for each columns and 12 elements for each rafters.

Table 2.1 Combinations of different numbers of elements

It was realised that, at the connection between the column and rafter, both the vertical and horizontal strains are free at this particular node. However, the second-order effect at the connection is thought have little effect on the structural behaviour. Therefore, all the cases were analysed again with free strain at the rafter-to-rafter and column-to-column nodes, but all strain degrees of freedom were fixed at the rafter-to-column joint nodes.

It was found, in all the cases, that the results from the non-rotated frame were consistent. Figure 2.6 plots all the vertical displacements at mid-span from the cases of the rotated frame B.

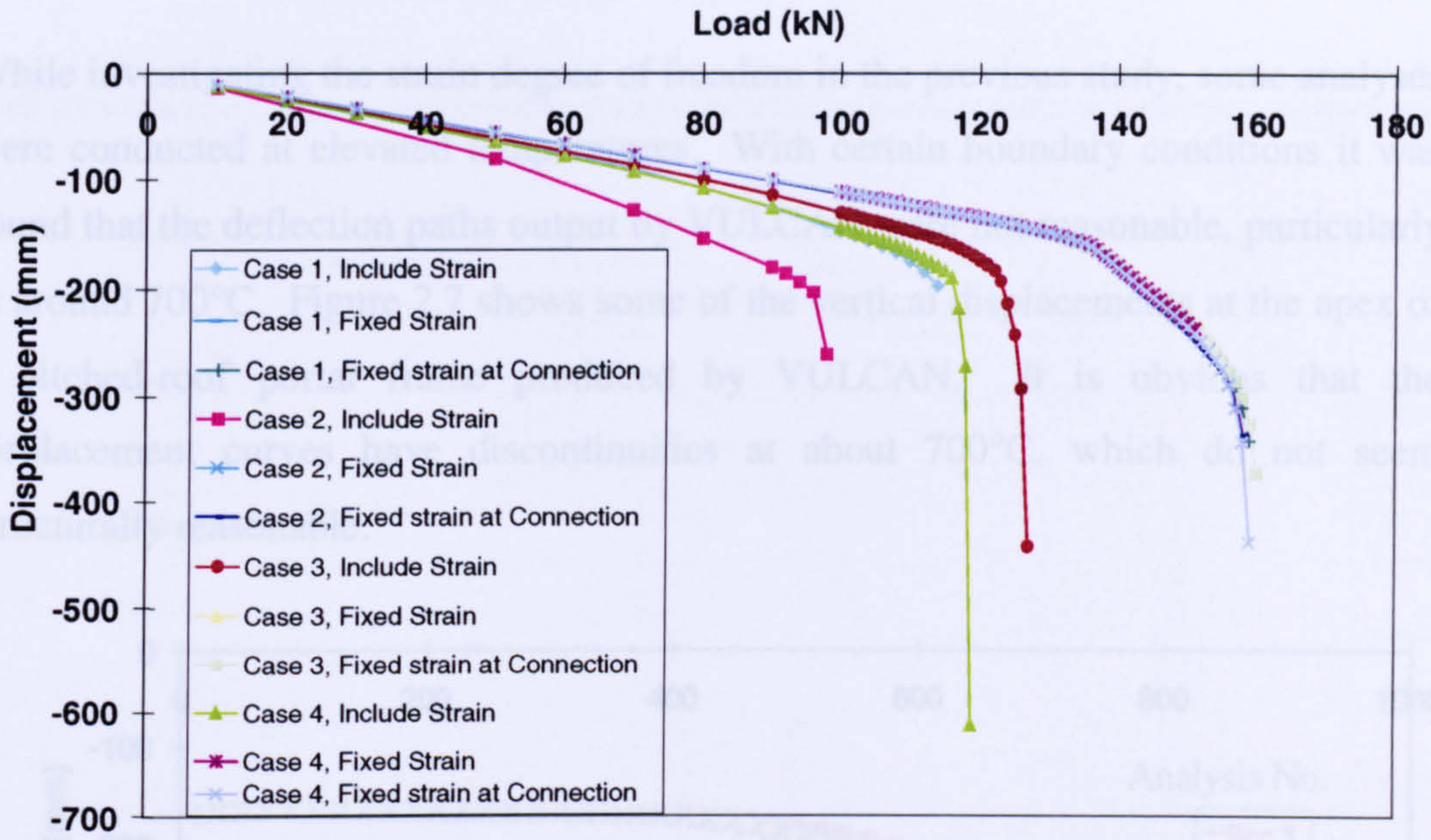

Figure 2.6 Vertical displacement for strain investigation of Frame B

From the displacement plot, some inconsistency can be seen in results when the strain degree of freedom is allowed. It also gives different displacements when different combinations of element numbers are used. However, when the strains are fixed at the connection nodes and left free elsewhere, then all cases give very similar results. These analyses also reach higher displacement levels compared to the fixed-strain cases.

It is therefore reasonable to model the inclined members with the strain degree of freedom fixed at the joints without compromising the geometrical non-linearity given by VULCAN analysis. The approach can be applied to the analysis of pitched-roof portal frames, where the strain degree of freedom of the node at the beam-to-rafter and rafter-to-rafter apex connection will be fixed. The secondary effect can be included at the nodes between connections.

Further tests on pitched-roof portal frames using this approach were conducted and it was found that results produced were consistent. All the analyses conducted for the parametric studies in the later chapters have adopted the same approach in modelling the frames.

2.2 Modification of Ramberg-Osgood Model

While investigating the strain degree of freedom in the previous study, some analyses were conducted at elevated temperatures. With certain boundary conditions it was found that the deflection paths output by VULCAN were not reasonable, particularly at around 700°C. Figure 2.7 shows some of the vertical displacements at the apex of a pitched-roof portal frame produced by VULCAN. It is obvious that the displacement curves have discontinuities at about 700°C, which do not seem structurally reasonable.

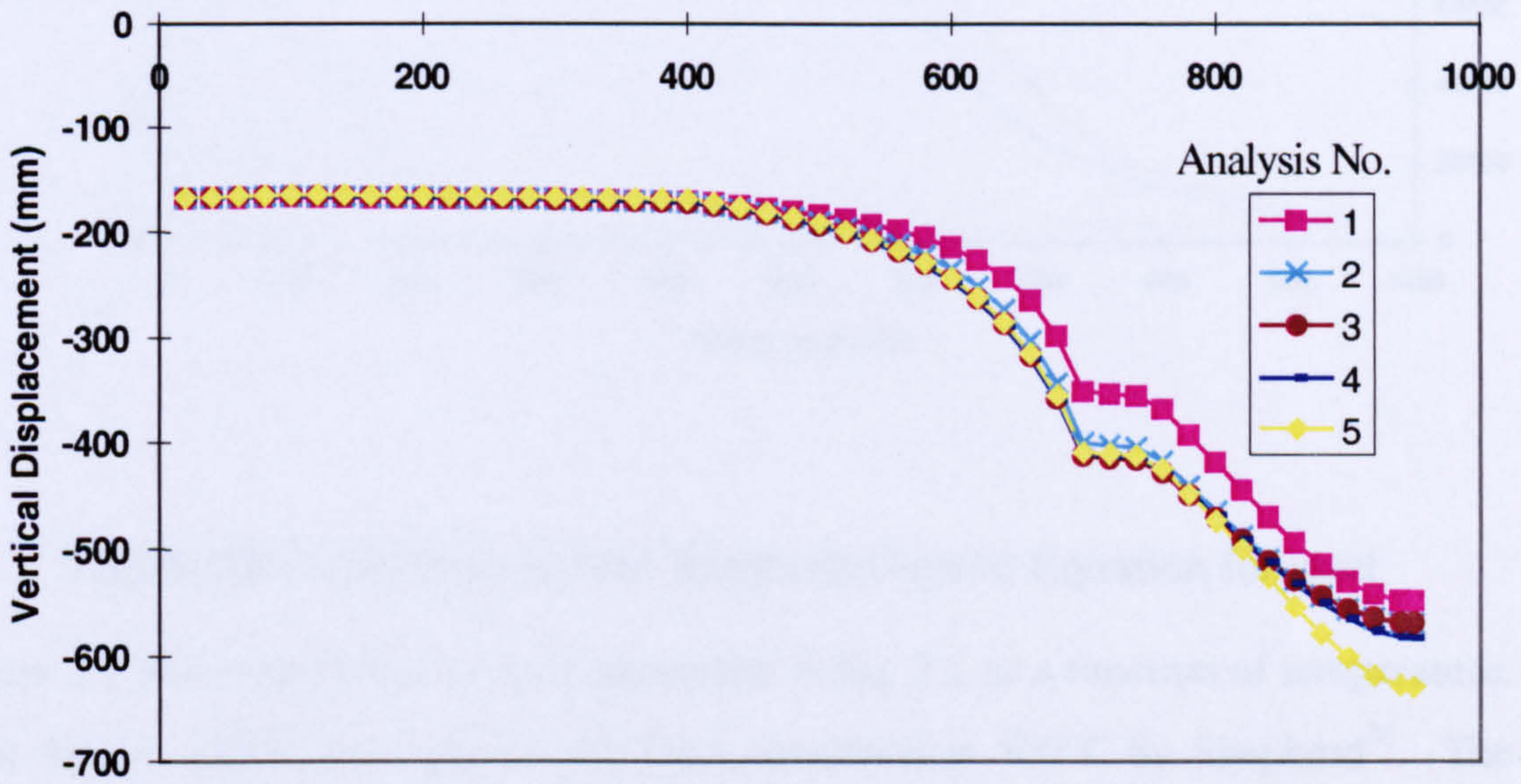

Figure 2.7 VULCAN analysis

It was thought that this phenomenon was related to the form of the existing Ramberg-Osgood stress-strain curves adopted in VULCAN. The Ramberg-Osgood model[9] for stress-strain curves of steel at elevated temperatures modifies the strains at a given stress by the use of three temperature-dependent parameters, namely A_t, B_t and N_t. VULCAN uses this model for the analysis of structural behaviour at elevated temperatures.

The Ramberg-Osgood equation is given as

$$\varepsilon_T = \left(\frac{\sigma_T}{A_T}\right) + \left(\frac{\sigma_T}{B_T}\right)^{N_T} \qquad (2.1)$$

where ε_t and σ_t represent strain and stress respectively at temperature t.

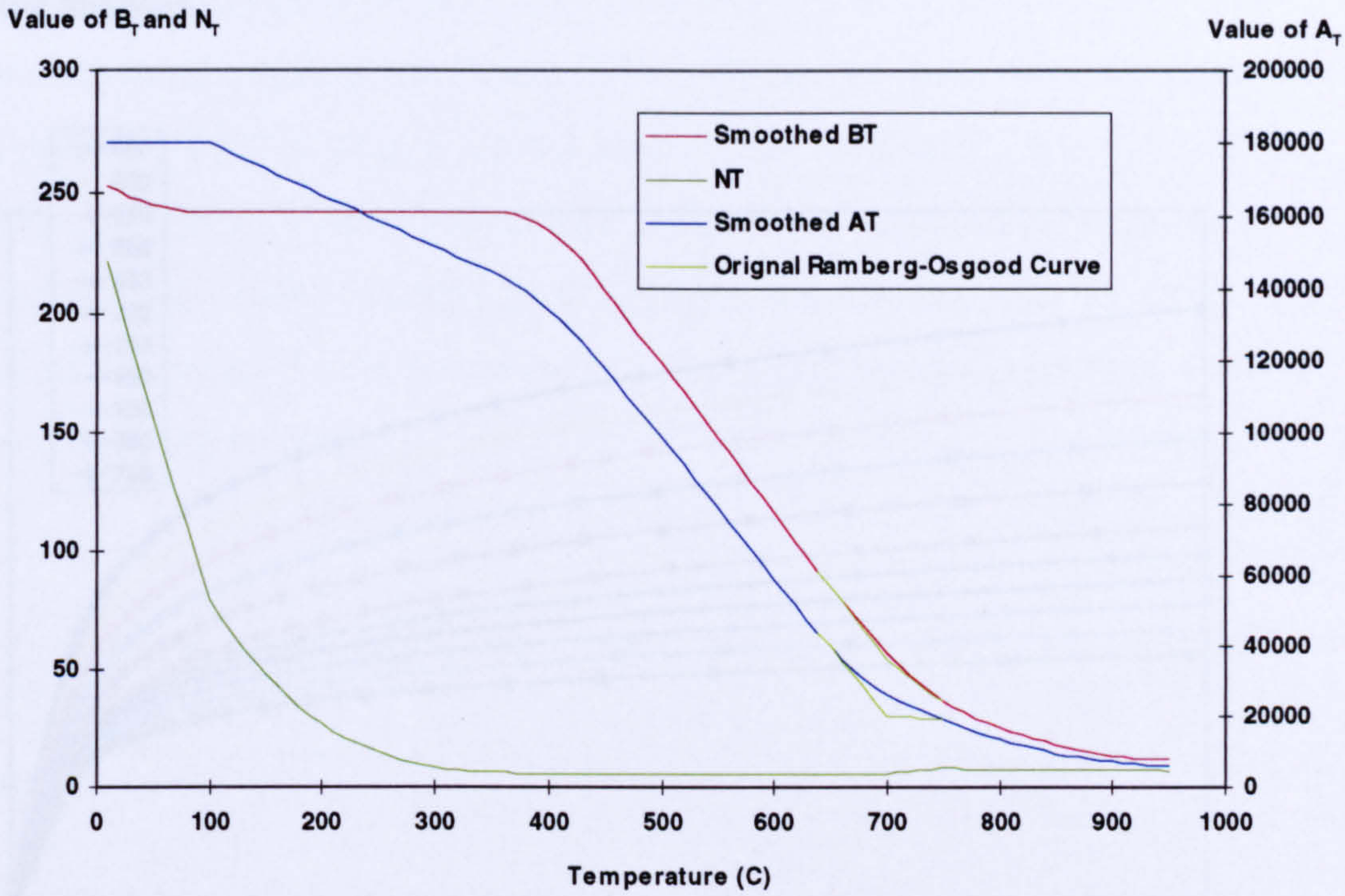

Figure 2.8 Coefficients for the Ramberg-Osgood Equation for steel

Figure 2.8 shows the value of each parameter in Eq. 2.1 as a function of temperature. Note that A_t and B_t have previously been smoothed at 400°C by Shepherd[32]. The green lines are the original Ramberg-Osgood curves for the coefficients A_t and B_t; it can be seen that there is a sudden change at 700°C.

In order to smooth the curves around 700°C, polynomials were derived to impose a gradual change on the coefficients between 650°C and 750°C, and these are shown as the red and blue lines in Figure 2.8. The minimal polynomials required to match the value and gradient of each coefficient are cubics, which are expressed between 650° and 750°C as

$$A_t = -0.01129522917\ t^3 + 25.04696979\ t^2 - 18637.68776\ t + 4673770.117 \qquad (2.2)$$

$$B_t = 0.000000094\ t^3 + 0.001356\ t^2 - 2.222025\ t + 1024.0875 \qquad (2.3)$$

From Figure 2.9 it can be seen that the stress-strains curves for the original Ramberg-Osgood model just below 700°C are more closely bunched than above 700°C. Figure 2.10 shows the modified model where the gaps between curves reduce

continuously. Therefore, there will not be a sudden change in the behaviour of steel during the analysis.

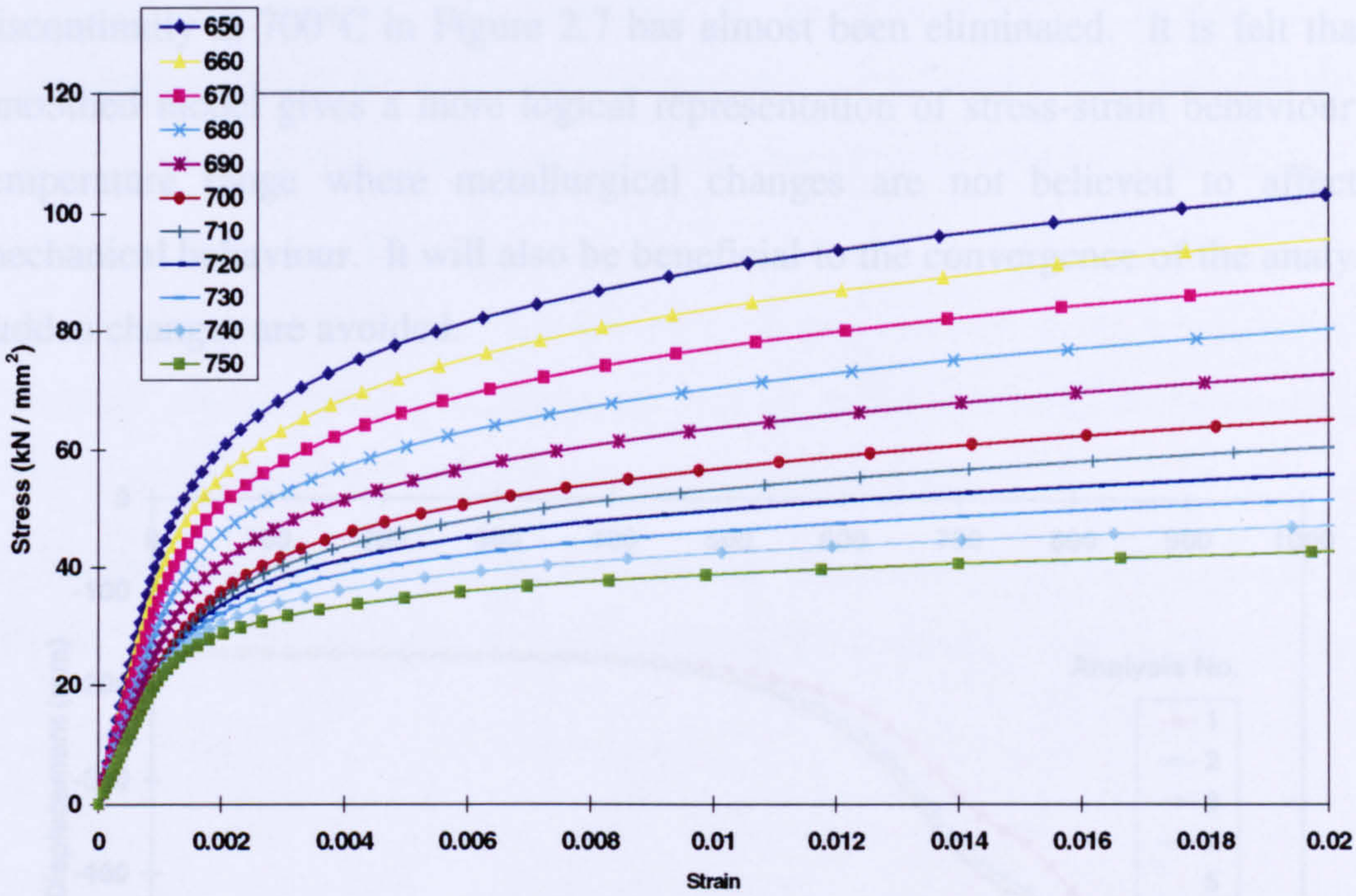

Figure 2.9 The original Ramberg-Osgood stress-strain curves for S275 steel

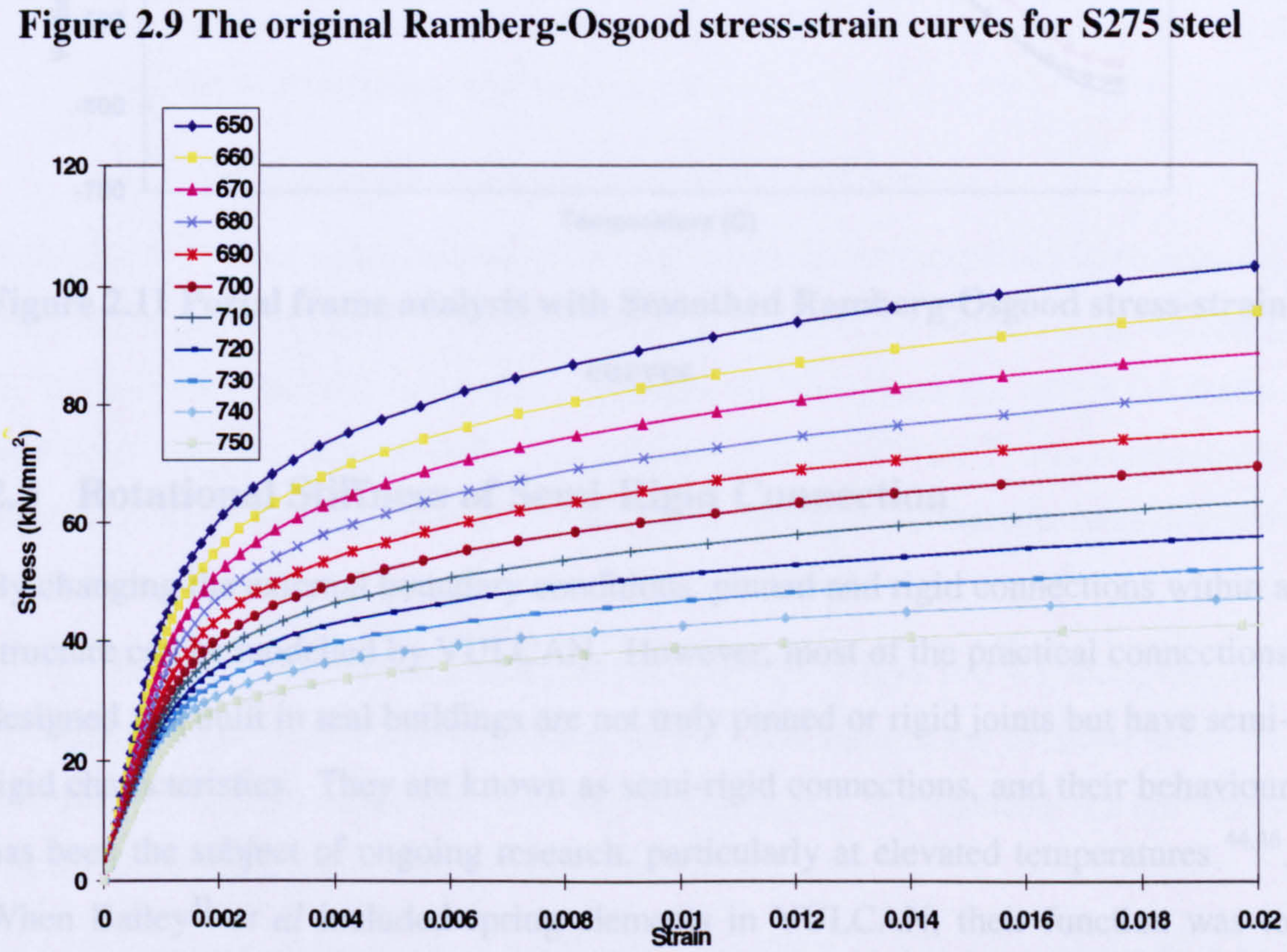

Figure 2.10 The modified (Smoothed) Ramberg-Osgood stress-strain curves for S275 steel

The modified Ramberg-Osgood curves are denoted as Smoothed Ramberg-Osgood curves. The cases shown in Figure 2.7 were re-analysed using the smoothed curves. and the results are plotted in Figure 2.11. It can be seen that the apparent discontinuity at 700°C in Figure 2.7 has almost been eliminated. It is felt that the smoothed model gives a more logical representation of stress-strain behaviour in a temperature range where metallurgical changes are not believed to affect the mechanical behaviour. It will also be beneficial to the convergence of the analysis if sudden changes are avoided.

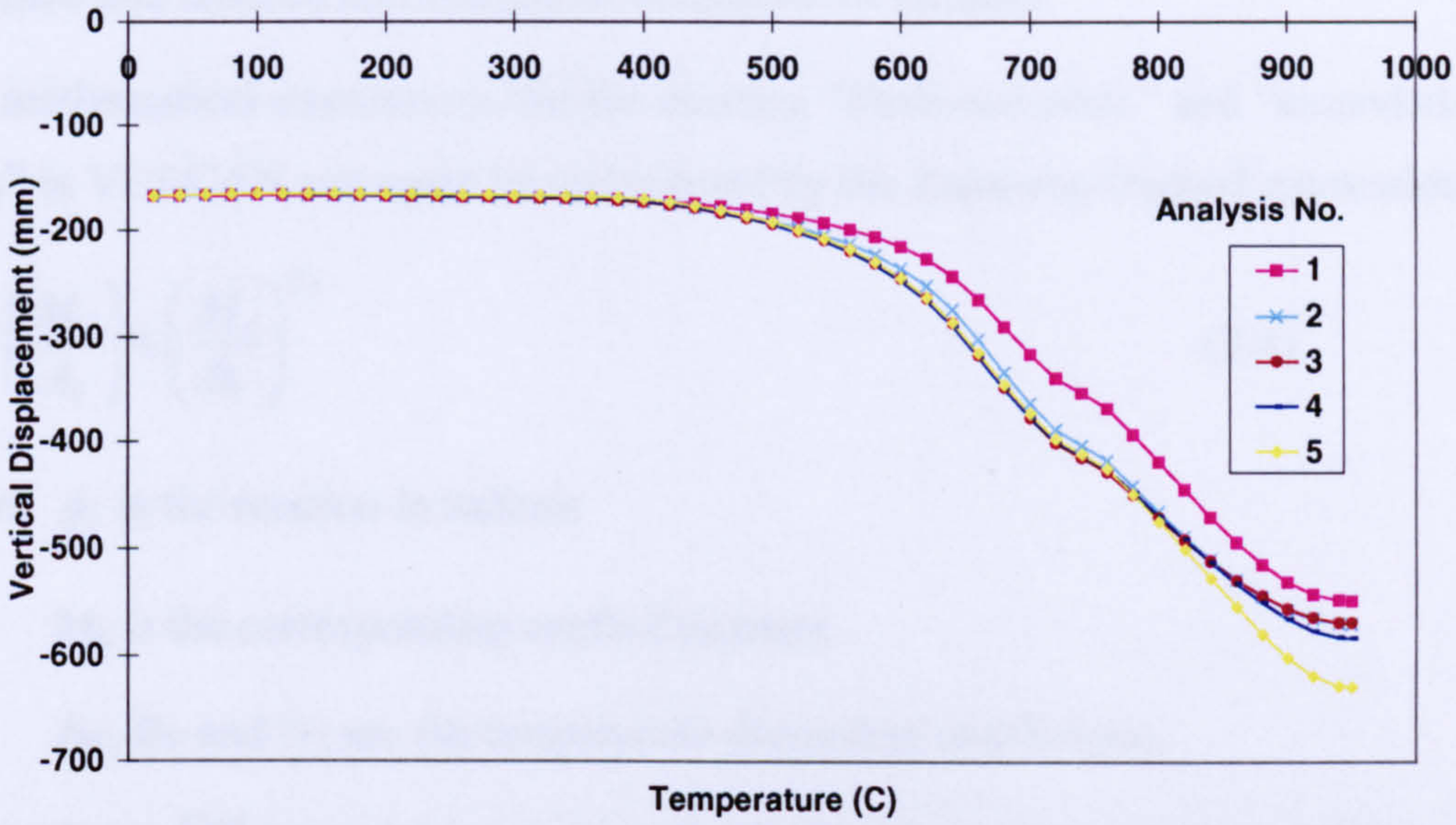

Figure 2.11 Portal frame analysis with Smoothed Ramberg-Osgood stress-strain curves

2.3 Rotational Stiffness of Semi-Rigid Connection

By changing the external boundary conditions, pinned and rigid connections within a structure can be modelled by VULCAN. However, most of the practical connections designed and built in real buildings are not truly pinned or rigid joints but have semi-rigid characteristics. They are known as semi-rigid connections, and their behaviour has been the subject of ongoing research, particularly at elevated temperatures [44,46]. When Bailey[31] *et al* included spring elements in VULCAN, their function was to represent the semi-rigid behaviour of connections. The pre-existing spring element could be modelled by:

- Specifying a rotational stiffness value, which remains constant at elevated temperature; or
- Choosing the existing "flush-end-plate" or "extended end plate" model, for which the degradation of the rotational stiffness at elevated temperature was determined from a series of fire tests[46,47] on a specific size of beam-column connections.

In order to have the flexibility to model various types and sizes of connection especially for the modelling of column bases in this research work, it was necessary to develop a new semi-rigid routine so that an initial rotational stiffness could be specified and reduced accordingly as temperatures increase.

The mathematical expressions for the existing "flush-end-plate" and "extended-end-plate" in VULCAN can again be represented by the Ramberg-Osgood expression as

$$\phi_c = \left(\frac{M_c}{A_T}\right) + \left(\frac{M_c}{B_T}\right)^{N_T} \qquad (2.4)$$

where ϕ_c is the rotation in radians

M_c is the corresponding applied moment

A_T, B_T and N_T are the temperature-dependent coefficients.

Leston-Jones [43,44] has conducted some elevated temperature moment-rotation tests on connections, and adopted the same expression to represent the results by curve-fitting A_T, B_T and N_T. Studies were also performed to investigate the effect on frame behaviour. The same approach has also been adopted by Al-Jabri[46] who conducted a subsequent study of the influence of elevated-temperature connection behaviour on overall frame behaviour.

Among the three temperature-dependent coefficients within the Ramberg-Osgood expression, A_t has the dominant influence on the initial tangent for the curve whereas the maximum plateau value is mainly dependent on B_T. N_T controls the curvature between the initial slope and the plateau.

Once the moment-rotation curve for ambient temperature has been determined by experiment or numerical modelling (e.g. by using the component method proposed in Eurocode 3 Annex J) it can be represented mathematically by the Ramberg-Osgood

expression, choosing suitable coefficients. The initial rotational stiffness ($\frac{\delta\phi_c}{\delta M_c}$) of the connection can represented by the coefficient A_t and yielding of the connection can be represented by B_T.

When the coefficients are obtained, they can then be reduced accordingly to represent the elevated temperature characteristic. The reduction factors for the stress-strain relationship of steel at elevated-temperature given by Eurocode3 Part 1.2 have been chosen to represent the degradation of the semi-rigid connections, as shown in Table 2.2.

Temperature (°C)	Reduction factor for A_T (Taken as $k_{E,\theta}$ from EC3 Part 1.2)	Reduction factor for B_T (Taken as $k_{y,\theta}$ from EC3 Part 1.2)
20	1.0	1.0
100	1.0	1.0
200	1.0	0.9
300	1.0	0.8
400	1.0	0.7
500	0.78	0.6
600	0.47	0.31
700	0.23	0.13
800	0.11	0.09
900	0.06	0.0675
1000	0.04	0.045
1100	0.02	0.0225
1200	0	0

Table 2.2 Reduction factors for the semi-rigid connection

As N_T represents the curving between the initial slope and the plateau, Leston-Jones made it constant in his degradation model and stated that N_T does not degrade with increasing temperatures. Al-Jabri had a similar finding from his experiments. Therefore, N_T was not degraded in the rotational stiffness model at elevated temperature.

A spreadsheet was created to assist in determining the values of A_T, B_T and N_T at ambient temperature from a given moment-rotation curve. These values can then be entered into VULCAN so that the appropriate semi-rigid characteristic at elevated temperature can be modelled. For example, to model a semi-rigid column base the ambient temperature moment-rotation curve can be determined using the component method and represented by the Ramberg-Osgood expression. The coefficients A_T,

B_T and N_T are then used by VULCAN to produce appropriate rotations at particular moment and temperature levels.

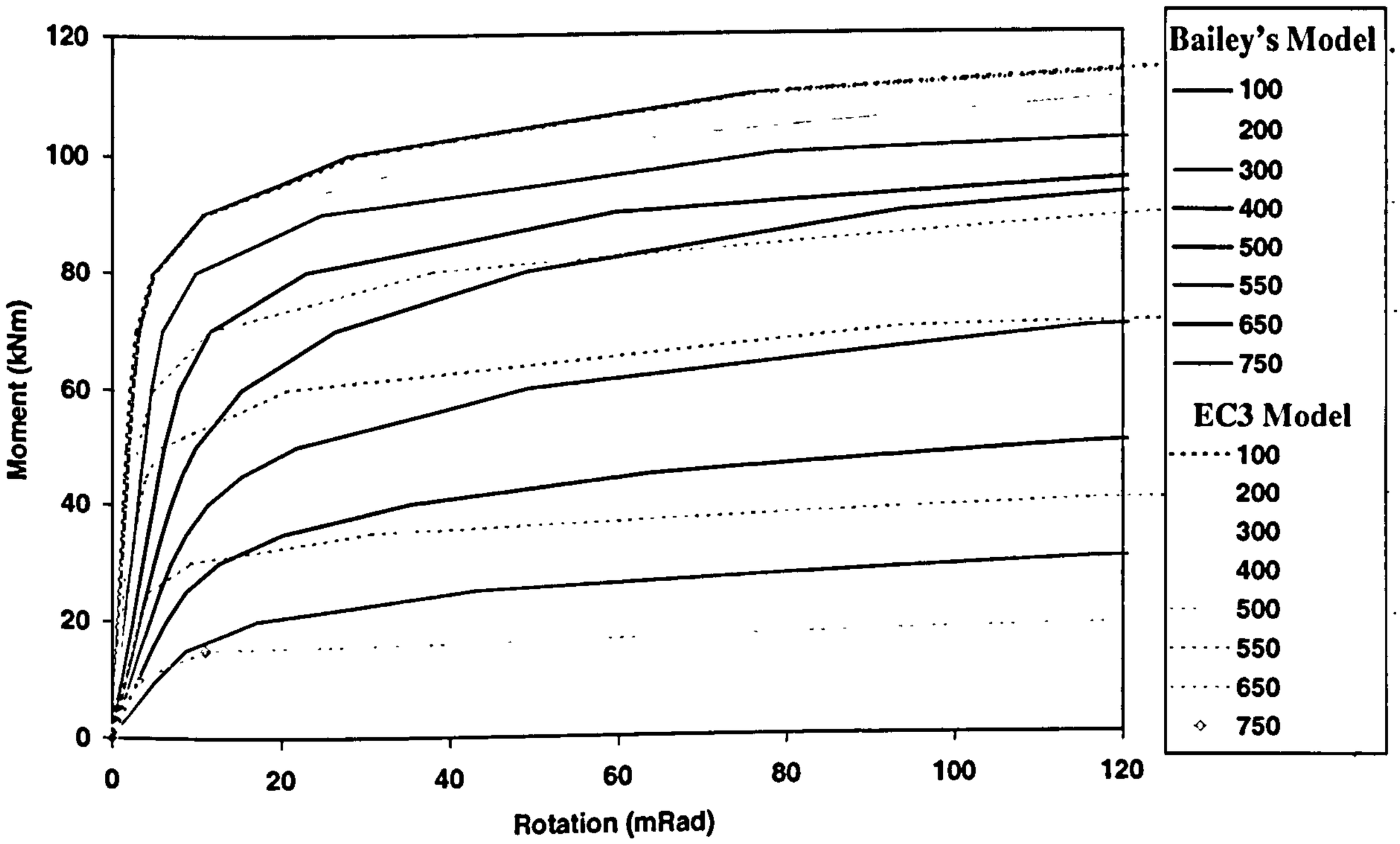

Figure 2.12 Comparison between Bailey's and EC3 degradation model

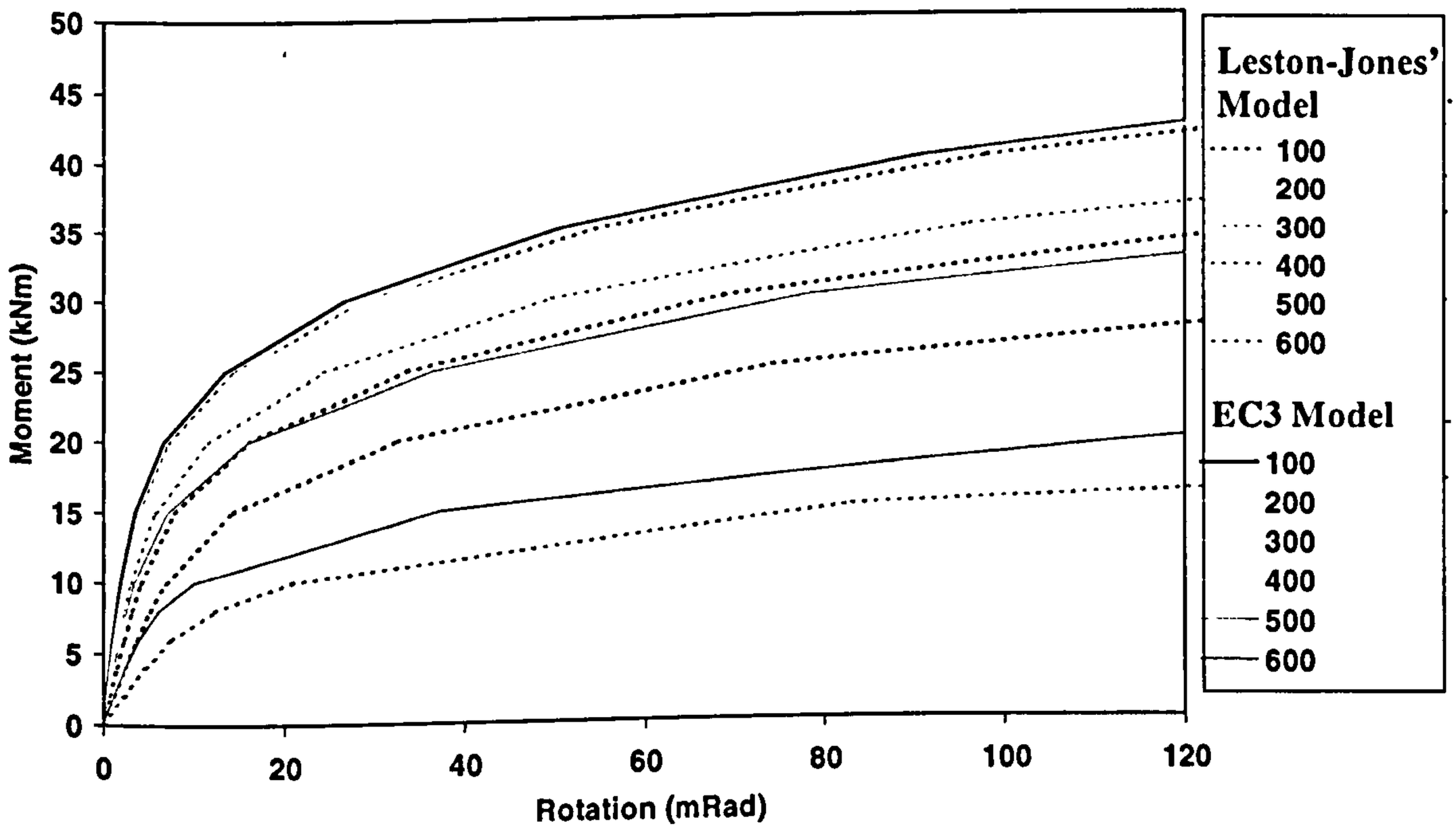

Figure 2.13 Comparison between Leston-Jones' and EC3 degradation model

The degraded moment-rotation curves can be plotted from the spreadsheet and compared against the models proposed by Bailey, which was the pre-existing model in VULCAN, and Leston-Jones is curve-fit from his experimental results. Figures 2.12 and 2.13 show the comparisons.

Although some of the results are not close in the comparions, the new rotational stiffness model is believed to provide a comprehensive numerical method representing the degradation of semi-rigid connections at elevated temperature. The model has now been introduced into VULCAN. However, it is beyond the scope of this research project to further investigate the validity of the model for all ranges of connections, including various sizes and types.

2.4 Solution Procedure for VULCAN

An iteration process is commonly used in non-linear finite element programs to obtain a solution, which is usually the displacements from a given set of applied forces, using the stiffness matrix of the element. There are a number of solution procedures available to be adopted with the finite element method. The Newton-Raphson method is one of the favourite choices, due to its relative simplicity and high accuracy within a common set of problem types.

VULCAN currently adopts the Newton-Raphson[49] method to obtain a displacement solution at given load level, and from that other unknowns are calculated. The whole process is to be repeated at each higher temperature (with reduced stress-strain curves) so that the series of elevated temperature solutions is determined. This type of solution procedure is normally adequate for most practical problems, unless it is necessary to find solutions beyond limit points.

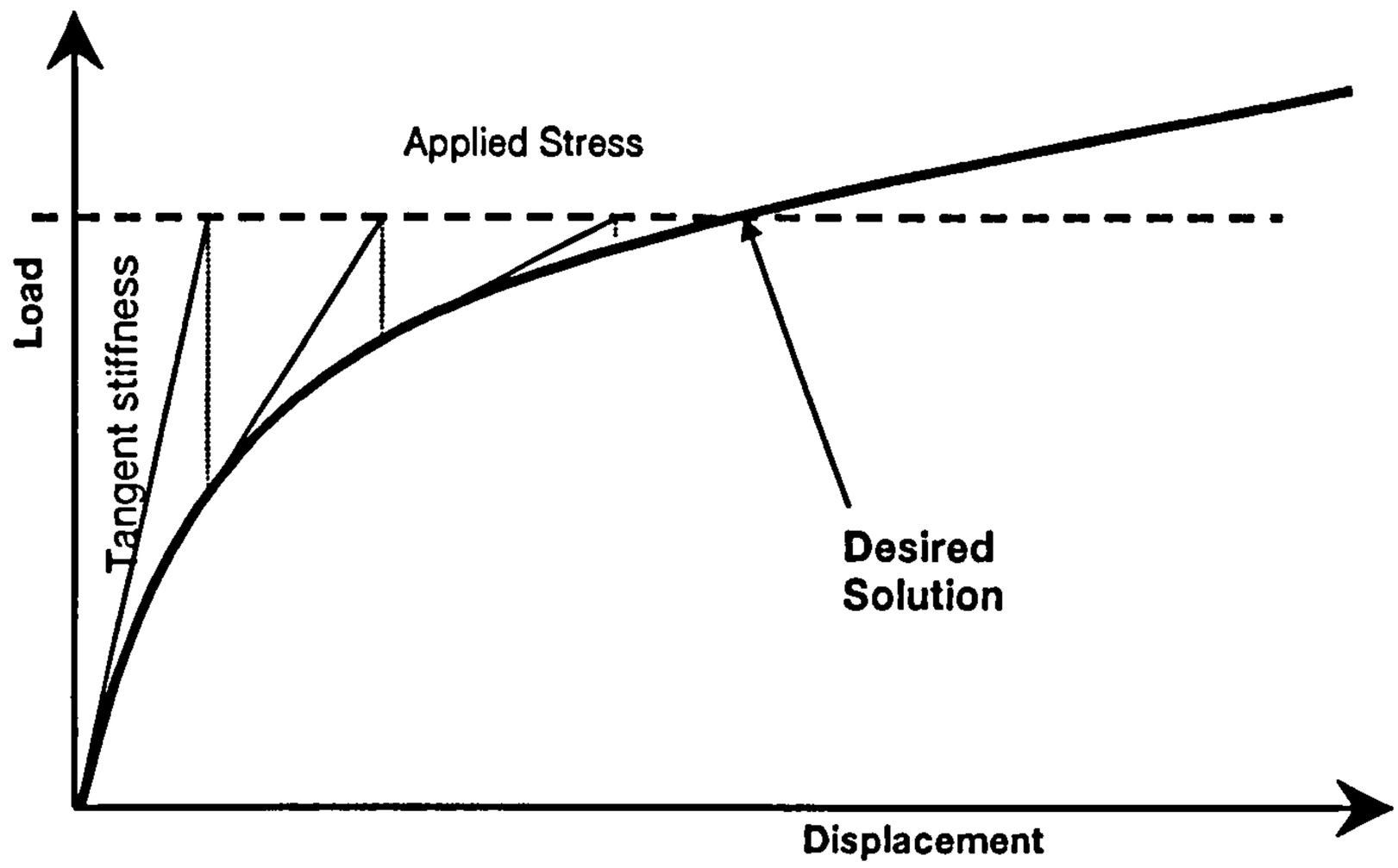

Figure 2.14 Newton-Raphson solution procedure

Figure 2.14 shows a typical solution path in a one-dimensional manner. It can be seen that each iteration step is governed by the load increment, and the changes in displacement become larger when approaching the desired solution, hence becoming less easily convergent. If the tangent stiffness changes from positive to negative, the iteration process will diverge and fail to produce an answer. The solution nearest to zero tangent stiffness (the limit point) will be the final solution and is taken as the failure point for the structural system.

In some circumstances where the overall structural system experiences a snap-through or snap-back behaviour, the response of the structure is prompt and the displacement increases dramatically as the internal forces decrease due to the sudden loss of stiffness. However, the structure manages to regain stability after the snap-through and continues to deflect further in a stable fashion as load increases. The Newton-Raphson method is not usually able to follow such a the displacement path, and often takes the limit point as the "failure" of the structure. Figure 2.15 illustrates the phenomenon.

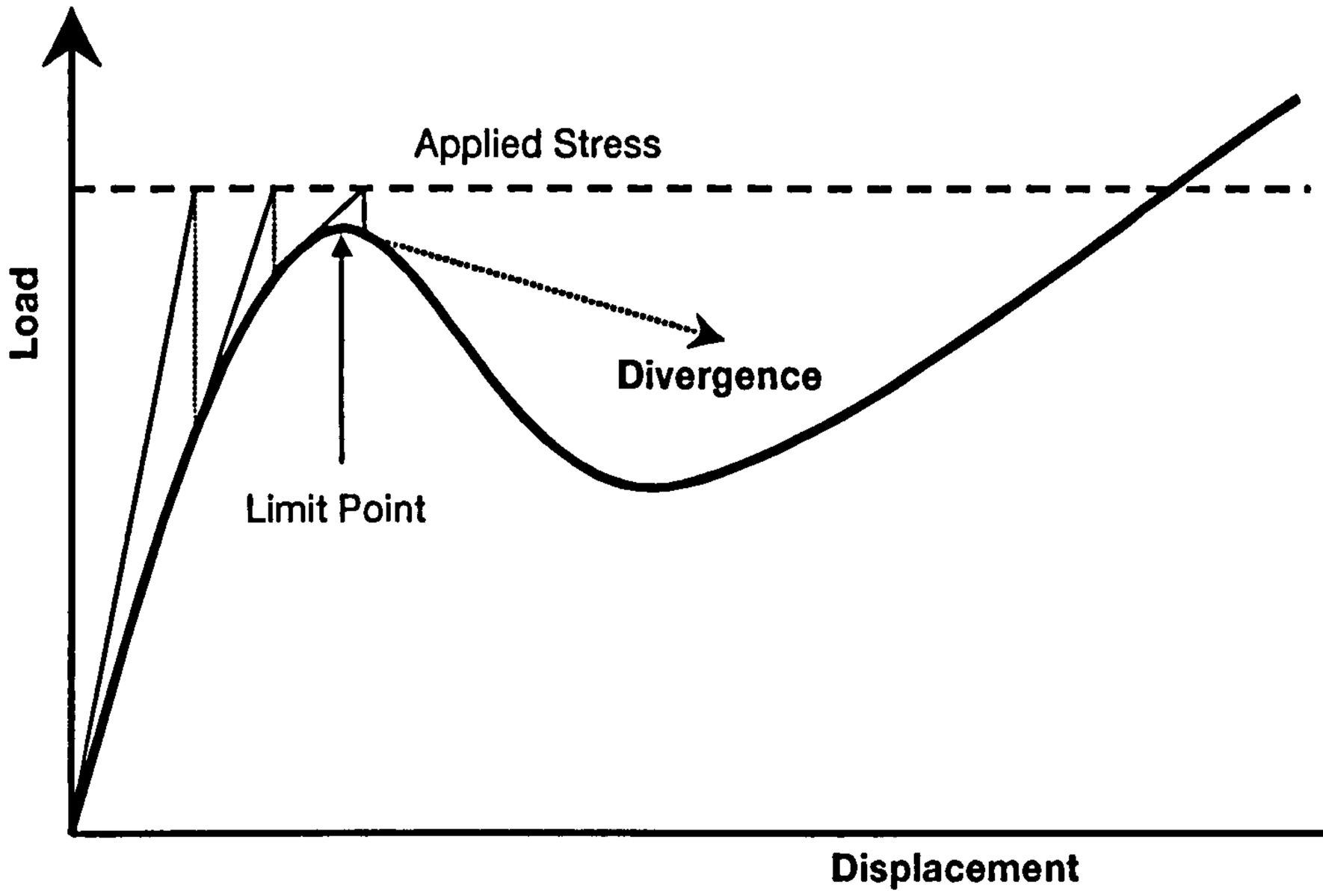

Figure 2.15 Snap-through behaviour

Snap-through behaviour can happen to pitched-roof portal frames. The columns of the portal frame restrain the rafters from deflecting when loaded or heated in fire, thus generating horizontal compression forces up to a point where the rafter angle is sufficiently shallow for the apex to dive vertically in a dramatic fashion. The portal frame can then regain stability for a further load range before collapsing.

Other solution procedures are available to overcome the problem, but usually involve a longer iteration process. Crisfield[50] proposed a modified Rik's approach to overcome limit points and to be able to solve for convoluted load-deflection paths. This is applied in conjunction with the Newton-Raphson method by introducing an extra constraint equation. Other possible solution procedures include the Displacement Control Method[49] , which displacement increment steps are applied rather than load increment steps. Arc-Length method[51] · involves controlling a norm of all degrees of freedom to achieve a more stable solution procedure and to handle snap-through behaviour.

Shepherd[32] *et al* have recently conducted an investigation into various solution procedures and the possibility of implementing extra options to be used in conjunction with the existing Newton-Raphson method for VULCAN. It was found that the Arc-Length method is indeed suitable to be included into VULCAN analysis. Simple structural tests were set up to test these alternative solution procedures.

To date the Arc-Length method has not been fully implemented in VULCAN. Hence post-snap-through behaviour of the pitched-roof portal frame can not be predicted by the finite element program.

2.5 Initial Studies of Portal Frames in Fire

The objective of this section is to test the capability of VULCAN in analysing portal frame structures. The study was conducted prior to an extensive rationalisation of the code, and therefore the strain degrees of freedom were fixed so that reliable analytical results could be obtained for moderate deflections. Several models were set up to examine the response predicted by the program with different cases of frames and heating zones. Only 2-dimensional frames were examined, without haunches at the eaves or apex. In most cases only a small proportion of the frame was heated, rather than assuming that the fire covered the entire width of the frame.

2.5.1 Goal-Post Portal Frame

Figure 2.16 shows the general layout of the model which was set up, and Figure 2.17 shows the elements used to represent it. Several different heating regimes were imposed, and the details of these are provided in Table 2.3.

From the analysis using VULCAN, results in terms of displacements, rotations and strains at each node were obtained. A graph of the mid-span deflections of the roof beam against temperature is shown in Figure 2.18 to allow examination of the trends in behaviour of the heated frame in the different heating regimes. A typical deflected shape, amplified with respect to the original dimensions, is also presented in Figure 2.19.

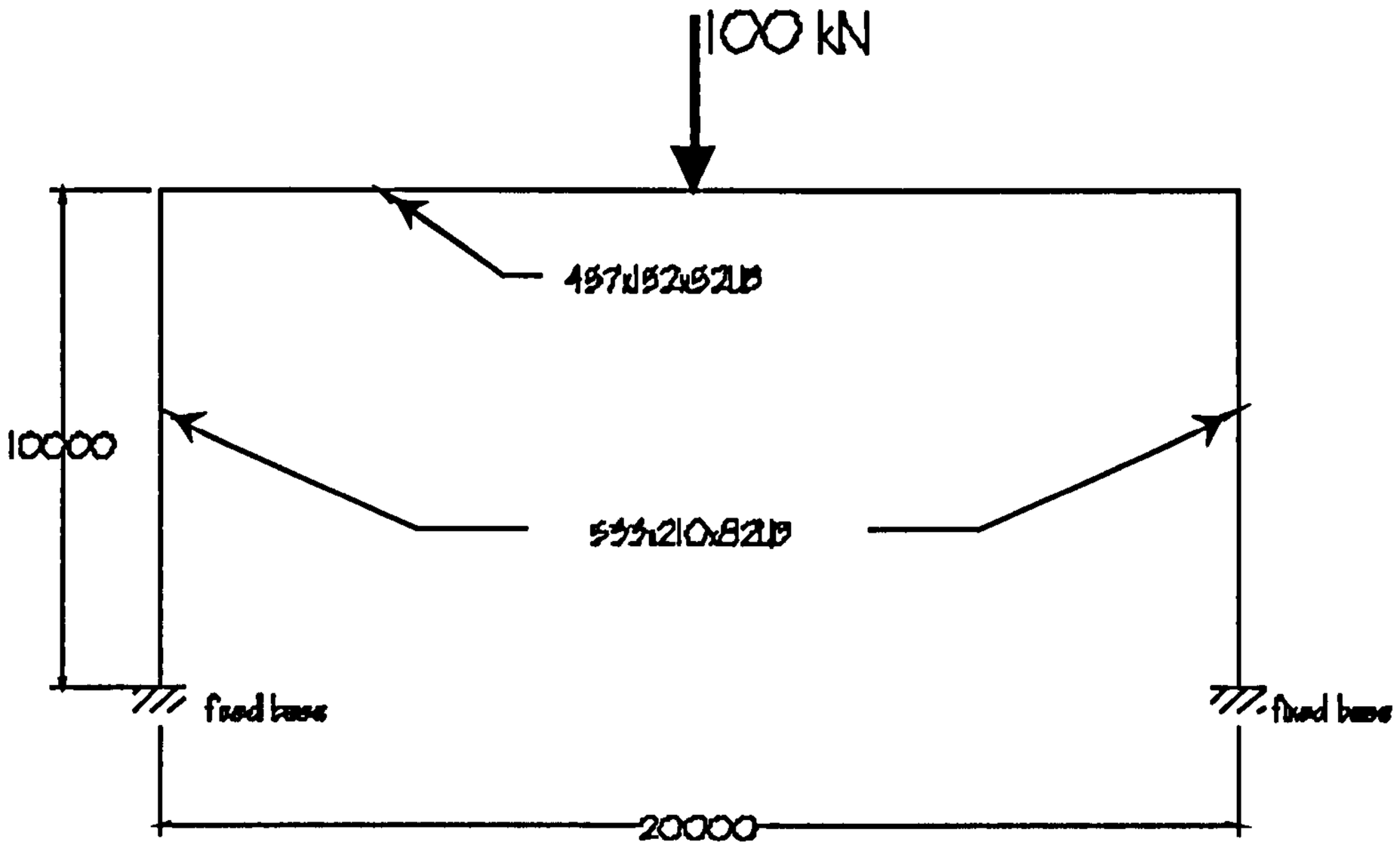

Figure 2.16 General layout of the goal-post portal frame

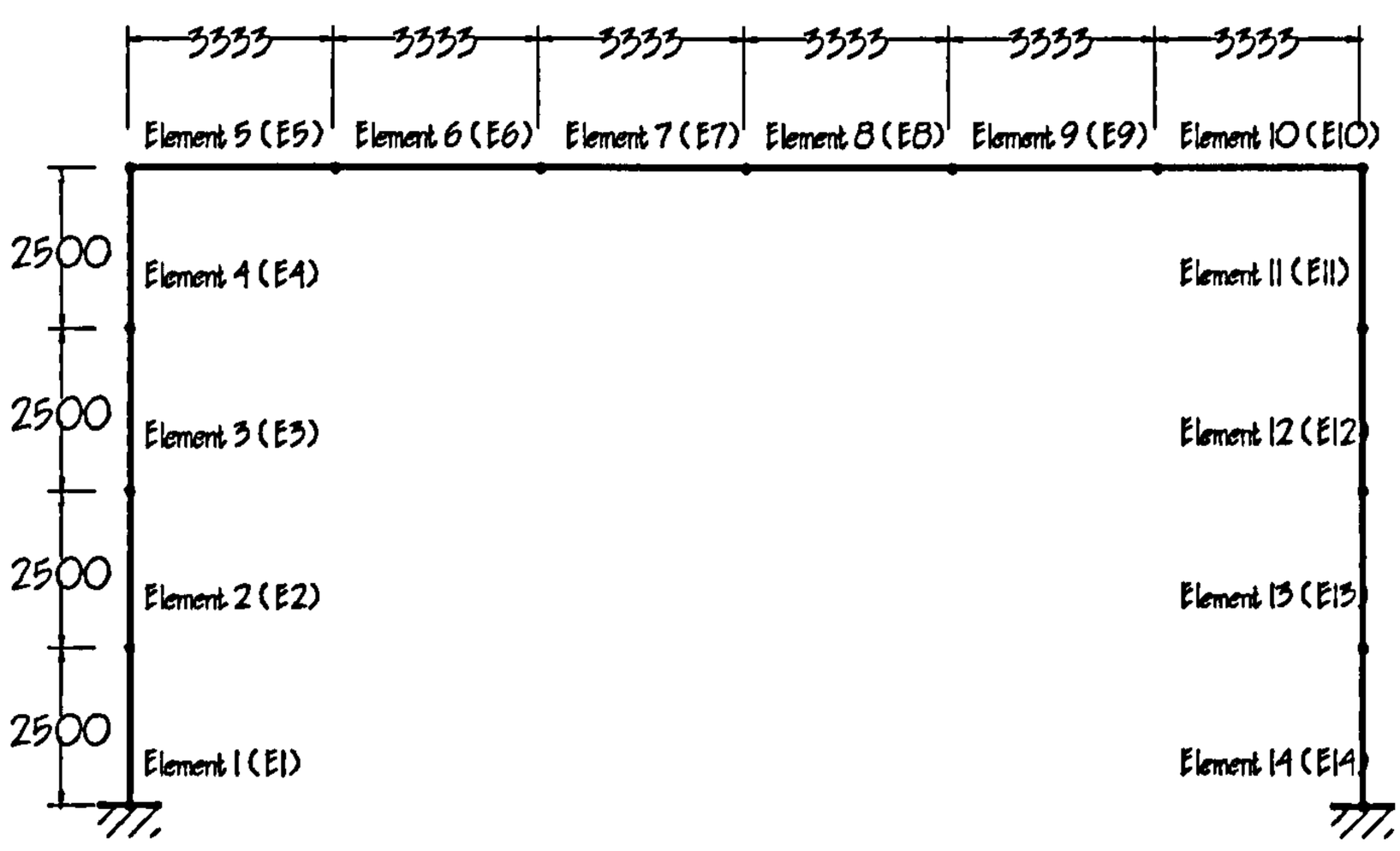

Figure 2.17 Element layout

Profile No.	Heated Element
1	E4, E5
2	E4, E5, E6
3	E3, E4, E5
4	E3, E4, E5, E6
5	E5
6	E5, E6
7	E5, E6, E7, E8, E9, E10
8	Whole frame was heated

Table 2.3 The Heating Regimes

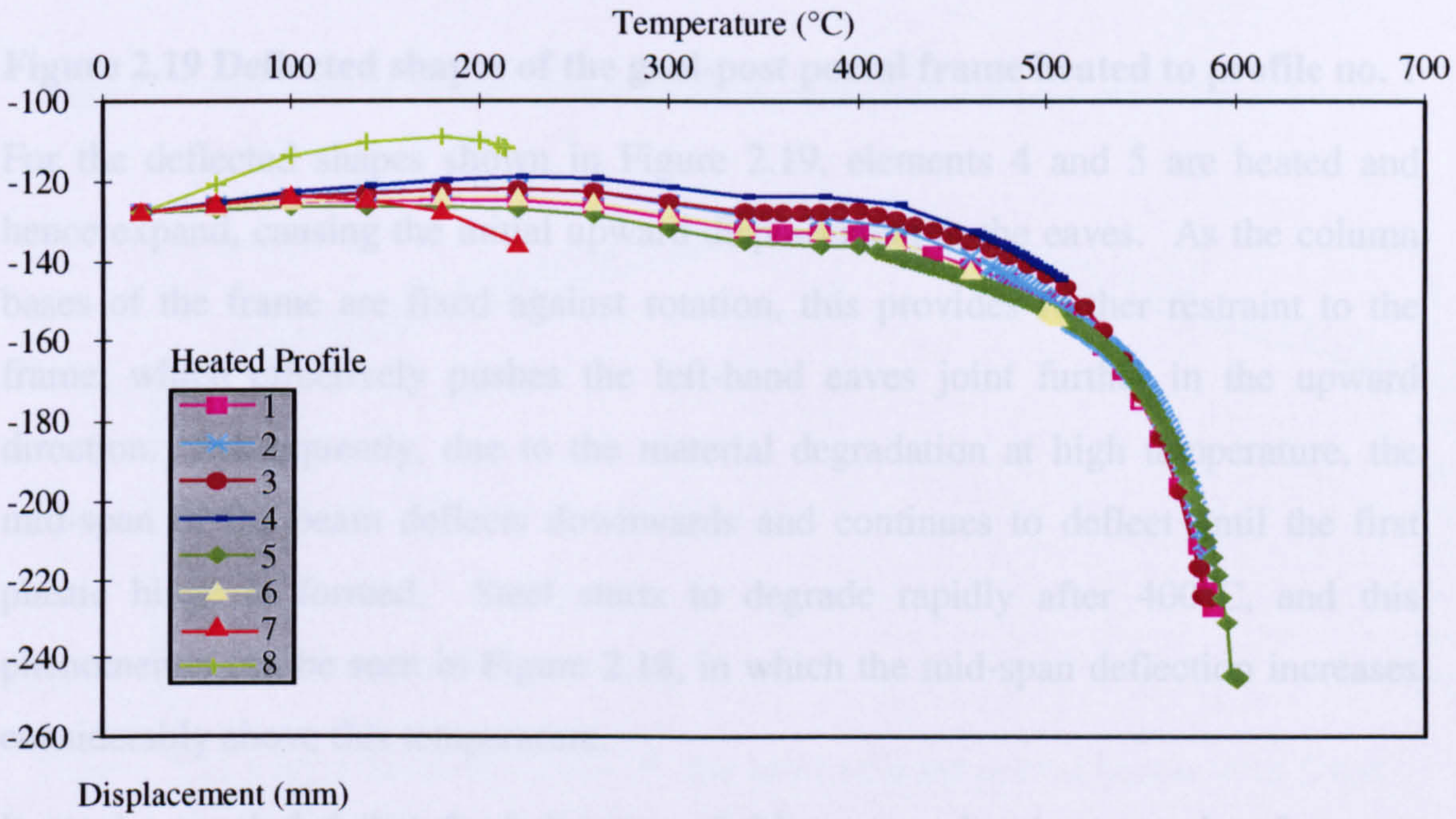

Figure 2.18 Vertical displacement at the beam mid-span for different heating regimes

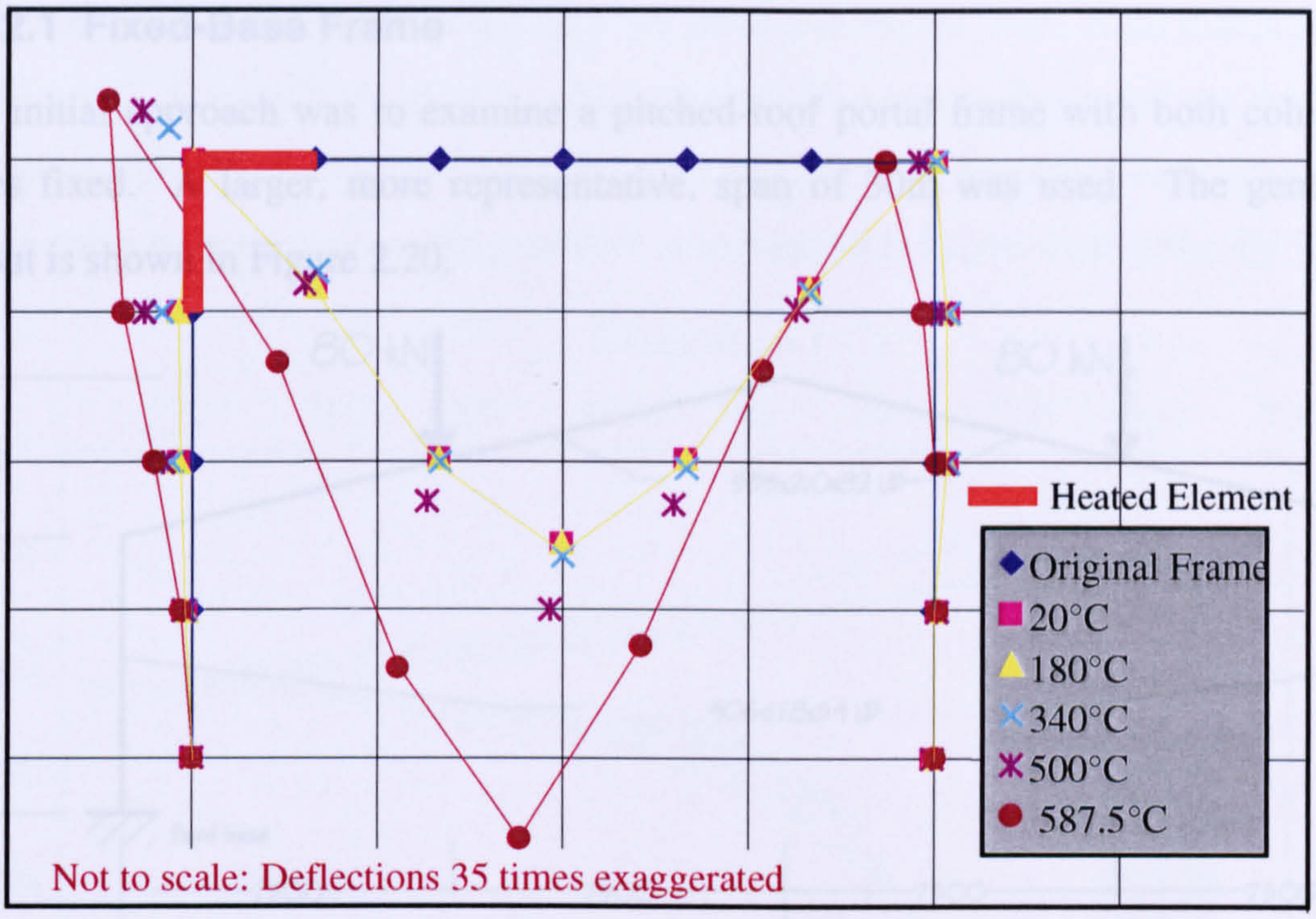

Figure 2.19 Deflected shapes of the goal-post portal frame heated to profile no. 1

For the deflected shapes shown in Figure 2.19, elements 4 and 5 are heated and hence expand, causing the initial upward displacement at the eaves. As the column bases of the frame are fixed against rotation, this provides further restraint to the frame, which effectively pushes the left-hand eaves joint further in the upward direction. Subsequently, due to the material degradation at high temperature, the mid-span of the beam deflects downwards and continues to deflect until the first plastic hinge is formed. Steel starts to degrade rapidly after 400°C, and this phenomenon can be seen in Figure 2.18, in which the mid-span deflection increases considerably above this temperature.

It can be concluded that the behaviour of this rectangular three-member frame as analysed by VULCAN is perfectly logical.

2.5.2 Pitched-Roof Portal Frame

It was decided to conduct a test similar to that on the goal-post frame on a pitched-roof portal frame, to see whether similar behaviour occurred.

2.5.2.1 Fixed-Base Frame

The initial approach was to examine a pitched-roof portal frame with both column bases fixed. A larger, more representative, span of 30m was used. The general layout is shown in Figure 2.20.

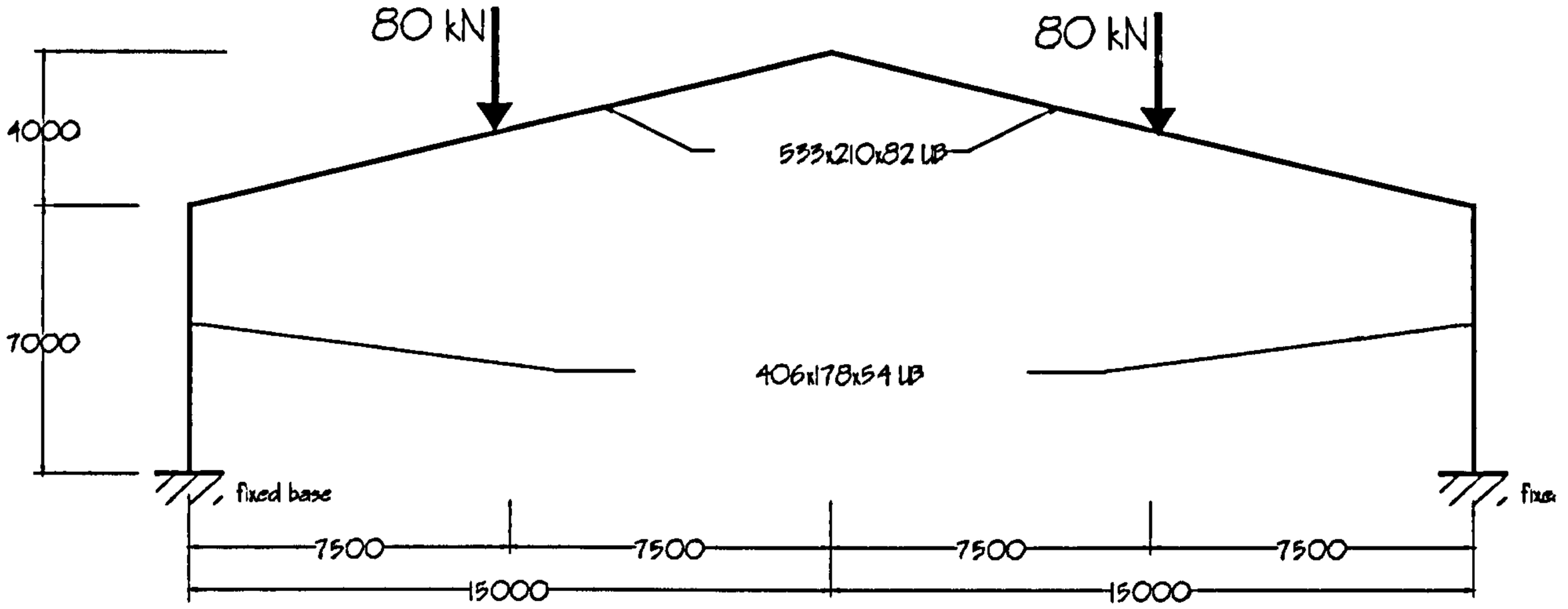

Figure 2.20 General layout of the pitched-roof portal frame with fixed bases

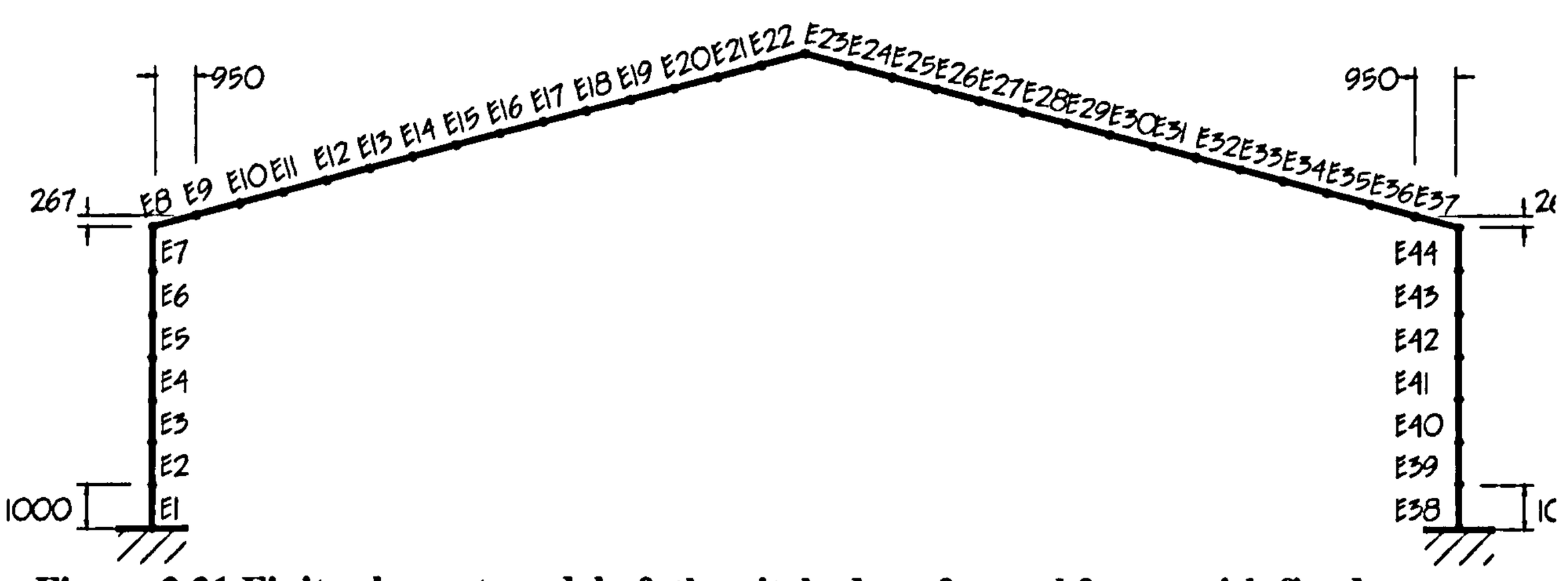

Figure 2.21 Finite element model of the pitched-roof portal frame with fixed bases

Profile No.	Heated Element(s)
1	E7, E8
2	E7, E8, E9
3	E7, E8, E9, E10
4	E7, E8, E9, E10, E11
5	E7, E8, E9, E10, E11, E12
6	E22, E23
7	E21, E22, E23, E24
8	E20, E21, E22, E23, E24, E25

Table 2.4 Heating regimes for the pitched-roof portal frame with fixed bases

The predicted displacements at the apex are plotted in Figure 2.22. Note that heating profiles 1, 2, 3, 4 and 5 are cases in which the top left eaves of the frame was heated, whereas profiles 6, 7 and 8 are cases in which the apex was heated. These are cases where the apex acts as a "smoke reservoir" and hence it is heated symmetrically.

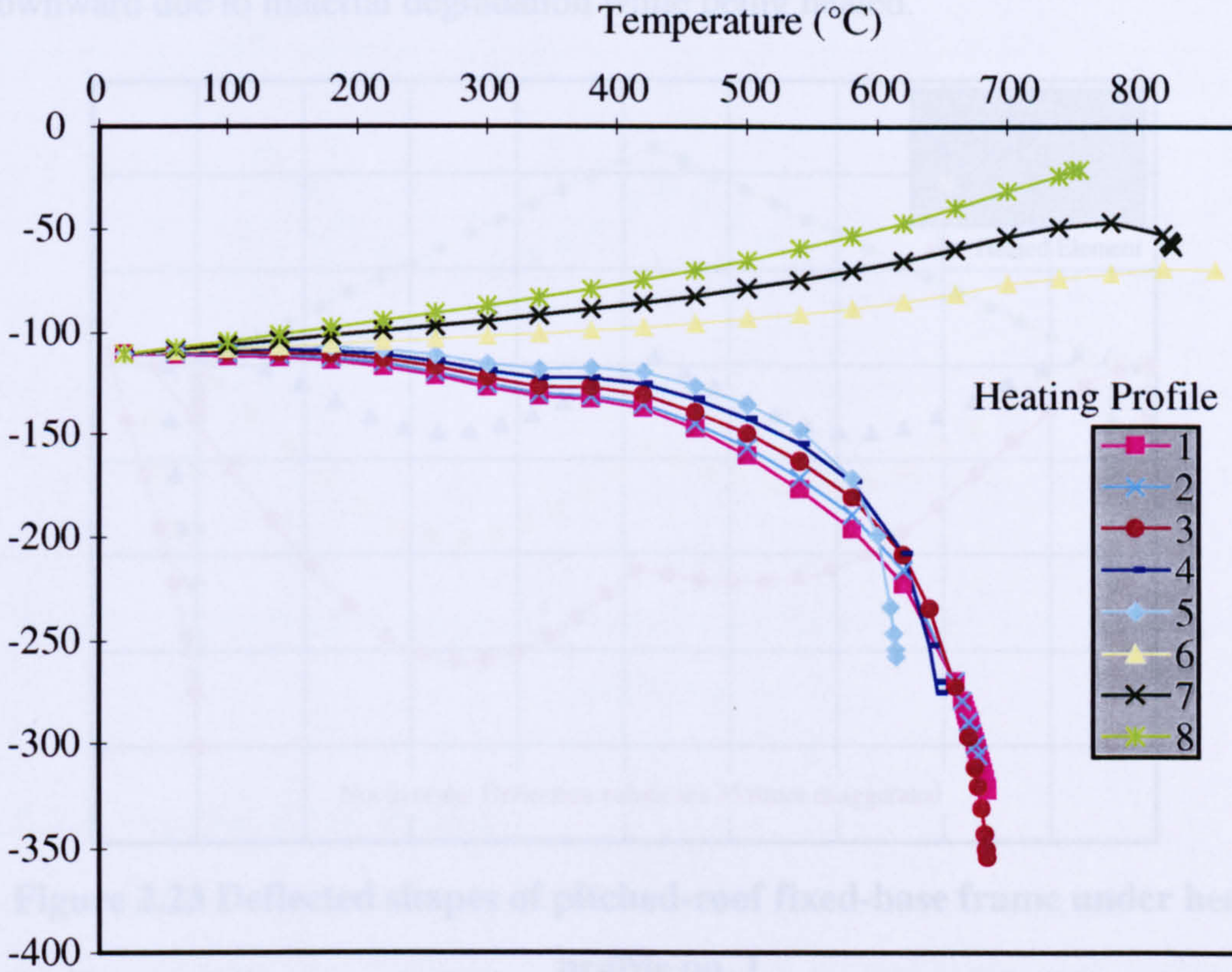

Figure 2.22 Vertical displacement at the apex under different heating profiles.

From Figure 2.22, it can be seen that the corner-heated frames have a trend of deflection which is very similar from one case to another, but is quite different from the cases which are heated in the region of the apex. Several deflected shapes of the frame are shown in Figure 2.23 and Figure 2.24.

For the cases where the eaves region is heated it can be seen that, as the heated zone temperature increases, the rafter near to the heated corner experiences higher deflection, which is to be expected. Similarly to the goal-post portal frame described earlier, the fixity of the bases against rotation provides restraint to the frame against severe sway displacement. Inevitably there is a slight upward displacement of the heated corner due to thermal expansion of the column.

From Figure 2.22 it can be seen that in the centrally heated cases the apex displaces upward gradually as temperature increases. This can be explained by inspection of

the deflected shapes plotted in Figure 2.25. The fixed bases provide stiffness which prevents the column from being pushed outwards, and hence prevents downward deflection at the apex. At the same time, thermal expansion again forces the apex to deflect upward. However, the centres of both of the rafters deflect gradually downward due to material degradation while being heated.

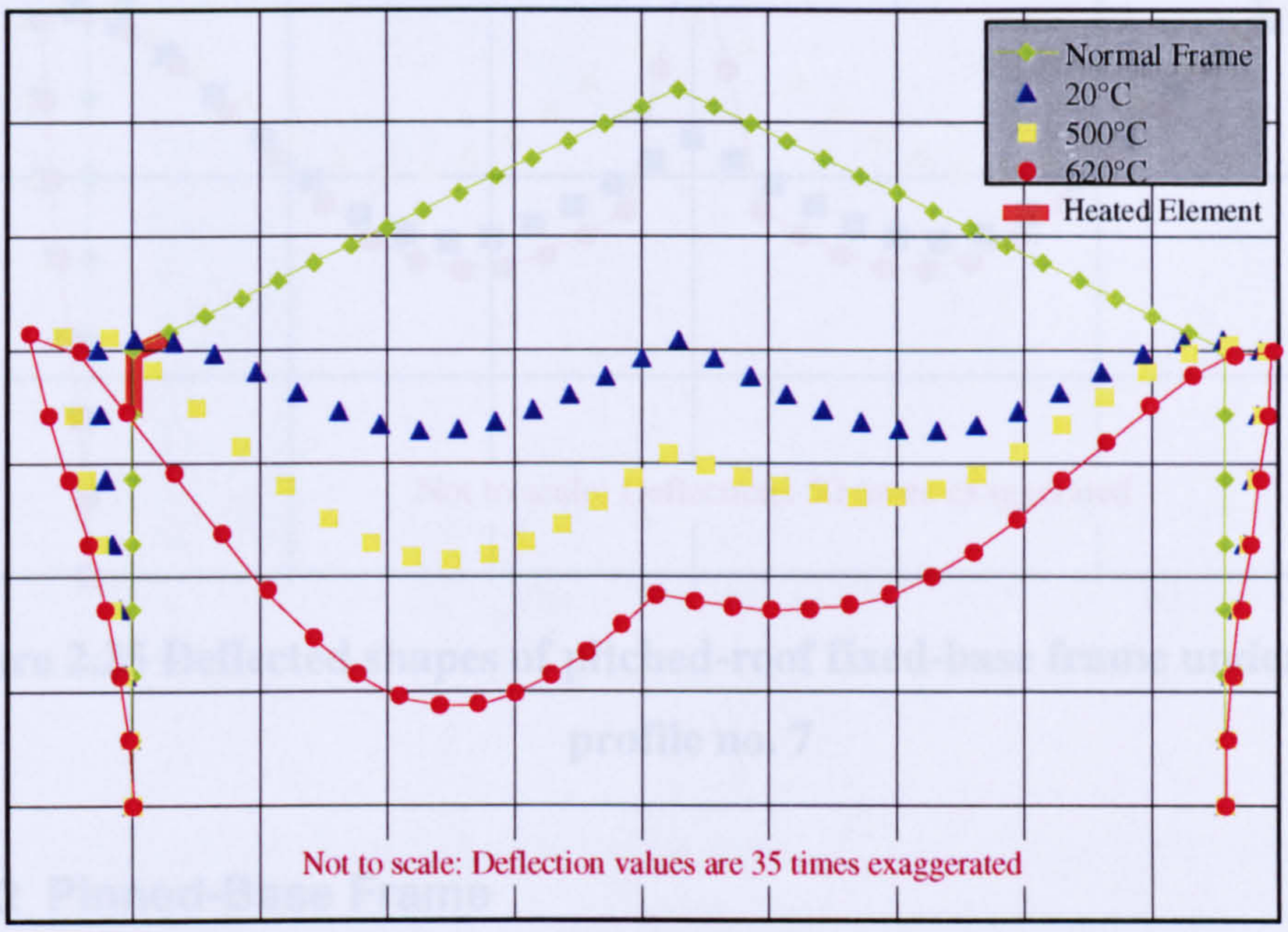

Figure 2.23 Deflected shapes of pitched-roof fixed-base frame under heating profile no. 1

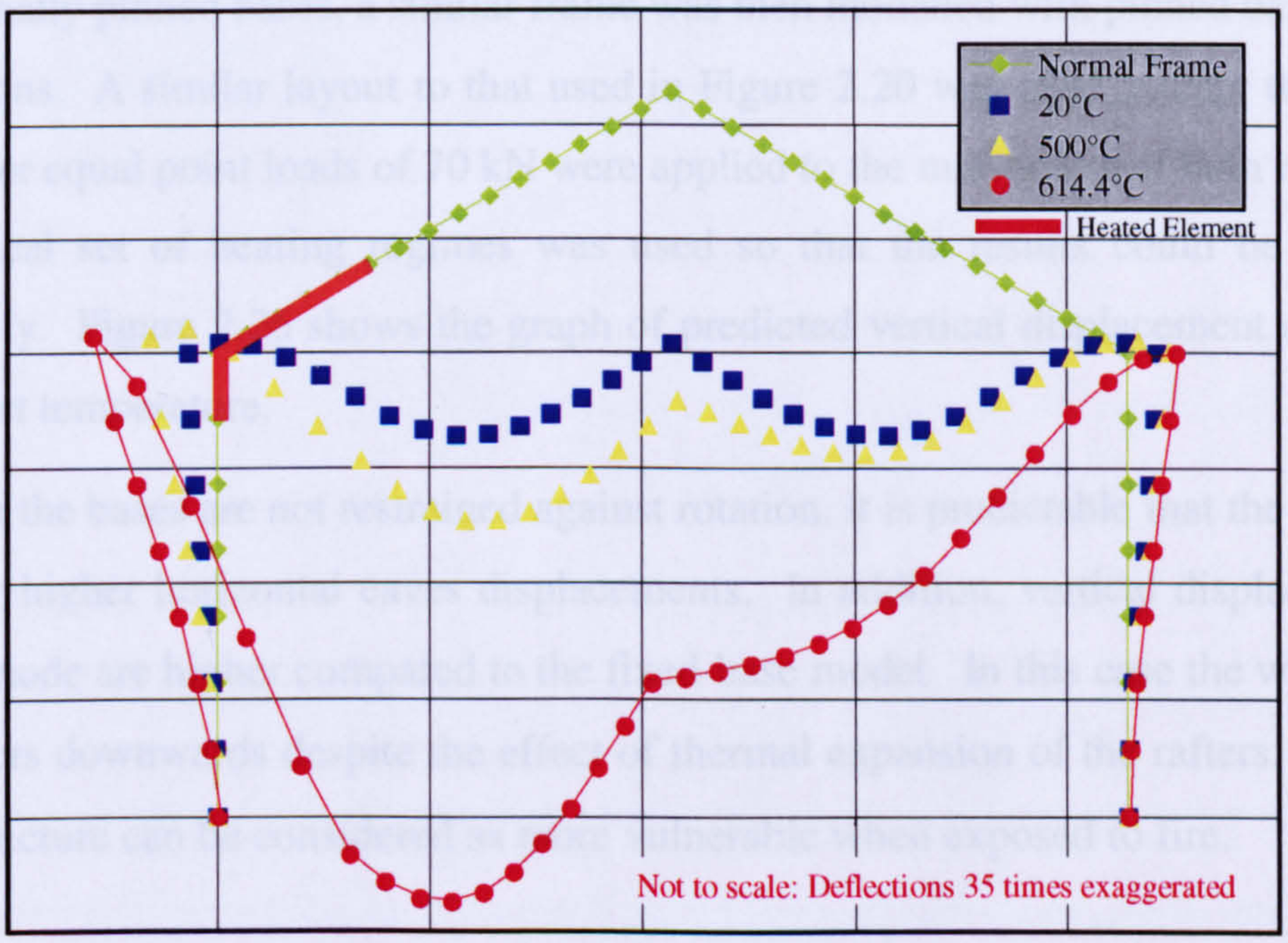

Figure 2.24 Deflected shapes of pitched-roof fixed-base frame under heating profile no. 5

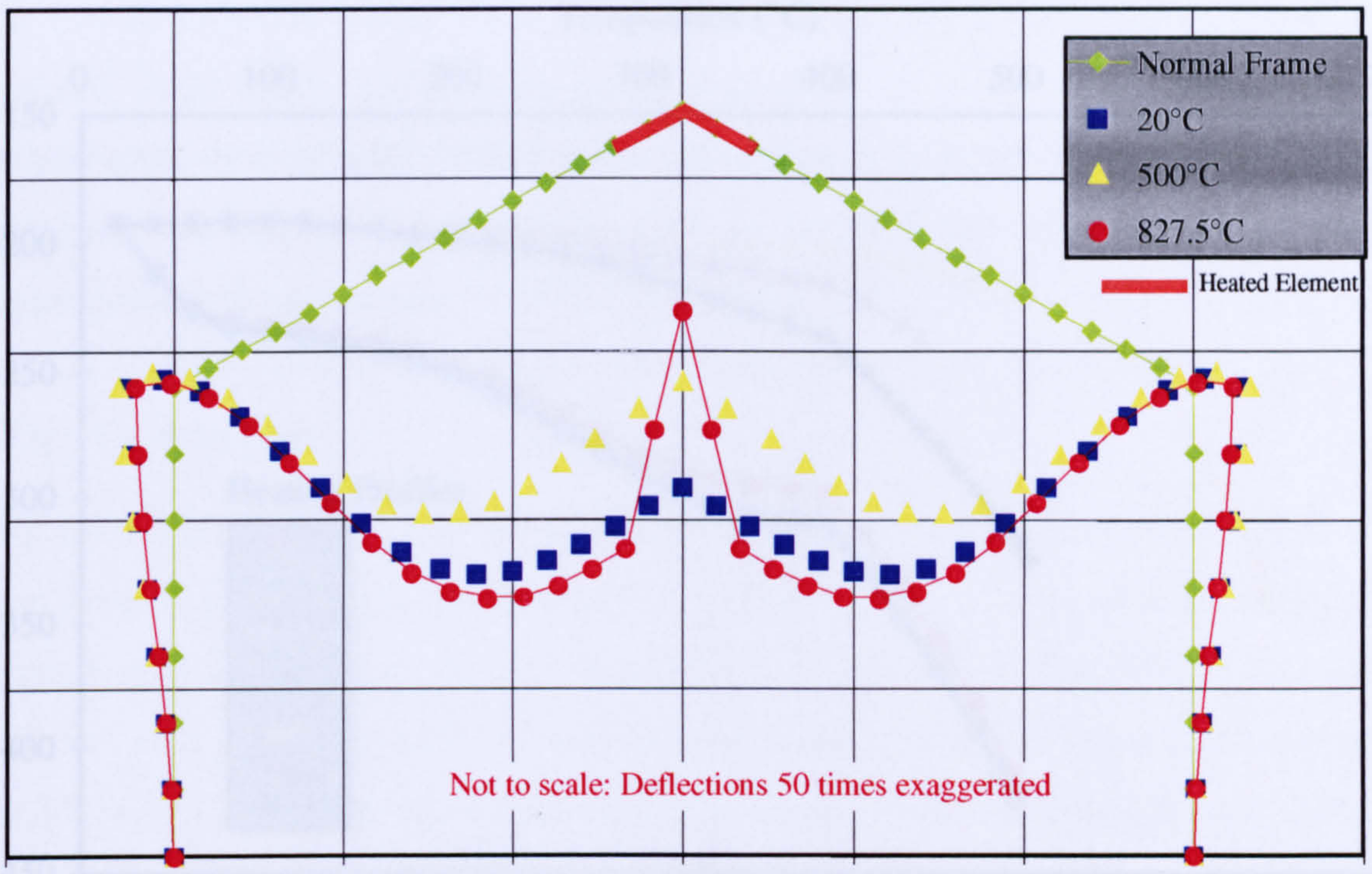

Figure 2.25 Deflected shapes of pitched-roof fixed-base frame under heating profile no. 7

2.5.2.2 Pinned-Base Frame

Having realised that fixed bases have a considerable effect on the frame while it is being heated, and also because in reality most industrial portals are designed with nominally pinned bases, a similar frame was then modelled with pinned bases to both columns. A similar layout to that used in Figure 2.20 was used, except that slightly smaller equal point loads of 70 kN were applied to the mid-points of both rafters. An identical set of heating regimes was used so that the results could be compared directly. Figure 2.26 shows the graph of predicted vertical displacement at the apex against temperature.

When the bases are not restrained against rotation, it is predictable that the frame will suffer higher horizontal eaves displacements. In addition, vertical displacements at each node are higher compared to the fixed-base model. In this case the whole frame deflects downwards despite the effect of thermal expansion of the rafters. This kind of structure can be considered as more vulnerable when exposed to fire.

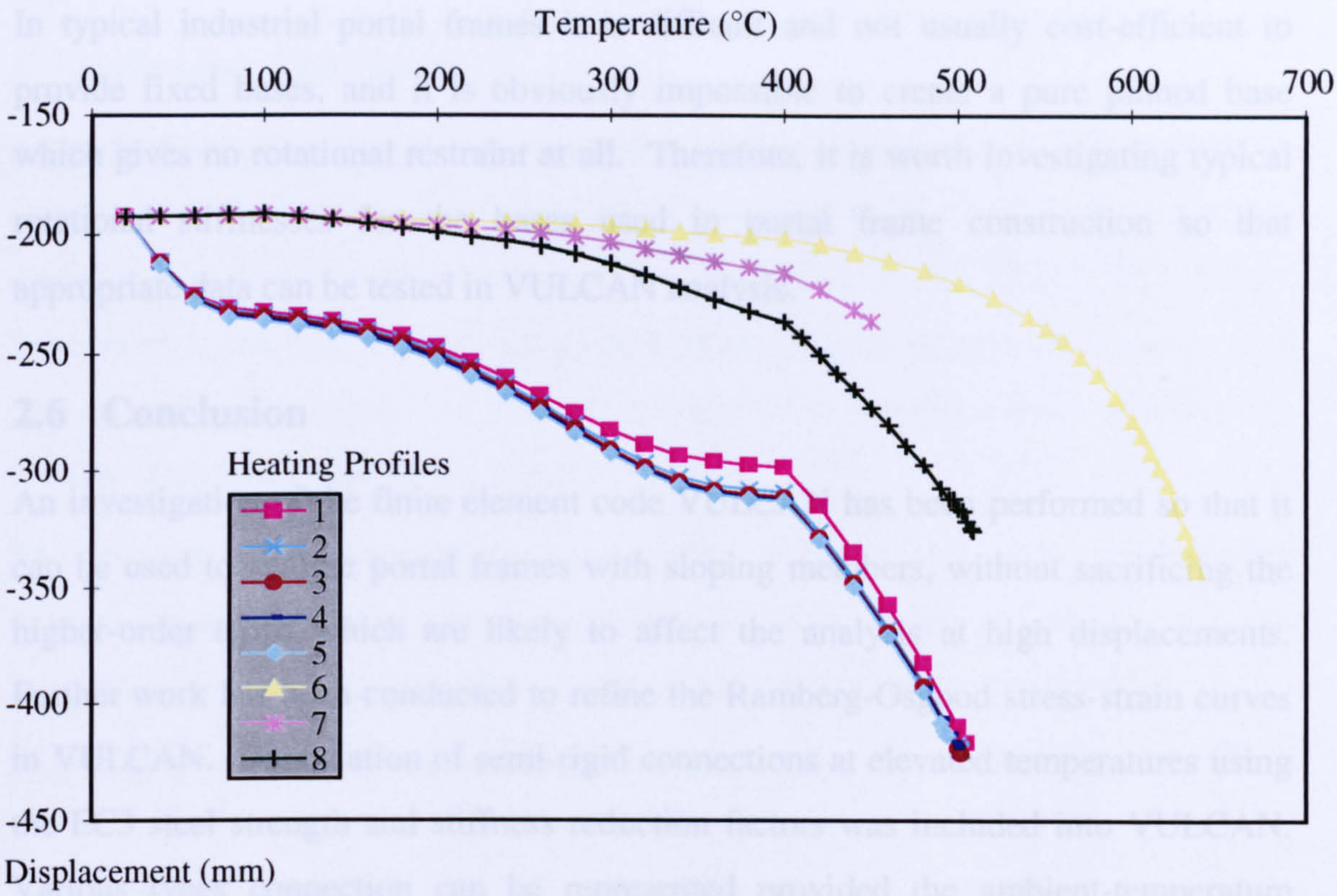

Figure 2.26 Vertical displacement at the apex of pitched-roof portal frame with pinned bases

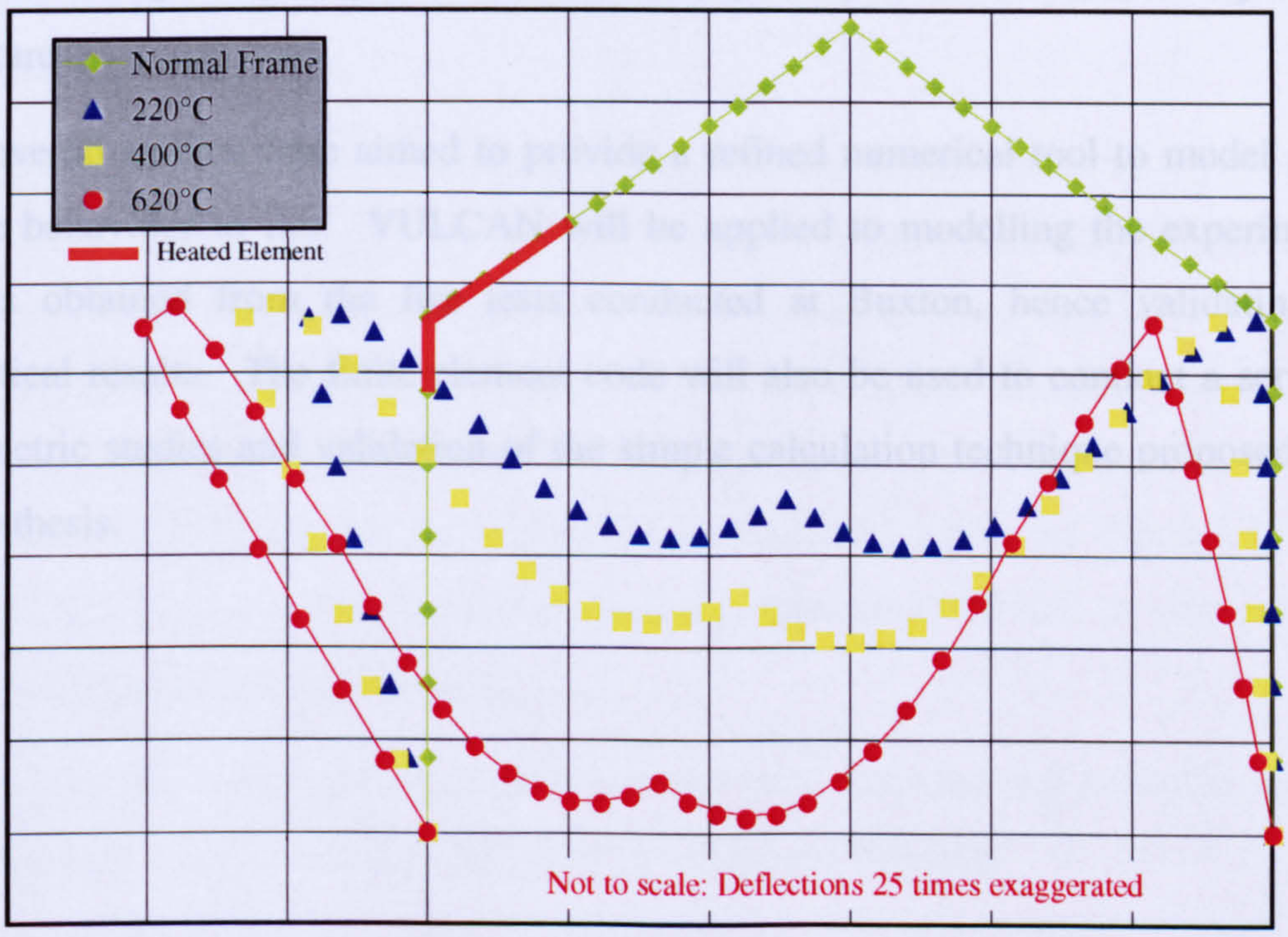

Figure 2.27 Deflected shapes of pitched-roof pinned-base frame under heating profile no. 5

In typical industrial portal frames it is difficult and not usually cost-efficient to provide fixed bases, and it is obviously impossible to create a pure pinned base which gives no rotational restraint at all. Therefore, it is worth investigating typical rotational stiffnesses for the bases used in portal frame construction so that appropriate data can be tested in VULCAN analysis.

2.6 Conclusion

An investigation of the finite element code VULCAN has been performed so that it can be used to analyse portal frames with sloping members, without sacrificing the higher-order terms which are likely to affect the analysis at high displacements. Further work has been conducted to refine the Ramberg-Osgood stress-strain curves in VULCAN. Degradation of semi-rigid connections at elevated temperatures using the EC3 steel strength and stiffness reduction factors was included into VULCAN. Various types connection can be represented provided the ambient-temperature behaviour is available.

Preliminary studies of the behaviour of portal frames were performed using VULCAN. The plots of the portal frame deflections at elevated temperatures were found to be logical, giving confidence in the capability of VULCAN to analyse such structures.

The overall studies were aimed to provide a refined numerical tool to model portal frame behaviour in fire. VULCAN will be applied to modelling the experimental results obtained from the fire tests conducted at Buxton, hence validating the analytical results. The finite element code will also be used to conduct a series of parametric studies and validation of the simple calculation technique proposed later in the thesis.

3 Indicative Fire Tests

As part of the research project sponsored by Health and Safety Laboratories to investigate the behaviour of industrial portal frames, a series of fire tests on a scale-model portal frame were planned to be conducted at the Health and Safety Laboratory at Buxton. The laboratory had relatively little experience in conducting fire tests on real structures and it was proposed first to conduct a series of indicative tests on steel panels prior to the portal frame tests.

The 1/5 scale portal frame structure will be described at a later stage. It is intended to represent the behaviour of real portal frames in fire, mainly by ensuring that the geometry and load level are realistic compared to contemporary construction.

This chapter will describe the indicative panels and their significance in detail.

3.1 Introduction

This section describes the indicative fire tests conducted on the 6th and 11th November 1997. The tests involved a steel panel, supported by Z-purlins and I-beams and heated by a gas flame. The purpose of these tests was to give a general indication of the temperature distributions to be expected in the region of the purlins and cladding panels.

The opportunity was taken to investigate the instrumentation available at Health and Safety Laboratories for this type of experiment. It was necessary to record the atmosphere and steel temperatures throughout the test, which can be recorded by thermocouples conventionally. The use of a thermal imaging camera was introduced, enabling the temperatures of any part visible to the camera to be recorded and distinguished using colour coding. The benefit of using the thermal imaging camera was to reduce the number of thermocouples required and to maximise the information obtained from the tests.

It was essential to ensure that all data required were recorded and available for each fire test, as it is costly and time-consuming to repeat a fire test.

Figure 3.1 shows a picture of the panel before the experiment. The surfaces of the steel panels, beams and purlins were all painted black so that the surface emissivity

was close to unity, thus allowing the use of the thermal imaging camera to show the surface temperatures during the test.

Figure 3.1 The indicative test panel

Three tests were performed, using different fire intensities and durations.

3.2 Design of the Indicative Panel

Given the purpose of conducting the indicative tests, the structural performance of the panels was not the critical factor and therefore the panels were supported in the most convenient way possible.

Figure 3.2, 3.3 and 3.4 show the design of the panel for the indicative tests. Since the members do not support any loading other than self-weight, the smallest size of UB section was used. The panel was suspended from chains at the four corners to the roof of the shed in which the experiment took place.

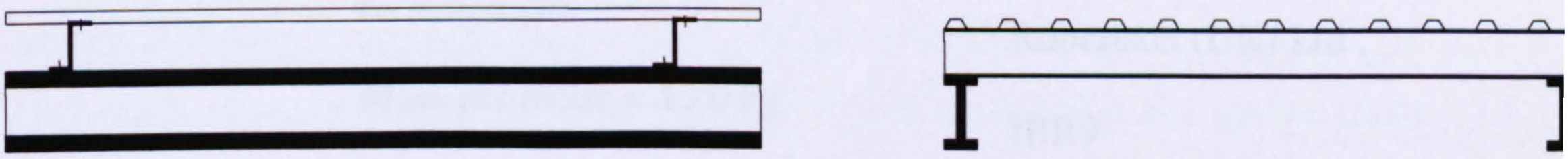

Figure 3.2 Front view (left) and Elevation (right) of the panel

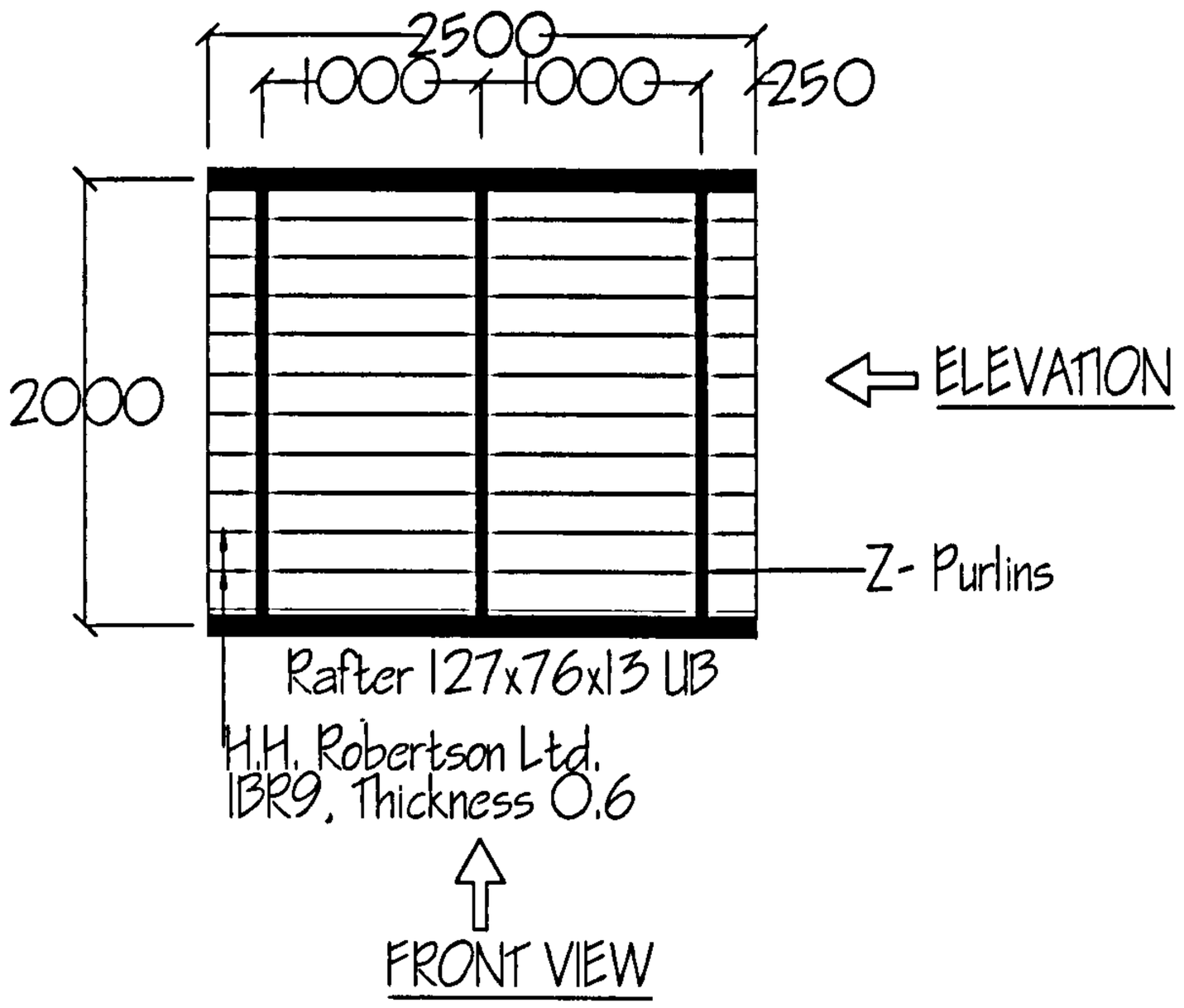

Figure 3.3 Plan View of the indicative

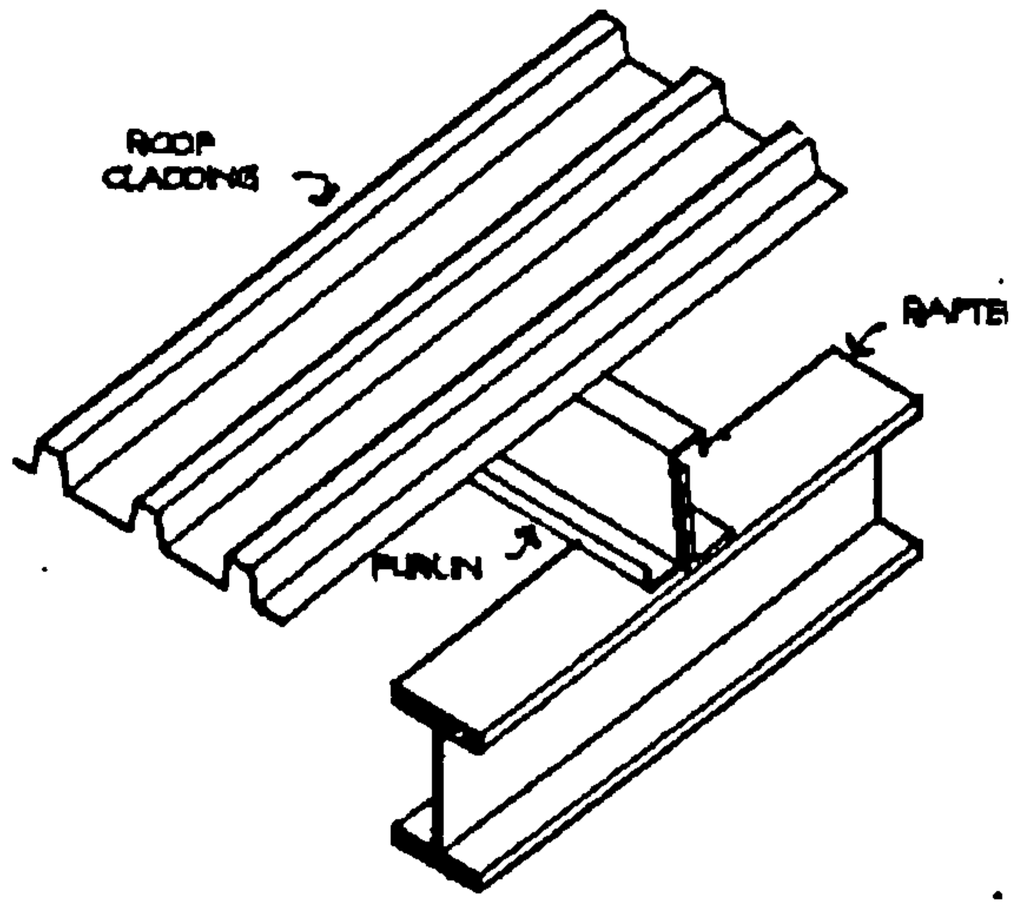

Figure 3.4 Isometric sketch of the connection details

Structural details: Rafter size: 127x76x13 UB

$A = 16.5\ cm^2$

$I_{xx} = 473\ cm^4$

Mass per metre = 13.0 kg

Hp/A = 325 (4 sided profile)

Purlin size: 142x58x1.8 Z pulins

$A = 8.53\ cm^2$

$I_{xx} = 74.1\ cm^4$

Mass per metre = 6.7 kg

Roof Cladding: H.H. Robertson (UK) Ltd., IBR9

Thickness = 0.6 mm

3.3 The First Indicative Test

The first test was carried out on 6th November 1997. Six thermocouples were used in this test; Figure 3.5 shows the positions relative to the fire. None of the thermocouples were welded onto the steel, which means that they were only measuring the air temperatures around the steel. The steel surfaces were viewed using the thermal imaging camera, so that temperature distributions could be obtained.

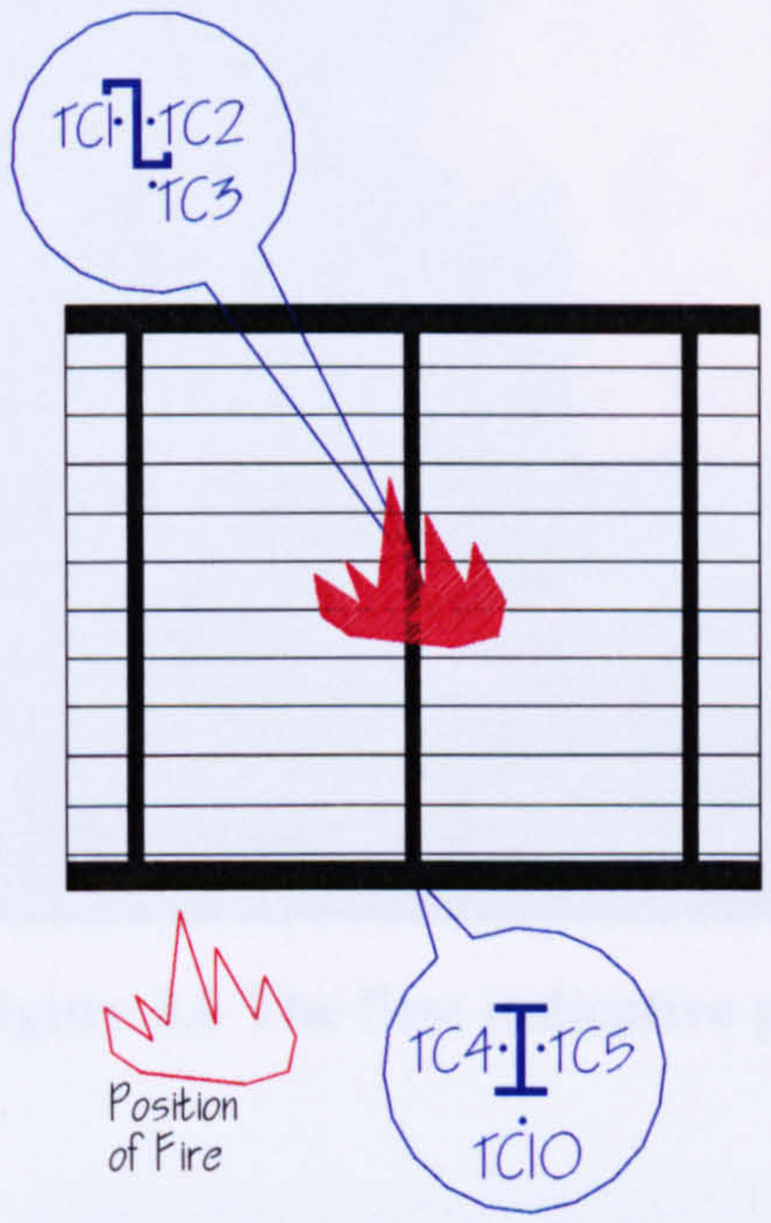

Figure 3.5 Positions of thermocouples

The gas flame burned for about 3 minutes with a gas flow of 100 litres/min. Thermocouples 1,2 and 3 measured the temperatures around the Z-purlins; 4, 5 and 10 measured temperatures around the I-beam.

Figure 3.6 shows a picture taken during the test. Figure 3.7 plots the recorded temperatures of each thermocouple against time. A computer program, TASEF[52], written in Fortran77 code was then used to predict the temperature distribution of the steel purlins from the gas temperatures, and the results were compared against those indicated by the thermal camera images. Figure 3.8 illustrates the results from the program. Figure 3.9 is a thermal image of the whole panel towards the end of the test. Figure 3.10 shows the condition of the panel and the purlin after the test.

Figure 3.6 The first indicative panel test

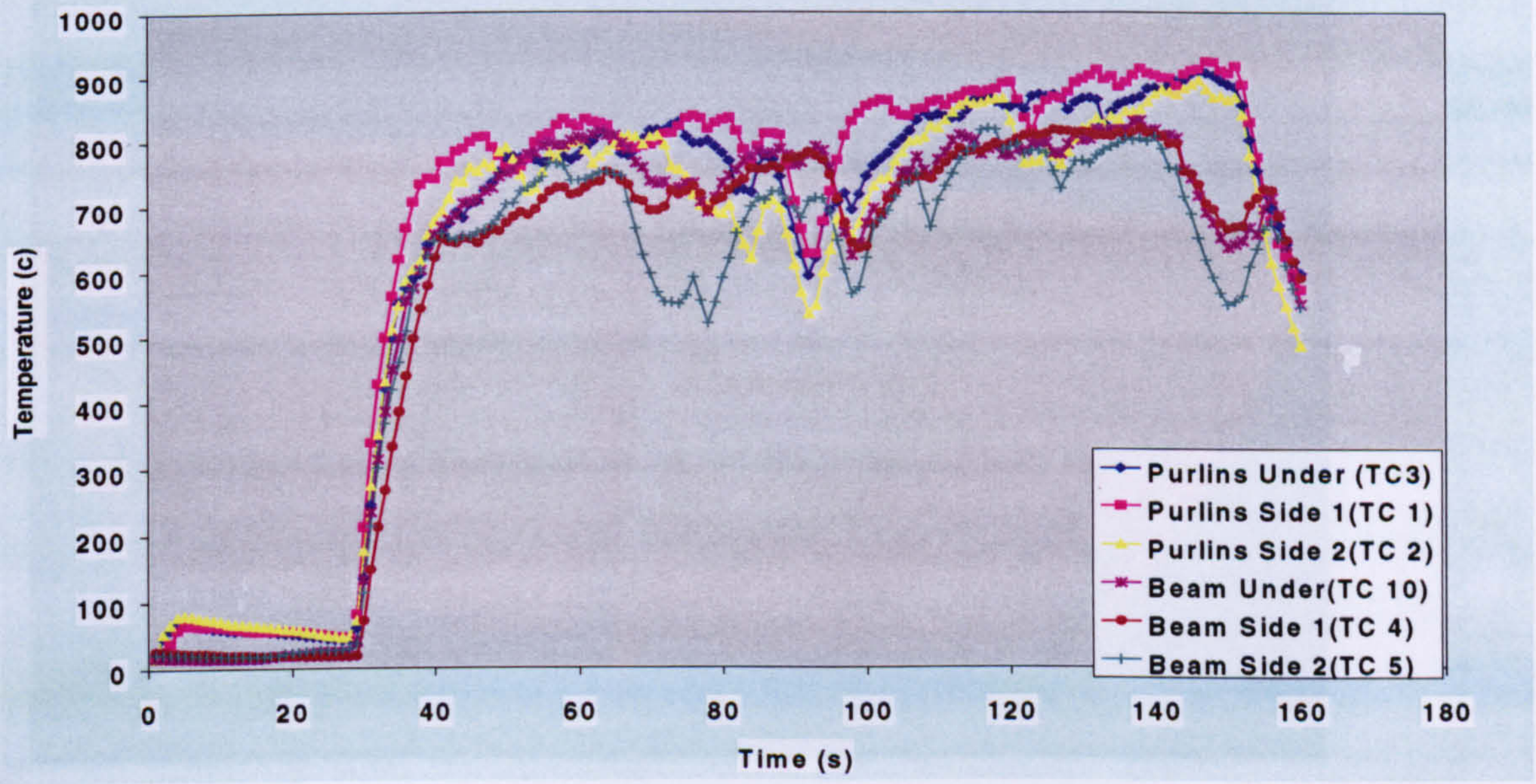

Figure 3.7 Temperatures recorded from the first indicative panel test

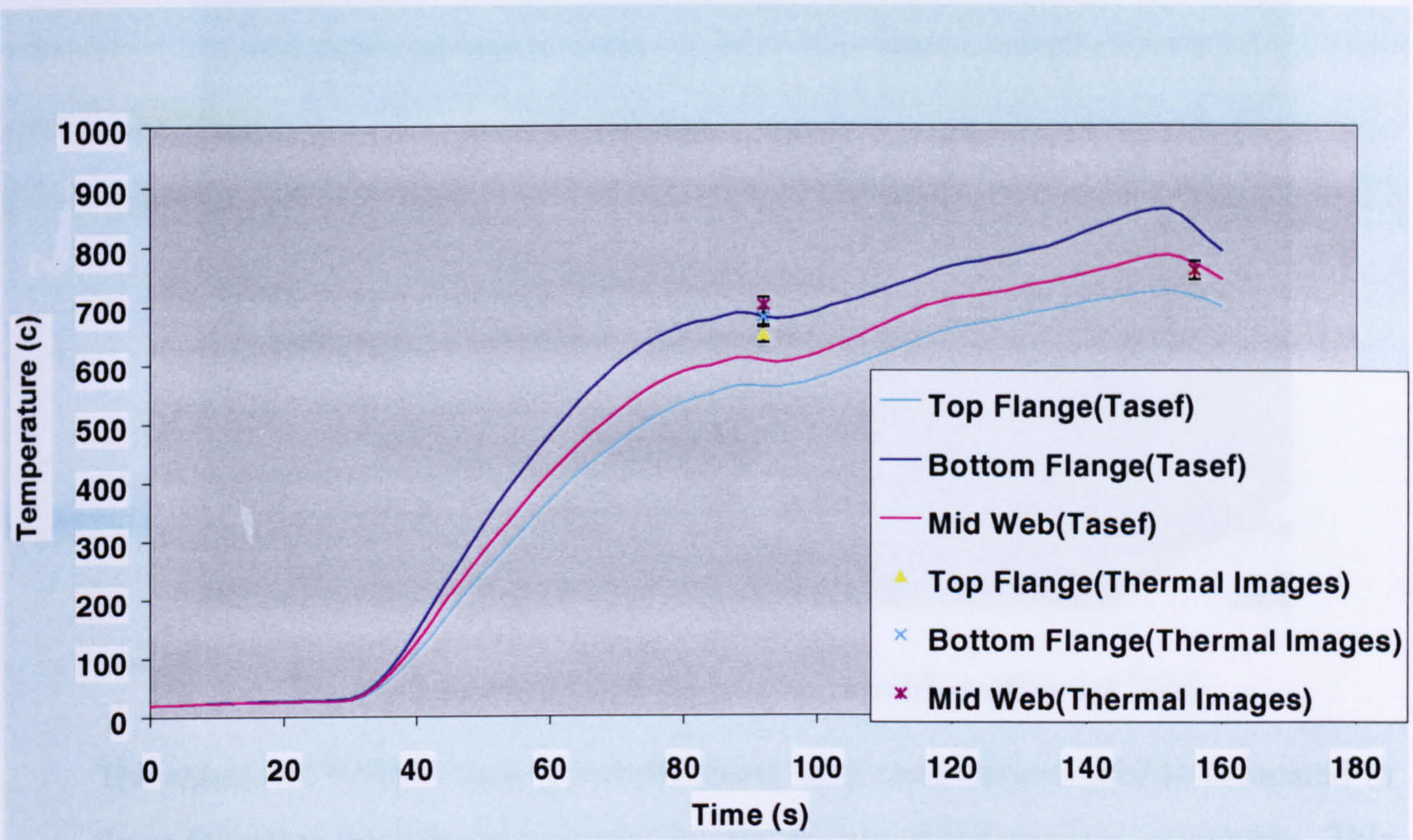

Figure 3.8 Comparison between results from TASEF and thermal images

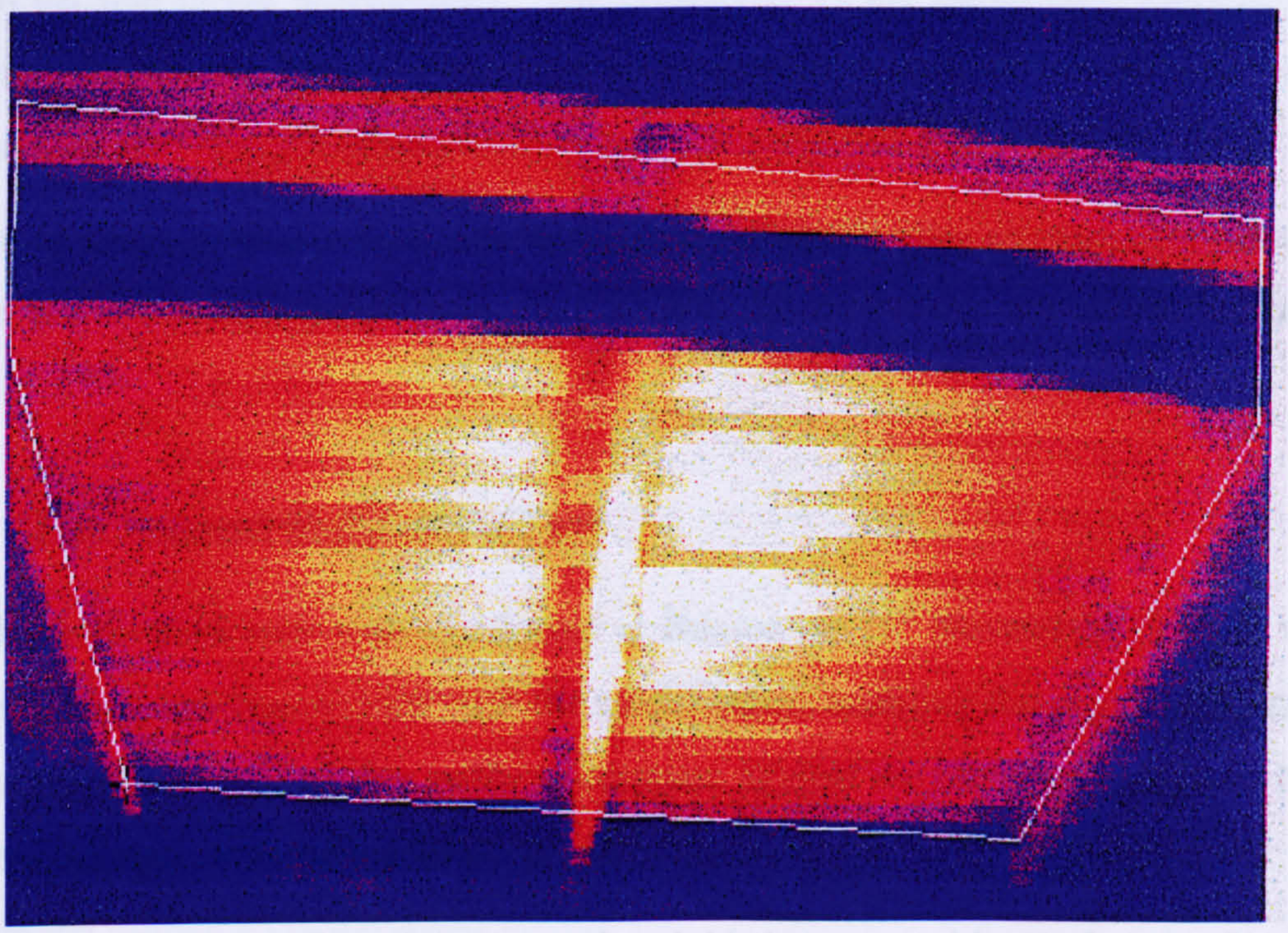

Figure 3.9 An example of the thermal image

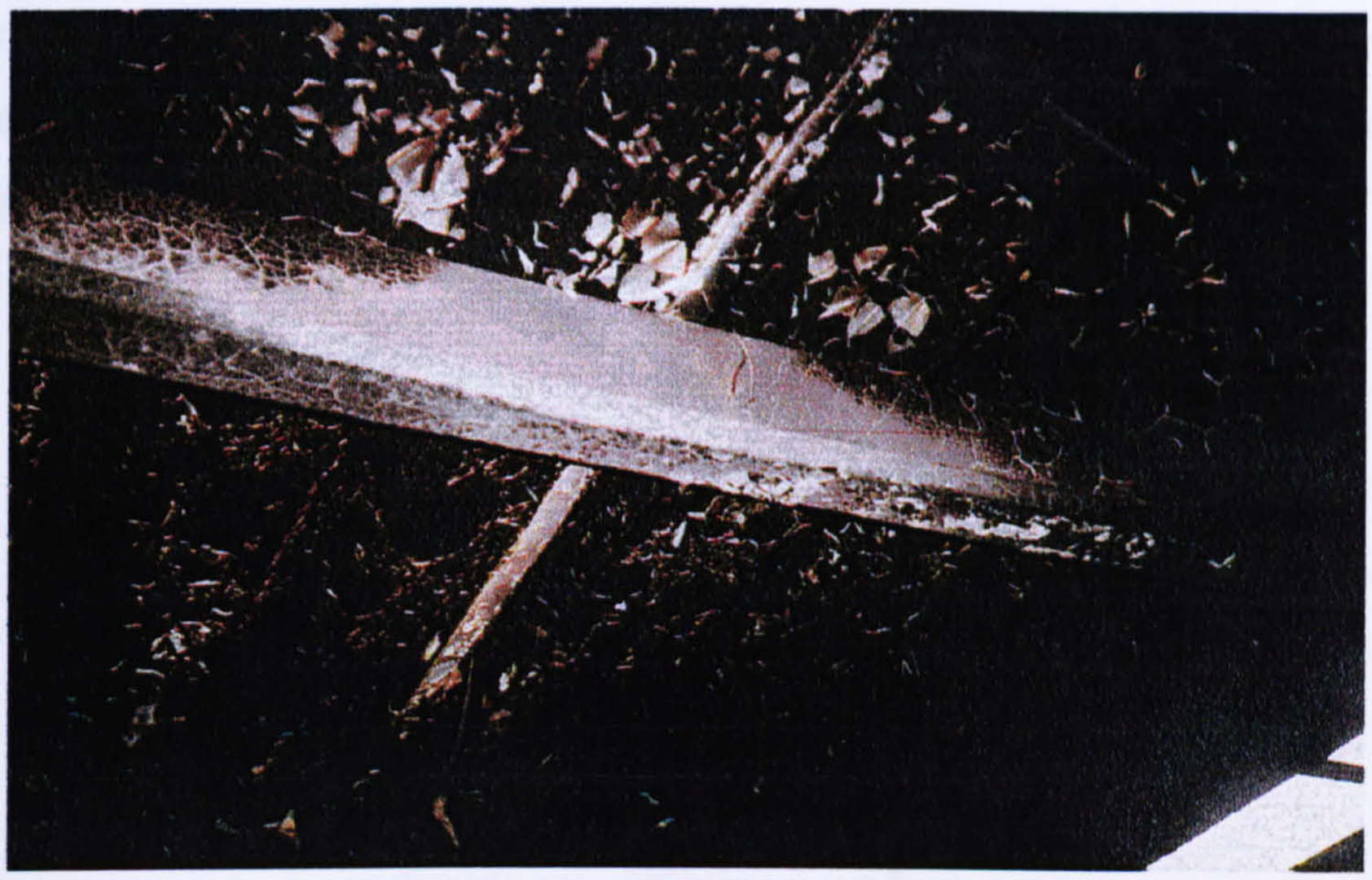

Figure 3.10 Panel and the purlin condition after 1st Test

The results of TASEF show generally lower steel temperatures profile compared to those indicated from thermal images, but the margin of difference is acceptable. This gives confidence that TASEF is capable of predicting steel temperatures 2-dimensionally with good accuracy. However, from inspection after the test, it could be seen that some of the black paint on the purlin and underside of the panel had fallen off due to the intense heat. The emissivity of the purlin may therefore vary throughout the test. Hence, there may be some reason to doubt the accuracy of the thermal images in representing the real element temperatures.

There was no significant structural damage to the panels after the test. This is logical since the beams and purlins were not loaded and they were not restrained at their ends.

3.4 The Second Indicative Test

Further indicative tests were conducted at Buxton on 21st November 1997, in which 2 thermocouples were welded onto the steel I-beam, enabling the actual temperatures of the steel to be recorded in order to compare against the temperatures given by the thermal images from the camera.

The design of the panel for these second and third tests was identical to the first. The positions of the thermocouples were slightly changed, as some of them were to measure steel temperature instead of the air temperature. Figure 3.11 shows the

positions in detail. Thermocouples 1, 2 and 3 were placed near to the Z-purlins; 9, 10 and 12 were placed near to the I-beam, and 11 and 16 were actually welded onto the top and bottom flanges of the beam respectively.

Figure 3.11 Position of thermocouples for the second and third indicative tests

For the second test, a baffle was put underneath the centre of the panel so that the gas flame and the heat flow were essentially 2-dimensional and hence concentrated on the heating of the sections of which thermocouples were placed. Fig. 3.12 illustrates the set-up of the baffle in a picture taken before the test was carried out. For this experiment the steel temperature was expected to be high, as most of the heat released was collected and concentrated within the baffle. 160 lit/min of gas flow was maintained throughout the test, which lasted for about 5 minutes.

Although the baffle was designed to contain the fire and heat, the actual fire was so intense during the test that the flame extended out of the baffle. As a result, the beam section with the welded-on thermocouple was fully engulfed in the fire for most of the time. Therefore the temperatures surrounding the beam thermocouples can be expected to be similar to those recording temperatures around the Z-purlin.

Figure 3.14 shows the steel beam engulfed in flame during this test.

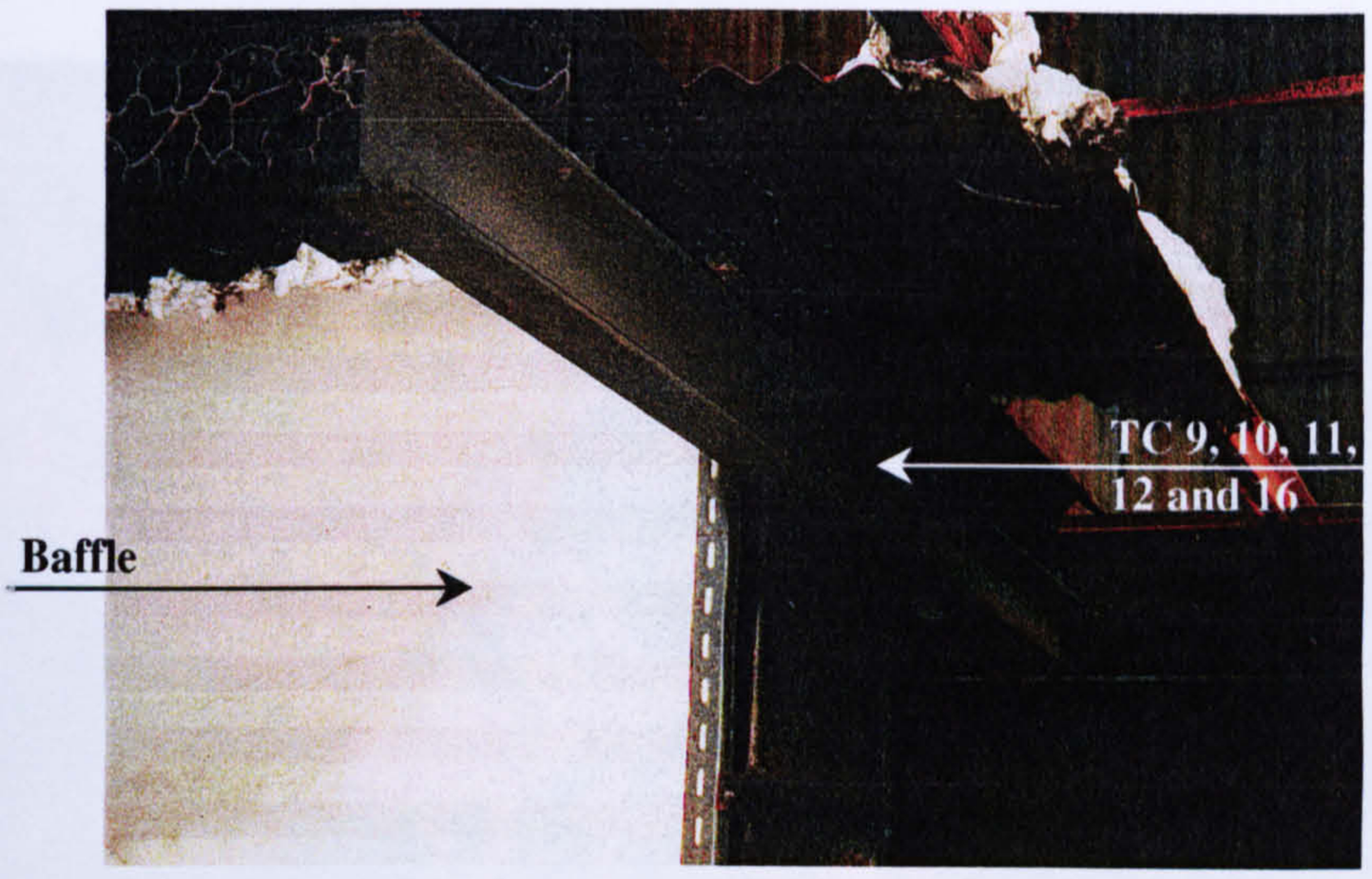

Figure 3.12 Set-up of the second test with baffle in place

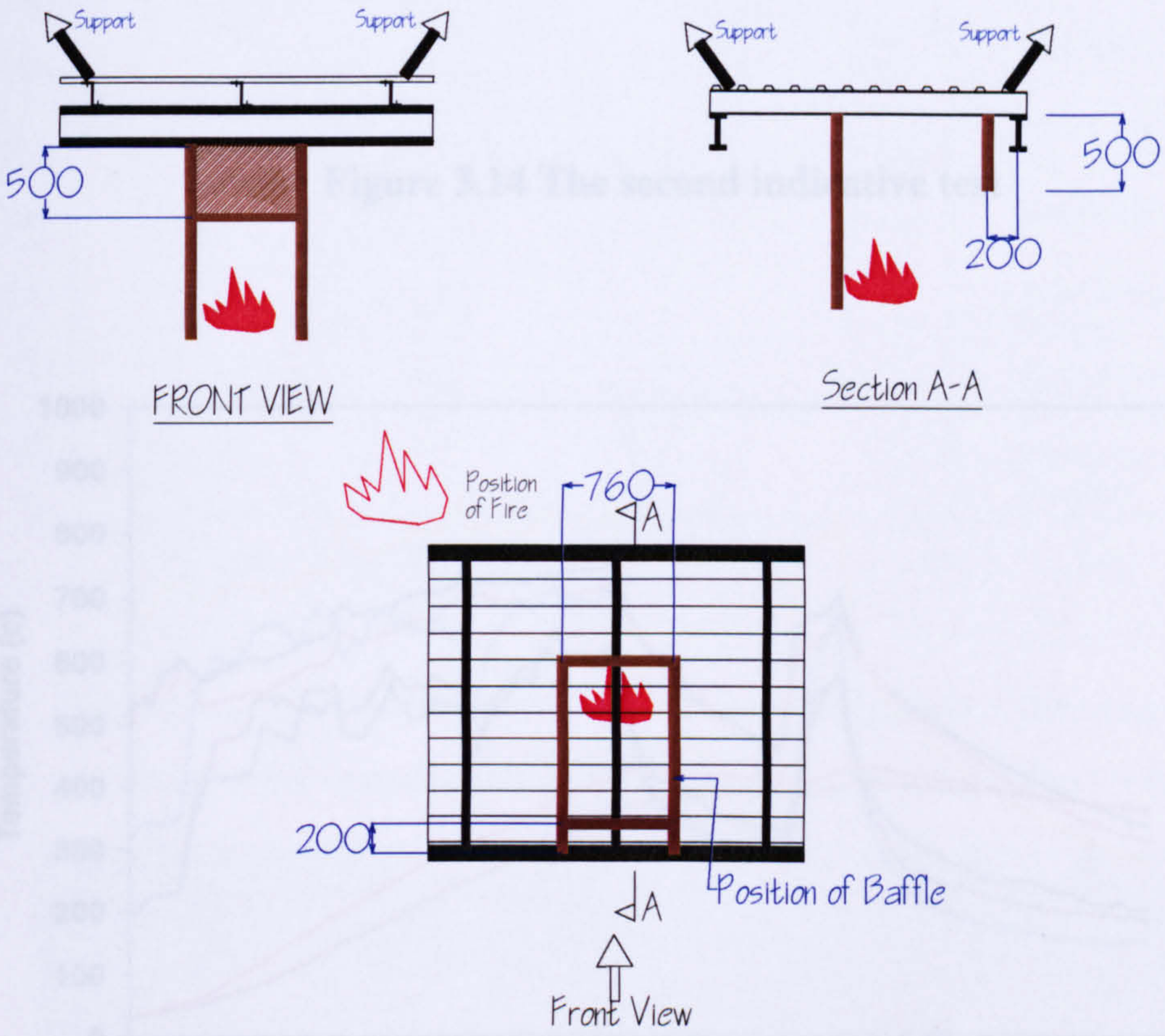

Figure 3.13 Set-up of the baffle for the second test

Figure 3.14 The second indicative test

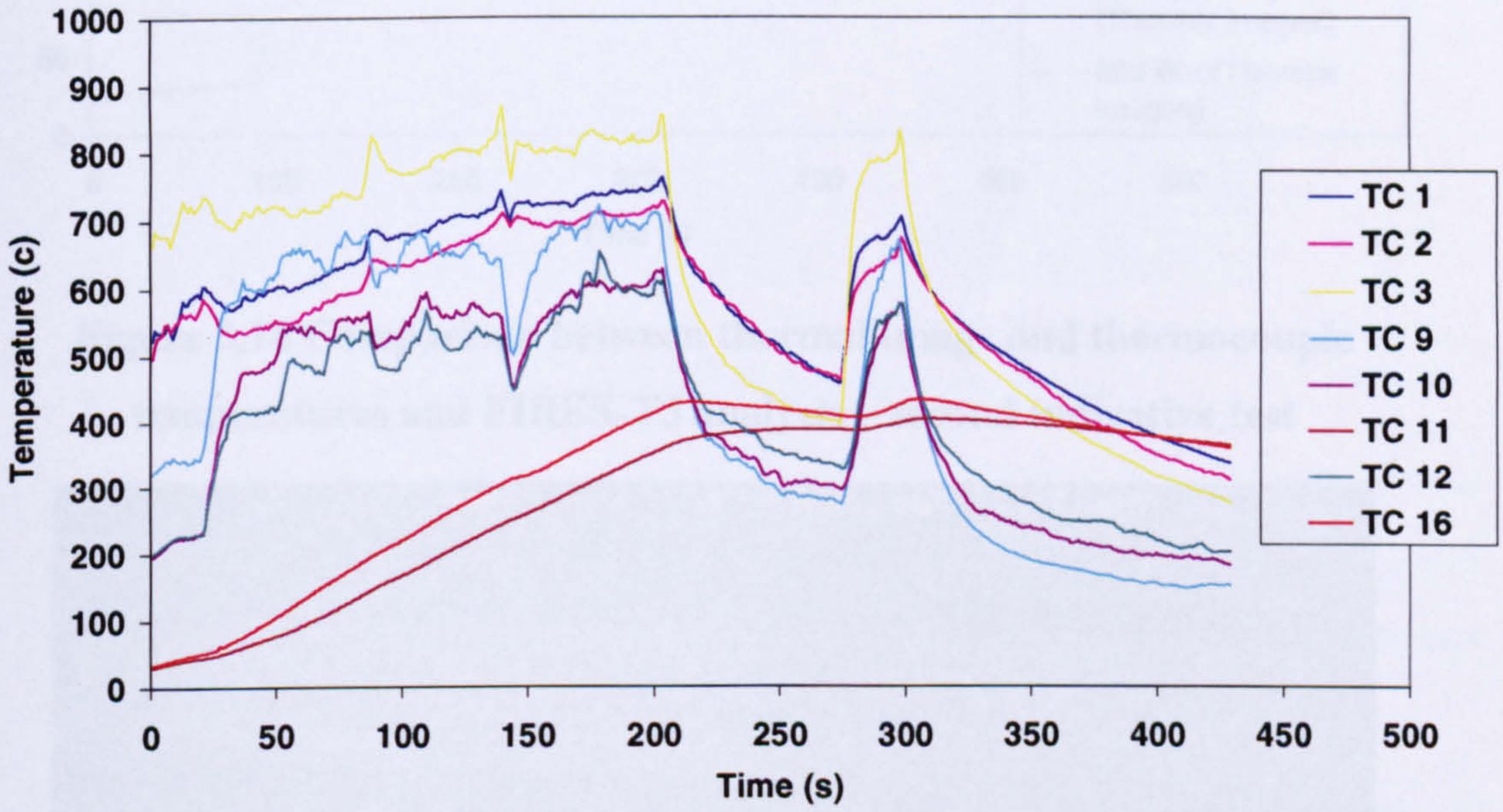

Figure 3.15 Temperature distribution recorded from the second indicative test

Figure 3.15 shows the recorded temperatures for each thermocouple. A separate computer program, FIRES-T3[53], was obtained and made executable in Fortran77 code. The program is capable of predicting steel temperatures, given the surrounding atmosphere temperature, and can perform a 3-dimensional analysis. With the gas temperature data from the test, FIRES-T3 was used to predict the temperatures of the I-beam section on which thermocouples were placed. Figure 3.16 shows the

comparison between the experimental results and the output from FIRES-T3. The temperature readings from the thermal images are plotted with an indication of their range of error. This is because the thermal images can only show refined colour variation due to thermal changes to an accuracy of ±5%. Temperatures of the steel surface obtained from the thermocouples are plotted to the same figure so that comparison can be made and hence the accuracy of the thermal images assessed.

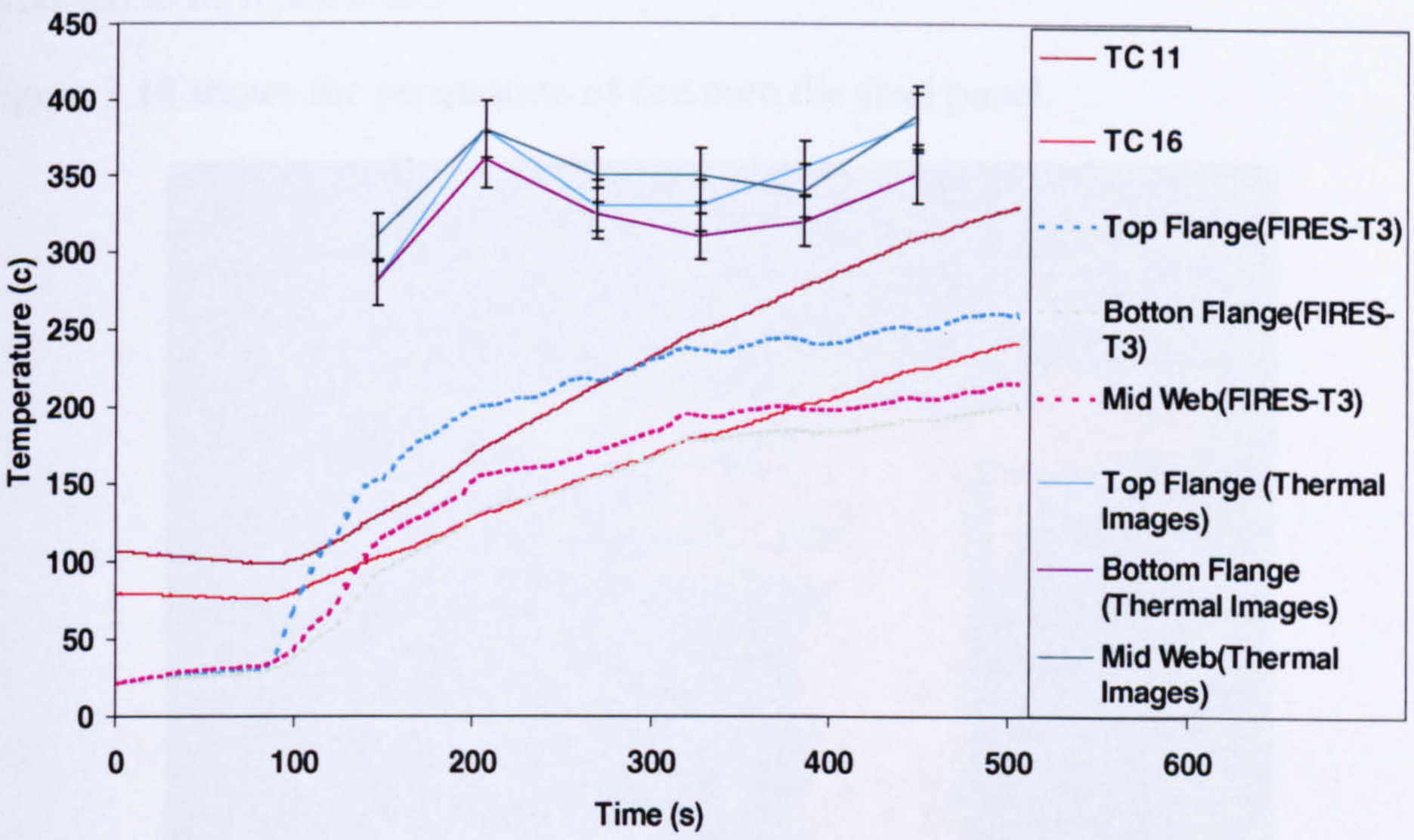

Figure 3.16 Comparison between thermal image and thermocouple temperatures and FIRES-T3 analysis – second indicative test

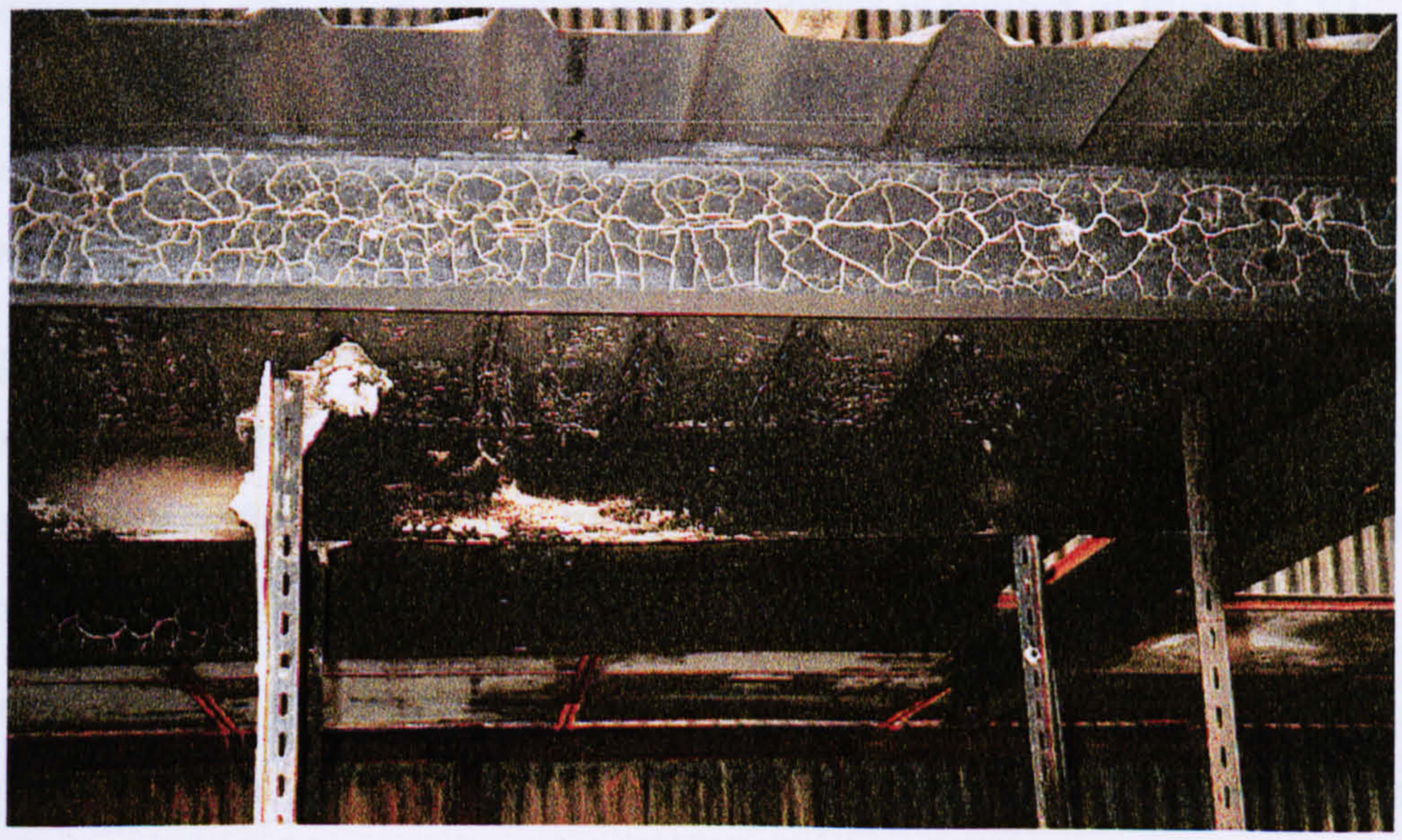

Figure 3.17 Condition of panel after the second indicative test

3.5 The Third Indicative Test

As soon as the panel had cooled after the second indicative test, the baffle was removed and the third test was conducted.

The arrangement of the thermocouples was unchanged, and the same gas burner was used. A slight reduction in gas flows was made for this test, and a discharge of 150 lit/min was applied. It was expected that the fire would spread over the whole panel, and the heat was not contained. Therefore, the steel temperatures in this test were expected to be much lower.

Figure 3.18 shows the penetration of fire onto the steel panel.

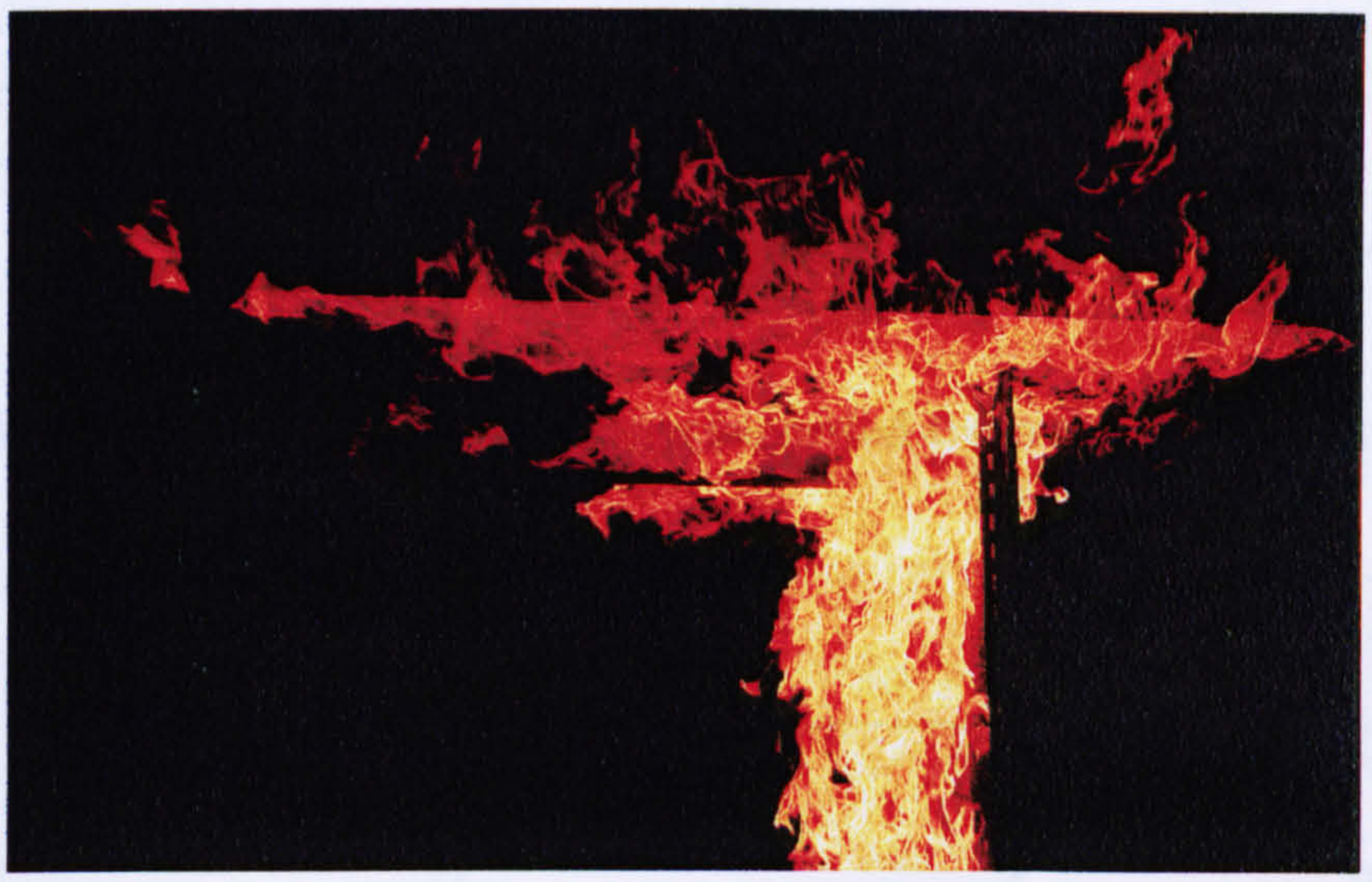

Figure 3.18 The third indicative panel test

The temperature data taken from the thermocouples is plotted in Figure 3.19. It can be seen that the gas temperatures near the I-beam are much lower than those around the purlin which was engulfed in the flame. The beam steel temperatures closely follow the gas temperature.

The gas temperatures were again fed into the program FIRES-T3 for prediction of the steel temperatures. Figure 3.20 compares the recorded thermocouple temperatures against the analysis from FIRES-T3. The reading from the thermal images is also plotted in the figure with bars indicating the range of error.

Figure 3.21 shows the condition of the purlin and beam after the tests. The black paint on the surface of the hottest part of purlin was seen to have fallen off, and the

purlin was slightly distorted by the intense heat. No further significant damage was observed.

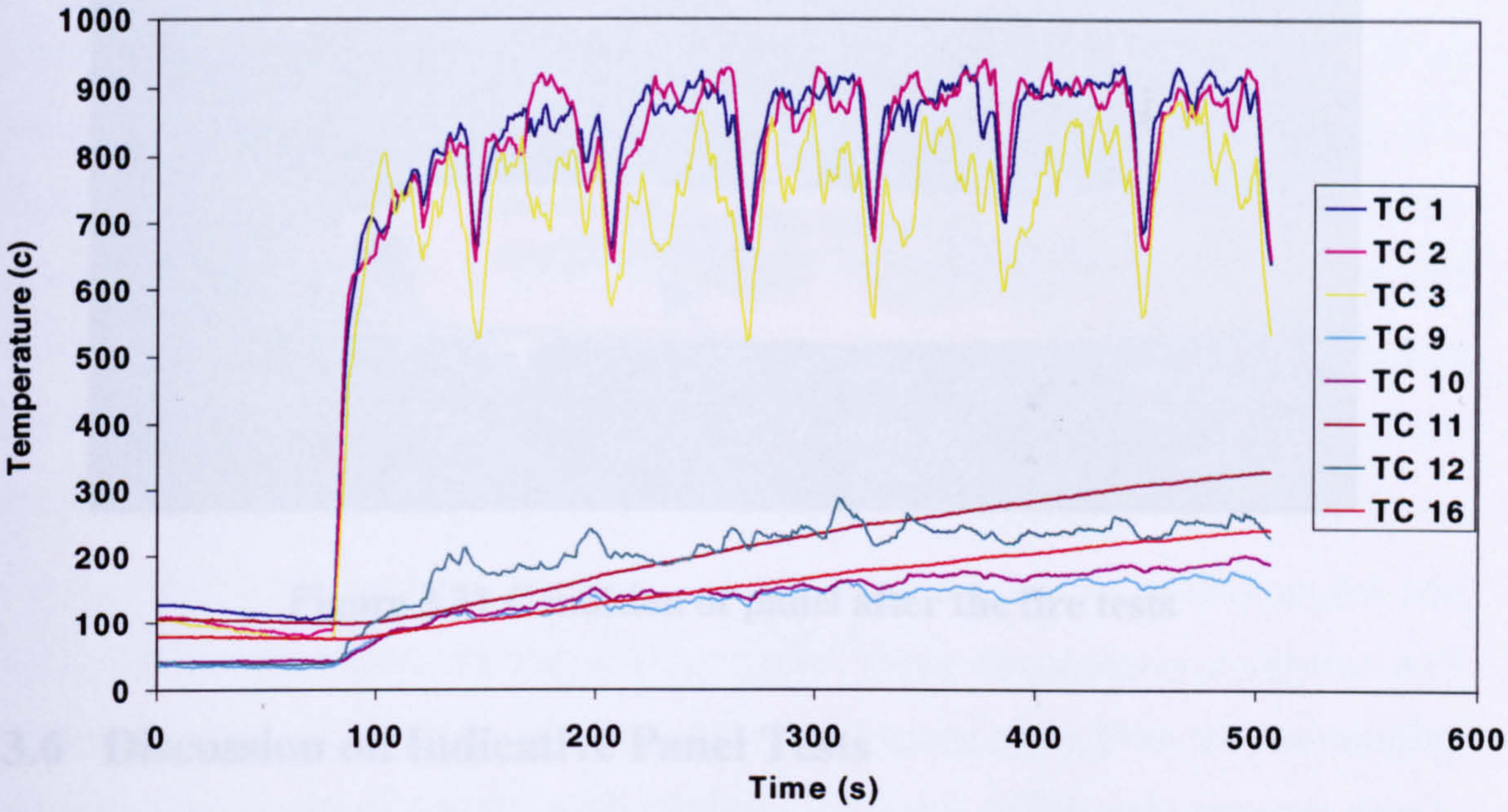

Figure 3.19 Temperature distributions recorded from the third indicative test

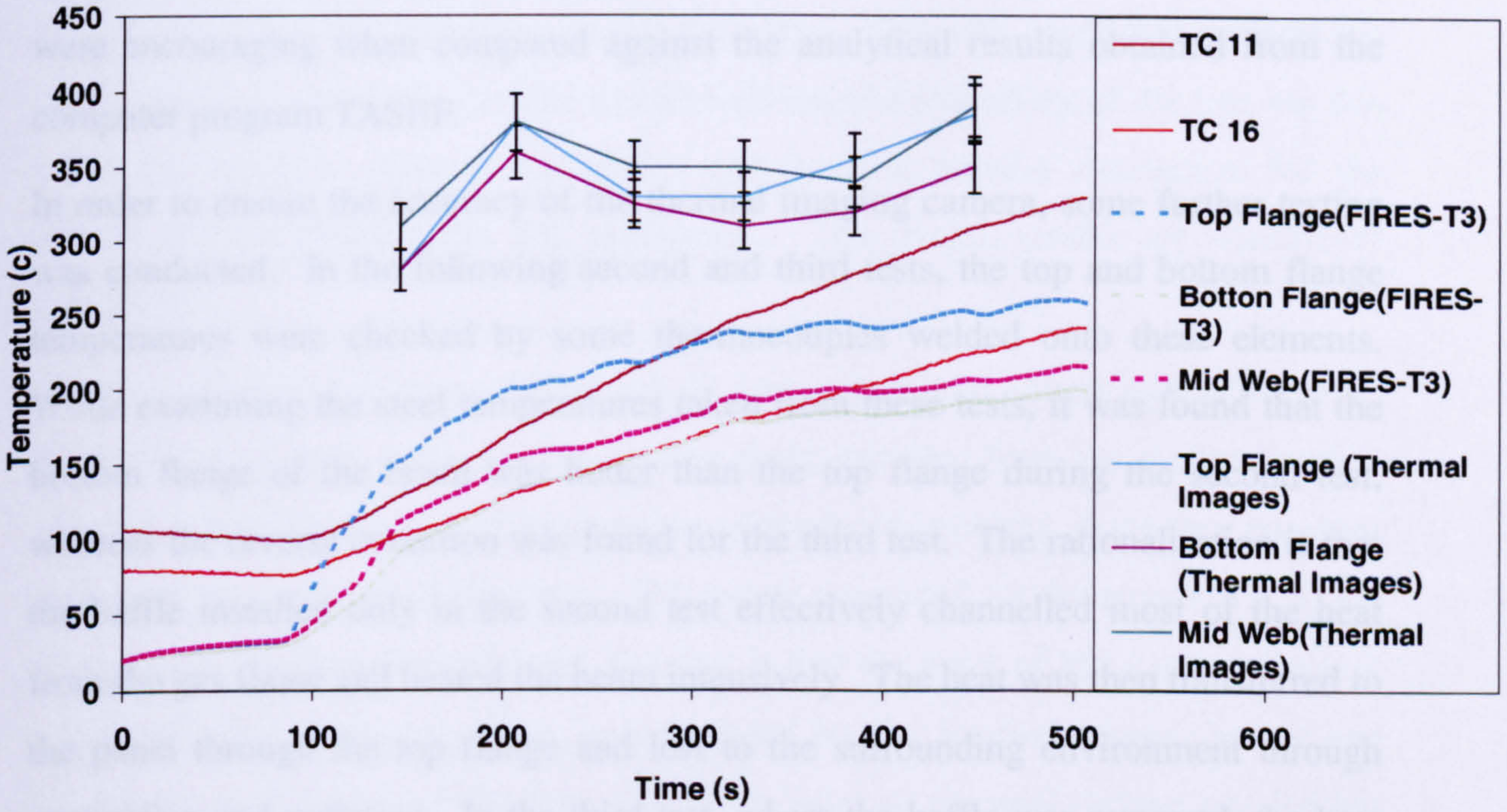

Figure 3.20 Comparison between thermal imaging temperatures and FIRES-T3 analysis – third indicative test

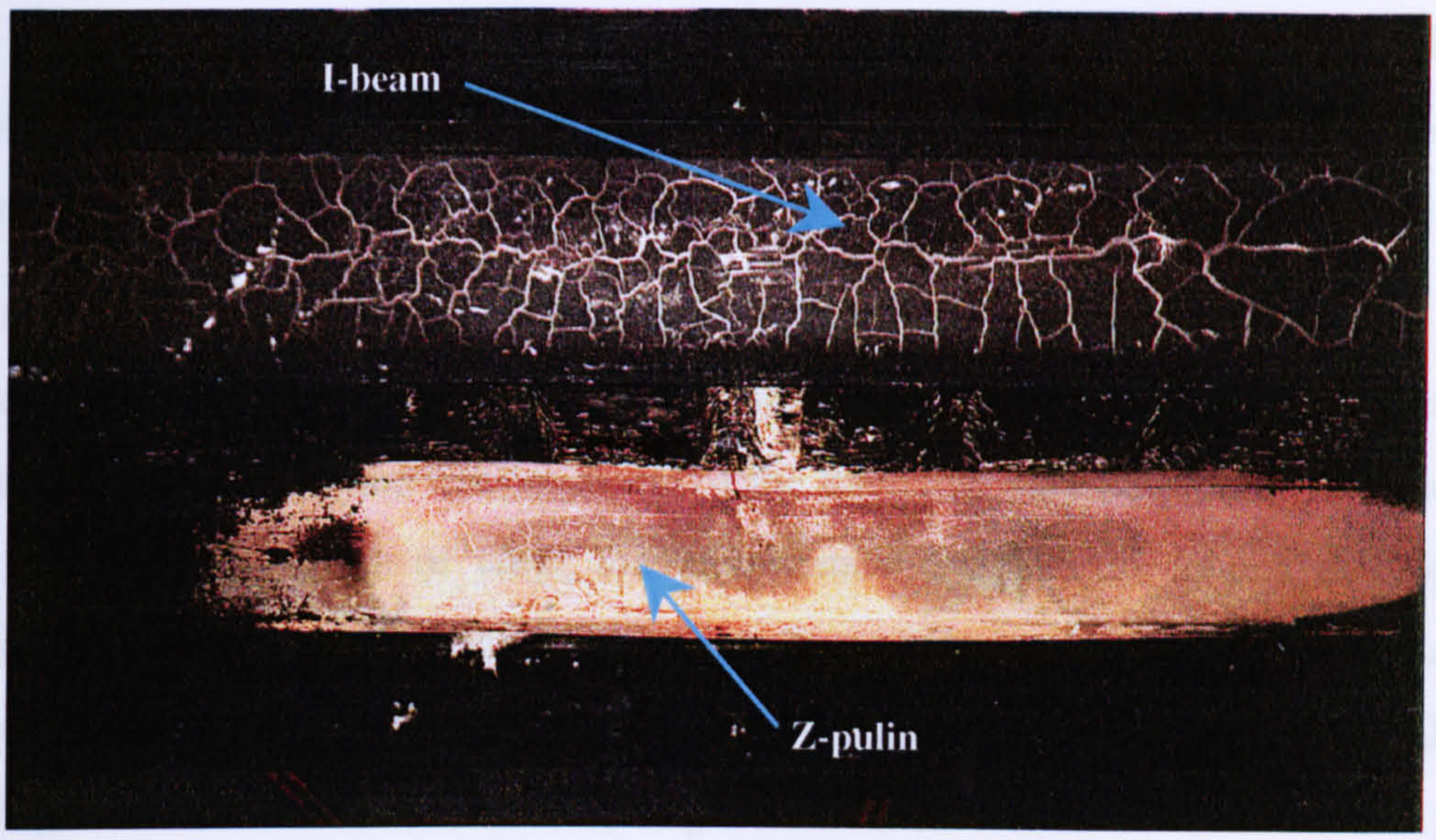

Figure 3.21 Condition of panel after the fire tests

3.6 Discussion on Indicative Panel Tests

The first test was significant in developing the experimental techniques to be used and generating some thoughts for the fire tests, for instance on the use of the thermal imaging camera and the necessity of having thermocouples to record steel temperatures. The temperatures read from the thermal images from the first test were encouraging when compared against the analytical results obtained from the computer program TASEF.

In order to ensure the accuracy of the thermal imaging camera, some further testing was conducted. In the following second and third tests, the top and bottom flange temperatures were checked by some thermocouples welded onto these elements. While examining the steel temperatures taken from these tests, it was found that the bottom flange of the beam was hotter than the top flange during the second test, whereas the reverse condition was found for the third test. The rationalisation is that the baffle installed only in the second test effectively channelled most of the heat from the gas flame and heated the beam intensively. The heat was then transferred to the panel through the top flange and lost to the surrounding environment through convection and radiation. In the third test, where the baffle was removed, the heat was distributed to the surroundings evenly and the panel formed a shield to collect hot gases underneath it. The rate of heat loss beneath the panel was greater than the convection and radiation through the air above it. It is believed that a layer of hot air,

with thickness of approximately 10% of the height from the fire to the panel, was formed beneath the panel. Therefore, the top flange was hotter than the bottom flange.

During a warehouse fire, the condition of the second test may be expected if an intense fire is ignited and flash-over takes place with high fuel load. However, if a small local fire occurs, the fire condition of the third test may be predicted. However, from the structural point of view, the temperature difference between the top and bottom flange is not significant enough to cause any thermal bowing to take place in the beam. It is therefore suggested that an evenly distributed temperature profile can be adopted across the section in analysing the structural behaviour.

On the other hand, comparing steel temperatures taken from the thermocouples and analytical results for the second and third tests, these temperatures compares well with each other. Analytical tools can predict steel temperature from the surrounding air temperature with relatively good accuracy, provided sufficiently accurate data is obtained for input.

The temperatures measured in the second test are more precisely predicted by FIRES-T3 compared to results from the third test. This is because there was more uncertainty about fire conditions in the third test. This was conducted without the baffle, and hence variations in the wind condition, the emissivity of the fire, etc can affect the analysis. This fire condition and the heat transfer mechanism for the second test are more stable and predictable. The overall results are considered acceptable.

It can be seen from Figures 3.16 and 3.20 that temperature values indicated by the thermal images were generally higher than those recorded from the thermocouples. There is little reason to doubt the accuracy of the thermocouples, since they compare well with the analytical predictions. The reason suggested for the apparently higher temperature readings from thermal imaging is that the layer of hot gases collecting underneath the panel may have been recorded by the thermal image camera and interpreted as the steel temperature. The black paint on the steel surface was flaking off throughout the test but the thermal imaging camera has assumed an unchanged emissivity throughout the test.

The general rule of radiation is governed by heat leaving a surface due to both reflection and emission, and on reaching a second surface, experiencing reflection as well as absorption. When the approximation of a blackbody is assumed, the process can be simplified by eliminating reflection from the equation. As soon as the black paint on the beam peels off, the thermal image camera can be over-estimating the temperature by recognising the natural colour of the beam as a high temperature surface. However, it is rather difficult to quantify the level of errors, and amount of paint which came off during the test.

Consequently, a decision was made to abandon the use of the thermal imaging camera in the following tests, and conventional thermocouples were used instead.

3.7 Design of the Portal Frame Warehouse

Following the indicative panel tests conducted at Buxton, a 1/5 scaled portal frame structure was built and tested under fire conditions. Displacements and temperature were measured and recorded with reference to time during these experiments. The experience from the indicative tests was beneficial in the setting up of the testing apparatus.

The major purpose of the frame model tests was to observe the collapse behaviour of a portal frame at elevated temperature, and the numerical data were used to validate the analytical results produced by VULCAN.

It was intended to design the portal frame to BS 5950, with the appropriate load level and resistance. The designed structure is a scaled-down model of a portal frame of 30m span and 12m column height with a scale reduction of 1:5. The rafter pitch is 14.9°

Figure 3.22 shows the layout of the structure, as designed by the author. It was later realised that even with the smallest UB section available, this would still be too strong to be adopted with the given geometry and self-weight to achieve a reasonable design. It was therefore decided to add extra imposed loading to the roof, so that the total loading (including the self-weight) was equivalent to a load ratio of 0.2 on the internal portal frames. This load level was an estimate of the extreme case likely to be encountered during a fire in reality.

A fire was to be ignited below internal portal frame, and temperatures were measured along the rafters and columns. Displacements would be taken at the ridge and eaves of the heated portal frame. It was planned to investigate different fire scenarios, with the details of the portal frame design being improved if necessary so that a typical portal frame structure could be modelled.

Further details on the instrumentation and the tests themselves will be described in Chapter 4, along with the results and numerical modelling.

3.8 Conclusion

Three indicative tests were conducted prior to the fire tests on scaled portal frame structures which were planned for the research project. These indicative tests were mainly aimed at examining the temperature distributions around frame members and purlins in the roof-space of a portal frame subjected to a local fire. Experience on conducting structural fire tests was also gained. It was found that the steel temperatures could be predicted with acceptable accuracy by existing thermal analysis software. This is significant in that it allows structural fire analysis to be conducted with reasonable confidence that the temperature distributions in the steelwork are representative of reality.

A 1:5 scale model of a portal frame structure was designed and constructed for the actual fire tests. The following chapter will give details on these experiments.

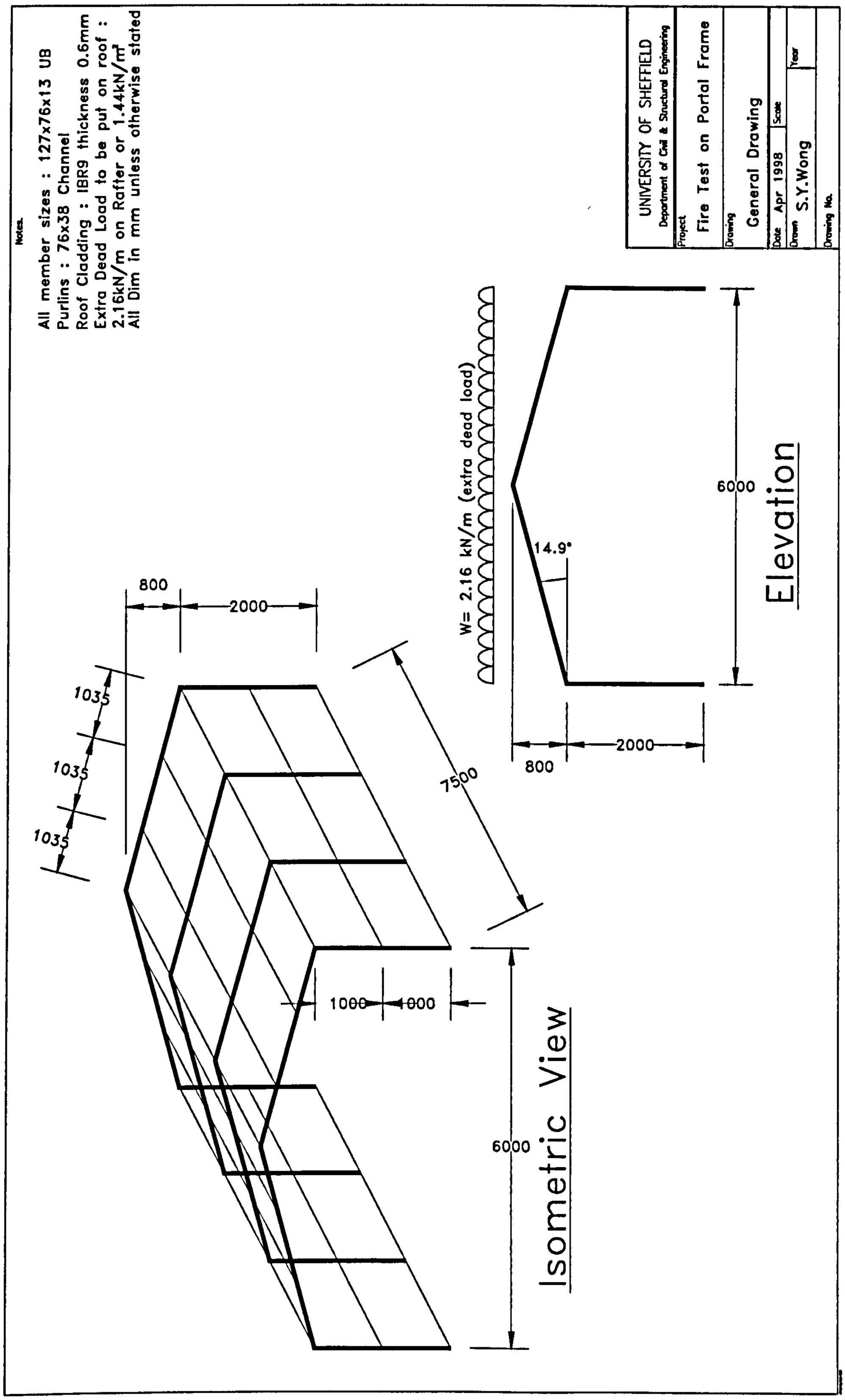

Figure 3.22 General layout of the experiment structure

4 Fire Tests on a Scaled Portal Frame and Computer Modelling

Following the series of indicative fire tests described in Chapter 3, a scaled portal frame warehouse model was constructed at the Health and Safety Laboratory, Buxton to be tested under fire. The portal frame has been designed and shown in Chapter 3. The main purpose of conducting these tests was to investigate the structural behaviour of steel portal frames at elevated temperature. Figure 4.1 shows the completed portal frame structure model. A goal post frame was constructed outside the test structure, which acted as a reference datum for the purpose of measuring displacements.

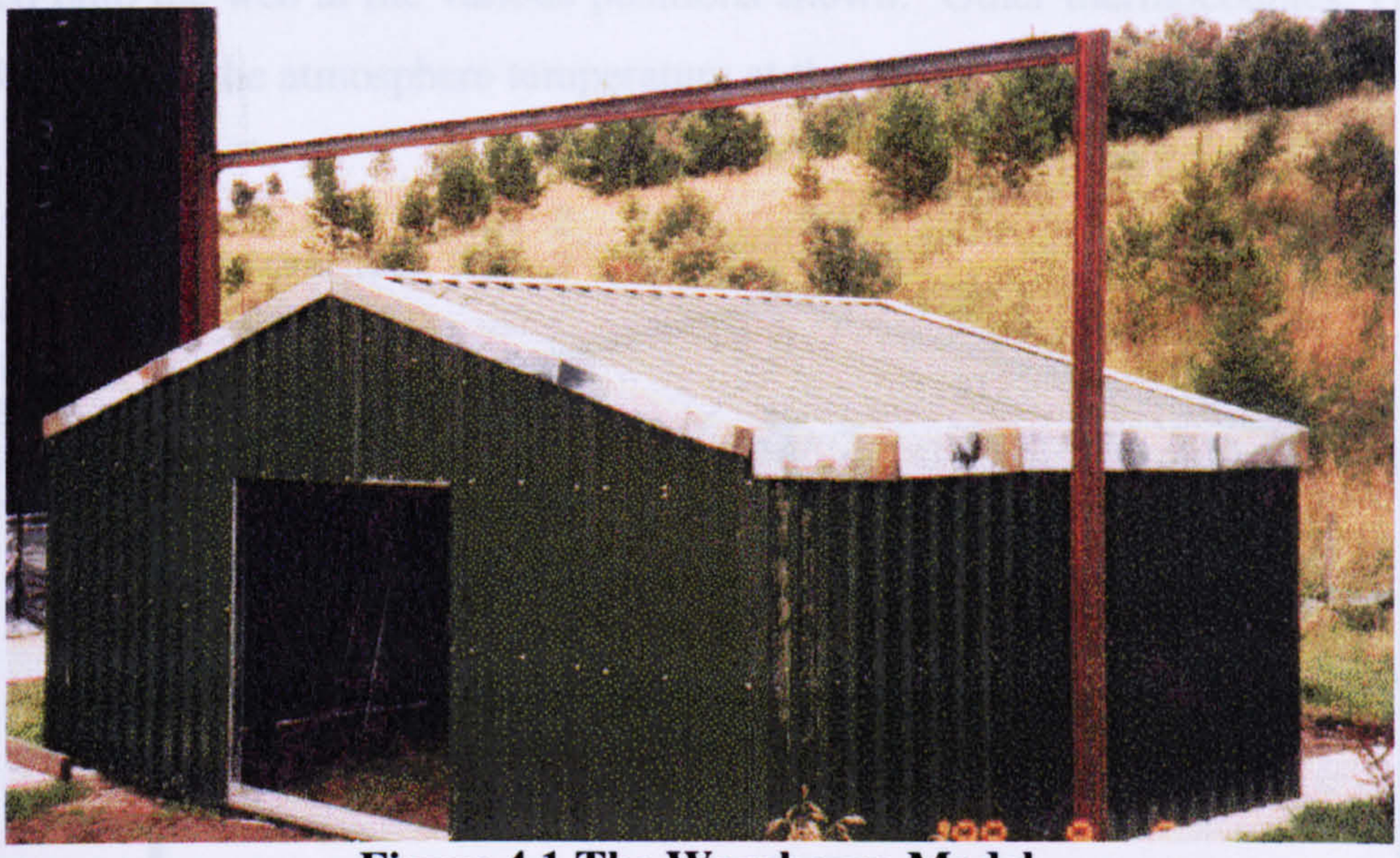

Figure 4.1 The Warehouse Model

Three major fire tests were conducted on the internal frame. This chapter describes these experiments in detail, and shows the recorded test results. The structural behaviour will then be modelled with VULCAN after the test so that the results can be compared and validated.

4.1 The Testing System and Instrumentation

This section describes the setting-up of the series of fire tests on the portal frame structure, including the instrumentation used for measuring the temperatures and deflections. A gravity loading system was included, since it was necessary to add extra loading to the frame to represent typical portal frame action.

4.1.1 Temperatures Measurement

With the experience gained from the previous indicative test it was decided to adopt conventional thermocouples for measuring the steel and gas temperatures. It was important to record accurate temperature profiles across the portal frame under test so that they could be applied to the computer modelling.

Figure 4.2 shows the positions of the thermocouples used in the tests. S1 to S16 denote the thermocouples welded onto the steel. Thermocouples S4, S5, S6 and S9, S10 and S11 were welded onto the top, mid-web and bottom flange of the steel section at the eaves and apex respectively. The other steel thermocouples were welded onto the web at the various positions shown. Other thermocouples, Gas1, 2 and 3 measured the atmosphere temperature at the two eaves and the apex.

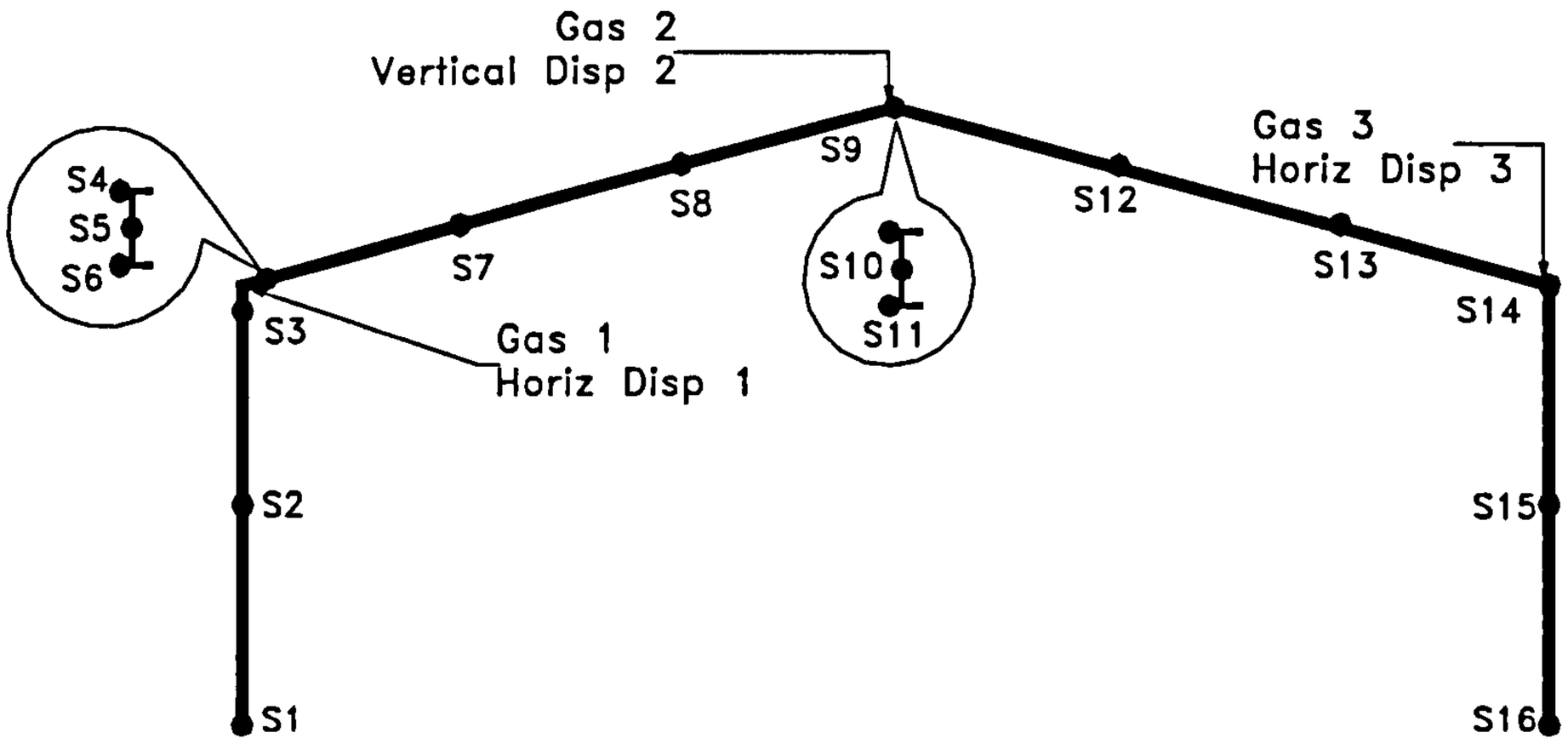

Figure 4.2 Positions of thermocouples

All thermocouples were connected to a data logger away from the test structure, using insulated wires and cables. Care was taken to ensure that the measurements would not be affected by heat during the experiment.

It was recognised that temperature measurement on the purlins spanning between portal frames could be potentially useful. However the purlins were very thin and hence it was difficult to weld on the thermocouples. It is relatively accurate to assume that the purlin temperature is nearly equal to the gas temperature under these circumstances.

4.1.2 Displacement Measurement

Three position sensors were acquired for the purpose of displacement measurement. The position sensor is an accurate electromechanical device which translates linear motion into a proportional electrical signal that can be recorded by data logger. It consists of a measuring cable which winds onto a machined calibrated cable drum. The drum is mounted onto a shaft which is tensioned by a coil spring providing constant pull-in force to maintain cable tension and control.

In operation, the free end of the measuring cable is attached to the measurement point of the portal frame, where the sensor then converts the linear cable movement into a rotary motion as it winds on or off the cable drum. The motion is then converted into an electrical output signal which can be calibrated and read as displacement measurement. The particular position sensor was manufactured by ASM with a model number of WS10-1000-10V-L10. The measurement range is 1m with a 0-10 V signal condition and linearity of ±0.1%.

With three position sensors available, it was decided to measure the horizontal movements of the two eaves and the vertical movement of the apex. The devices were fixed and secured on the reference frame and calibration of movements was done before every test.

4.1.3 The Loading System

As described in the previous chapter, it was necessary impose some extra vertical load onto the portal frame so that a representative loading level could be achieved. For a normal industrial portal frame warehouse the extreme loading case likely to be encountered during a real fire was estimated to be 0.2 of the failure load. In order to represent this accurately, the most practical way was to impose three point loads, at the apex and the two mid-points of the rafters respectively. This is relatively similar to the representation of a uniformly distributed load.

The extra loading was achieved by hanging a barrel filled with water onto the portal frame rafters at each loading point. The amount of water was controlled to the intended load level. The barrels were covered by additional insulation during the fire tests in order to prevent loss of water due to evaporation in the heated environment. Figure 4.3 shows the set-up of the loaded frame. This same loading system was

adopted for all fire tests conducted and was proven to be a relatively efficient solution for the purpose.

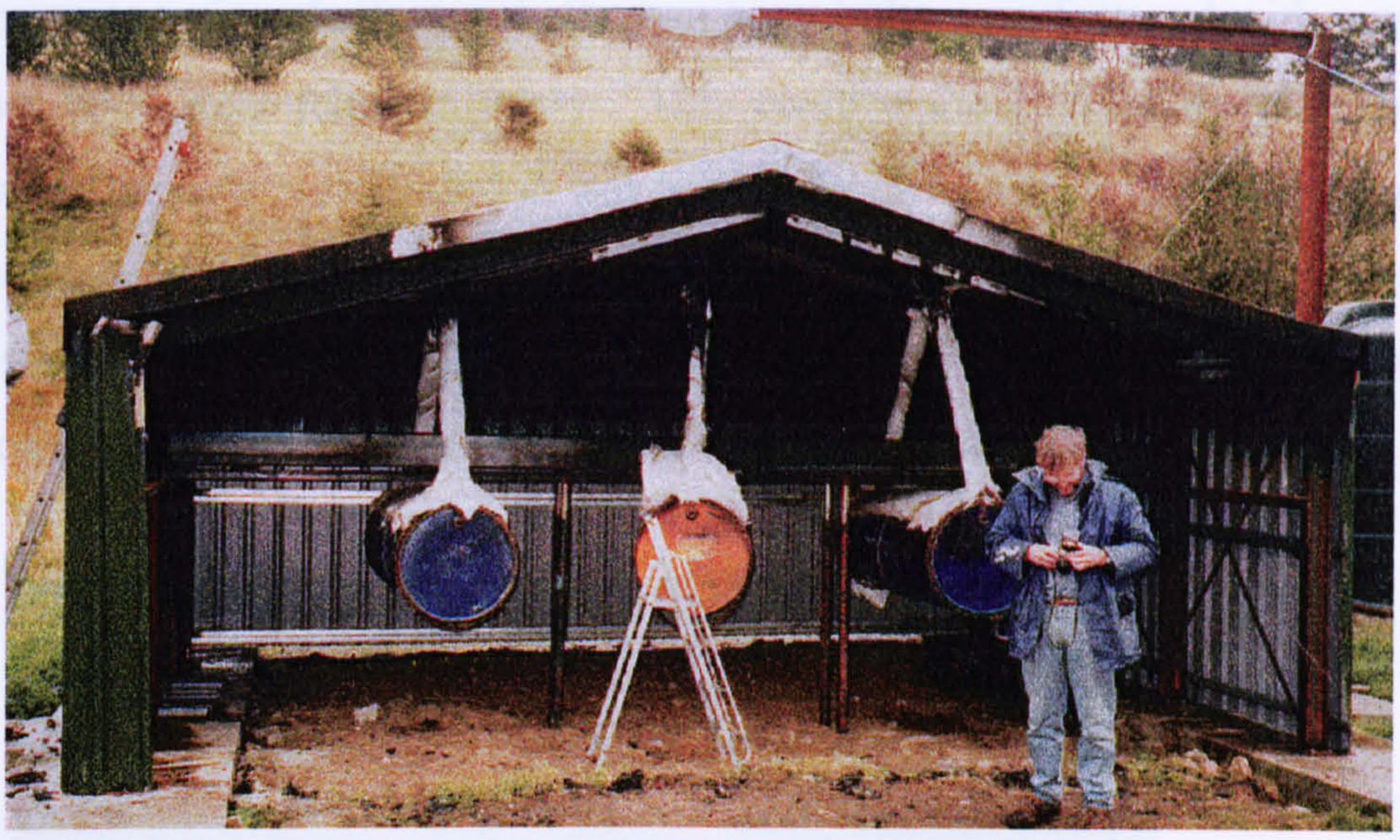

Figure 4.3 The Loading system for the portal frame

4.1.4 Base Connection

It was intended to create nominally pinned base connections for the test frame, but also to represent a practical portal frame. The test frame was constructed with a base plate welded onto the column and placed onto four bolts which were embedded into a rectangular concrete footing. The concrete footing supports one side of all the portal frame columns.

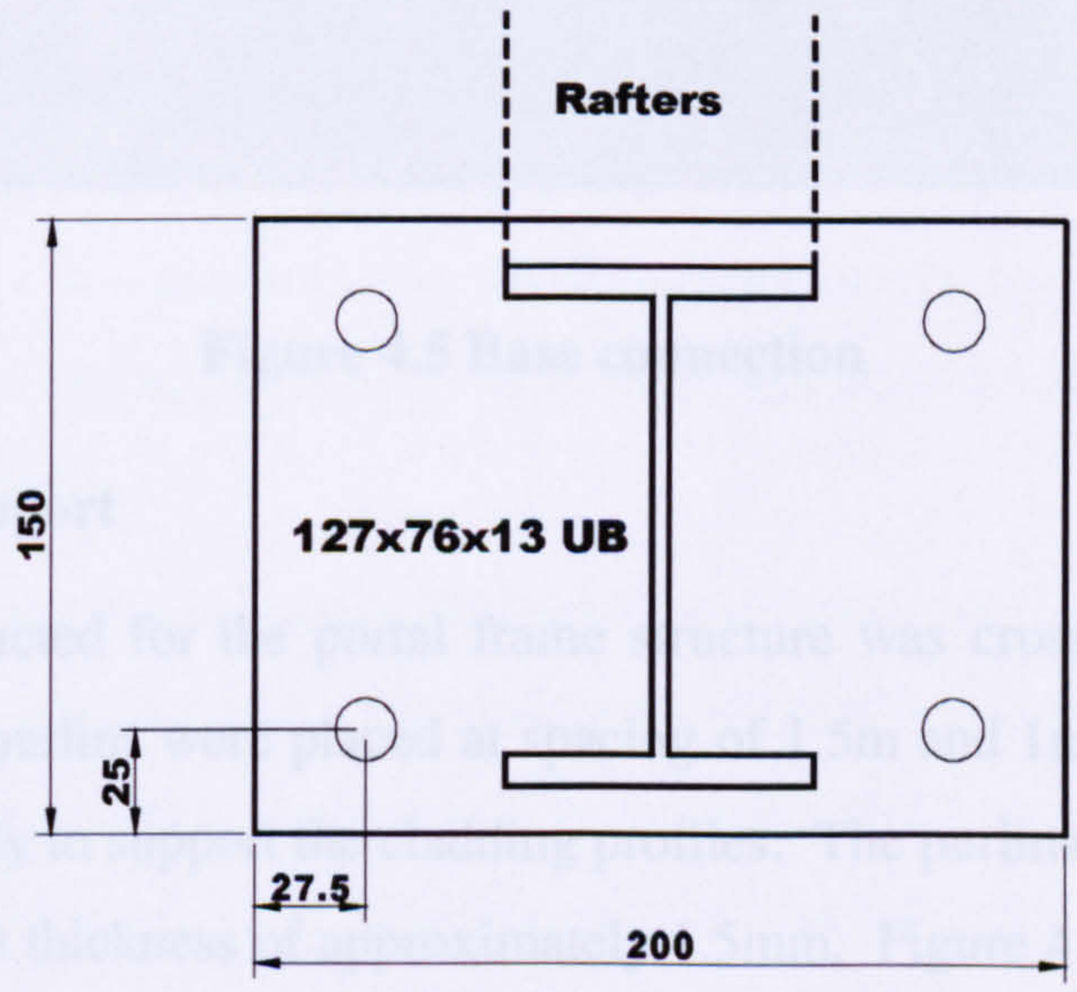

Figure 4.4 Dimensions of base connection

The base plate was 150mm x 200mm with a thickness of 12mm. The bolts are 12mm in diameter. Figure 4.4 shows the actual dimensions of the base plate. In order to create a pinned effect, only the two outer bolts were fastened with nuts while the inner bolts were released freely. This enabled the column to rotate outward easily when the rafters expanded. It was not totally obvious that this represented well a pinned base, but a typical industrial portal frame would have a base with four bolts and this would be regarded as a pinned base. It was intended to review the base condition after the first test if any refinement was necessary.

Figure 4.5 Base connection

4.1.5 Lateral Support

Each frame constructed for the portal frame structure was cross braced with steel strip. In addition, purlins were placed at spacing of 1.5m and 1m on the rafters and columns respectively to support the cladding profiles. The purlins were 120mm deep by 50mm wide with thickness of approximately 1.5mm. Figure 4.6 shows the lateral support system.

Figure 4.6 Lateral support system

4.2 The First Experiment – Heating of the Whole Rafter

This test aimed to produce a fire extending across the whole rafter. The initial thought was to have the temperature along the entire rafters increased evenly until the portal frame failed. Hence a line fire was produced to achieve the intended heating profile.

Due to the nature of the testing environment, which was situated within the HSL and office compound, smoke releases were a concern and it was intended to keep the test as short as possible. It was decided to use liquid heptane as the burning fuel, which can produce a high level of heat with a relatively low level of smoke, and is relatively easy to handle.

A separate support system was made to hold a long rectangular metal tray which was used to contain the burning fuel. The independent framework was to ensure that its self-weight was not added to the portal frame. The metal tray was raised about 1.5 metres above ground level. The intention was to concentrate heating on the rafters with majority of the column lengths remaining relatively cool. The entire setup can be seen in Figure 4.3.

It can be seen from the same figure that the entire front gable sheeting had been removed (as compared to Figure 4.1). This was to provide sufficient ventilation for the burning fuel. A preliminary test had been conducted in the presence of a front cladding with an opening of 1.5m by 1.5m. Due to the lack of ventilation, only part of the liquid heptane ignited, but the majority evaporated and incinerated just outside the opening where more oxygen was available. Consequently, high temperatures within the portal frame compartment could not be achieved.

When sufficient ventilation was available, all the heptane fuel was ignited and burnt underneath the rafters, and efficiently heated the section. Figure 4.7 shows the initial stage of the fire. The smoke produced was solely due to burning of the plastic coating on the cladding, which created a slight concern from the local occupants.

Figure 4.7 Early stage of the first test

However, the fire was more susceptible to the surrounding air movements with the large opening. At a late stage in the test it was realised that there was some difficulty in controlling the burning rate due to the ventilation condition. It was almost impossible to heat up the rafter evenly as the fire and heat were drawn naturally to the apex of the frame, and a small amount of wind could deflect the effect of the fire so that the heating became asymmetric.

The fire lasted only for about 10 minutes, although 120 litres of heptane were used. Some parts of the steel were heated to just over 900°C, and a certain extent of deflection was observed and recorded. However, the frame did not collapse totally.

4.2.1 Experimental Results

Figure 4.8 and 4.9 plot temperature and deflection against time respectively. The positions of the thermocouples can be found in Figure 4.2. The Standard ISO 834 fire curve has been plotted in the temperature graph as a reference for the heating rate during the test.

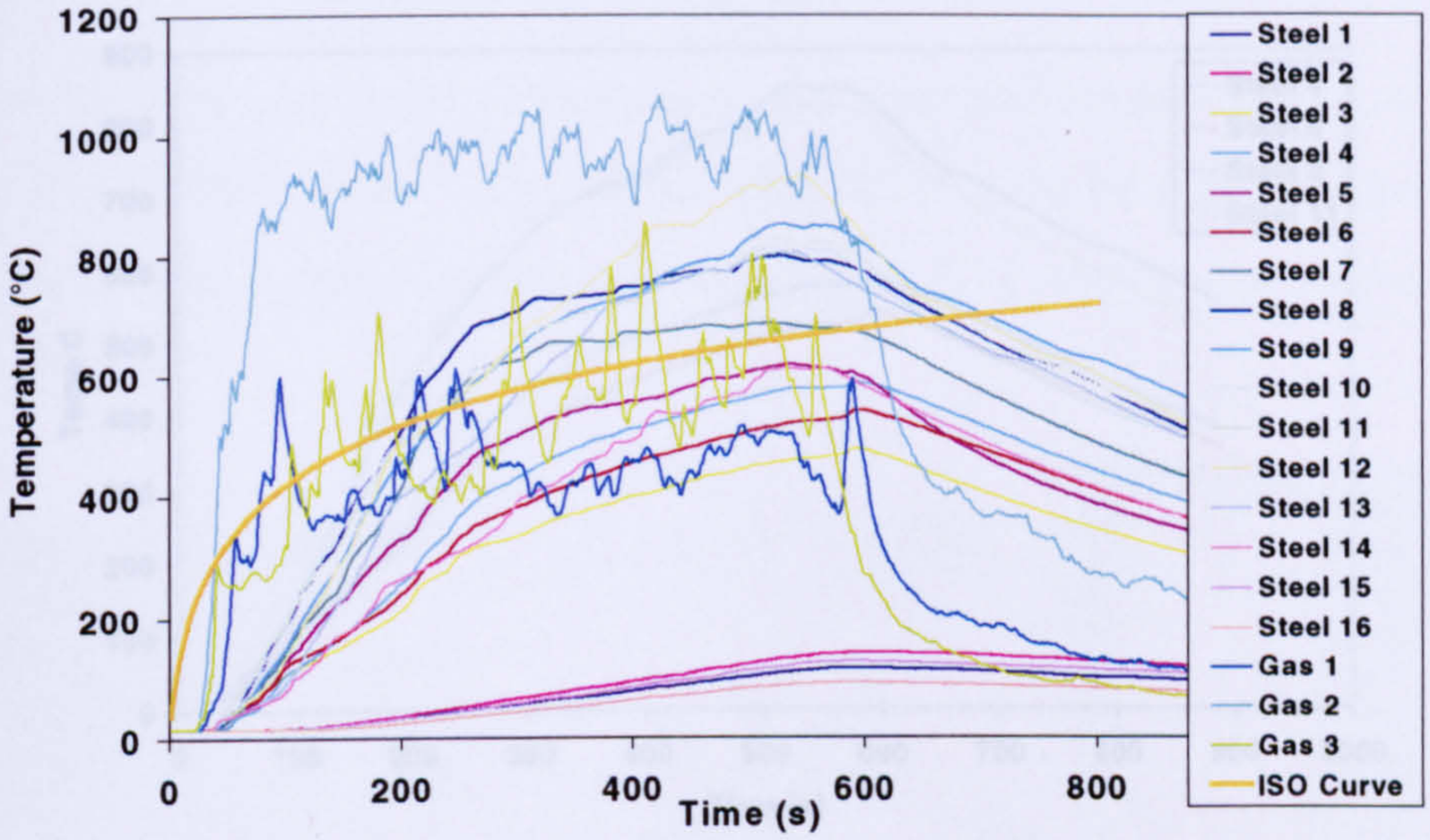

Figure 4.8 Recorded temperatures during the first test

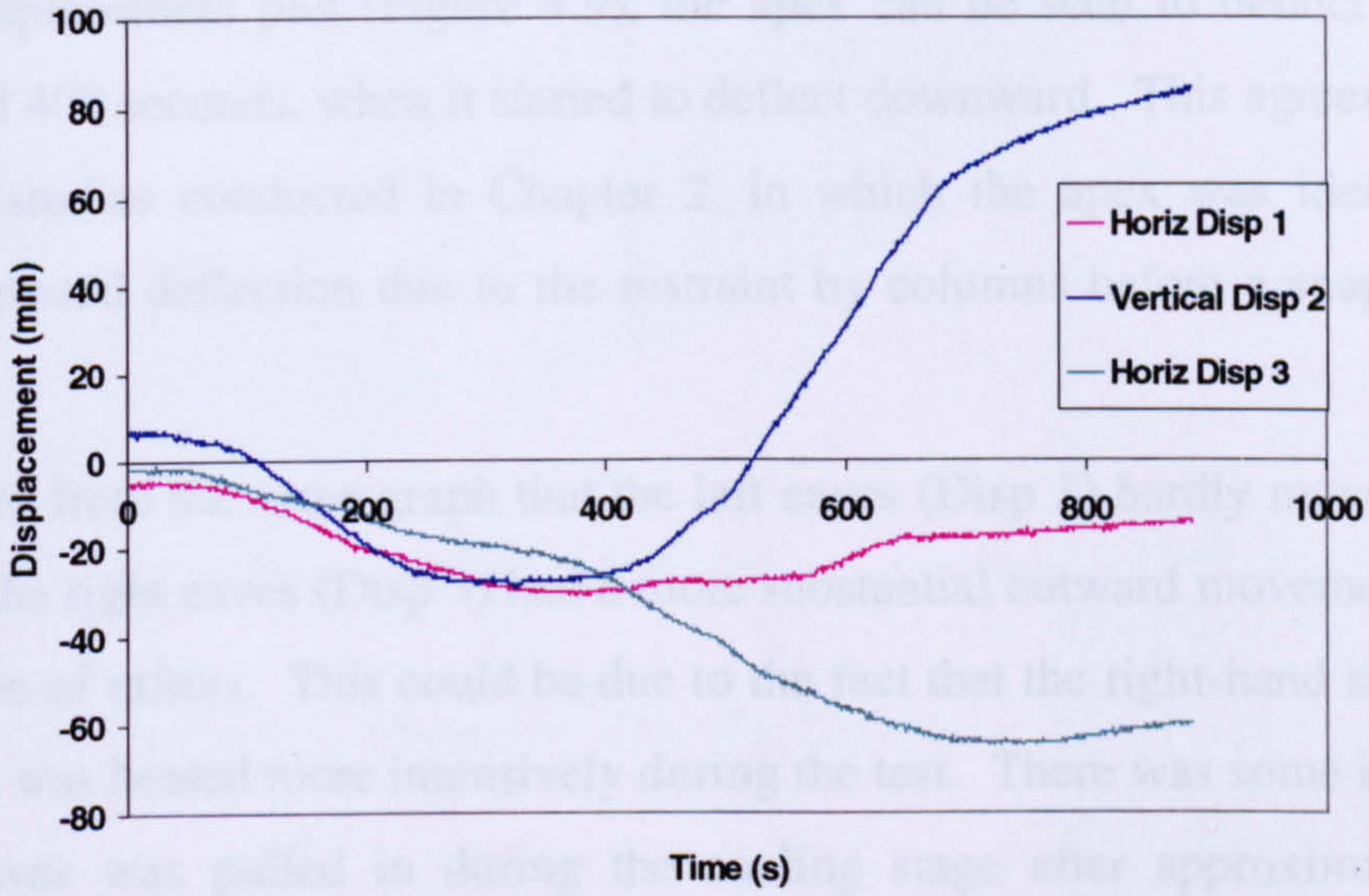

Figure 4.9 Recorded displacements during the first test

From the temperature plots, the hottest part of the portal frame was the apex and the temperature gradually reduced towards the two eaves (Steel 3 and Steel 14). Heating was more intense across the right rafter due to the air movement, which resulted in a higher temperature at the right eaves. The column sections below the level of the heating tray remained below 150°C, as recorded by steel 1, 2, 15 and 16. Cooling

started to take place as soon as the fuel finished burning, after approximately 600 seconds.

The temperature difference between the top and bottom flanges at the apex was almost negligible, but a temperature gap of up to 55° was seen at the left eaves. The top flange was hotter than the bottom flange at both locations. Figure 4.10 compares the temperatures at these locations.

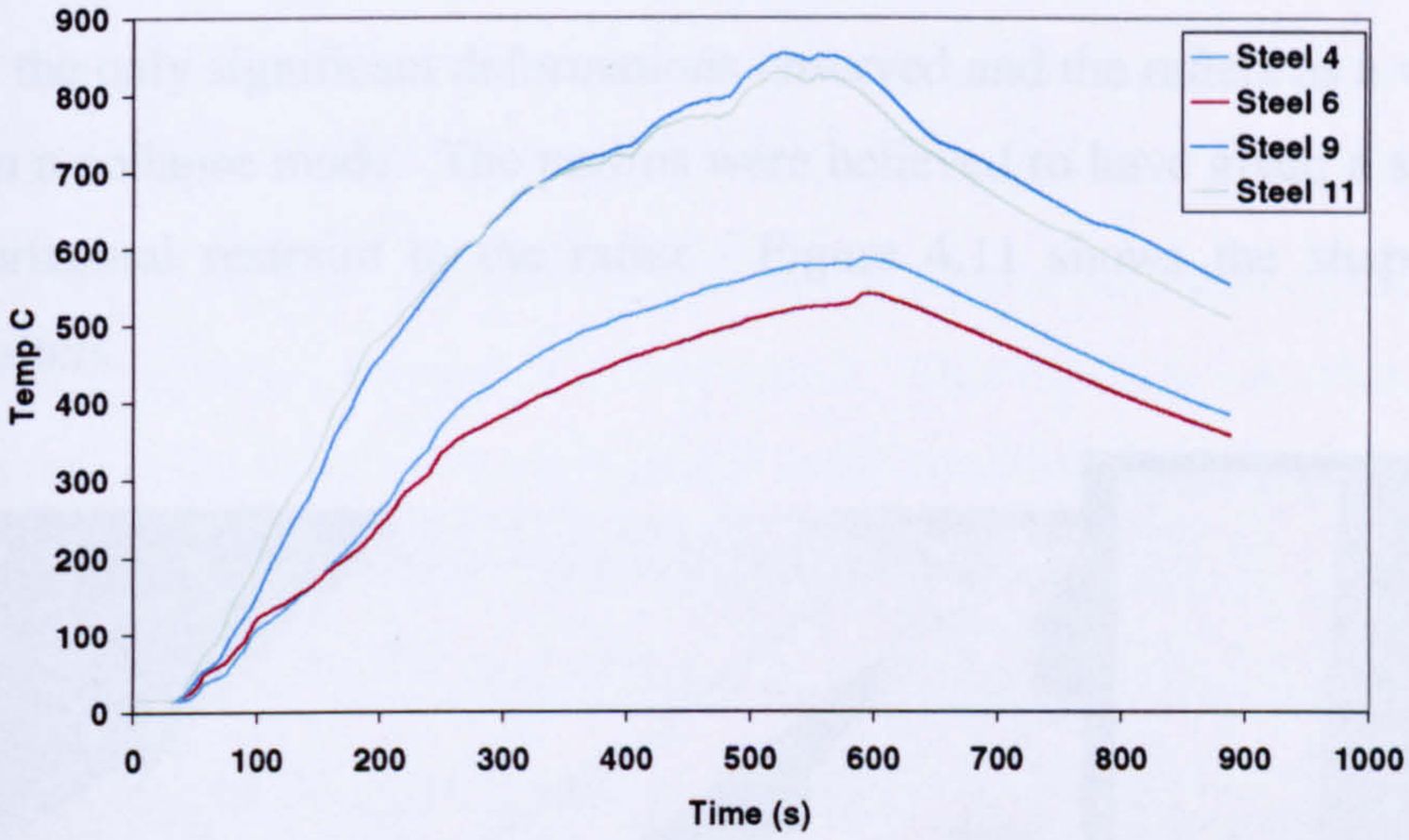

Figure 4.10 Temperature comparison between top and bottom flanges

From the displacement plot (Figure 4.9), the apex can be seen to deflect upwards initially until 400 seconds, when it started to deflect downward. This agrees with the preliminary studies conducted in Chapter 2, in which the apex was identified as having an upward deflection due to the restraint by columns before a snap-through took place.

It can be seen from the same graph that the left eaves (Disp 1) hardly moved during the test but the right eaves (Disp 3) had a more substantial outward movement due to the expansion of rafters. This could be due to the fact that the right-hand side of the portal frame was heated more intensively during the test. There was some indication the right eaves was pulled in during the cooling stage after approximately 700 seconds.

4.2.2 Post-test Inspection

On inspecting the portal frame visually after the test, it was found that the whole of each rafter had been deflected into an S-shape in the vertical plane. The mid-span purlin point (which is also one of the three loaded positions) appeared to be the point

with zero curvature. The upward bowing of the half rafter near to the eaves may be explained by the temperature difference between top and bottom flange recorded by from the thermocouples. However, the extent of damage due to this phenomenon is insignificant.

On the hotter half of the frame, the rafters had deformed laterally to a certain extent with a slight rotation. This is due to the fact that the top flange was restrained by the purlin, where as the bottom flange was free to deform.

These were the only significant deformations observed and the rafters as a whole had not failed in a collapse mode. The purlins were believed to have given a substantial level of horizontal restraint to the rafter. Figure 4.11 shows the shapes of the deformed rafters.

Figure 4.11 The Rafter deformations after the first test

4.2.3 Computer Analysis

The first fire test was modelled with the finite element program VULCAN. Due to the nature of the test, in which only one portal frame was heated and the others remained relatively cool, a two dimensional analysis should be sufficient at this stage for the purpose of comparison. The cross bracing between columns should provide

significant lateral restraint, especially since most of the columns stayed cool below the burning tray.

The temperature profile for the model was input as obtained from the thermocouples; this was considered sufficient to represent the overall test situation accurately.

However, one of the major uncertainties for the modelling was to predict the rotational stiffnesses of the base connection. It is believed that significant stiffness exists at the base, although the connections had been made as simple as possible. It was found during the analysis that the base rotational stiffness affects the amount of deflection significantly.

Two analyses were therefore conducted, one with a pinned-base assumption and the other with a semi-rigid connection of 2 kNm/mrad. This figure is considered to be a reasonable finite value between the imaginary fixed and pinned assumptions used by the program, from the previous investigation into the base stiffness.

The results in terms of displacement from the VULCAN analysis were plotted against temperature and compared against the experimental figures. The reference temperature was taken as the highest temperature in the steel, and the comparison was made at the apex and the two eaves. Figure 4.12, 4.13 and 4.14 show the comparison at left eaves, right eaves and apex respectively.

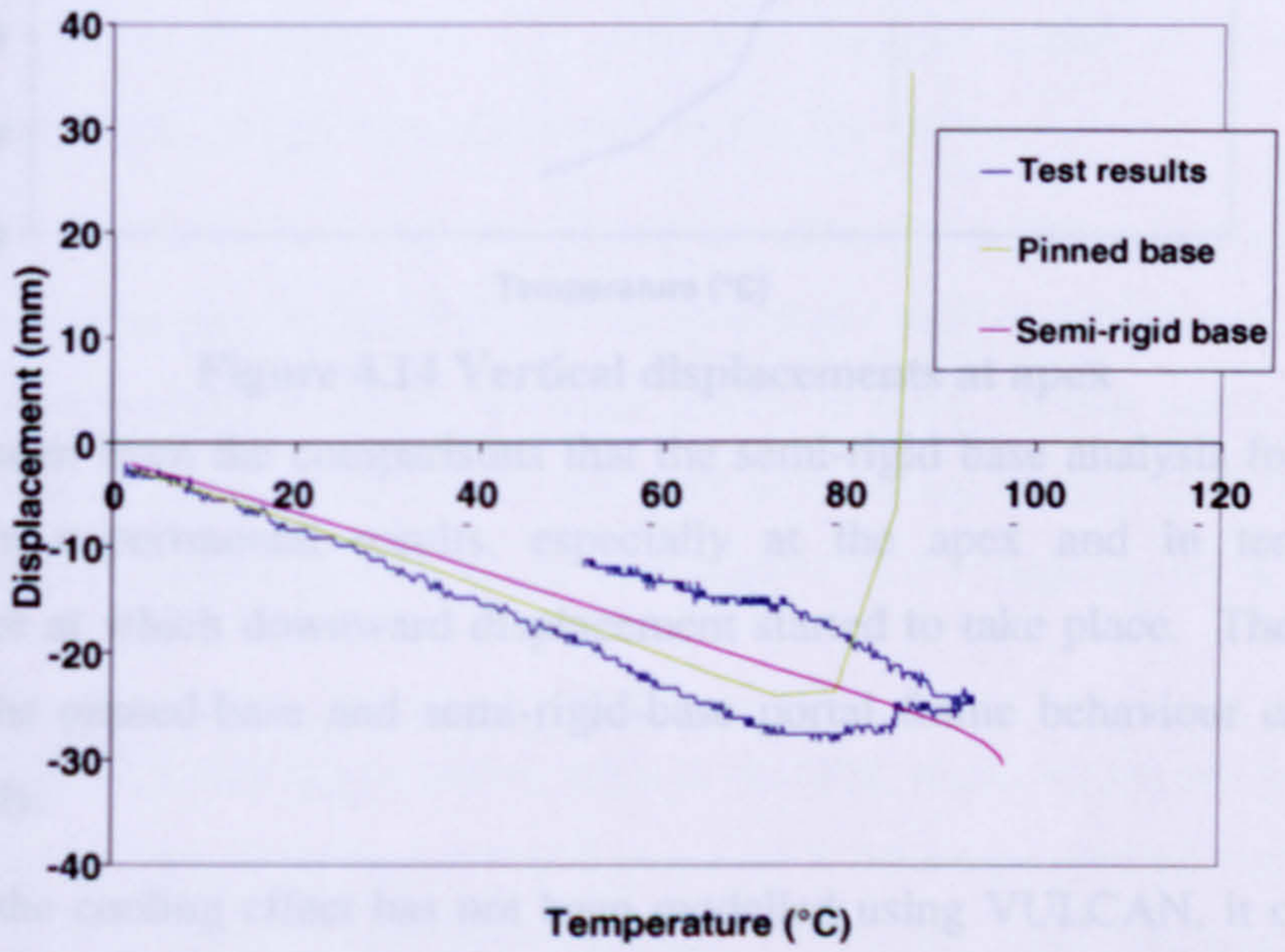

Figure 4.12 Horizontal displacements at left eaves

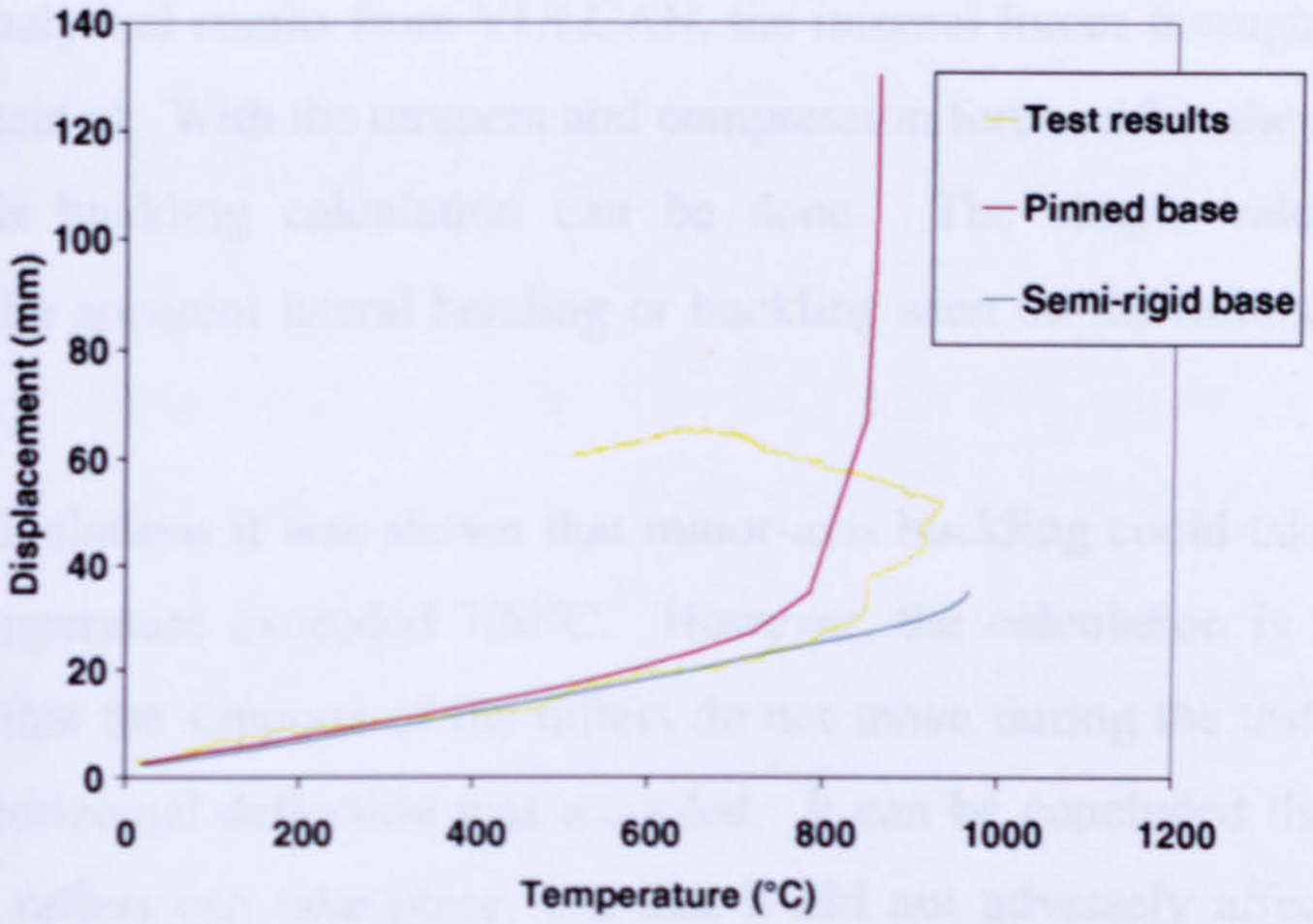

Figure 4.13 Horizontal displacements at right eaves

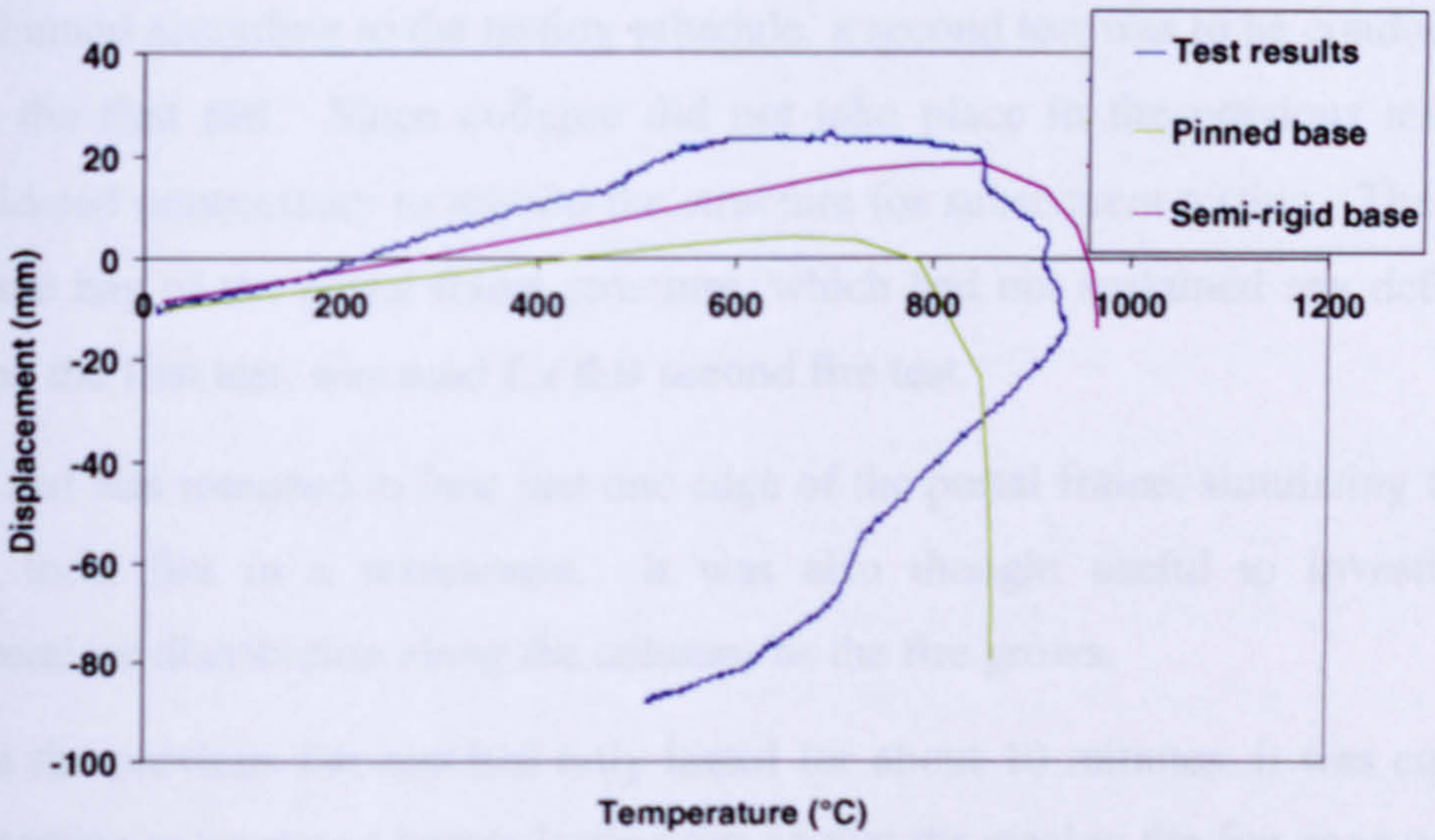

Figure 4.14 Vertical displacements at apex

It can be seen from the comparisons that the semi-rigid base analysis follows more closely the experimental results, especially at the apex and in terms of the temperature at which downward displacement started to take place. The difference between the pinned-base and semi-rigid-base portal frame behaviour can be seen quite clearly.

Although the cooling effect has not been modelled using VULCAN, it can be seen from the experimental curves that permanent strains within the test frame were apparently present. The frame could be near to the failure stage if it had been heated further.

Using the analytical results from VULCAN, the internal forces throughout the frame could be obtained. With the moment and compression force within the rafter section, a minor-axis buckling calculation can be done. The simple calculation is to investigate the apparent lateral bending or buckling seen on the rafters after the test (Figure 4.11).

From the calculations it was shown that minor-axis buckling could take place when the steel temperature exceeded 720°C. However, the calculation is based on the assumption that the supports of the rafters do not move during the test, while small amount of horizontal deflection was recorded. It can be concluded that minor-axis buckling of rafters can take place, but that it did not adversely affect the overall behaviour of the portal frame in fire.

4.3 The Second Experiment - Edge Fire Test

As planned according to the testing schedule, a second test was to be conducted soon after the first test. Since collapse did not take place in the previous test, it was considered unnecessary to rebuild the structure for subsequent testing. The adjacent internal bay of the portal frame structure, which had not sustained any deformation during the first test, was used for this second fire test.

This test was intended to heat just one edge of the portal frame, simulating the effect of a local fire in a warehouse. It was also thought useful to investigate the temperature distribution along the columns as the fire grows.

Since the previous fire test had only lasted for about 10 minutes, it was considered appropriate to arrange a longer-lasting fire so that the steel in the fire zone could stay at the maximum temperature for a longer period of time. It was again intended to create a collapse mechanism in this test, and preliminary studies indicated that the steel temperature would have to reach over 1000°C if a collapsing portal frame was to be seen.

It was therefore decided to use timber cribs as the fuel, replacing the burning tray and heptane. The timber cribs were stacked in a 1 x1 x 2m shape, placed underneath the rafters of the test frame at the left-hand edge. The cribs were estimated to have a burning-time of more than an hour.

The front of the structure was again left open again for ventilation purposes. The testing conditions and all measurement devices were similar to the first test. All the measuring devices, including the reference frame outside the portal frame, were moved to the location of the new test frame.

Figure 4.15 shows the test. It can be seen that flame front extended almost to the apex of the structure, with the entire left-hand column engulfed in fire.

Figure 4.15 The second fire test: Early stages

The entire test lasted for well over 40 minutes before the fire was manually extinguished. The compartment temperature achieved a state of equilibrium after approximately 10 minutes, when the heat input balanced the loss of heat to the surroundings. This equilibrium state prevented a further increase in temperature. The hottest part of the steel achieved a similar temperature to the fire atmosphere and stayed unchanged for approximately 30 minutes. Most of the rafter achieved an equilibrium temperature which continued for at least 30 minutes.

The maximum steel temperature recorded was about 800°C. With this temperature, it was not surprising to see no collapse mechanism of the portal frame during the test. Beside this, there was no significant asymmetric movement or deformation observed throughout the test, although one half of the frame was much hotter than the other. A decision was made to terminate the test after the fire had burned for 40 minutes.

4.3.1 Experimental Results

Figure 4.16 plots the steel and gas temperatures recorded during the fire test, along with the Standard ISO 834 fire curve. The gas temperature of the hottest part matches the ISO curve well, by pure coincidence.

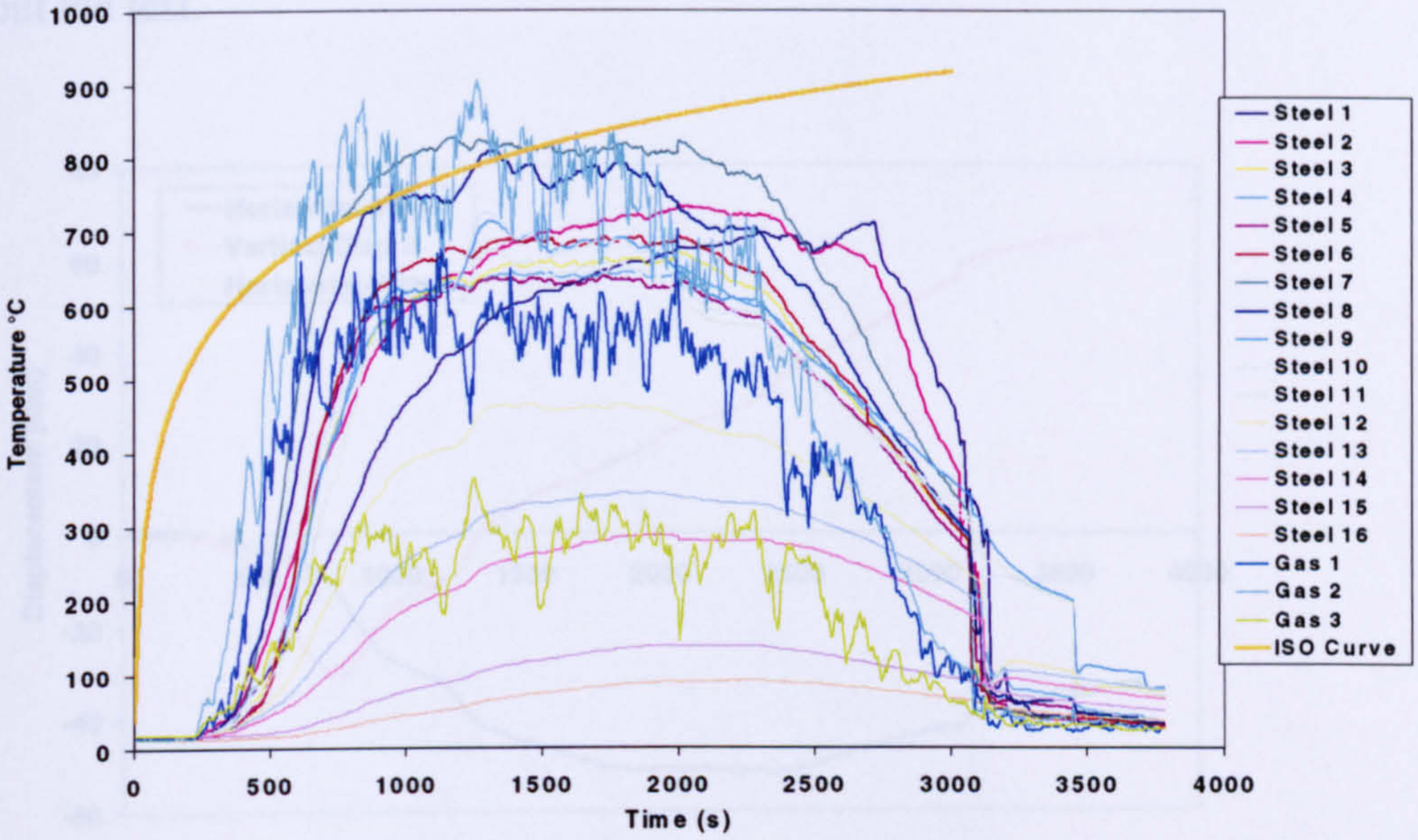

Figure 4.16 Temperatures recorded throughout the second fire test

While comparing the gas temperatures at the three different positions, it was found that the apex within the compartment was the hottest part, with a maximum temperature of 870°C. This effect was first encountered during the indicative test where the steel sheeting collected the hot gas and channelled it to the higher part of the structure, rather than the eaves. The unheated eaves remained relatively cool, with a maximum temperature just below 320°C.

Comparing the top and bottom flange temperatures at apex and eaves, the difference between them was almost negligible. This is because the rate of heating is relatively slow with the burning cribs, compared to the rapid ignition of the heptane used in the previous test. The longer-lasting test also enabled the temperature to be distributed more evenly to the entire section rather than just heated locally.

The temperature distribution along the column near the fire was rational. The mid-section temperature was very similar to that at the top of the column; the bottom of the column heated more slowly but eventually caught up with the top part. As for the cooler half of the frame, temperatures reduced as the distance from fire increased, with the bottom of the column temperature remaining close to ambient temperature.

Figure 4.17 shows the displacements measured during the fire test. Since only one side of the portal was heated vigorously, the vertical displacement was predictably smaller compared to the first test. The vertical displacement at the apex was approximately 80mm, and the heated eaves (Disp 3) sustained a larger horizontal deflection than the cooler eaves. The cooler eaves sustained negligible movement throughout the test.

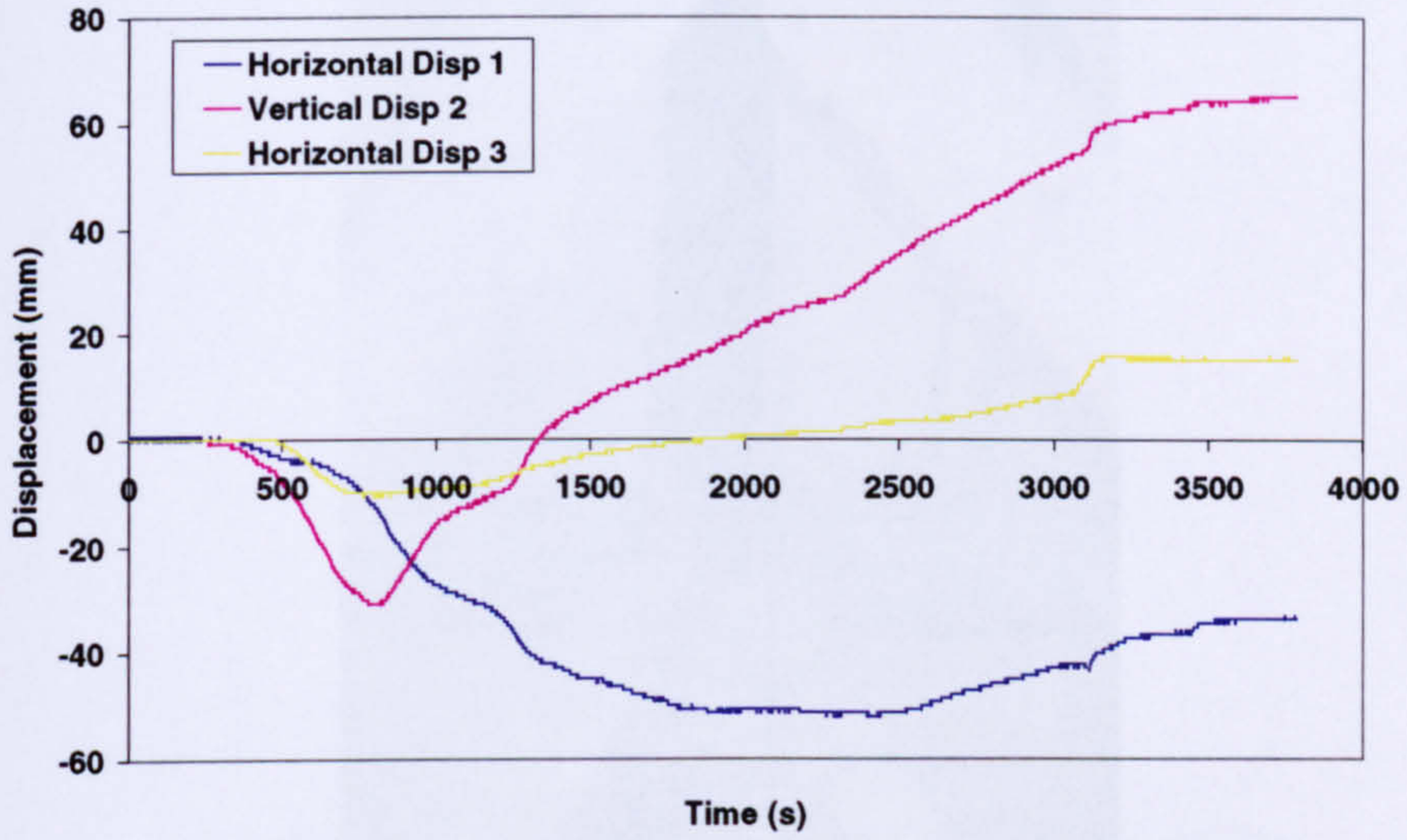

Figure 4.17 Recorded displacements for the second fire test

4.3.2 Post-test Inspection

Although this fire lasted longer than the first test, the temperatures were not as severe. Due to the asymmetric heating of the frame there was a slight swaying to the left, which could not be detected visually.

Apart from this, the local deformations observed were very similar to those in the first test, where the most apparent visual deformation was lateral bending over the hottest part of the rafters, buckling between purlin points. This could be anticipated since the previous calculation on combined bending and compression had indicated that minor-axis buckling could take place at temperature in excess of 750°C. Again, an S-shape deformation in the vertical plane could be seen on the rafters. Figure 4.18 shows the lateral deformation of the rafters.

It is interesting to see that even when the majority of the column was heated to approximately 700°C, there was no visible local or overall deformation of the column. Its post-test condition was almost intact apart from some char marks.

Similarly, the cladding and purlins did not sustain any significant damage, in the sense that they stayed intact on the roof and the side façade throughout the test. Minor twisting and bending were seen on the purlins. However, the cladding and purlins were relatively lightly loaded compared to their normal state when used in a real portal frame warehouse.

Figure 4.18 Lateral deformation of rafter from the second fire test

The detail of the deformed shape and the amount of displacement sustained was recorded by measuring after the frame had cooled down.

4.3.3 Computer Analysis

The test was again modelled with VULCAN, applying the same assumptions as in the previous modelling. The temperatures recorded from the testing were fed into the input file as closely as possible. The same frame was modelled with pinned base and semi-rigid base connections.

The vertical displacements at the apex and the horizontal displacements at the two eaves were extracted from the analytical output. These were then plotted on the same graph together with the experimental data, so that the comparison could be seen. Figure 4.19, 4.20 and 4.21 show the plots, in which the displacements have been plotted against the highest temperatures in the steel so that a more comprehensive comparison can be made.

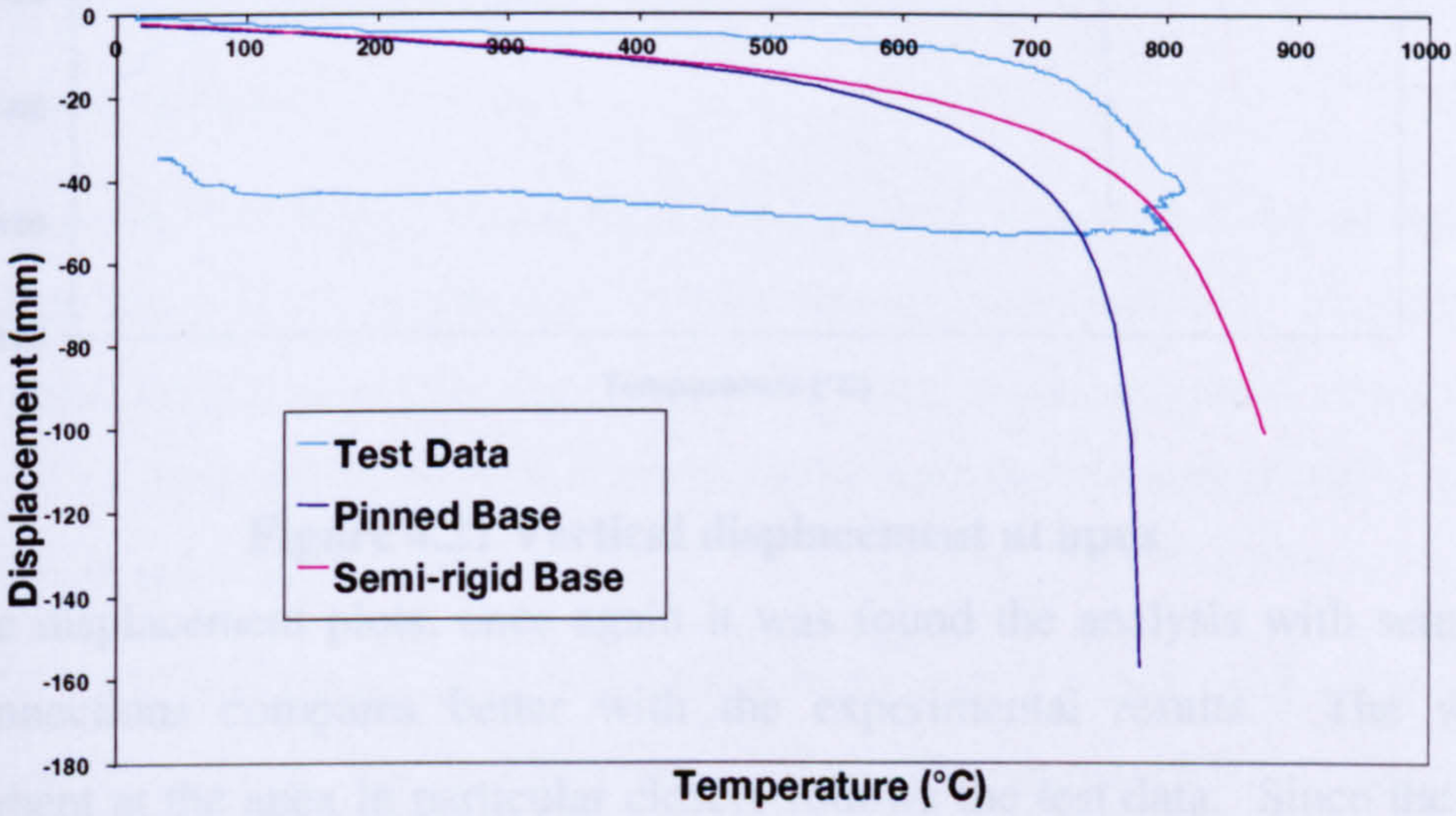

Figure 4.19 Horizontal displacement at left eaves

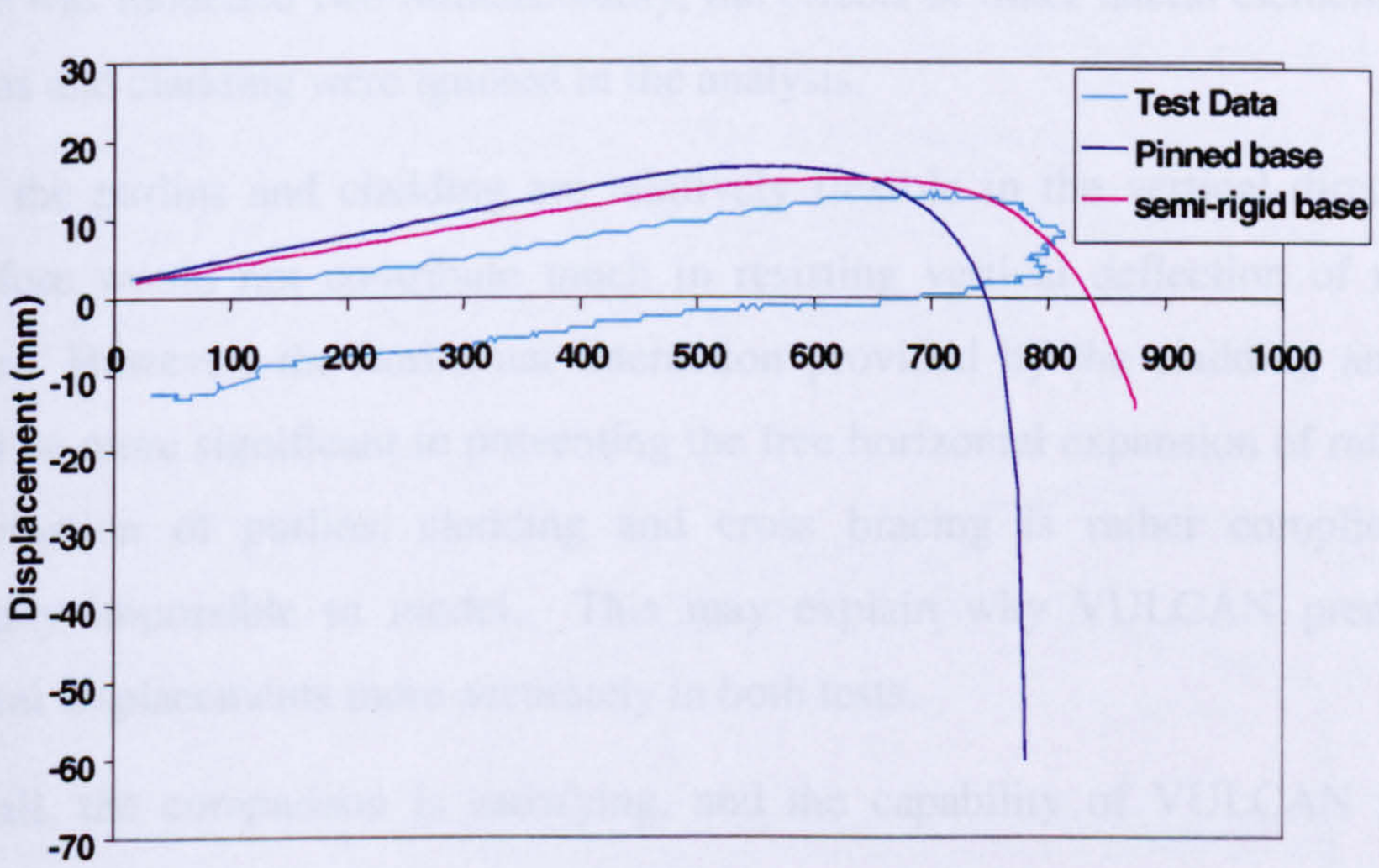

Figure 4.20 Horizontal displacement at right eaves

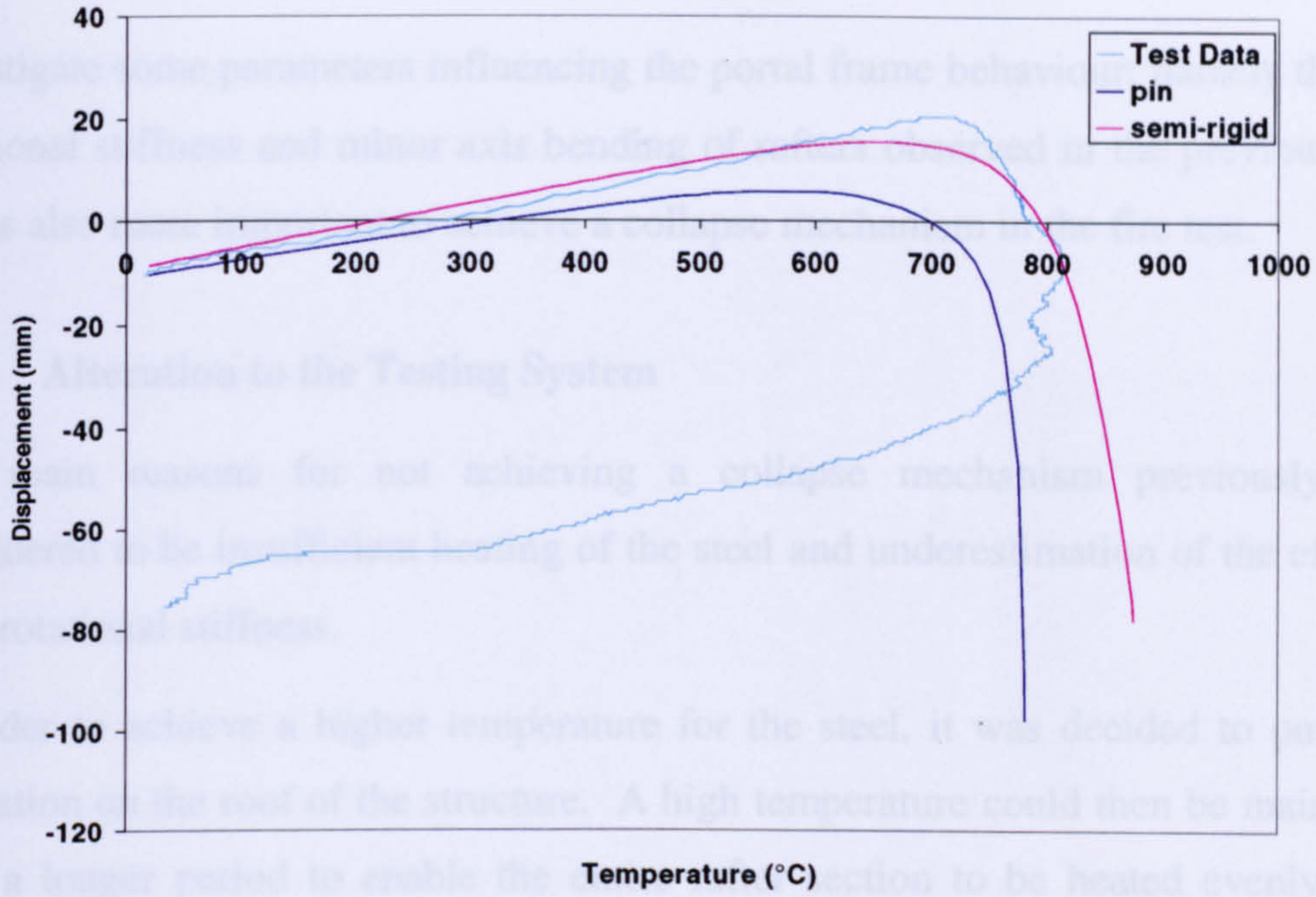

Figure 4.21 Vertical displacement at apex

From the displacement plots, once again it was found the analysis with semi-rigid base connections compares better with the experimental results. The vertical displacement at the apex in particular closely follows the test data. Since the portal frame was modelled two-dimensionally, the effects of other lateral elements such as purlins and cladding were ignored in the analysis.

Both the purlins and cladding are relatively flexible in the vertical direction, and therefore would not contribute much in resisting vertical deflection of the portal frame. However, the horizontal interaction provided by the cladding and purlins could be more significant in preventing the free horizontal expansion of rafters. The combination of purlins, cladding and cross bracing is rather complicated and virtually impossible to model. This may explain why VULCAN predicted the vertical displacements more accurately in both tests.

Overall, the comparison is satisfying, and the capability of VULCAN is further validated.

4.4 The Third Test – Overall Rafter Heated

It was rather disappointing not to have a structural collapse in the previous two tests. It was planned to have the following test reproducing the heating scenario of the first one, (i.e. overall rafters heated). Several refinements were made to the test frame to

investigate some parameters influencing the portal frame behaviour; namely the base rotational stiffness and minor axis bending of rafters observed in the previous tests. It was also more important to achieve a collapse mechanism in the fire test.

4.4.1 Alteration to the Testing System

The main reasons for not achieving a collapse mechanism previously were considered to be insufficient heating of the steel and underestimation of the effect of base rotational stiffness.

In order to achieve a higher temperature for the steel, it was decided to put some insulation on the roof of the structure. A high temperature could then be maintained over a longer period to enable the entire rafter section to be heated evenly. The majority of the length of the rafters would have to reach an average of 900°C to have a more significant failure.

The use of liquid heptane as fuel is efficient in heating, and a controllable fuel supply system was devised as shown in Figure 4.22. The liquid heptane reached the burning tray at a rate controlled by its natural pressure difference through the connecting pipe, and a valve was fitted onto the pipe so that more fuel could be provided during the fire if necessary. This was to ensure a continuous combustion until collapse of the frame occurred. The burning tray was slightly tilted so that the heptane could reach the end remote from the feeding point.

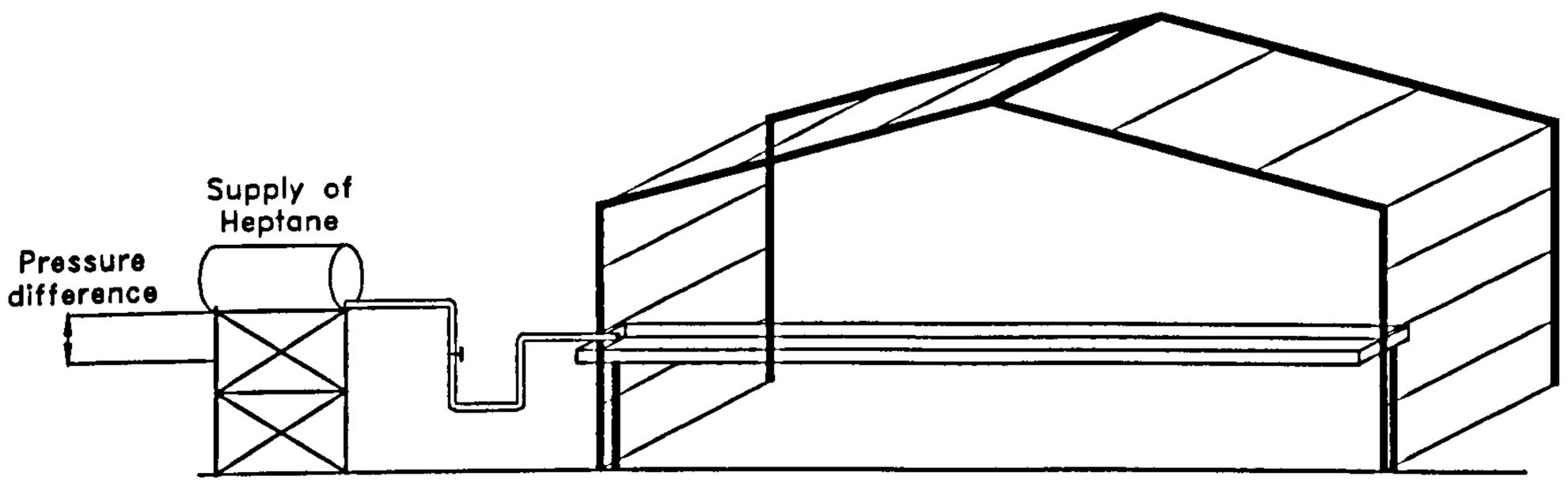

Figure 4.22 Fuel supplying system

On the portal frame itself, the two internal frames were rebuilt after the first two tests. An attempt was made to achieve pinned base conditions to the greatest extent possible for the test frame. This was intended to eliminate the uncertainty from the VULCAN analysis.

To enable free rotation at the base, a bar of approximately 6mm diameter was placed underneath the base plate of the column. All the nuts were loosened so that the base plate could rotate freely. Figure 4.23 shows the details.

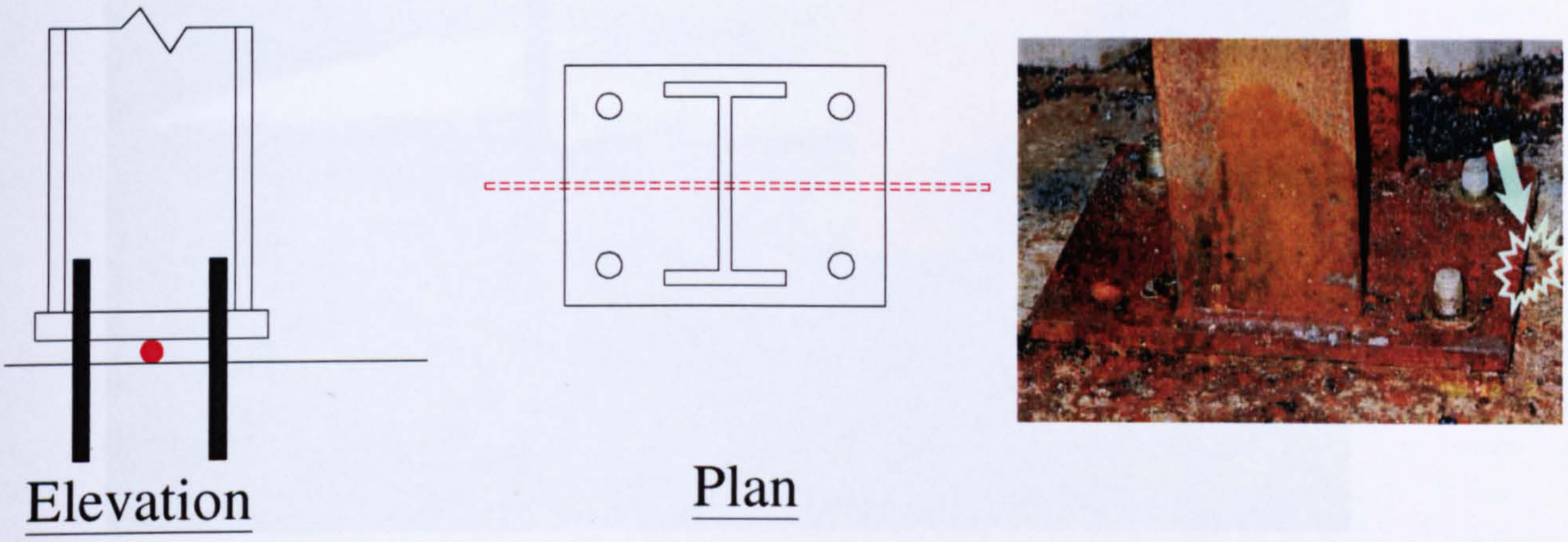

Figure 4.23 Base connection details

To counteract the lateral buckling found in the exposed rafter zone between purlins, it was decided to weld one steel strip between frames mid-way between adjacent purlin points, parallel to the purlins. The steel strip was attached to the top flanges of the rafters by welding, and reduced the effective buckling length of the rafter about its minor axis. However, having artificially created a pinned base for the columns, the axial thrust within the rafters was expected to be lower due to the reduced restraint at the column tops.

4.4.2 The Test

With the testing experience gained from the previous two fire tests, the setting-up of this test went relatively smoothly. A video camera was used to record the entire experiment. The fire was ignited with a shallow depth of heptane in the burning tray. The entire burning tray was soon ignited, heating the full length of the rafters. Supply of heptane was required occasionally.

Shortly after 5 minutes into the test, the apex was seen to be starting to deflect downward. Without much warning a little later, the apex underwent a vertical dive and the entire rafters were seen to collapse rapidly. This was the snap-through failure always predicted by VULCAN analysis. The alterations proposed for this test had proven to be significant in creating a collapse mechanism. Figure 4.24 shows a picture taken shortly after the snap-through failure, where the flame was still fiercely heating the steel.

Figure 4.24 Snap-through failure during the third fire test

4.4.3 Experimental Results

Figure 4.25 plots the temperatures recorded by the thermocouples during the test. The results can be compared against the ISO 834 fire temperature, although the fire only lasted for approximately 500 seconds. In fact, the displacement plot shown in Figure 4.27 indicates that the snap-through took place at approximately 280 seconds after ignition. Average gas temperature stayed at around 900°C.

With such a short-lived but intense fire, the column section below the fire was not exposed to much radiation and remained near to ambient temperature throughout the test. The steel above the burning tray was totally engulfed in flame once the fire was ignited. This was shown from the gas temperature curves, which fall in the same temperature region across the whole portal frame for the duration of the test.

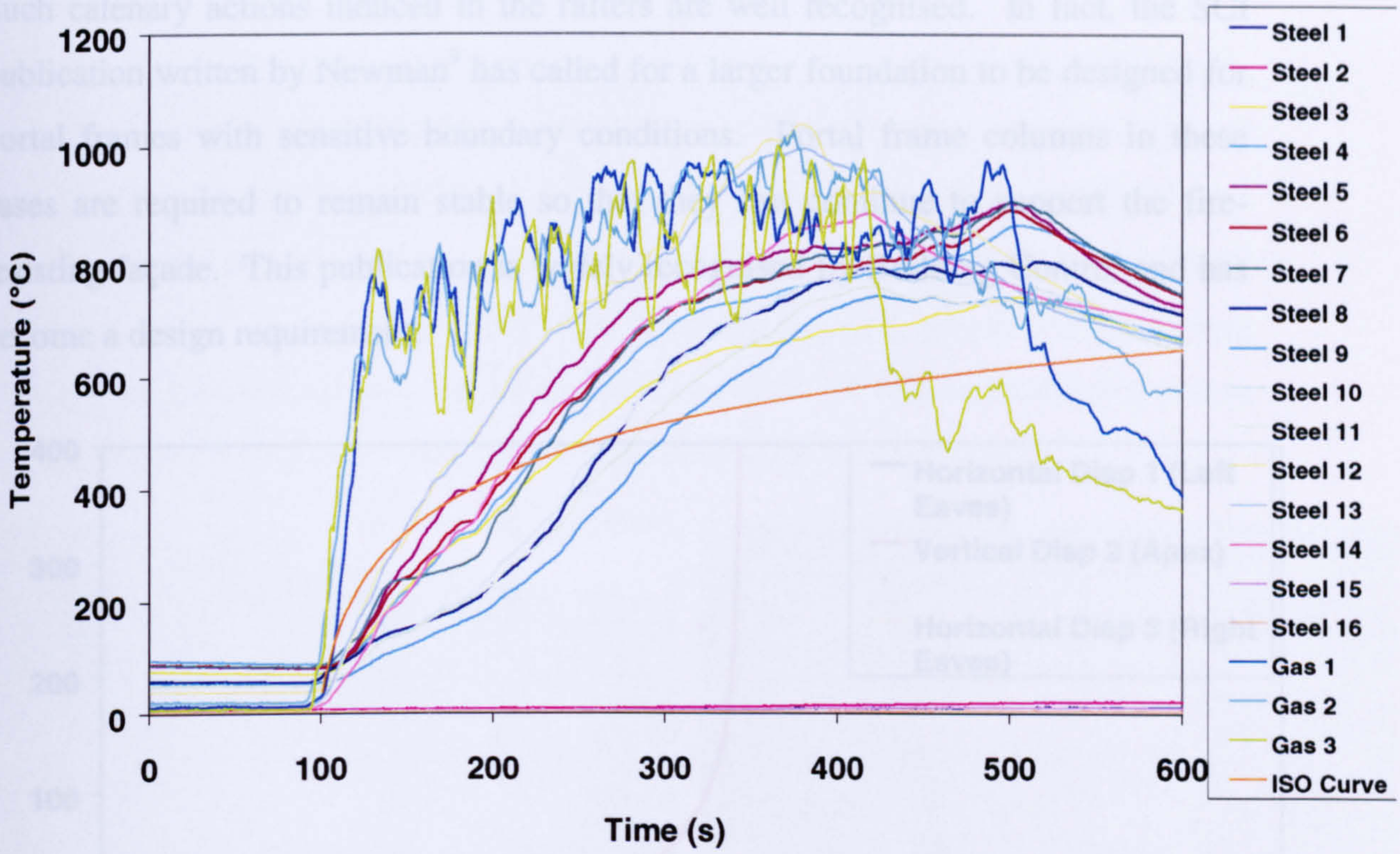

Figure 4.25 Recorded temperatures from the third test

With this intense heating, steel temperatures along the rafters were relatively even. The eaves area appeared to be heating slightly behind the mid-section of the rafters, since the eaves were less exposed to the fire. The temperature difference between the top and bottom flanges was not significant as a result of the totally engulfing fire. Maximum steel temperature reached just below 1040°C at thermocouple S12, which is just right to the apex. It was later found from the inspection after test that a plastic (fire) hinge had formed in this region.

From the plot of displacements shown in Figure 4.26, the apex did not deflect until 300 seconds into the test, when it started to deflect downward quickly and eventually dived vertically. Both eaves were initially deflected outward due to the steel expansion until the snap-through took place, after which they were both pulled inward (the reversal of displacement shown in the curves) by the rafters in catenary action.

Such catenary actions induced in the rafters are well recognised. In fact, the SCI publication written by Newman[9] has called for a larger foundation to be designed for portal frames with sensitive boundary conditions. Portal frame columns in these cases are required to remain stable so that they can continue to support the fire-resisting façade. This publication is widely recognised by Building Control and has become a design requirement.

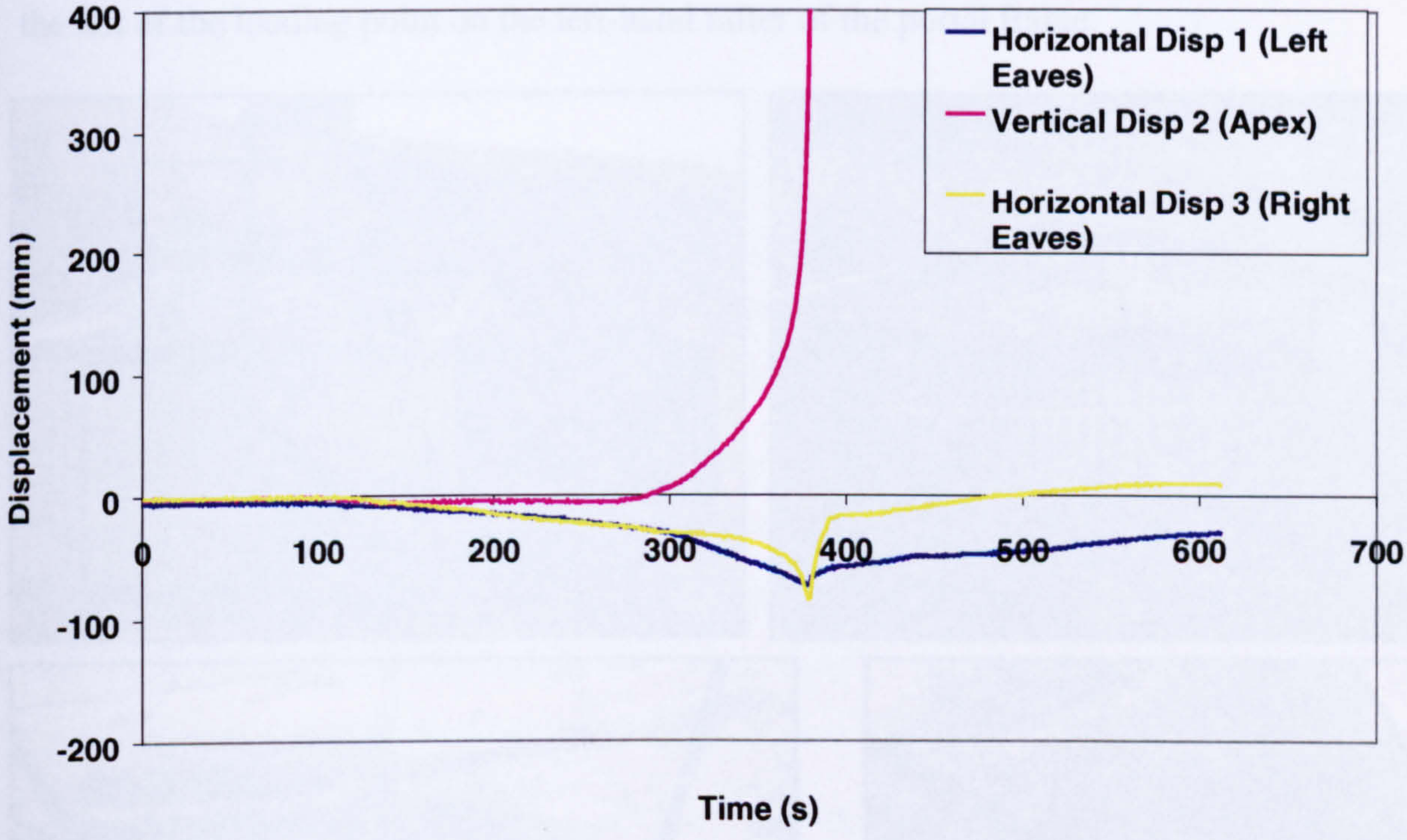

Figure 4.26 Recorded displacements from the third test

If the horizontal displacement graph is investigated more closely, it can be seen that the right-hand eaves (Disp 3) has been pulled in by a bigger margin than the left eaves (Disp 1). In fact, the reversal effect on the left eaves is much gentler compared to the sharp effect at the right eaves. This indicates that the failure of the portal frame was not induced by a "beam mechanism", but was more likely a "combined mechanism". (Obviously the sway mechanism has been ruled out, given the loading details.)

A detailed study on failure modes of portal frames in fire has been conducted, and parametric studies are presented in Chapter 5.

4.4.4 Post-test Inspection

An inspection of the collapsed frame was carried out after the steel had cooled down. A collapse mechanism had been produced in which the rafters had deflected considerably. In fact, the rafters only stopped deflecting when the water-filled barrel touched ground and relieved the vertical load on the rafters. The formation of plastic hinges on the rafters could be clearly seen. Two hinges were seen to be located near to the eaves, one at each side. An additional hinge could be seen to be forming just to the left of the loading point on the left-hand rafter of the portal frame.

Figure 4.27 Collapse of the portal frame (top) and fire hinges formed during the test (bottom)

If the temperatures were uniform along the rafters, bending moments could create four plastic hinges in the snap through situation (two near to the apex and two near to the eaves). However, three hinges is sufficient to induce a snap-through failure in combined mechanism. The form of failure mechanism will be investigated at a later stage in these studies.

Figure 4.27 shows the collapsed shape of the portal frame It can be seen from this figure that the steel rafter section has rotated by approximately 90° about its axis, starting a short distance from the right-hand eaves (at the position of the third plastic hinge formed). The section at this position had detached from the purlins and steel strips which normally provided the restraint against rotation. Such phenomena could happen to industrial portal frames in fire. The purlin section used for the test frame is relatively large compared to the rafter section, and the restraint provided by purlins in a normal portal frame structure will be less compared to the test situation. The rafters will be subject to minor axis bending as soon as this rotation takes place, and become more vulnerable at elevated temperatures.

On the other half of the portal frame the purlin was still attached to the rafters and this rotation did not take place. It is believed that the purlins could help substantially in providing restraint, although they were seen to have deformed rather badly.

Despite the massive deformation sustained by the rafters of the portal frame the columns had remained relatively undamaged. Due to the low level of restraint from the column bases, these bases effectively only resist horizontal force, without resisting bending. It was shown from the thermocouples that the steel of the columns remains almost unheated throughout the transient testing period.

While inspecting the roof cladding, it was found that this was not ripped through during the test, but actually managed to maintain its integrity throughout the test. There was no observation of fire penetration of the roof cladding, even when the portal frame had collapsed. This may be of interest if further research is to be done on the behaviour of steel cladding in fire.

The vertical cladding on the side façade did not sustain any damage. Similarly, the cross bracing did not appeared to have deformed.

Overall, the failure of the portal frame was primarily due to the collapse of the rafters. Higher temperatures and less stiffness at the base connection were the major causes for the differences seen between this test and the first one.

4.4.5 Computer Analysis

VULCAN analysis was again brought into use for modelling of the third test. There was little uncertainty regarding the base rotational stiffness for the test frame as it must be very close to a pinned base due to the special arrangements made.

When a two-dimensional analysis was conducted, it was found that the computer program predicted an earlier failure than happened in the test. The remaining factor which was not modelled was the existence of secondary members, in particular the Z-purlins which had a section depth of 120mm. Although the thickness of the purlins was only1.5mm, they can contribute to the vertical stiffness of the rafters.

A three-dimensional model was set up with purlins simply supported between the adjacent portal frames and attached to the test frame. Figure 4.28 shows the set-up of the model. The purlins were modelled with only two elements each since their detailed behaviour was not the major concern.

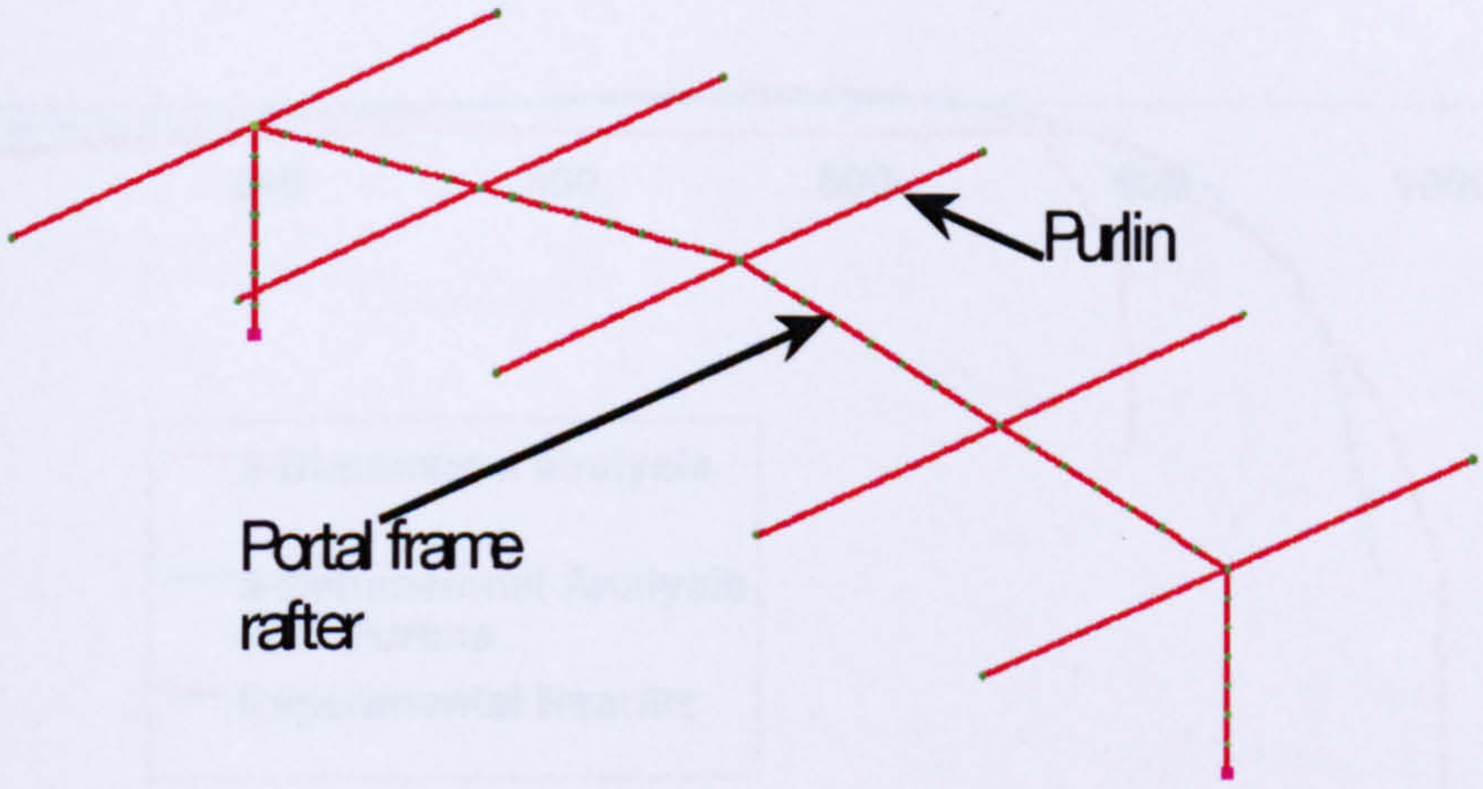

Figure 4.28 Three-dimensional VULCAN model on the third test

The results from the computer analyses were plotted against temperature together with the experimental results. Figure 4.29, 4.30 and 4.31 show the comparisons; the reference temperature is that of the hottest part of the steel. It can be seen from the graphs that three-dimensional analysis, including the purlins, predicted the failure temperature more accurately than the two-dimensional modelling. This again demonstrates that the purlins were beneficial in resisting fire collapse of the tested portal frame structures.

Figure 4.32 shows the predicted shape of the test frame just before failure, using an enlarged vertical displacement scale

Apparently the VULCAN analysis was terminated once the snap-through failure took place, and hence large-displacement movement after failure could not be followed. However, the deflection shown is indeed very similar to the deformation of the portal frame in the test, with the plastic hinge locations matching up with the deformed shape seen in Figure 4.27.

The horizontal displacement predicted by VULCAN was marginally greater than the experimental results. The rationalisation of this may be that the cross bracing and sheeting rails (Z-purlins) attached to the columns were providing additional horizontal restraint which has not been modelled to the column movement. Furthermore, these secondary elements were attached to the adjacent frames which remained relatively cool during the test.

Given the minor uncertainty about the effect of the secondary elements, the VULCAN prediction was considered satisfactory in analysing this structural system.

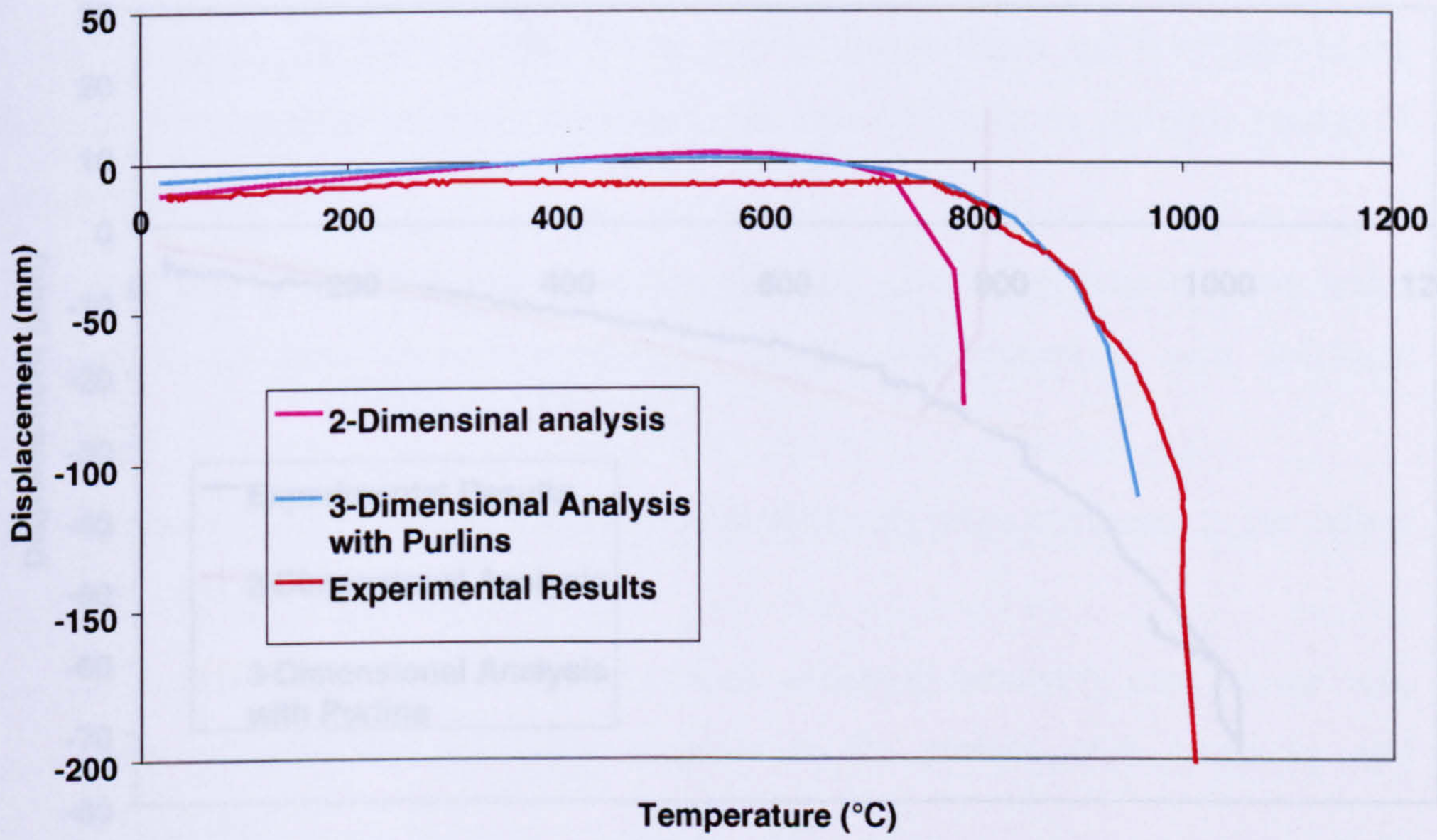

Figure 4.29 Vertical displacement at apex

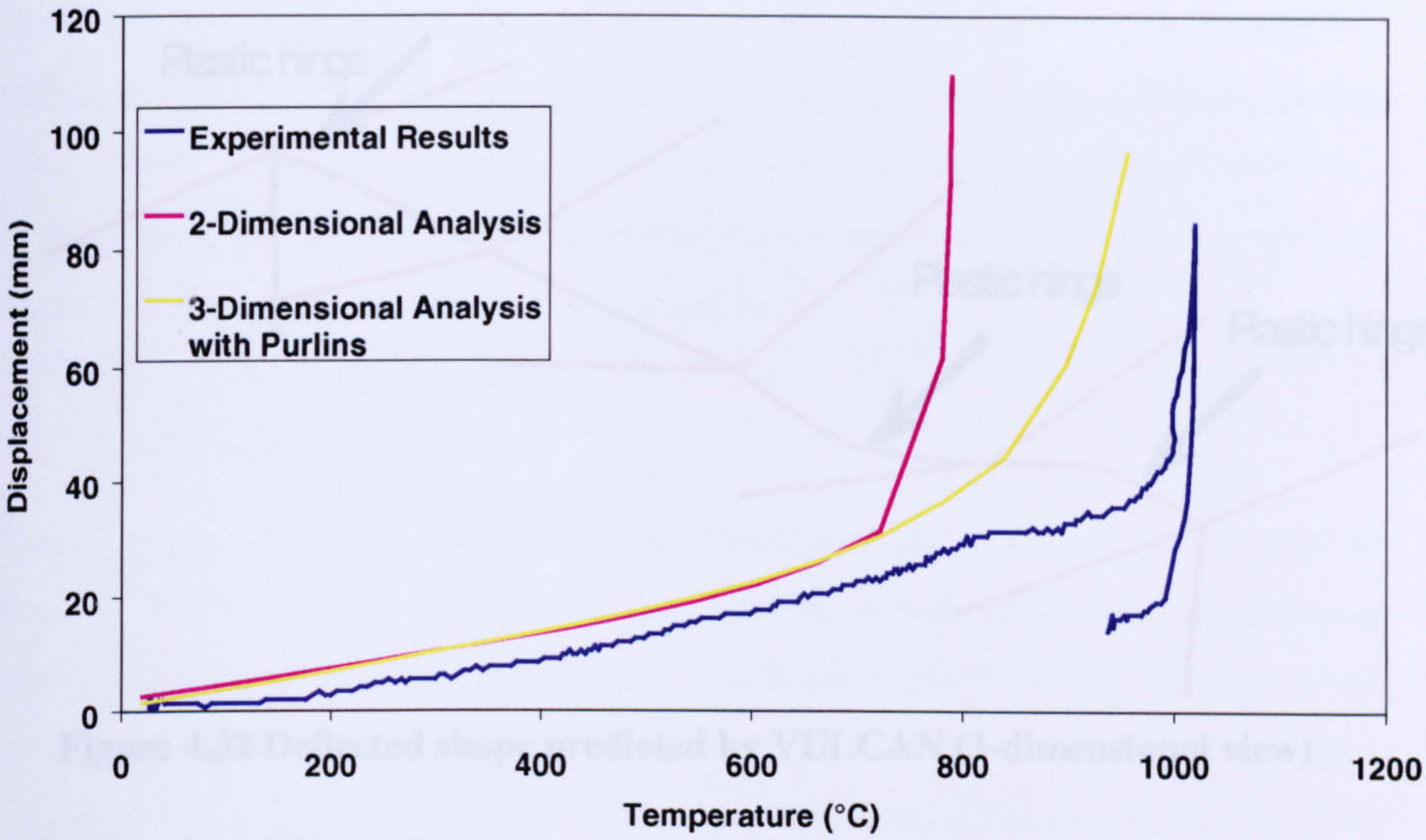

Figure 4.30 Horizontal displacement at right eaves

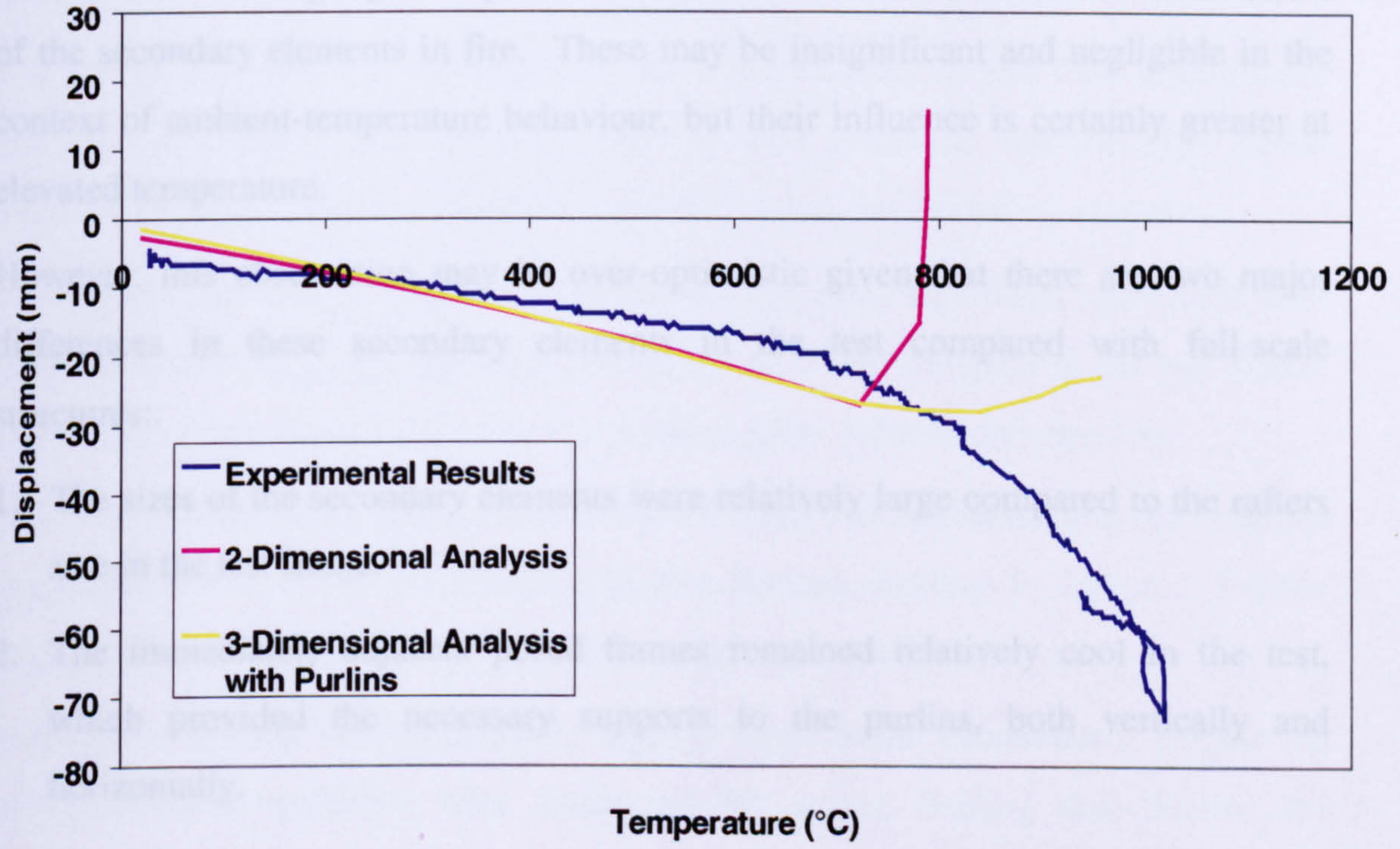

Figure 4.31 Horizontal displacement at left eaves

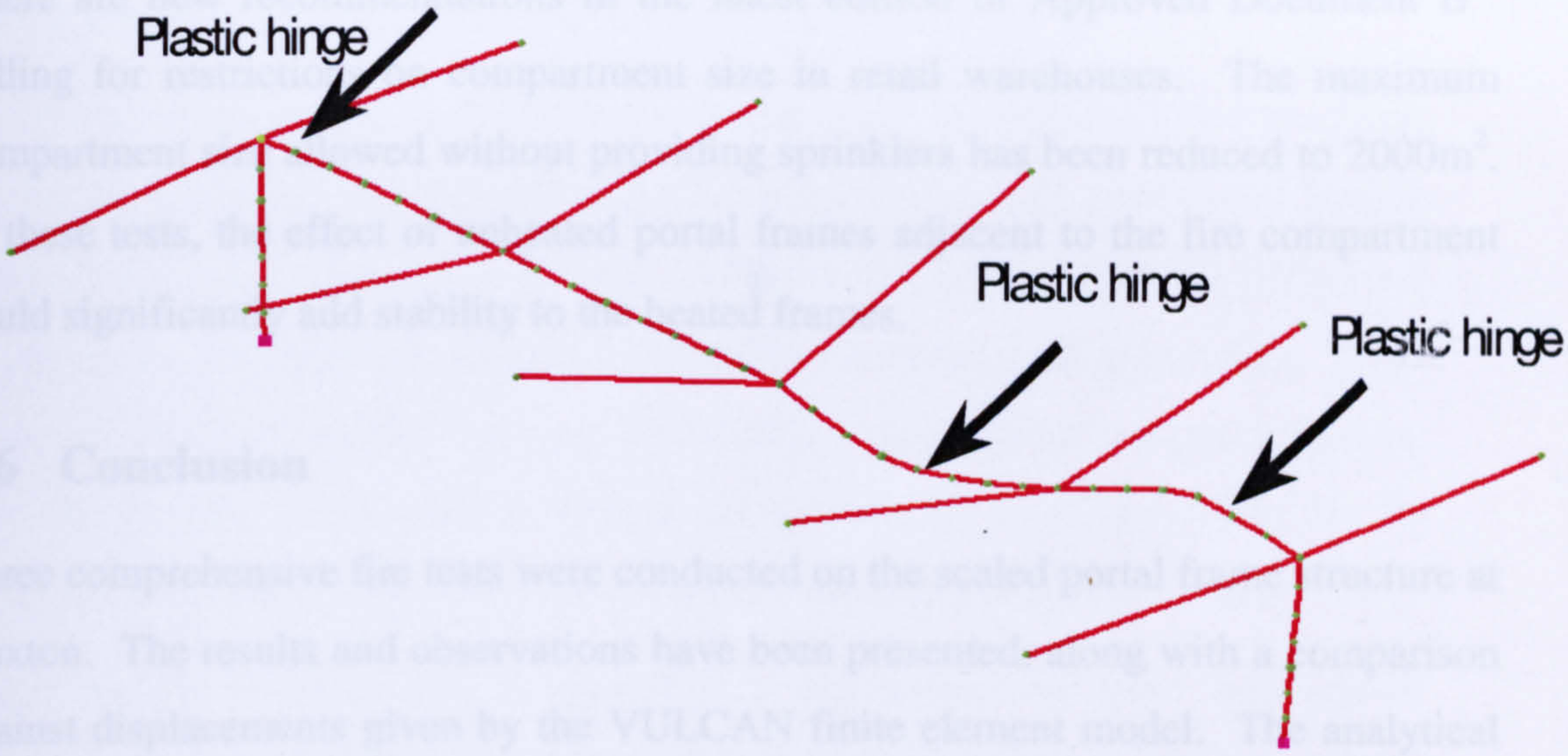

Figure 4.32 Deflected shape predicted by VULCAN (3-dimensional view)

4.5 Further Discussion

One of the issues highlighted by the three fire tests conducted at Buxton is the effect of the secondary elements in fire. These may be insignificant and negligible in the context of ambient-temperature behaviour, but their influence is certainly greater at elevated temperature.

However, this observation may be over-optimistic given that there are two major differences in these secondary elements in the test compared with full-scale structures::

1. The sizes of the secondary elements were relatively large compared to the rafters size in the test frame.
2. The immediately adjacent portal frames remained relatively cool in the test, which provided the necessary supports to the purlins, both vertically and horizontally.

Because of the very local heating, unless there is a total burn-out of the entire portal frame structure, there will always be some cooler portal frames which can provide extra strength to the hotter ones. A total flashover within a large compartment is however rarely seen, statistic figures and discussions[12,54,55,56] are available for further investigation.

There are new recommendations in the latest edition of Approved Document B[57] calling for restrictions on compartment size in retail warehouses. The maximum compartment size allowed without providing sprinklers has been reduced to 2000m^2. In these tests, the effect of unheated portal frames adjacent to the fire compartment could significantly add stability to the heated frames.

4.6 Conclusion

Three comprehensive fire tests were conducted on the scaled portal frame structure at Buxton. The results and observations have been presented, along with a comparison against displacements given by the VULCAN finite element model. The analytical results are close to the experimental data taken from the tests, which provides confidence in using VULCAN to analyse portal frames. Parametric studies were therefore planned to investigate further their behaviour at elevated temperatures using VULCAN.

The results and post-test investigations have been described and their significance has been discussed, including the effect of base rotational stiffness, the lateral buckling of rafters, rotation of rafters and the effect of the secondary elements.

Having seen no collapse mechanism in the first two tests, significant alterations were made to the set-up of the third test, which led to a total collapse of the test frame. The third test was the most significant, yielding some valuable information.

The failure mode of the portal frame in the third test was examined, and the evidence suggested that a combined mechanism had formed, leading to failure. Further investigation will be conducted within the parametric studies.

In general the tests were successful, with no major faults encountered, despite the complication of recording data, setting up the correct loading and creating the intended fire scenarios.

5 Parametric Studies 1 -Two Dimensional Analysis

Much of the work illustrated in the previous chapters has demonstrated that the finite element model VULCAN can be used to predict the behaviour of steel portal frames in fire with reasonable accuracy. Further understanding of portal frame behaviour can be gained by investigating various factors that affect the failure in a fire. Such investigations can be conducted by using VULCAN to analyse series of portal frames, changing the desired factor only in each study so that the resulting effect can be clearly detected and discussed. Such analyses are known as parametric studies.

The major benefit of parametric studies is to avoid conducting large numbers of experiments which can be difficult to control and highly expensive. More detailed studies can also be done by concentrating on just one area at a time. The studies will concentrate on pitched-roof portal frames, as these are the most common form of modern construction for single storey warehouses.

In order to simplify the studies and minimise the computer run time, two-dimensional portal frames are initially defined and analysed, investigating the effect of load ratio, span and height of the portal frames, heating profiles in real fires, horizontal wind forces, base-rigidity and the angle of the pitched roof. Out-of-plane failure and the interaction between adjacent portal frames are not considered. The frame is allowed to deflect out of its plane but no external out-of-plane forces (transverse load) are included in the analyses. The pinned column bases, where applicable, are only allowed to rotate in-plane.

The failure point of the portal frame is defined as the point where an uncontrollably large displacement occurs in a relatively small temperature increment, causing a snap-through of the rafters. The analyses do not continue to model the post-snap-through phase, even if stability is regained later by other means.

The results and discussions are presented in this chapter. They are then related to another series of parametric studies presented in Chapter 6, where three-dimensional portal frames are analysed.

5.1 The Effect of Load Ratio

The effect of vertical load on the behaviour of plane portal frames in fire is investigated in this section. The vertical load is applied as a uniformly distributed load on the roof, defined using a load ratio -the ratio of applied load to the ultimate load capacity of the portal frame. A typical pitched roof portal frame, which spans 30m with column height of 7m is defined and is then designed to resist typical loading. The height of the apex is 11m, which results a rafter inclination of 14.9°. Haunches have not been included in the design since they do not influence the overall behaviour of the portal frame (plastic hinges will form at the ends of the haunches instead of the nearest point to the eaves).

Plastic analysis and design are used to determine the section sizes of the rafters and columns, and pinned bases are assumed during the analysis. Figure 5.1 summarises the layout of the portal frame used for the parametric studies.

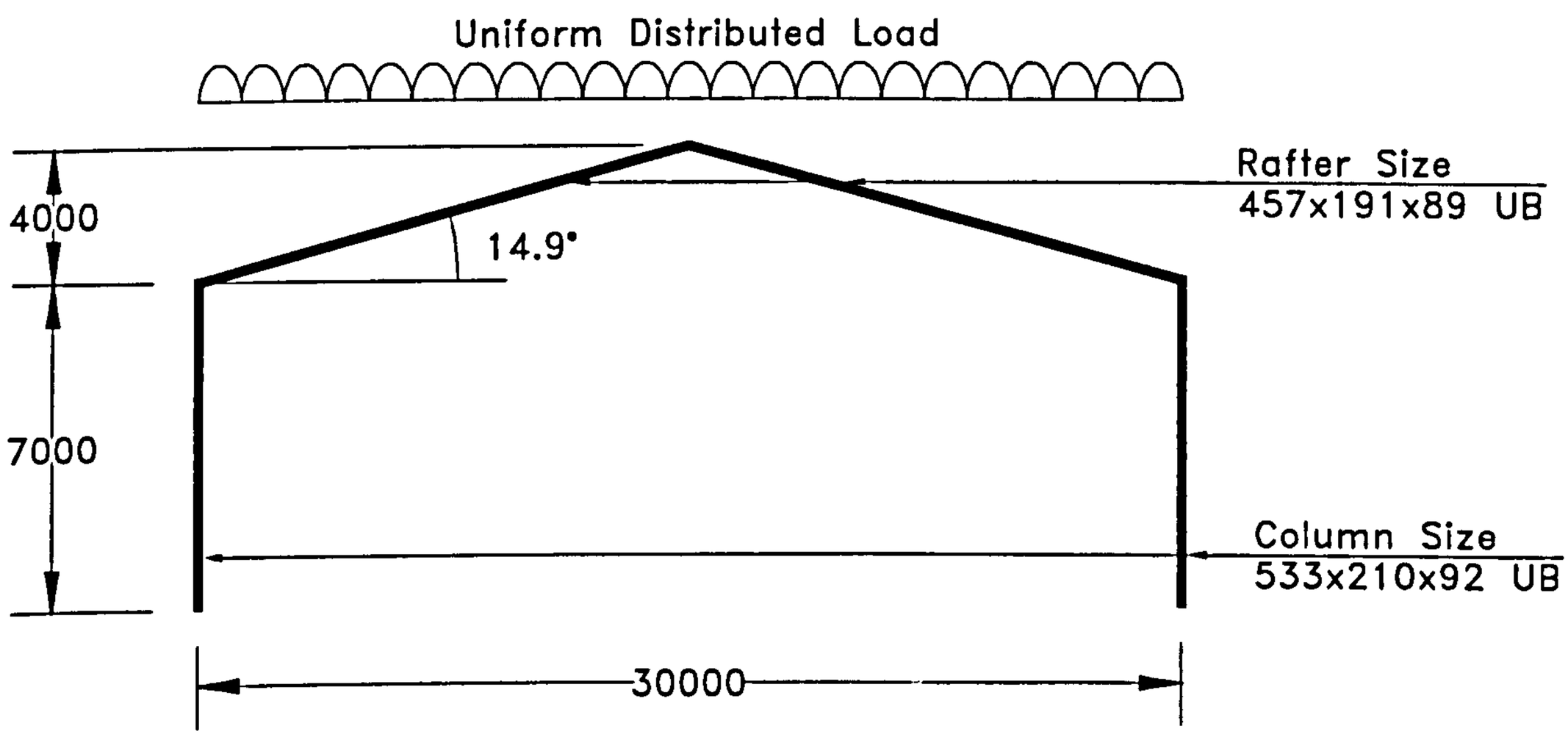

Figure 5.1 Parametric Studies – Load Ratios

Once the geometry of the problem had been set up within VULCAN, different levels of vertical loading were then applied to the rafter, varying the load ratio from 0.1 to 0.8. A very small horizontal force was used to avoid the possibility of bifurcation buckling.

In order to investigate the effect of load ratio, the fire scenario remains identical in each analysis. The chosen fire scenario, based on the most common cases, included the whole rafter being heated uniformly but the column remaining cold. This simply represents a fire within a large warehouse where the pitched roof provides a heat and smoke reservoir, and hence increases in temperature, whereas the columns remain relatively cold below the smoke zone.

When the portal frame warehouse is close to a boundary, and the boundary distance does not provide sufficient separation from adjacent buildings, the cladding is required to have a minimum of 60 minutes' fire resistance. This results in a requirement for the columns which support the cladding to have adequate fire resistance. Therefore the column temperatures will be relatively low compared to those of the rafters.

The results from this study are plotted in Figure 5.2, in terms of the vertical displacement at the apex. The apex initially deflects upwards due to the thermal expansion of the rafter and the restraint to this expansion from the columns; when the steel properties begin to reduce significantly as temperature increases, the rafters become softer until the point where snap-through takes place, which has been defined failure as by VULCAN. The failure temperature for a load ratio of 0.1 is about 800°C. This reduces steadily as the load level is increased, reaching 400°C at a load ratio of 0.8.

The spread of the eaves, which is defined as the difference between the horizontal displacements of the eaves, is plotted against temperature in Figure 5.3 for each load case.

The plot of eaves spread indicates that the two eaves connection continuously deflect further away from each other due to thermal expansion and rafter rotation, and demonstrate a rotational failure of the frame (as described in the previous chapters) as soon as the snap-through of the rafters takes place. The spread of eaves will remain more or less constant if a sway failure occurs, in which both eaves move in the same direction with about the same magnitude. The frames do not experience sway failure at any load level in these analyses, even though pinned bases are assumed. The significance of the base conditions will be explored in later sections.

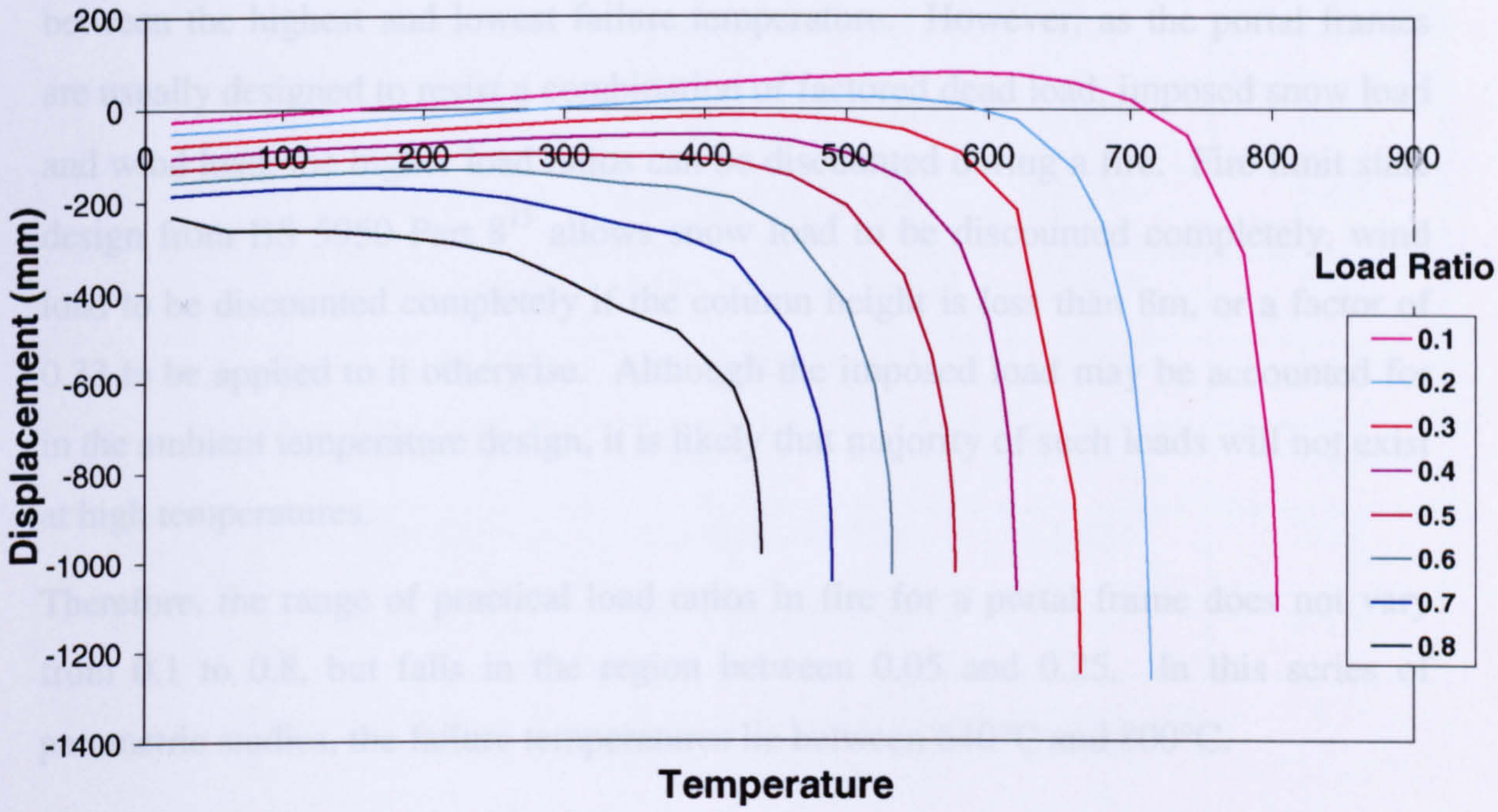

Figure 5.2 Vertical Displacement at Apex

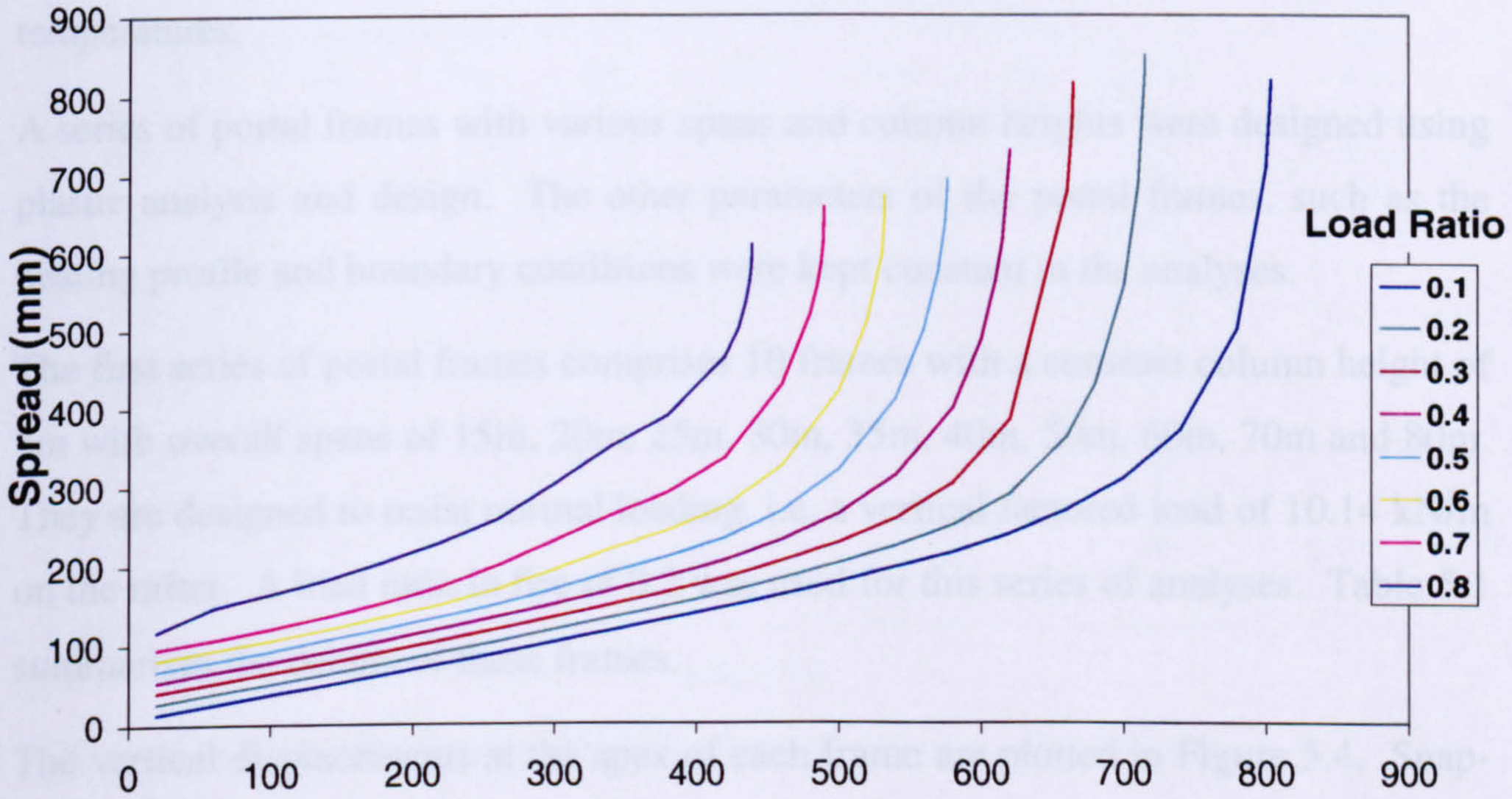

Figure 5.3 Spread of Eaves

From the analysis, it is obvious that load ratio has a considerable impact on the failure temperatures of portal frames; in this case there is approximately 400°C difference between the highest and lowest failure temperature. However, as the portal frames are usually designed to resist a combination of factored dead load, imposed snow load and wind load, the higher load ratios can be discounted during a fire. Fire limit state design from BS 5950 Part 8[13] allows snow load to be discounted completely, wind load to be discounted completely if the column height is less than 8m, or a factor of 0.33 to be applied to it otherwise. Although the imposed load may be accounted for in the ambient temperature design, it is likely that majority of such loads will not exist at high temperatures.

Therefore, the range of practical load ratios in fire for a portal frame does not vary from 0.1 to 0.8, but falls in the region between 0.05 and 0.25. In this series of parametric studies, the failure temperatures lie between 640°C and 800°C.

5.2 The Effect of Span and Column Height

The load ratio is found to have a significant influence on failure temperature from the previous analyses on a single portal frame. Different geometries of frames are investigated in this section, looking at the influence of geometry on failure temperatures.

A series of portal frames with various spans and column heights were designed using plastic analysis and design. The other parameters of the portal frames, such as the heating profile and boundary conditions were kept constant in the analyses.

The first series of portal frames comprises 10 frames with a constant column height of 7m with overall spans of 15m, 20m, 25m, 30m, 35m, 40m, 50m, 60m, 70m and 80m. They are designed to resist normal loading, i.e. a vertical factored load of 10.14 kN/m on the rafter. A load ratio in fire of 0.2 was used for this series of analyses. Table 5.1 summarises the details of these frames.

The vertical displacements at the apex of each frame are plotted in Figure 5.4. Snap-through failure is clearly detected, especially for the larger span portal frames. The failure temperature of each frame lies close to 700°C, which indicates that the load ratio of 0.2 dominates the failure temperatures. A larger variety of frame geometries is required to investigate this further.

Span (m)	Column Section (Grade 43)	Rafter Section (Grade 43)	Roof Inclination	0.2 Load Ratio (kN/m)
60	914×305×201 UB	914×305×201 UB	7.59°	2.51
50	838×292×176 UB	762×267×173 UB	9.09°	2.67
40	610×305×149 UB	610×229×125 UB	11.31°	2.47
35	610×229×113 UB	533×210×109 UB	12.88°	2.48
30	533×210×92 UB	457×191×89 UB	14.93°	2.42
25	457×152×60 UB	457×152×60 UB	17.74°	2.29
20	457×152×52 UB	406×140×46 UB	11.31°	2.23
15	305×102×33 UB	305×102×33 UB	14.93°	2.16

Table 5.1 Portal Frames with Fixed Column Height of 7m

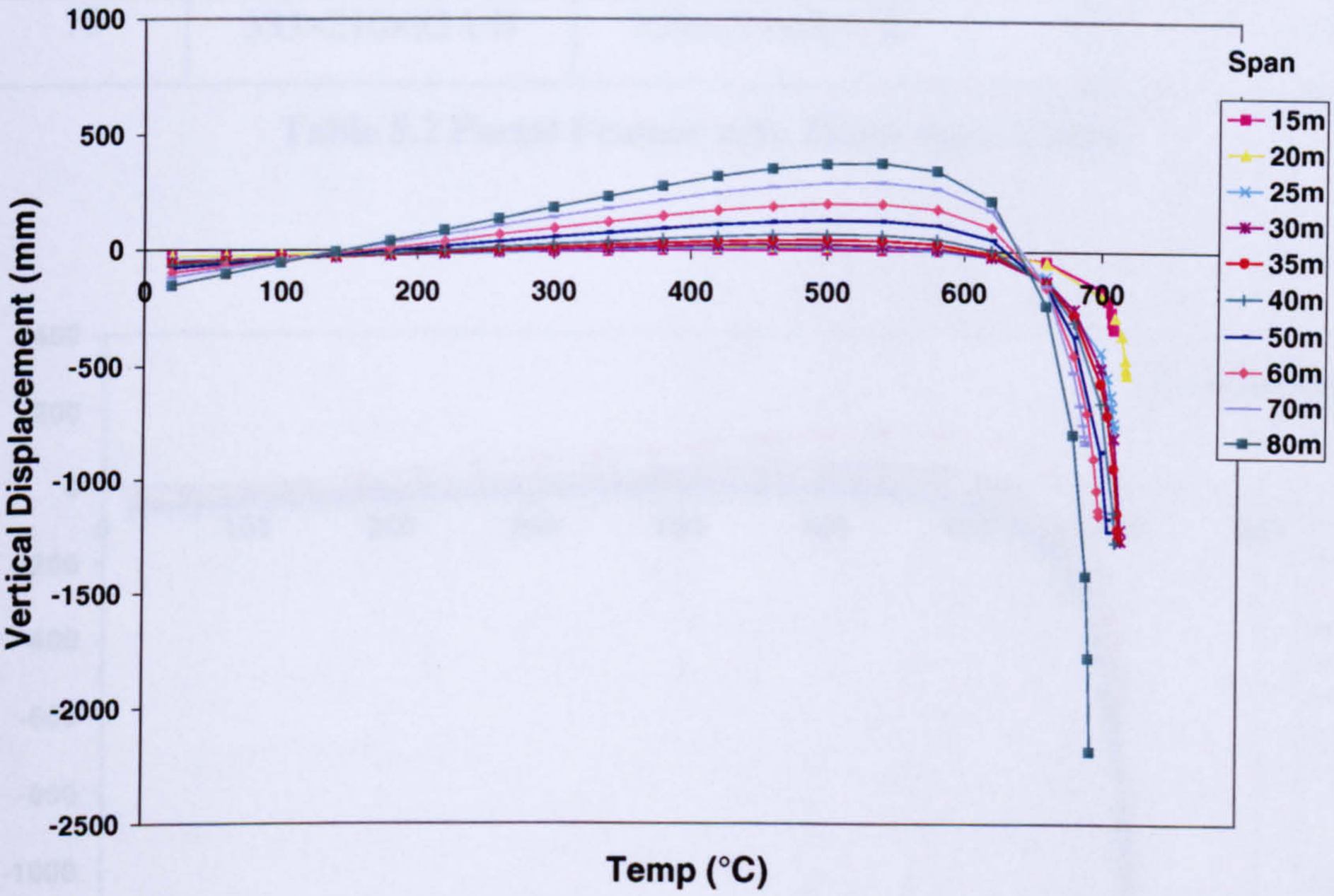

Figure 5.4 Vertical Displacement at Apex – Variable Span

The next series of portal frames was designed to have a constant span of 30m but with the column heights varying from 3m to 15m at one-metre intervals. A summary of the frames is shown in Table 5.2.

Height (m)	Column Section (Grade 43)	Rafter Section (Grade 43)	Roof Inclination	0.2 Load Ratio (kN/m)
3	457×191×74 UB	457×191×74 UB	14.9°	2.60
4	457×191×82 UB	457×191×82 UB	14.9°	2.60
5	457×191×82 UB	457×191×82 UB	14.9°	2.46
6	533×210×82 UB	533×210×82 UB	14.9°	2.61
8	533×210×82 UB	533×210×82 UB	14.9°	2.49
9	533×210×82 UB	533×210×82 UB	14.9°	2.44
10	533×210×82 UB	533×210×82 UB	14.9°	2.40
11	533×210×82 UB	533×210×82 UB	14.9°	2.38
12	533×210×82 UB	533×210×82 UB	14.9°	2.34
13	533×210×82 UB	533×210×82 UB	14.9°	2.32
14	533×210×82 UB	533×210×82 UB	14.9°	2.31
15	533×210×82 UB	533×210×82 UB	14.9°	2.29

Table 5.2 Portal Frames with Fixed Span of 30m

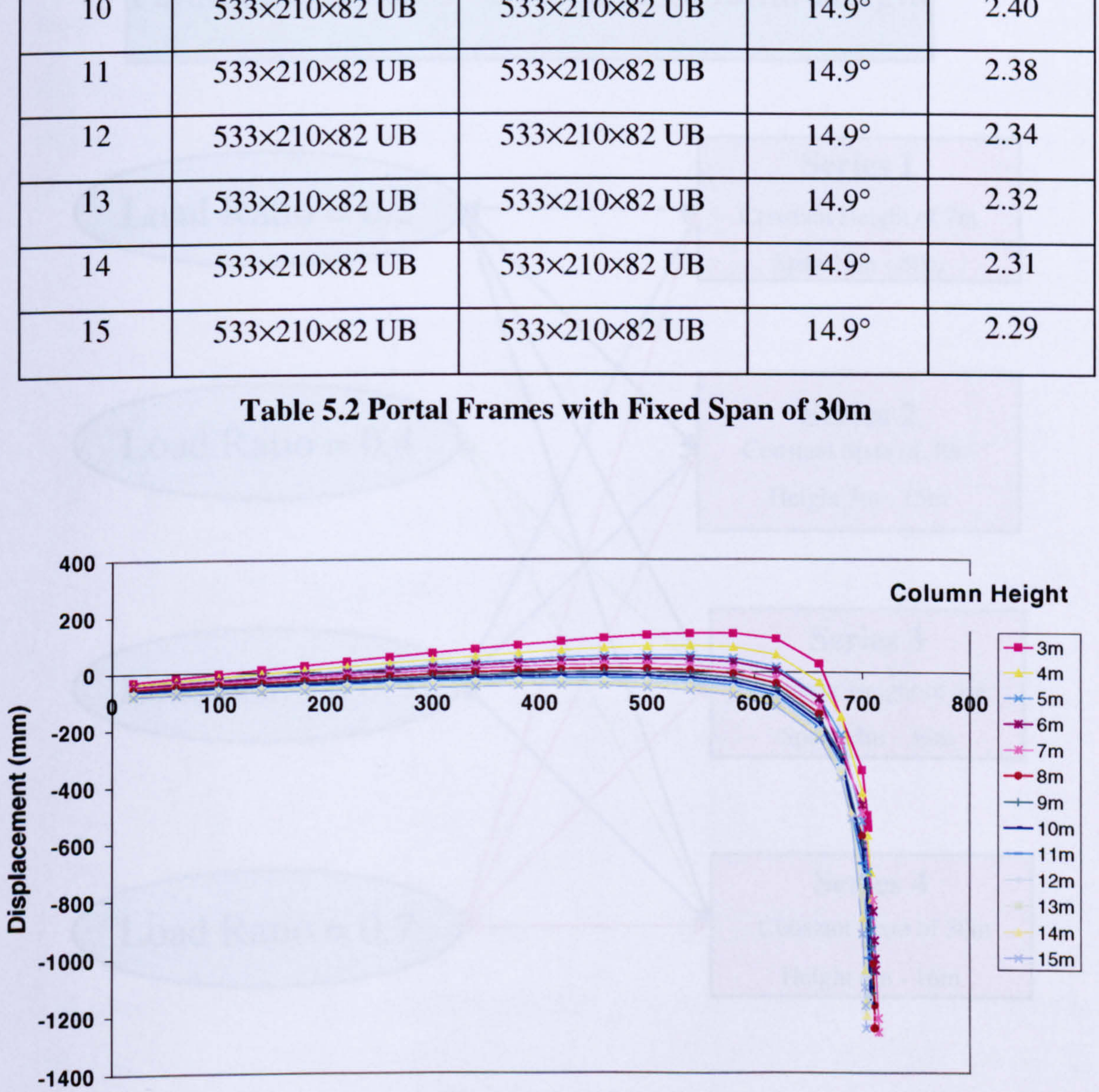

Figure 5.5 Vertical Displacement of Apex - Variable Column Heights

Figure 5.5 plots the results from the analyses, in terms of the vertical displacements at the apex. Combining the results from the previous series of analyses, it is demonstrated that the upward movement of the apex (before snap-through takes place) is larger for the frames with higher span/height ratio. However, all the frames fail at approximately 700°C, even though the span/height ratio varies from 2 to 12. The failure mechanism is similar in all the frames, comprising a rotational movement as described earlier.

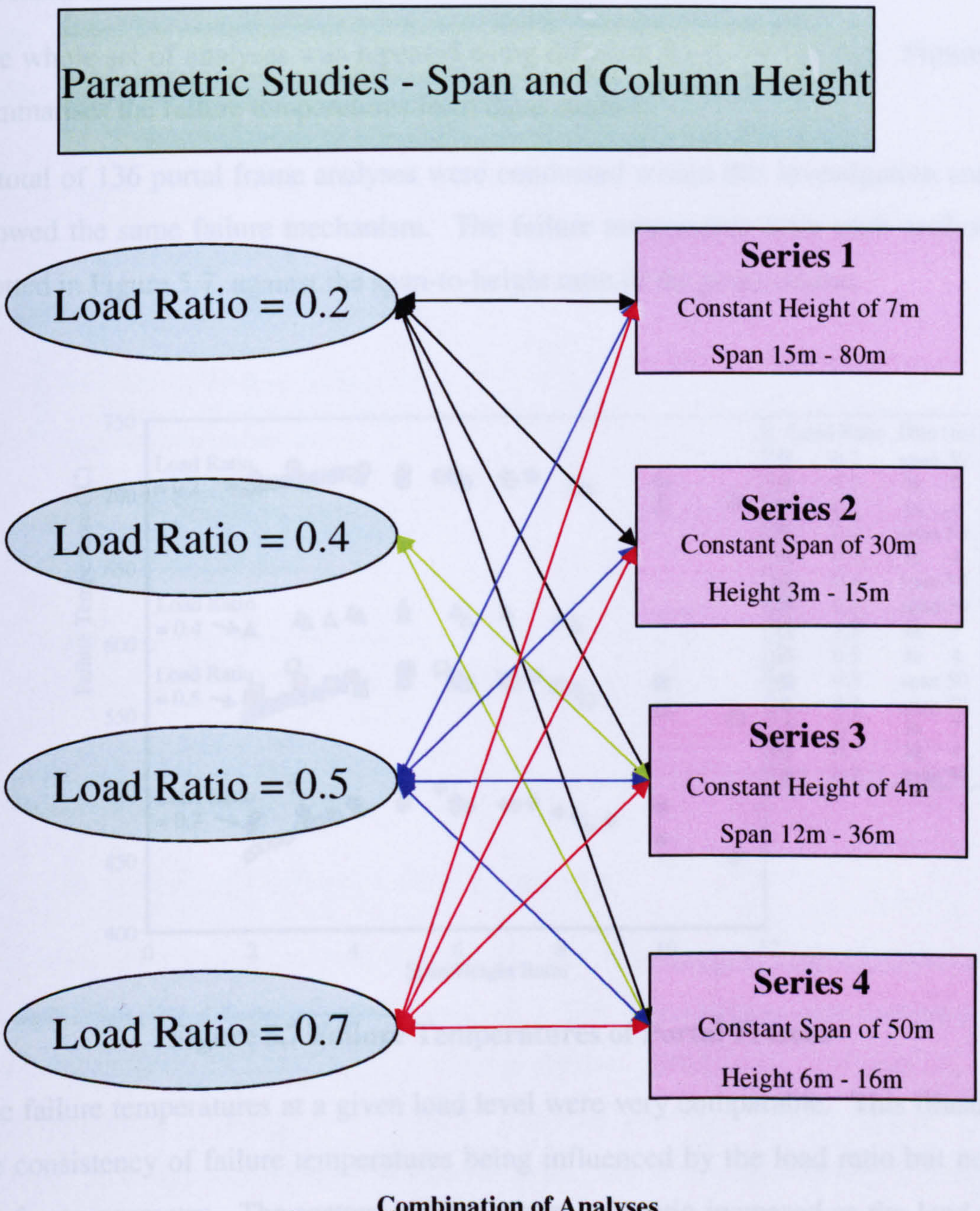

Figure 5.6 Parametric studies on Span and Column Height of Portal Frames

For the third series of portal frames the column height was made constant at 4m and the span was varied from 12m to 36m in 4m intervals. This was followed by a fourth series of frames with constant span of 30m and column heights ranging from 6m to 16m in 2m intervals. Both series were again analysed at a load ratio of 0.2.

Similar findings to the earlier analyses were obtained from the third and fourth series of parametric studies. The conclusion can almost be drawn that a portal frame with load ratio of 0.2 will have a critical temperature of approximately 700°C provided that the rafter is heated and bases are pinned.

The whole set of analyses was repeated using different levels of loading. Figure 5.6 summarises the failure temperatures from these studies.

A total of 136 portal frame analyses were conducted within this investigation and all showed the same failure mechanism. The failure temperature from each analysis is plotted in Figure 5.7, against the span-to-height ratio of the portal frame.

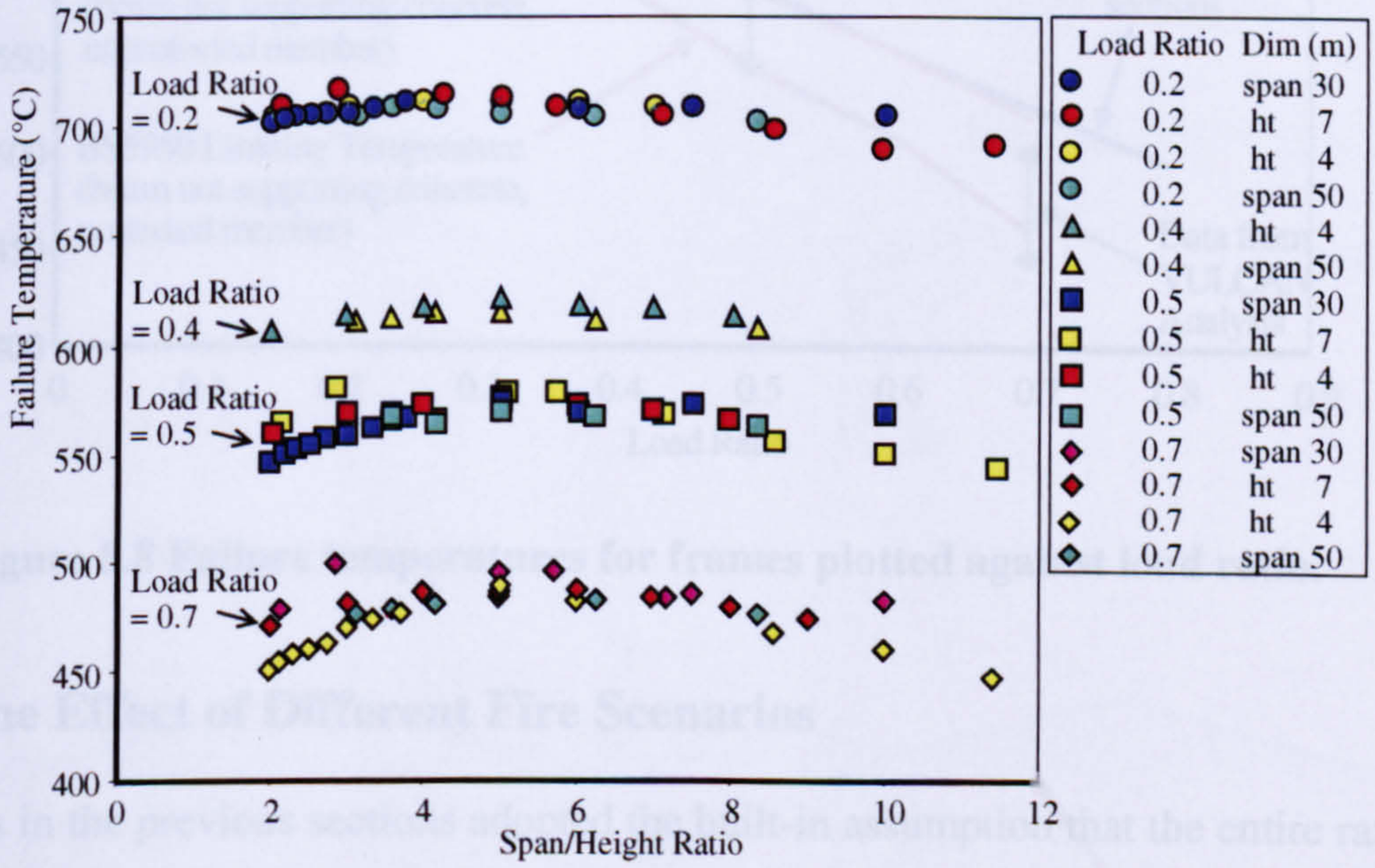

Figure 5.7 Failure Temperatures of Portal Frames

The failure temperatures at a given load level were very comparable. This illustrates the consistency of failure temperatures being influenced by the load ratio but not by the frame geometry. The scatter within a given load ratio increased as the load ratio increased. For the 0.7 load ratio, the difference between the highest and lowest failure temperature is approximately 50°C.

The range of failure temperatures from the analyses are plotted against load ratios in Figure 5.8, and they are also compared against the limiting temperatures extracted from BS 5950: Part 8[13] and Eurocode 3[15]. The limiting temperature for the BS 5950 category 'Member in bending not supporting concrete slabs: protected member' can be seen to form an approximate lower bound for the analytical results.

The nature of the analyses, in which rafters are heated but the columns stay relatively cold, has similarities with simple beams, except that rafters are inclined members. It has been seem that the limiting temperature data given in the Codes can provide a quick, approximate indication of the failure temperatures of portal frames given a similar heating scheme.

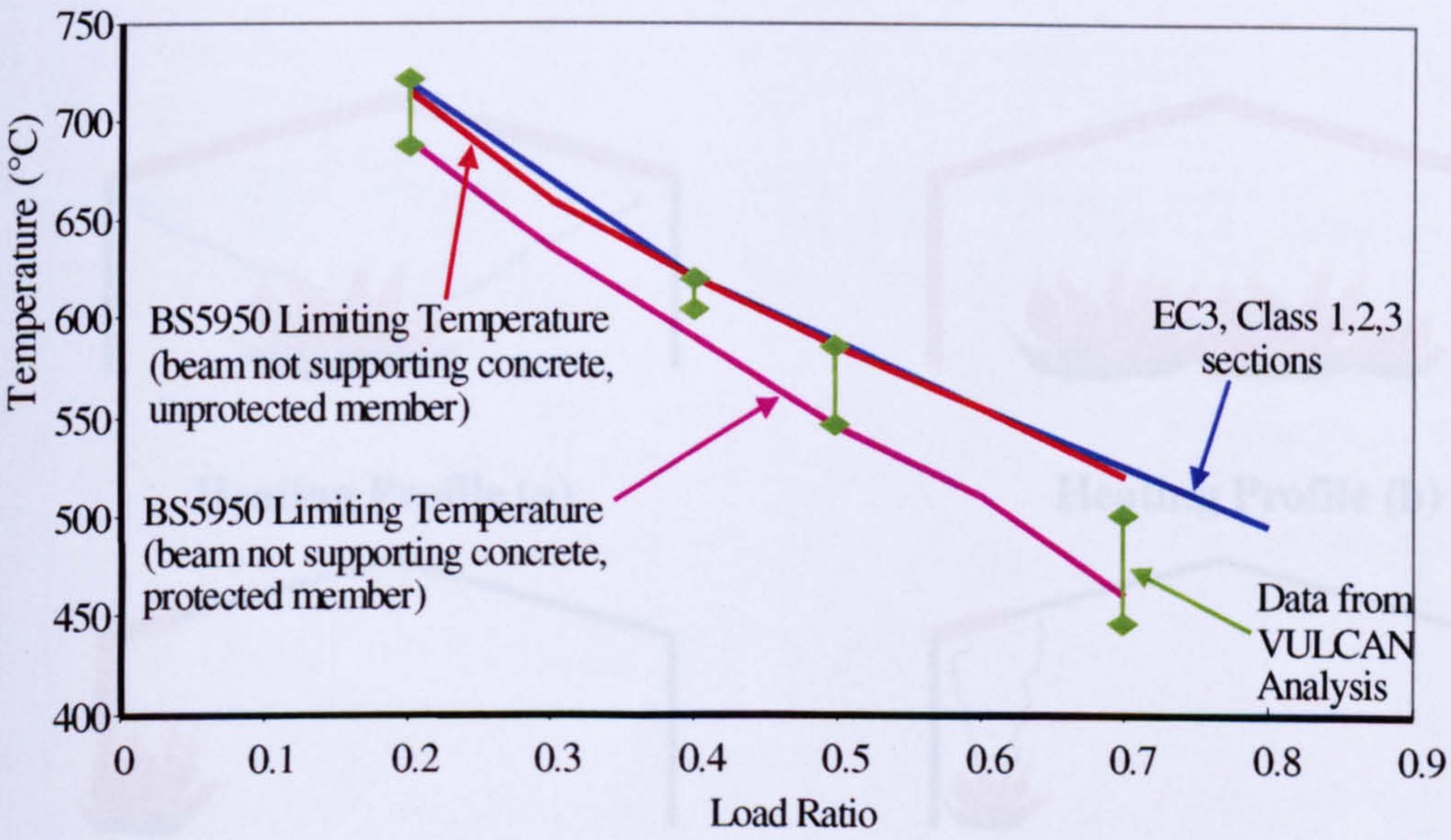

Figure 5.8 Failure temperatures for frames plotted against load ratio.

5.3 The Effect of Different Fire Scenarios

Analyses in the previous sections adopted the built-in assumption that the entire rafter is heated but the columns remain cold in a fire. A different fire scenario will inevitably create a different heating scheme for the portal frame. Especially in a large warehouse building, a fire can be localised and only heat a portion of the building. In a high rack-storage warehouse, a line fire across the building will lead to either a relatively small section of the frame being heated or the entire frame increasing in temperature.

Figure 5.9 illustrates the different heating schemes considered in the next parametric studies. Profile (a) represents the typical fire scenario used in the previous analyses, where a combination of fire and smoke heat up the rafters. In the most severe fire case of total burn-out of the entire storage accommodation, all the steel members will be heated as shown in Profile (b). Profiles (c), (d), (e) and (f) consider localised fires at different locations, i.e. near edges, mid-span and mid-rafters. These cases lead to some localised heating of portions of the rafters.

As the portal frame is loaded vertically, the bending moment experienced by the rafters will be negative (hogging) at the eaves, reducing gradually and changing to positive (sagging) in the region of the apex. The maximum moment is expected to be near to the eaves, and the mid-rafter zones are expected to experience least moment.

Heating Profile (a)

Heating Profile (b)

Heating Profile (c)

Heating Profile (d)

Heating Profile (e)

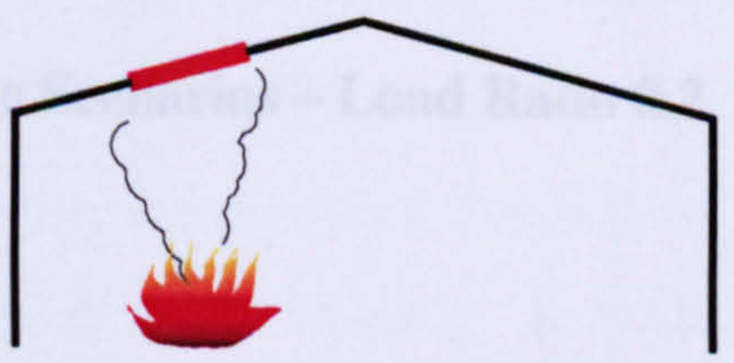

Heating Profile (f)

Figure 5.9 Heating Profiles of Portal Frames in Various Fire Scenarios

The portal frame under investigation is 30m in span and 7m in height to the eaves (as previously defined in Section 5.1). The analyses do not concentrate on the geometry

of the frame but on the vertical load applied, given that the load ratio seems to be the dominant factor affecting the frame behaviour.

Figures 5.10 and 5.11 show the results of the studies at load ratios 0.2 and 0.7 respectively. The vertical displacements at the apex are plotted against the steel temperatures in the heated zone. Comparing the heating profiles (a) and (b) for which the difference is the heating of the column, very similar behaviour is seen. This also applies when comparing profiles (c) and (d). This indicates that the heating of columns does not lead to very much worse or more critical failure behaviour of portal frames, provided that the out-of-plane deformation is prevented since the analyses are two-dimensional.

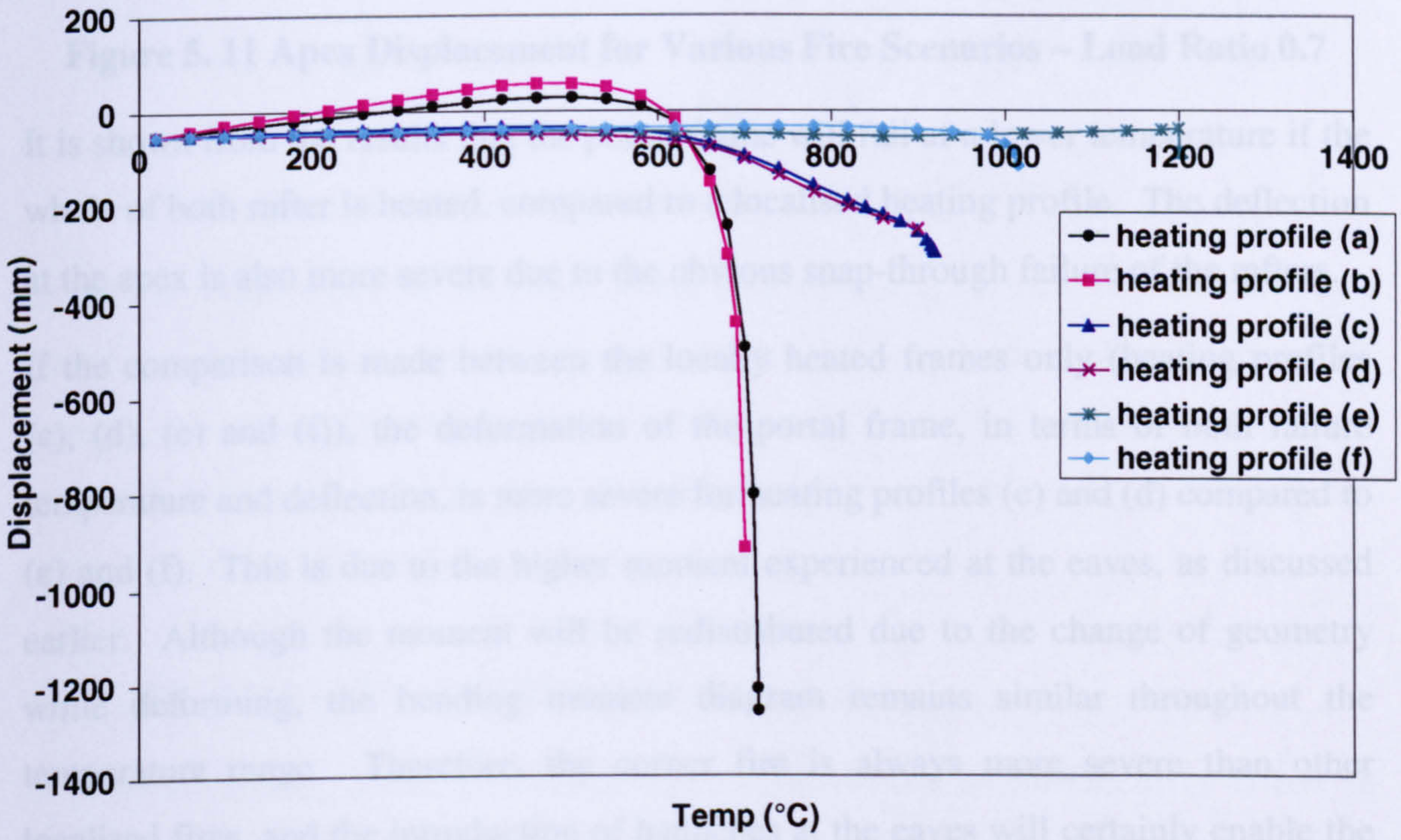

Figure 5.10 Apex Displacement for Various Fire Scenarios – Load Ratio 0.2

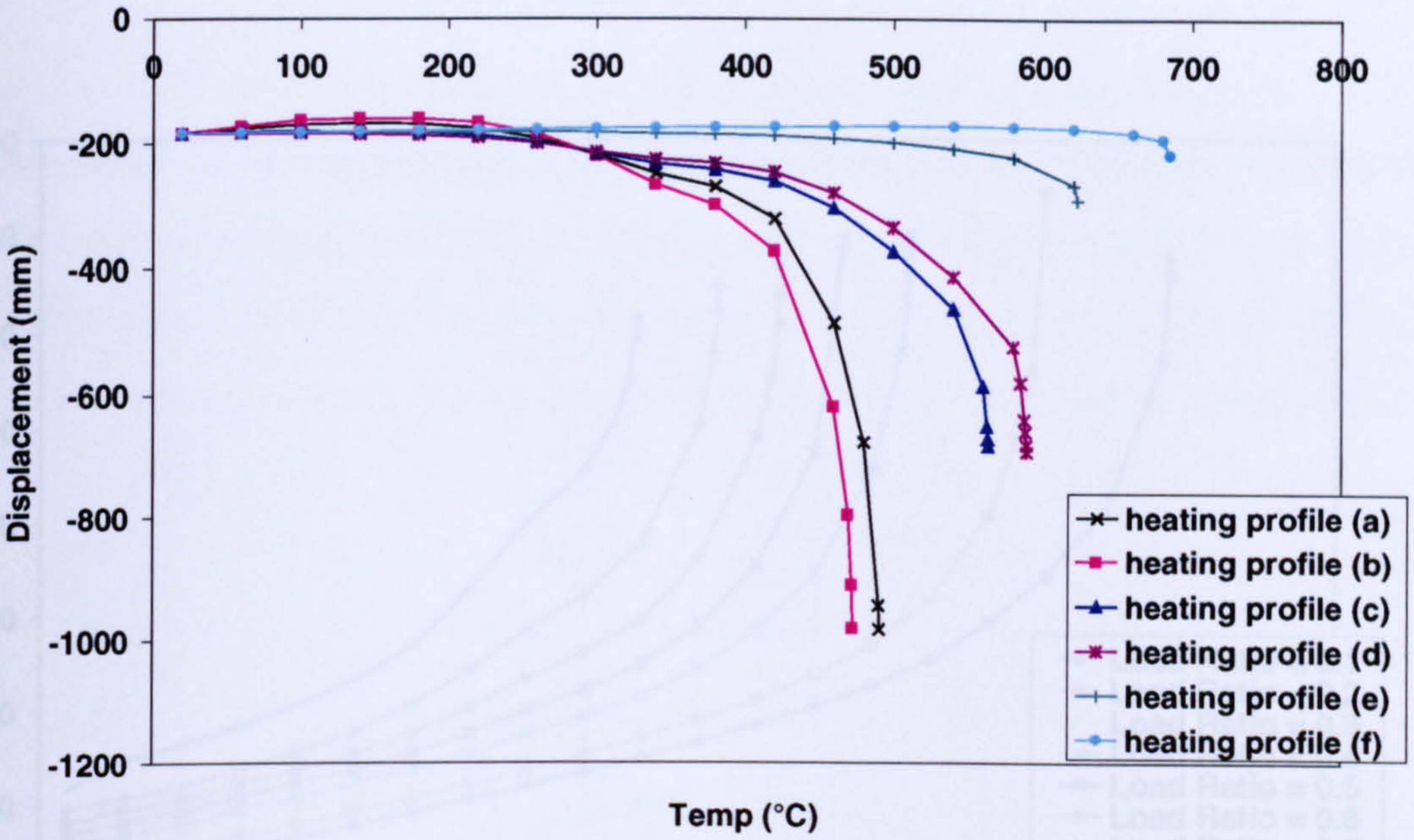

Figure 5. 11 Apex Displacement for Various Fire Scenarios – Load Ratio 0.7

It is shown from the results that the portal frame will fail at a lower temperature if the whole of both rafter is heated, compared to a localised heating profile. The deflection at the apex is also more severe due to the obvious snap-through failure of the rafters.

If the comparison is made between the locally heated frames only (heating profiles (c), (d), (e) and (f)), the deformation of the portal frame, in terms of both failure temperature and deflection, is more severe for heating profiles (c) and (d) compared to (e) and (f). This is due to the higher moment experienced at the eaves, as discussed earlier. Although the moment will be redistributed due to the change of geometry while deforming, the bending moment diagram remains similar throughout the temperature range. Therefore, the corner fire is always more severe than other localised fires, and the introduction of haunches at the eaves will certainly enable the formation of plastic hinges to be pushed further away from the eaves.

It should be noted that in a warehouse where skylights are provided, these tend to open in the early stages of a fire and provide ventilation to the building. It is likely that the hot smoke will escape through the skylight and only the top of the building (near the apex) forms a reservoir. This tends to cause heating profile (e) to form and this is likely to happen for most smouldering fires. However, It is not likely to be critical for the structural behaviour of the portal frame.

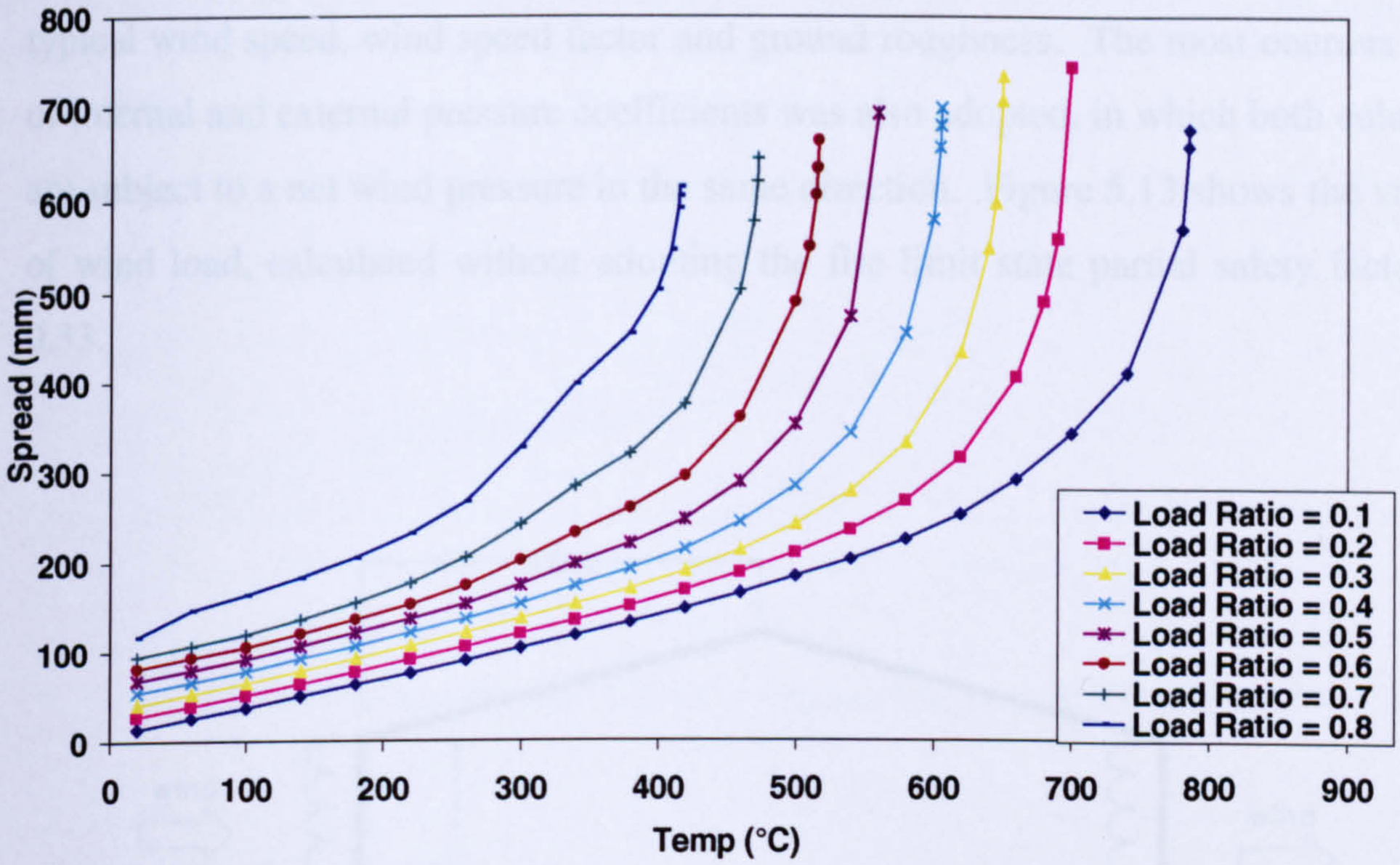

Figure 5.12 Spread of Eaves for Heating Profile (a)

When the failure mode of the portal frame is investigated for each fire scenario, it is found that sway failures do not take place. The plot of spread of eaves for the most severe fire scenario (heating profile (a)) is shown in Figure 5.12; the eaves are found to move further from each other as snap-though occurs, once again forming the rotational failure mechanism.

5.4 The Effect of Wind (Horizontal) Load

In order to contain the fire within the building in which it originated, sway failure of portal frames is not permitted. Sway failure is more likely to occur in the presence of horizontal wind force. However, under the current BS 5950 Part 8 provisions, the fire condition is considered as an accidental limit state. Therefore, it is considered unlikely that a fire will coincide with the maximum design wind force. This allows wind load to be omitted for buildings less than 8m, or wind load to be reduced by two-third otherwise.

Considering a portal frame warehouse with frames spaced at 6m centres with the typical portal frame dimensions of Section 5.1, the wind load was calculated using a typical wind speed, wind speed factor and ground roughness. The most onerous case of internal and external pressure coefficients was also adopted, in which both columns are subject to a net wind pressure in the same direction. Figure 5.13 shows the values of wind load, calculated without adopting the fire limit state partial safety factor of 0.33.

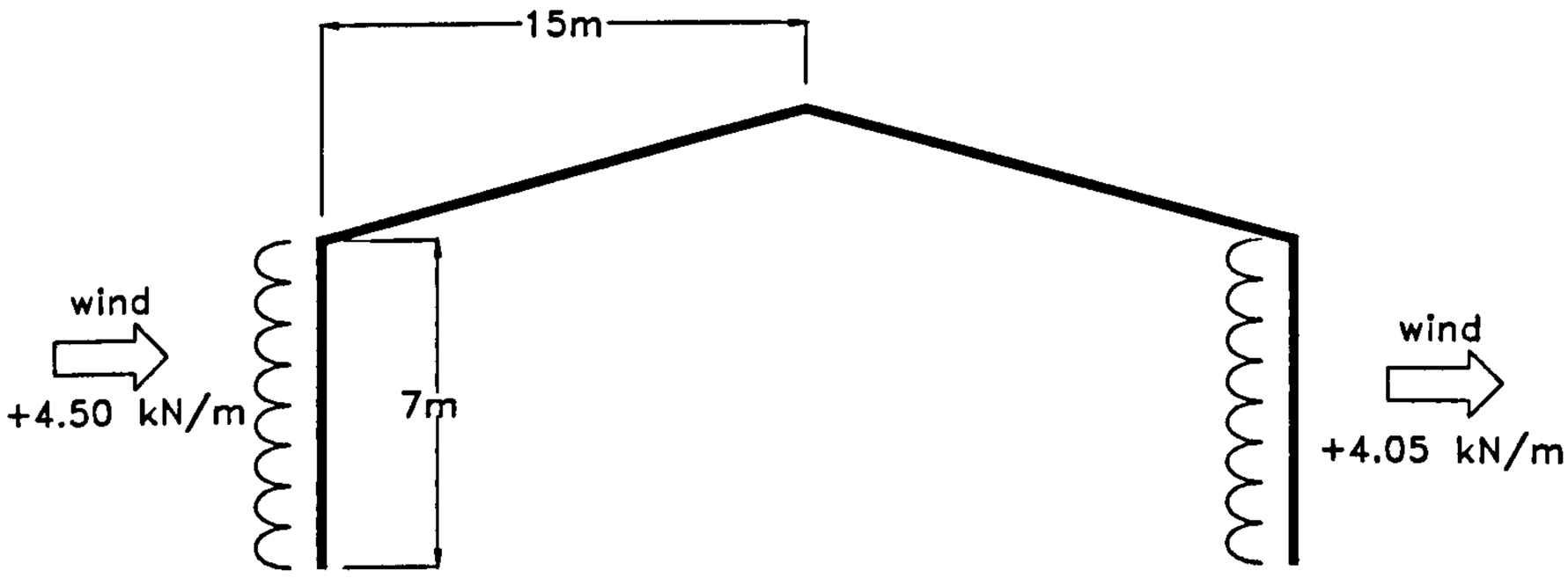

Figure 5.13 Wind Load

Analyses were conducted using this wind load, varying the vertical load on the rafters. The vertical load is represented as a load ratio for the portal frame, with a maximum load ratio of 0.4 being used since it is not practical to have high vertical load for portal frames in fire. The results from the analyses, expressed in terms of the spread of eaves, are plotted in Figure 5.14. The analyses were repeated applying a wind load with the recommended reduction factor of 0.33, and the results are plotted in Figure 5.15.

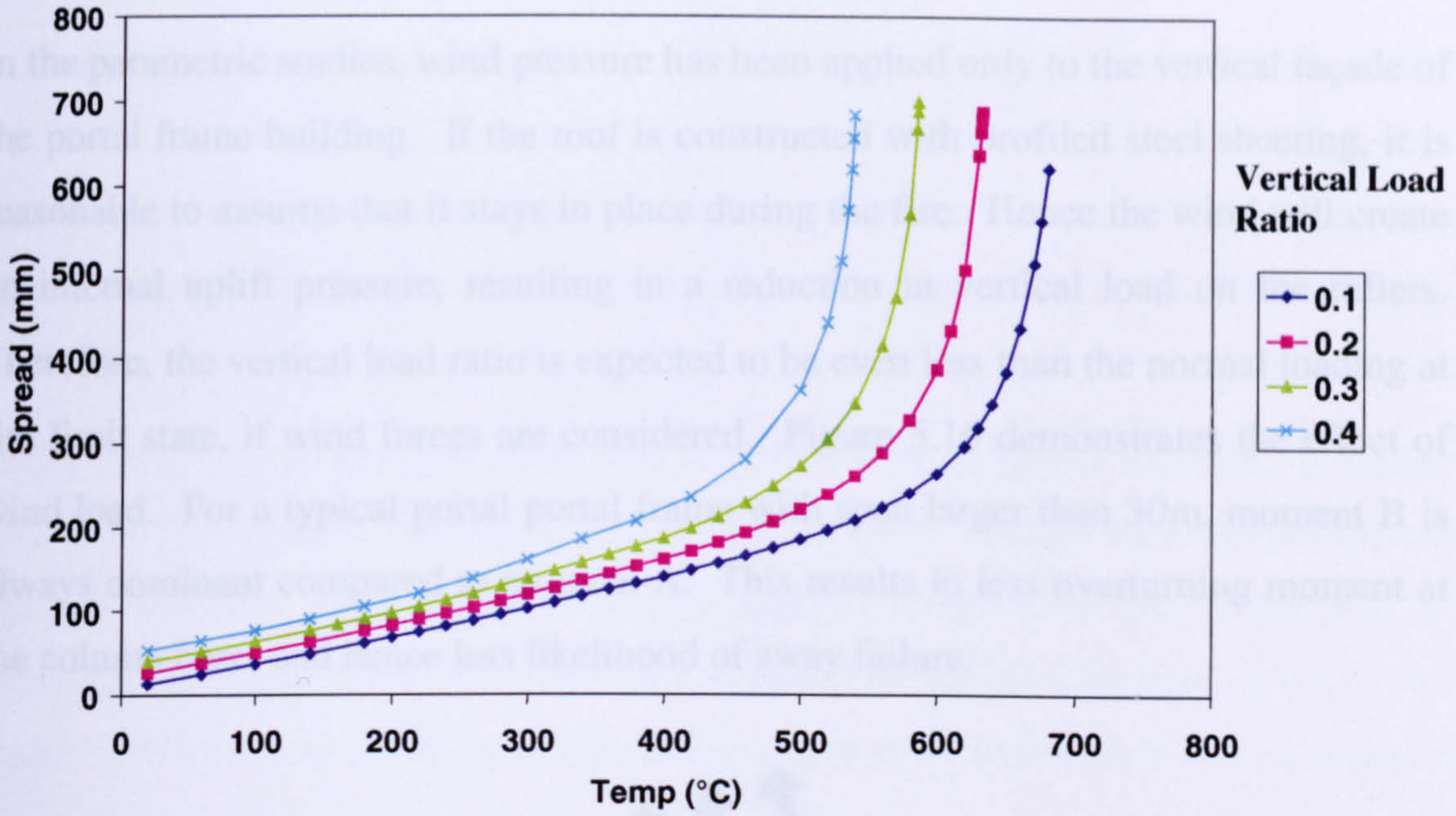

Figure 5.14 Spread of Eaves – Analyses with Full Wind Load

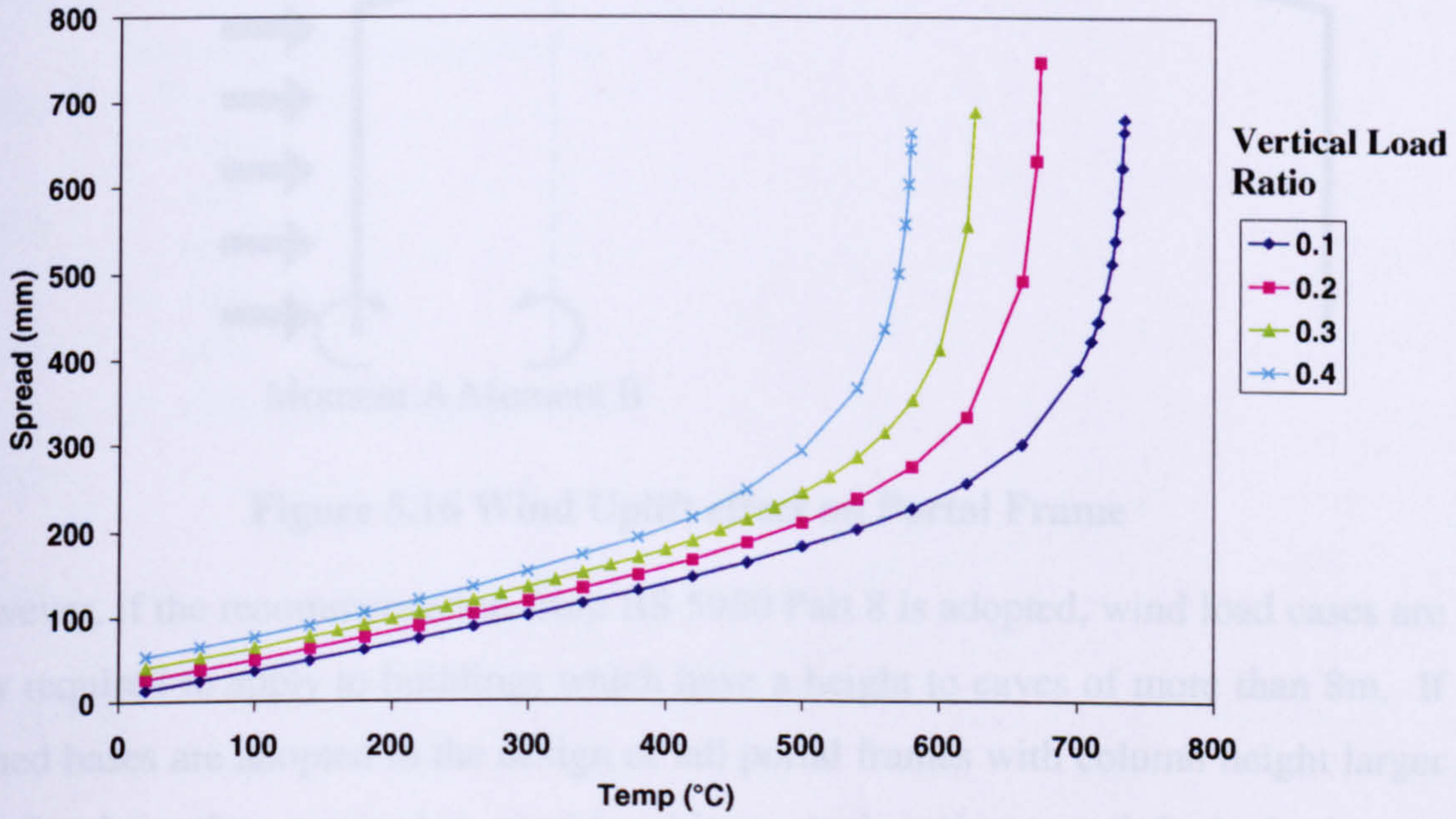

Figure 5.15 Spread of Eaves – Analyses with 0.33 Wind Load Factor

From the plot of eaves spread, there is no evidence that the portal frames are subject to sway failure. In fact, the horizontal distance between the eaves increases as the portal frames approach failure, suggesting that the failure mode in wind conditions is similar to that under purely vertical loading.

The introduction of reduced wind load makes little difference to the failure temperatures of the portal frames, compared to the effect of vertical load. This again demonstrates the dominant influence of the vertical load.

In the parametric studies, wind pressure has been applied only to the vertical façade of the portal frame building. If the roof is constructed with profiled steel sheeting, it is reasonable to assume that it stays in place during the fire. Hence the wind will create an internal uplift pressure, resulting in a reduction in vertical load on the rafters. Therefore, the vertical load ratio is expected to be even less than the normal loading at fire limit state, if wind forces are considered. Figure 5.16 demonstrates the effect of wind load. For a typical portal portal frame with span larger than 30m, moment B is always dominant compared to moment A. This results in less overturning moment at the column base, and hence less likelihood of sway failure.

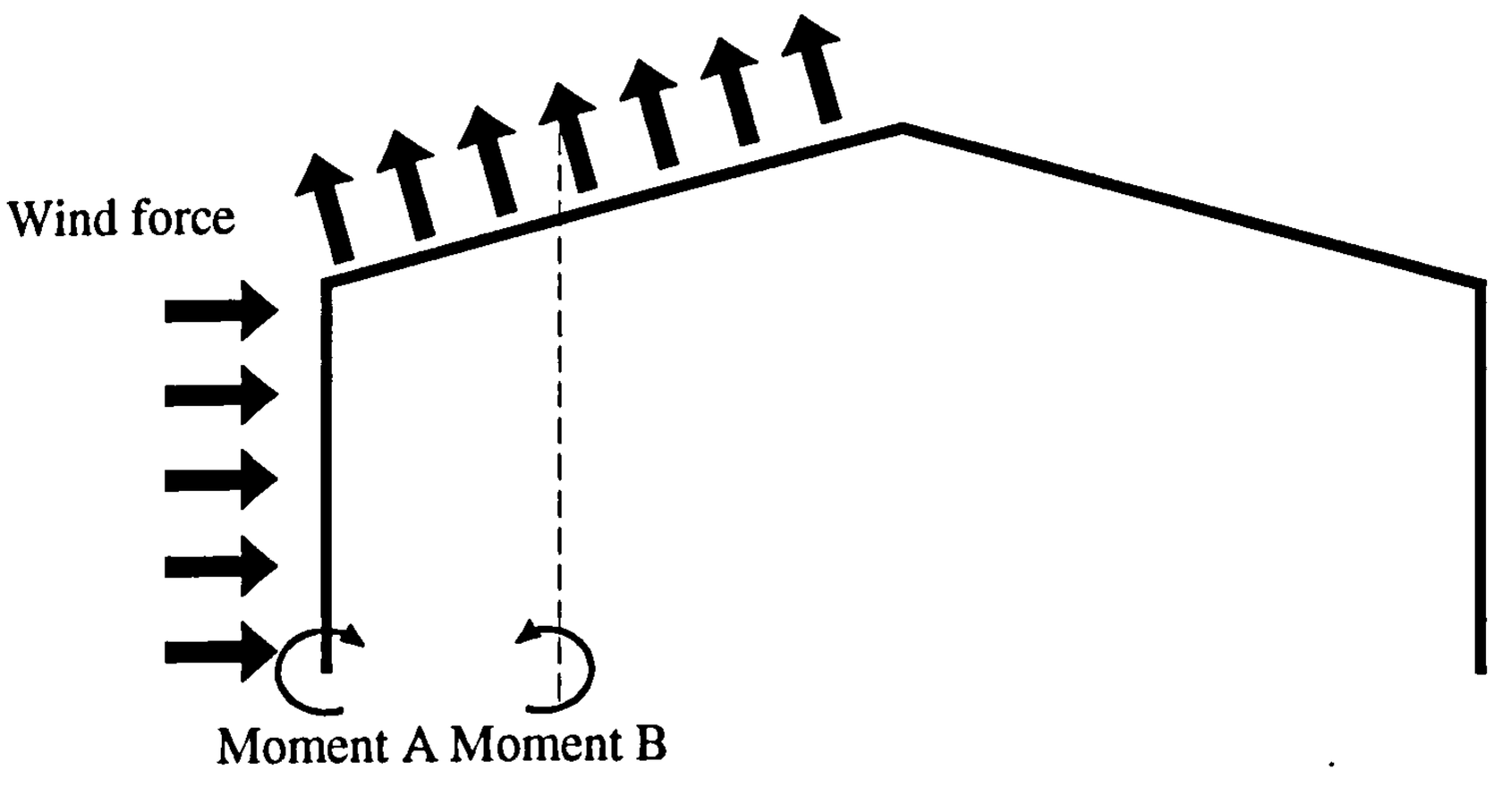

Figure 5.16 Wind Uplift effect on Portal Frame

However, if the recommendation from BS 5950 Part 8 is adopted, wind load cases are only required to apply to buildings which have a height to eaves of more than 8m. If pinned bases are adopted in the design of tall portal frames with column height larger than 8m, it is often required to provide a bigger steel section to satisfy the horizontal deflection criterion of the columns, due to the increased wind loading. Therefore, it is often found that wind loading is the less onerous case in the fire limit state for typical portal frame buildings. In consequence the lack of extensive research and reasoning behind the 8m recommendation given in BS5950 Pt 8 does not necessarily lead to major concern for portal frame buildings.

The purpose of these parametric studies is to investigate the likelihood of the occurrence of sway failure of a portal frame. A particularly slender frame was chosen, applying different levels of horizontal force combined with low vertical loading. The span of the frame is 15m and the height to eaves is 7m, which results in

a span/height ratio of 2.14. The frame is again designed using plastic analysis, and a vertical load ratio of 0.2 is adopted. The horizontal load is added to the frame as a percentage of the total vertical load, applied as a point load on one of the eaves. The typical wind force for a portal frame is approximately 20% of the 0.2 load ratio loading.

The results from the analysis are plotted in terms of the spread of the eaves in Figure 5.17. The results show a strong indication that the frame will have a rotational failure at a low horizontal force (<50%). The final analysis shown is the case where 80% of wind load is applied with half the vertical load (i.e. a vertical load ratio of 0.1). The results indicate a sway failure in which the spread of eaves does not experience 'runaway'.

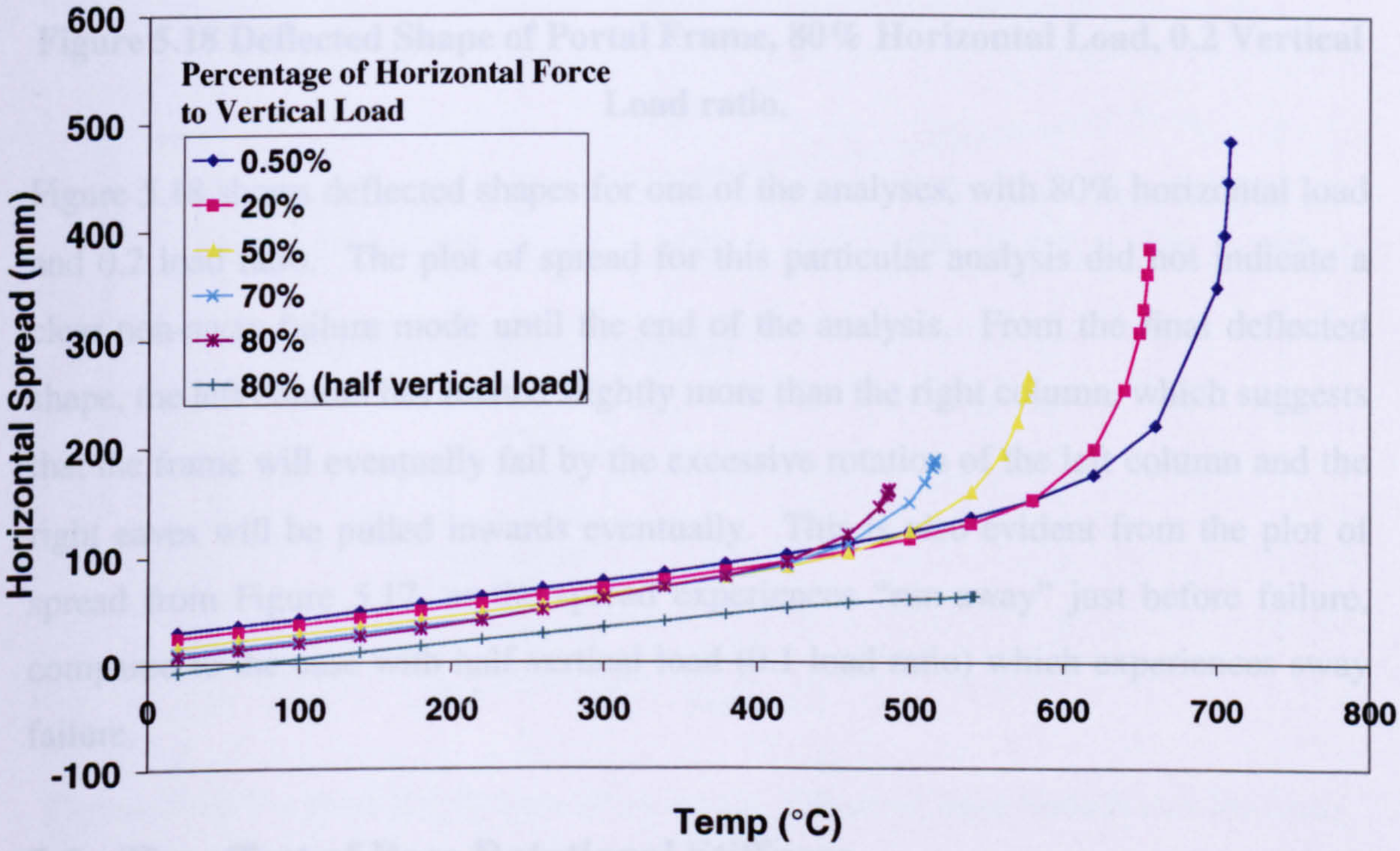

Figure 5.17 Spread of Eaves – The Effect of Horizontal Forces

Sway failure of a portal frame is theoretically possible . However, the analysis on the last case was based on a slender frame with extremely high horizontal force and low vertical load. This is not realistic for a portal frame building under normal circumstances. With a higher vertical load combining a horizontal force at one side, the P-δ will enable the column that resists the horizontal force to rotate more than the other column, creating the rotational failure mode.

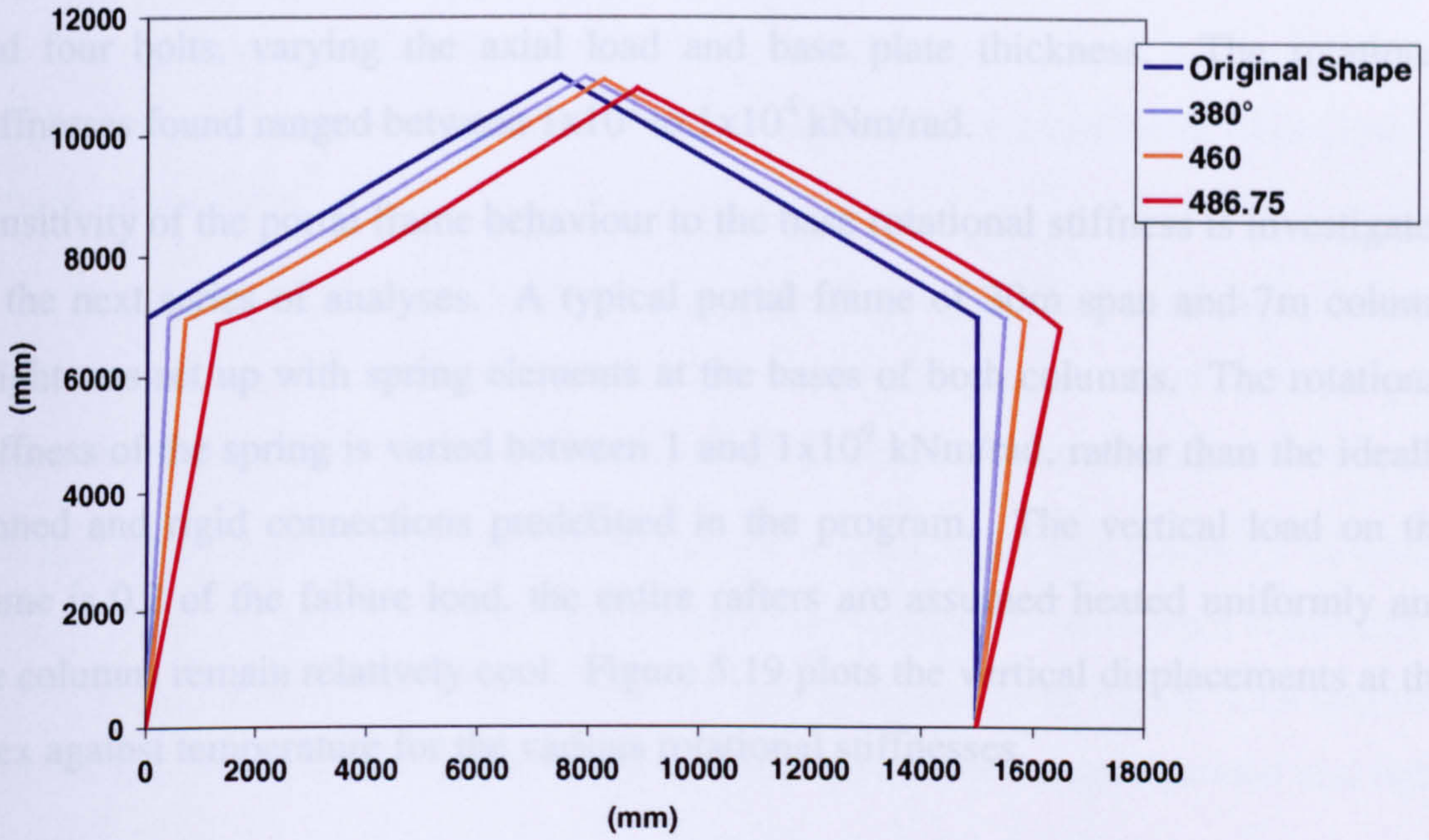

Figure 5.18 Deflected Shape of Portal Frame, 80% Horizontal Load, 0.2 Vertical Load ratio.

Figure 5.18 shows deflected shapes for one of the analyses, with 80% horizontal load and 0.2 load ratio. The plot of spread for this particular analysis did not indicate a clear non-sway failure mode until the end of the analysis. From the final deflected shape, the left column has rotated slightly more than the right column, which suggests that the frame will eventually fail by the excessive rotation of the left column and the right eaves will be pulled inwards eventually. This is also evident from the plot of spread from Figure 5.17, as the spread experiences "run-away" just before failure, compared to the case with half vertical load (0.1 load ratio) which experiences sway failure.

5.5 The effect of Base Rotational Stiffness

The analyses in the previous sections have adopted the assumption of pinned bases to the columns of the portal frames. Although the same assumption is widely used by engineers while designing portal frames, a connection with the column base plate bolted down to the concrete foundation is the common practice in specifying the details of these bases. These connections do not actually allow free rotation at the base. In fact, it has been shown from research and experiments[58,59,60,61] that such connections will provide significant rotational stiffness to the columns.

Jaspart and Vandegans[5.4] conducted a series of experiments on column bases with two and four bolts, varying the axial load and base plate thickness. The rotational stiffnesses found ranged between $1x10^2$ to $1x10^4$ kNm/rad.

Sensitivity of the portal frame behaviour to the base rotational stiffness is investigated in the next series of analyses. A typical portal frame of 30m span and 7m column height was set up with spring elements at the bases of both columns. The rotational stiffness of the spring is varied between 1 and $1x10^9$ kNm/rad, rather than the ideally pinned and rigid connections predefined in the program. The vertical load on the frame is 0.2 of the failure load, the entire rafters are assumed heated uniformly and the columns remain relatively cool. Figure 5.19 plots the vertical displacements at the apex against temperature for the various rotational stiffnesses.

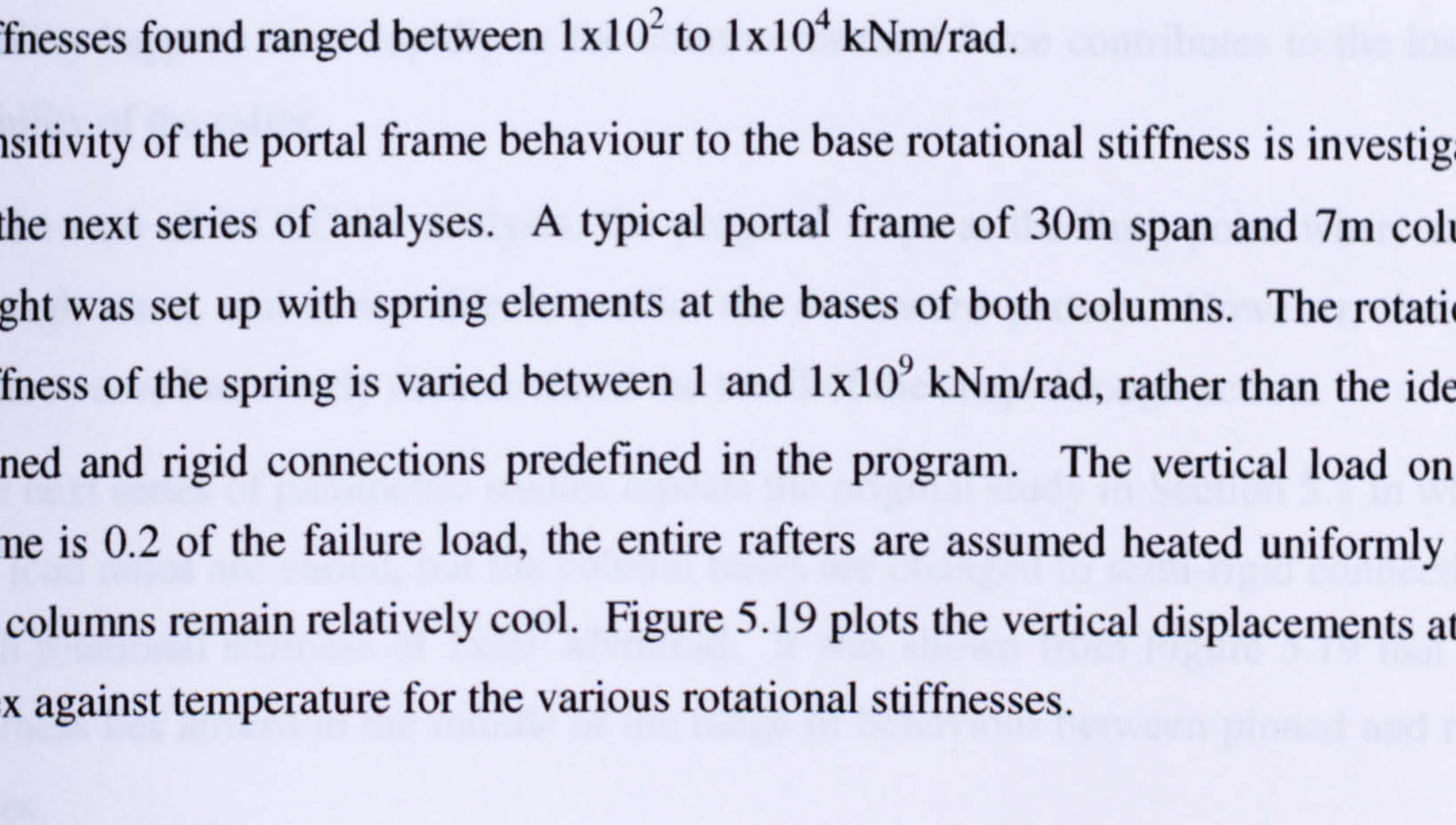

Figure 5.19 Vertical Displacement at Apex - Effect of Base Rotational Stiffness

The analyses show that rotational stiffnesses up to $1x10^2$ kNm/rad do not affect the portal frame behaviour as compared to "pinned", and a rotational stiffness of more than $1x10^6$ kNm/rad can be considered as "rigid". The portal frame behaviour is most sensitive to stiffnesses between $1x10^2$ and $1x10^5$ kNm/rad.

When the rotational stiffness is low, the restraint to the column is low and the rafter expansion causes the eaves to deflect outward. As the strength of rafters reduces at higher temperatures, the rafters deflect downward until snap-through takes place. When the column restraint is large due to higher rotational stiffness, the eaves can no

longer deflect outward as much, and instead the apex is pushed upward and the rafters experience greater axial force. As the rafters reach the snap-through point, the loss of stability happens more rapidly as the column restraint force contributes to the loss of stability of the rafter.

In the case of VULCAN analysis, the program stops at the limit point where snap-through starts, and is not able to predict the downward pattern. However, the pre-failure curve has clearly demonstrated the trend of the snap-through action.

The next series of parametric studies repeats the original study in Section 5.1 in which the load ratios are varied, but the column bases are changed to semi-rigid connections with rotational stiffness of $1x10^4$ kNm/rad. It was shown from Figure 5.19 that this stiffness lies almost in the middle of the range of behaviour between pinned and rigid bases.

Figure 5.20 and 5.21 show the vertical displacement at the apex and the spread of eaves for this case. The shape of the curves is similar to the results from Section 5.1 (Figures 5.2 and 5.3) except that the numerical values of failure temperatures and displacements differ. The failure temperatures for the frames with semi-rigid bases are higher, and the upward deflections at the apex are greater, with smaller values of horizontal eaves spread. This is due to the restraint effect explained earlier.

From the vertical displacement plot of the 0.1 load ratio case, the first indication of failure appears at approximately 800°C. This failure temperature is in line with the other cases in this series of analysis. However, due to the semi-rigid pinned bases and the low level of vertical load, the snap-through is not as dramatic as the other cases and VULCAN has managed to bring the analysis to a further stage, which can not be usually picked up by VULCAN. As temperature approaches 1000°C, the snap-through is more dramatic and VULCAN can not follow the sudden vertical dive of the apex. The three final solutions (indicated by the dots) of the analysis show the evidence of this dive.

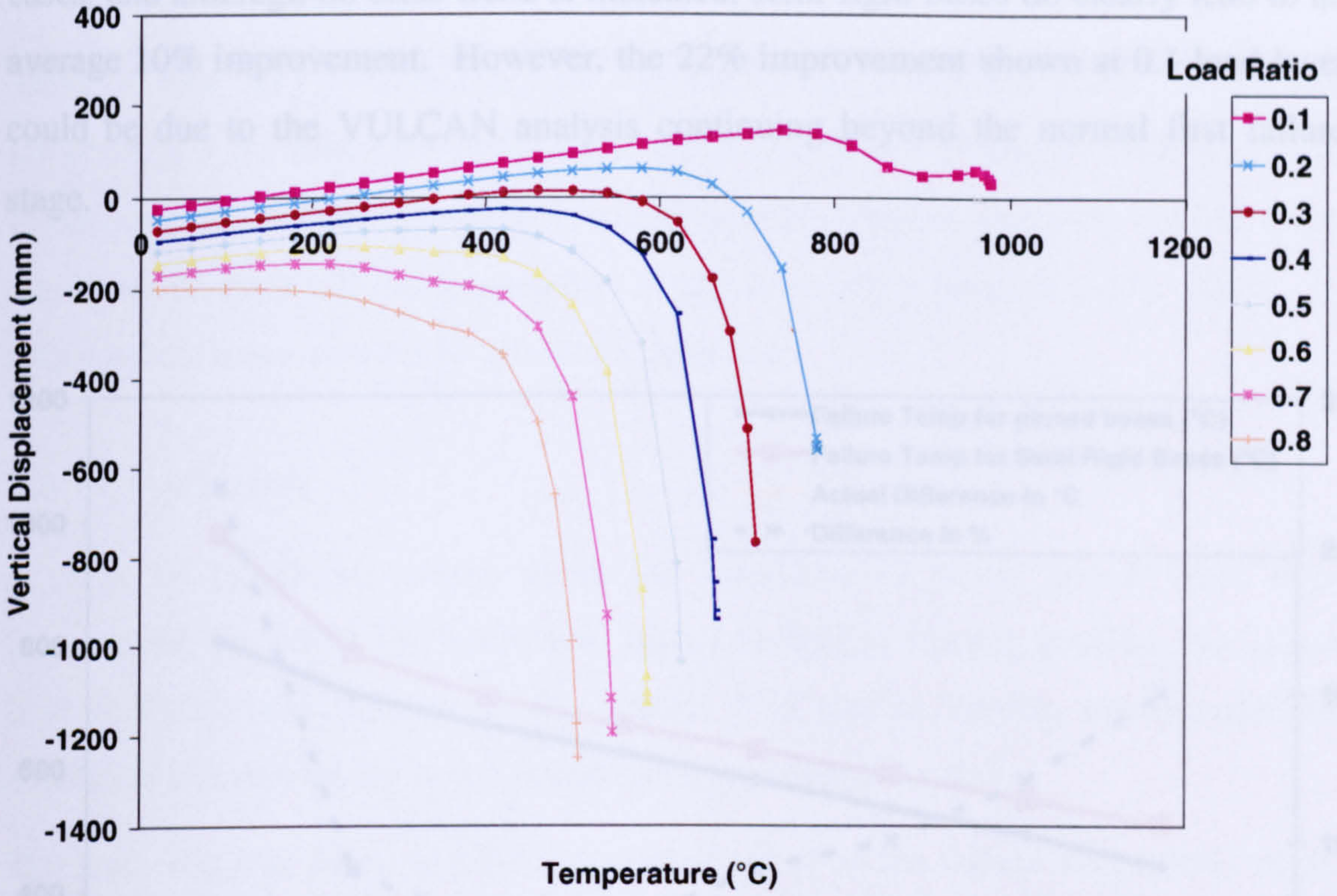

Figure 5.20 Vertical Displacement at Apex – Semi-Rigid Base with Various Load Ratios

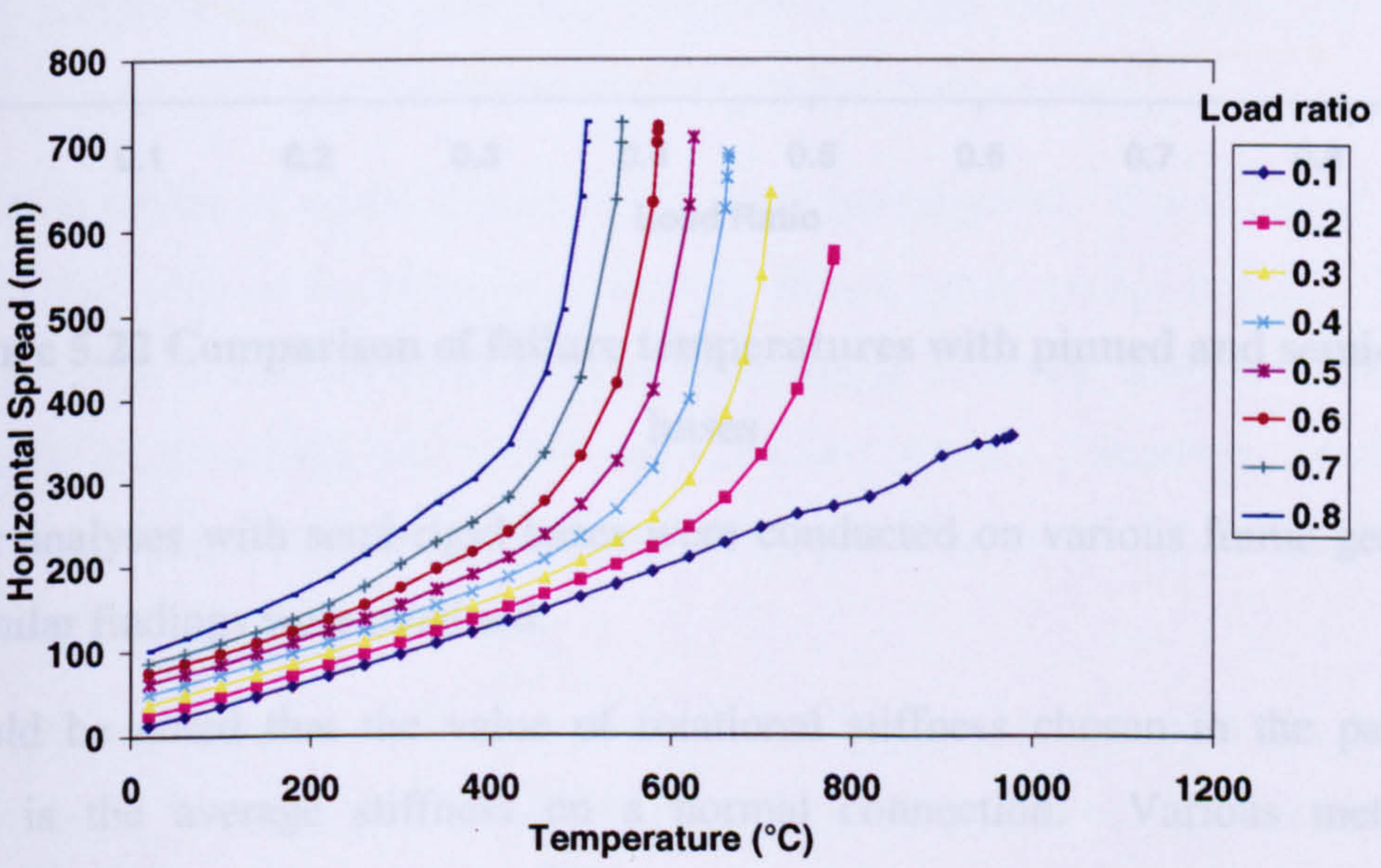

Figure 5.21 Horizontal Spread of Eaves – Semi-Rigid Base with Various Load Ratios

Figure 5.22 compares the actual failure temperatures of the pinned and semi-rigid cases, and although no clear trend is indicated, semi-rigid bases do clearly lead to an average 10% improvement. However, the 22% improvement shown at 0.1 load level could be due to the VULCAN analysis continuing beyond the normal first failure stage.

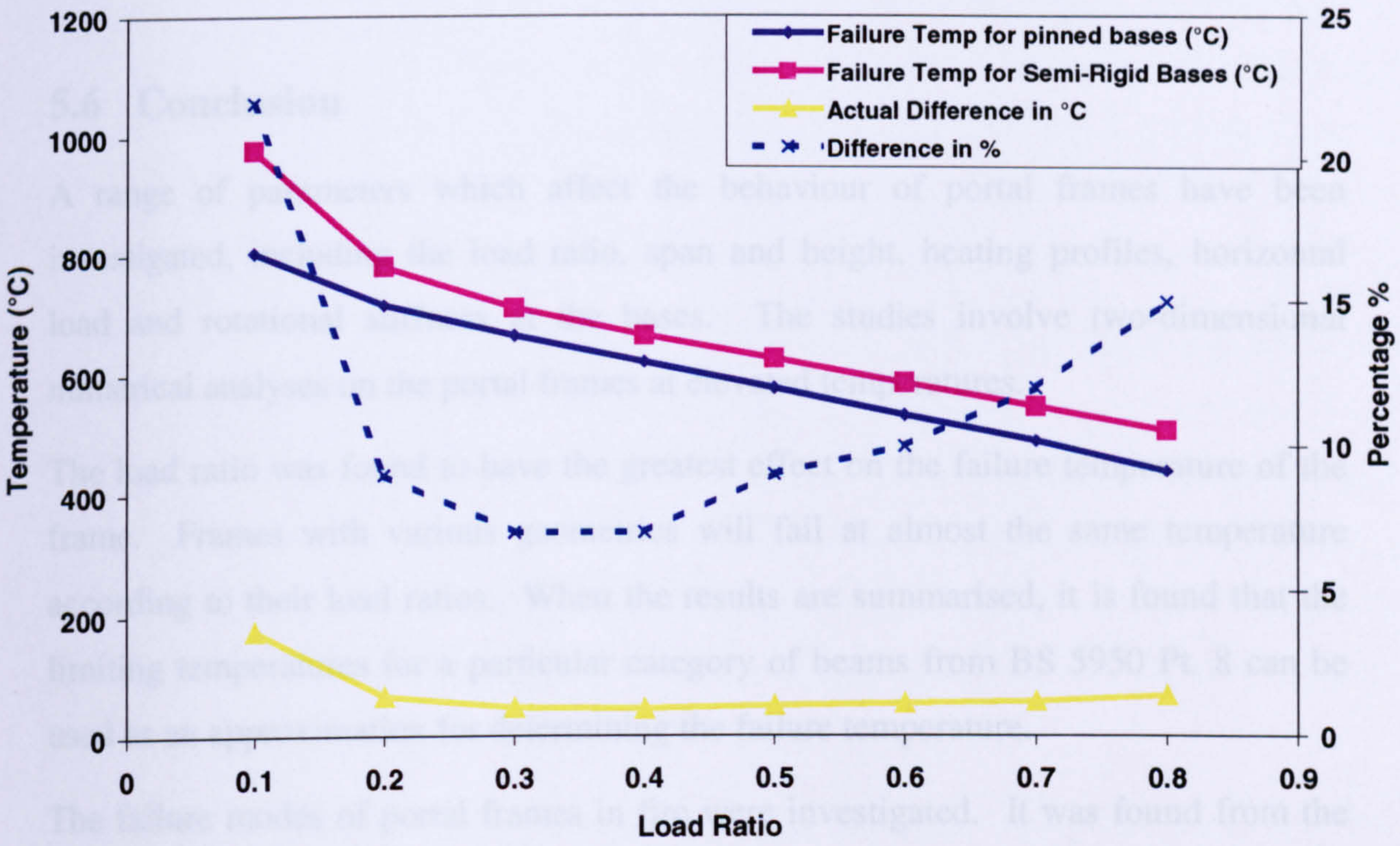

Figure 5.22 Comparison of failure temperatures with pinned and semi-rigid bases

Further analyses with semi-rigid bases were conducted on various frame geometries and similar findings were obtained.

It should be noted that the value of rotational stiffness chosen in the parametric studies is the average stiffness on a normal connection. Various methods of determining the actual rotational stiffness can be found based on current research[58,61]. However, the calculation for these stiffnesses would normally consider the interaction between the steel and concrete foundation only. The interaction between the soil and the foundation is little known. The fact that a relatively high factor of safety is often adopted in a foundation design has led to difficulty in determining the overall

rotational stiffness of the complete base. Therefore, the assumption of a pinned connection is considered always to be safe.

There is also very limited research and knowledge about the effect of elevated temperature a the rotational stiffness of base connections. However, it is reasonable to consider that the base connection would normally remain relatively cold in a fire due to its position. If the temperature of the connection remains below 400°C, its rotational stiffness may not be affected a great deal.

5.6 Conclusion

A range of parameters which affect the behaviour of portal frames have been investigated, including the load ratio, span and height, heating profiles, horizontal load and rotational stiffness at the bases. The studies involve two-dimensional numerical analyses on the portal frames at elevated temperatures.

The load ratio was found to have the greatest effect on the failure temperature of the frame. Frames with various geometries will fail at almost the same temperature according to their load ratios. When the results are summarised, it is found that the limiting temperatures for a particular category of beams from BS 5950 Pt. 8 can be used as an approximation for determining the failure temperature.

The failure modes of portal frames in fire were investigated. It was found from the analyses that none of the frames had a sway failure mode except one case in which extremely high horizontal force and low span-height ratio was adopted. This case is thought to be unrealistic and would not exist in practice. Therefore, wind loading does not normally produce a critical case for portal frames in fire, in particular for large-span frames.

When the heating profile of the portal frame has been investigated, it was found that the heating of columns does not affect the failure temperatures significantly. In the event of a local fire, the heating scheme in which the eaves are heated was found to be the most critical case.

The extra rotational stiffness of normally pinned bases is shown to be beneficial to the failure temperature of the portal frame compared to the normal assumption of pinned bases. However the overall rotational stiffness, in particular the interaction between the foundation and the soil, is little known and research on the effect of elevated

temperature on the connection is limited. Therefore, it is difficult to quantify the actual benefit of the semi-rigid behaviour of the column base.

6 Parametric Studies 2 – Three Dimensional Analysis

Following the series of 2-dimensional parametric studies on portal frame behaviour in fire, it was proposed to extend the analyses to 3-dimensional behaviour using the finite element program VULCAN. In previous studies, a relatively small model with just one portal frame bay had been set up to model one of the scaled frame fire tests at Buxton. It gave an indication of VULCAN's capability for the analyses. A more complete 3–dimensional analysis is now attempted in this study. Inevitably the 3-dimensional model will be much larger, and hence prolonged analysis time is required. The details of the model will be described in the following Section 6.1.

6.1 The 3-Dimensional Model and Assumptions

It is necessary to include the secondary members within the 3-dimensional model, and it is important how they are modelled. The major secondary members which contribute to the portal frame behaviour are the Z-purlins found in most industrial construction. The purlins are normally made of cold-formed galvanised steel, spaced close to each other (typically 1.5 – 2.0 metres apart). They are designed to resist the vertical load from roof and to restrain horizontal movement or minor-axis buckling of the main portal frame rafters.

However, the purlins are weak in minor-axis buckling. Under fire conditions, they are heated rapidly due to their minimal thickness and high H_p/A ratio. The bending resistance in fire is therefore almost negligible, and the fire tests at Buxton have given evidence of this. Nevertheless, the purlins were recognised to provide a certain degree of restraint to the rafters, through their tension capacity as interconnecting members.

Therefore although VULCAN analysis does not model the local behaviour of steel members, (i.e. local buckling and twisting) this was not considered essential in fire. In order to simulate the tension resistance of purlins, the Z-shape can be replaced by the I-shape traditionally used in VULCAN, approximating the width of the top/bottom flange as the width of the I member and adopting the same depth and thickness throughout.

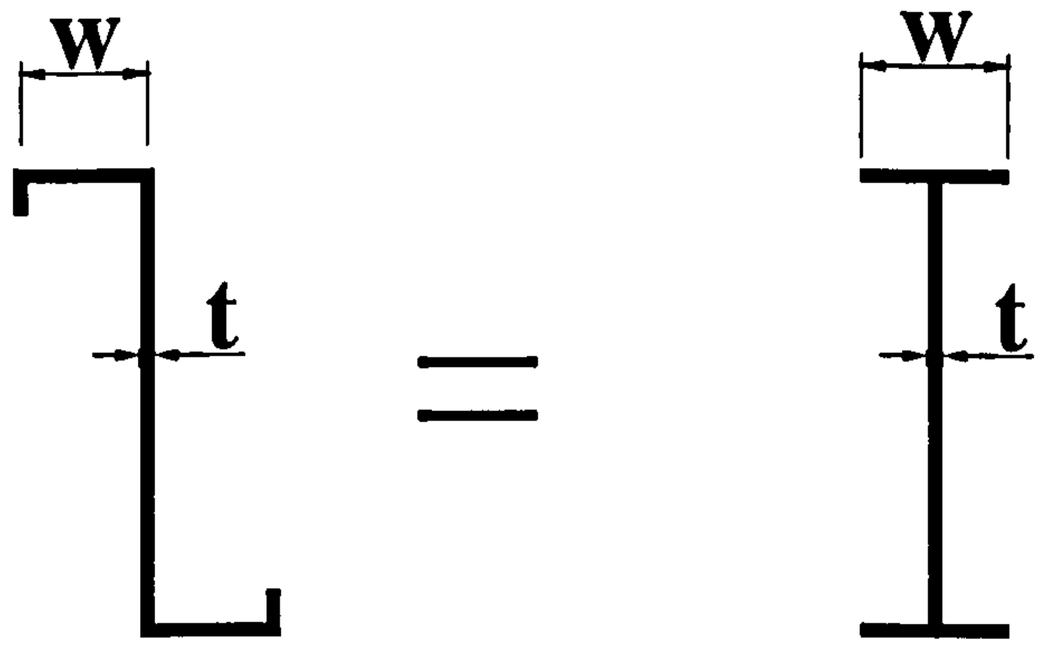

Figure 6.1 Simulation of Z-purlin in VULCAN

With such a thin and relatively deep section, the purlins are usually fixed to the roof cladding and support the vertical load. The interlocking roof cladding, spanning between purlins, nevertheless provides lateral restraint so that they do not buckle about the minor axis. This is particularly important in fire conditions because the expansion within the heated purlins alone could cause minor-axis failures of the sections in the early stages.

The potential problem was recognised when a preliminary VULCAN model was set up while excluding the consideration of any roof cladding effect. The analyses could not be extended to high temperatures because of the failure of purlins at an early stage. The difficulty was overcome by subsequently including imaginary members that connect the purlins together. These imaginary members span between purlins and lie parallel to the portal rafters. They have minimal area and thickness (10x10 mm H section with 1mm thickness) and only act in tension, simulating the effect of a roof cladding restraint.

Figure 6.2 shows the set-up of the finite element model, including the mesh representing the combination of purlins and roof cladding. The mesh enables the simulation of an orthotropic surface with the primary vertical resistance coming from the Z-purlins. The entire mesh will behave as a continuum and this is thought to be close enough in representing the real structure. Since both the purlins and the imaginary members are relatively small in section, the effects of connection on the entire portal frame are negligible, and therefore spring elements were not introduced.

The figure shows that the model only consists of three portal frames. Although it is not a full industrial warehouse shed, the model should be sufficient to generate representative results for the studies. The model consists of 237 nodes and 350 elements. The computer time required for a single analysis was much longer than for

a 2-dimensional analysis.

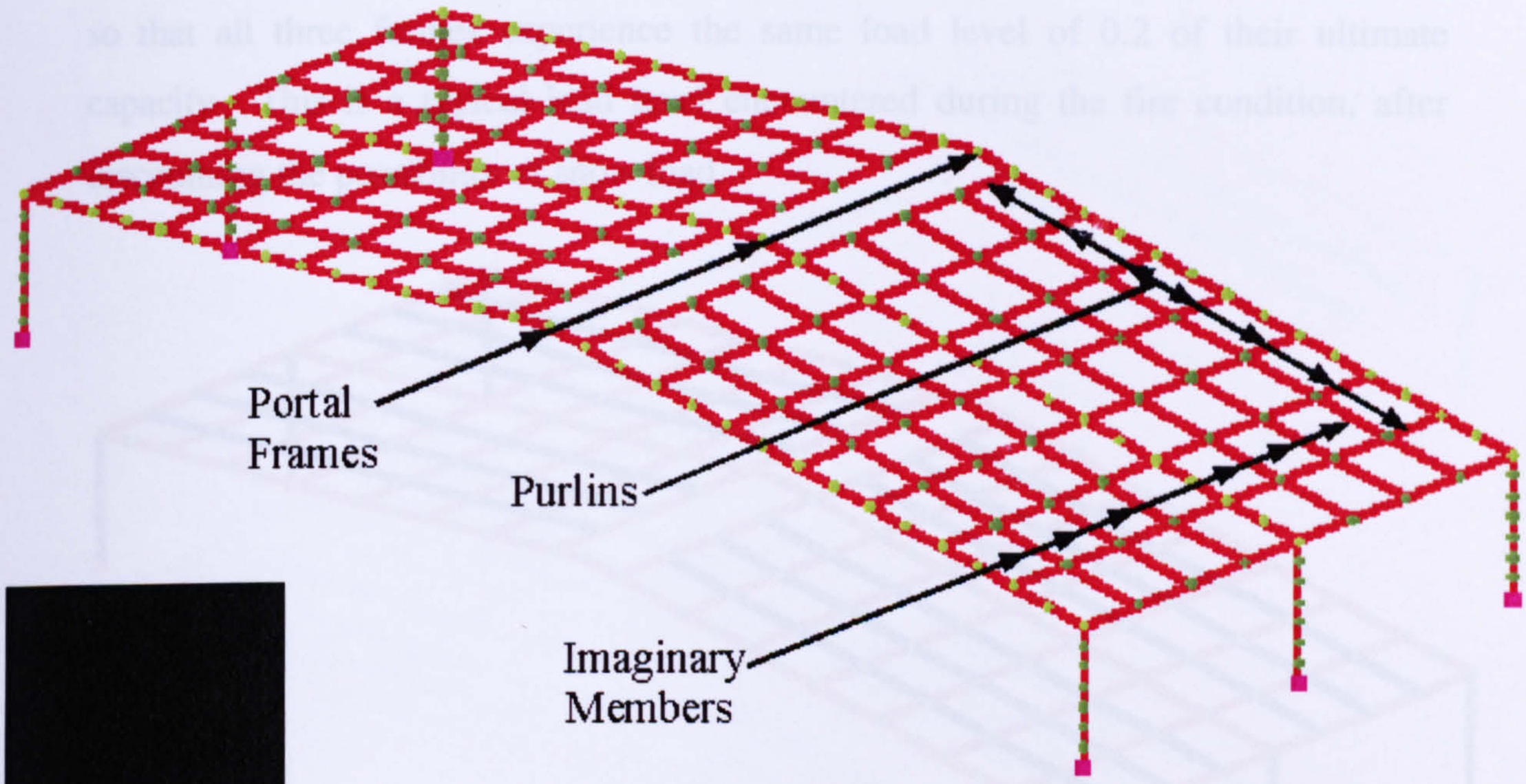

Figure 6.2 VULCAN Model of 3-Dimensioanl Portal Frame Warehouse

6.1.1 3-Dimensional VULCAN Model

In order to start the investigation of the 3-dimensional behaviour, a typical industrial portal frame layout was used. The span of the portal frames adopted is 30m and the frame centres are spaced 6m apart. The height to eaves is 7m with the roof pitched at 14.9°. The generic dimensions have often been adopted in the 2-dimensional parametric studies conducted previously. The same section sizes were again adopted and the assumption of no haunches remains.

It was decided to compare the 3-dimensional analysis with the previous 2-dimensional case as the basis of the studies. The basic model shown in Figure 6.2 was adopted and the details are presented in the following section.

6.2 Case 1 – Entire Roof Heated

Using the model described previously, a fire scenario involving heating of the entire roof member will be modelled in this section. The columns in this case are assumed to be protected and remain relatively cool. A conservative assumption of pinned bases is adopted so that like-against-like comparison to a 2-D analysis can be done. A uniformly distributed load of 0.4 kN/m^2 has been applied to the entire roof, spread

evenly between nodes. The load is equivalent to a load ratio of 0.2 on the central portal frame. Additional load has been applied to the portal frames at the two edges so that all three frames experience the same load level of 0.2 of their ultimate capacity. This is a typical load level encountered during the fire condition, after discounting the possibility of snow load.

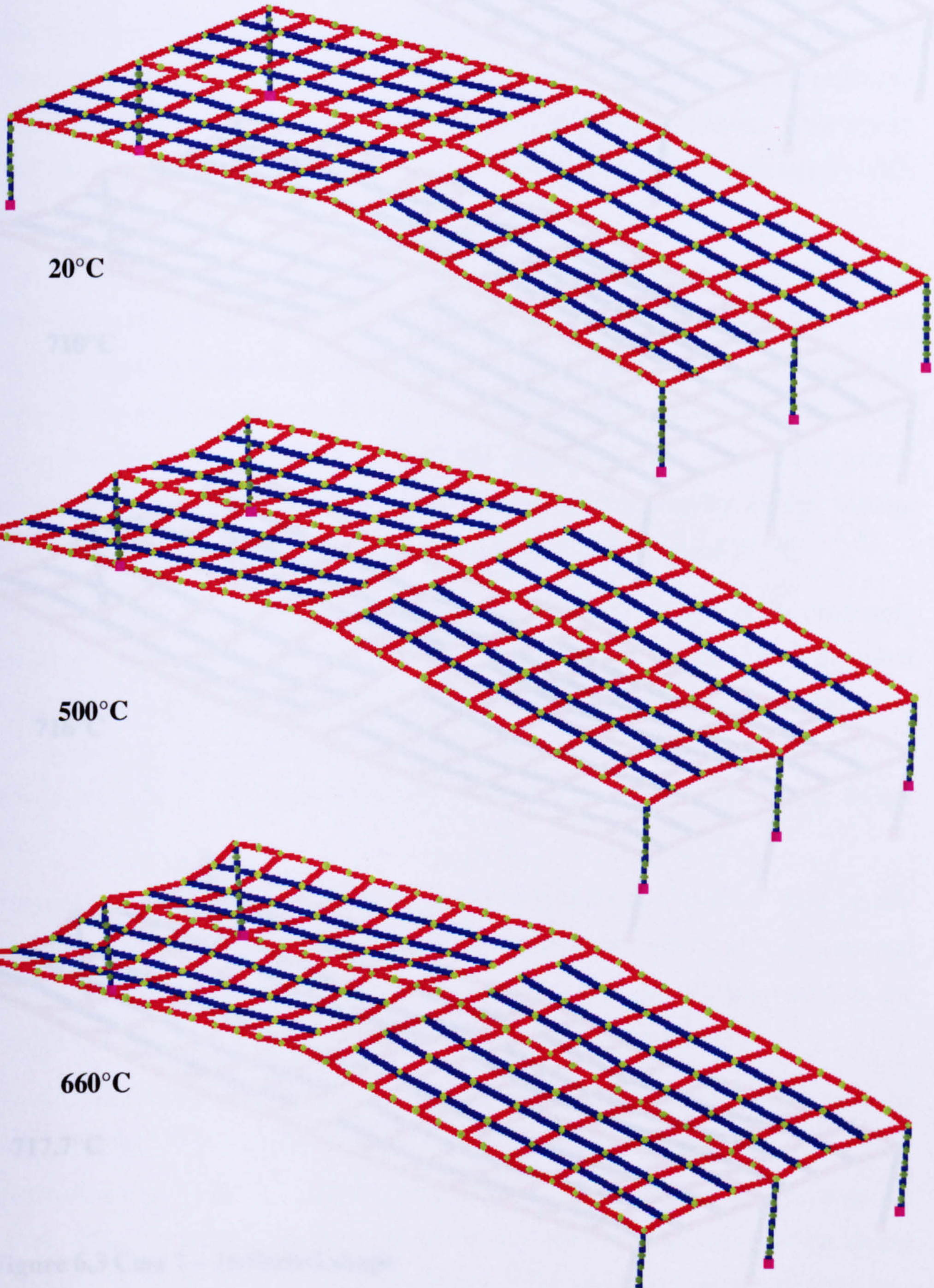

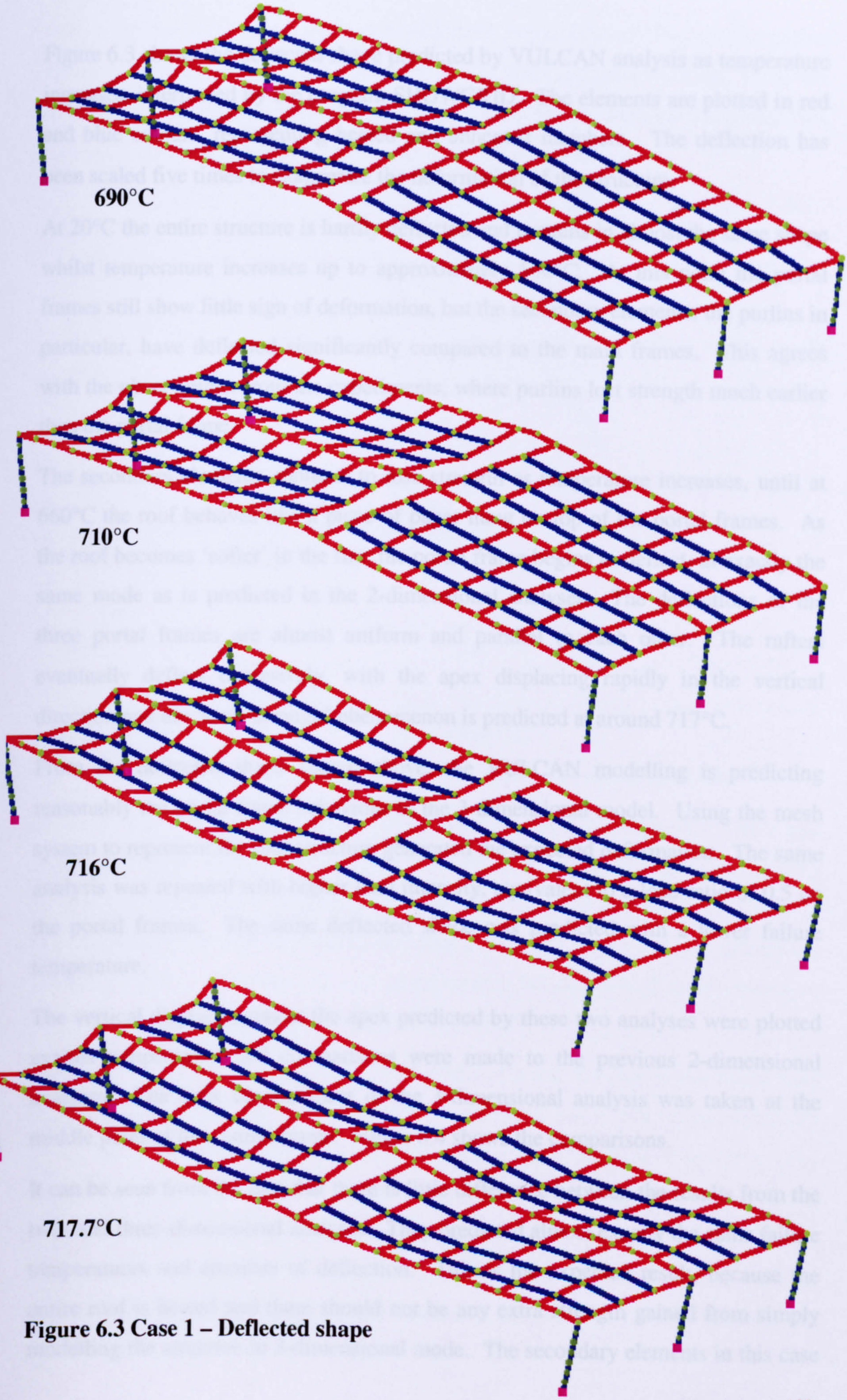

Figure 6.3 Case 1 – Deflected shape

Figure 6.3 shows the deflected shape predicted by VULCAN analysis as temperature increases, interpreted by the program SHOWGRID. The elements are plotted in red and blue colours, representing heated and unheated members. The deflection has been scaled five times to exaggerate the deformation of the structure.

At 20°C the entire structure is hardly deflected and remains in almost the same shape whilst temperature increases up to approximately 500°C. At this point the portal frames still show little sign of deformation, but the secondary elements, the purlins in particular, have deflected significantly compared to the main frames. This agrees with the observations from the experiments, where purlins lost strength much earlier than the portal frame.

The secondary elements continue to lose strength as temperature increases, until at 660°C the roof behaves like a piece of paper hung on top of the portal frames. As the roof becomes 'softer' in the fire, the portal frame begins to deflect, in exactly the same mode as is predicted in the 2-dimensional analyses. The deflections of the three portal frames are almost uniform and parallel to each other. The rafters eventually deflect excessively, with the apex displacing rapidly in the vertical direction and the 'snap-through' phenomenon is predicted at around 717°C.

From the deflected shape shown above, the VULCAN modelling is predicting reasonably the portal frame behaviour in the 3-dimensional model. Using the mesh system to represent the roof structure generated the expected deformation. The same analysis was repeated with higher load intensity, equivalent to a load ratio of 0.5 on the portal frames. The same deflected shape was predicted with a lower failure temperature.

The vertical displacements at the apex predicted by these two analyses were plotted against temperature, and comparisons were made to the previous 2-dimensional analyses. The apex displacement of the 3-dimensional analysis was taken at the middle point of the central frame. Figure 6.4 shows the comparisons.

It can be seen from the plot that there is little difference between the results from the two- and three-dimensional analyses. They predicted almost exactly the same failure temperatures and amounts of deflection. This is the expected result, because the entire roof is heated and there should not be any extra strength gained from simply modelling the structure in 3-dimensional mode. The secondary elements in this case

were only providing lateral restraint to the main portal frames. The purlin spacing has actually provided sufficient restraint to the rafters against buckling about the minor axis. The imaginary members were providing exactly the same restraint to the purlins as they would in reality, given the roof cladding interaction.

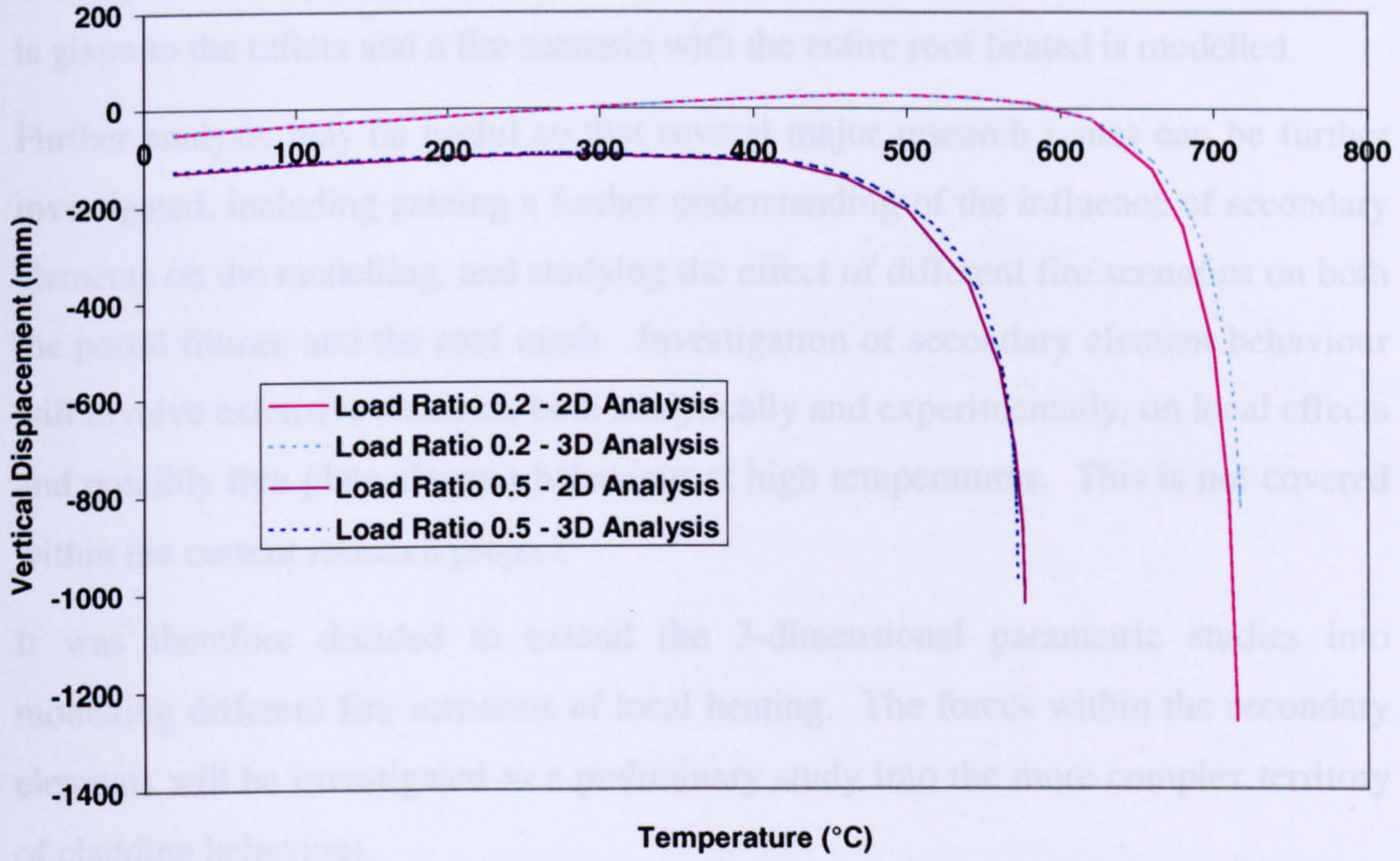

Figure 6.4 Vertical displacement at apex – 2D vs. 3D analysis

However, the forces within the imaginary members are not comparable with a real cladding. These members should not be used to represent the cladding without further investigation into cladding behaviour. The fact that they were not heated in the analysis simply assumes that the cladding is infinitely strong and will not split in the fire condition. In reality, the roof cladding may fail due to high temperatures, or may even fall off as the purlins deform excessively.

However, if the roof cladding fails in the event of a real fire, the portal frame may benefit from this situation. The load level on the portal frame will further reduce by losing the cladding self-weight and possibly a significant amount of services. The steel temperatures are likely to reduce as additional ventilation becomes available (assuming flashover has already taken place, as it would if the entire rafter is heated to the failure temperature). On the other hand, the failure of cladding may increase the life-safety risk of fire fighters, but whether or not the fire fighters remain in the

building the post-flashover stage is questionable. The issue will be further discussed later.

6.2.1 Further Analysis

The 3-dimensional analyses have demonstrated that portal frame behaviour can be well represented by 2-dimensional modelling, provided that sufficient lateral restraint is given to the rafters and a fire scenario with the entire roof heated is modelled.

Further analysis may be useful so that several major research issues can be further investigated, including gaining a further understanding of the influence of secondary elements on the modelling, and studying the effect of different fire scenarios on both the portal frames and the roof mesh. Investigation of secondary element behaviour will involve extensive research, both analytically and experimentally, on local effects and possibly thin plate element behaviour at high temperatures. This is not covered within the current research project.

It was therefore decided to extend the 3-dimensional parametric studies into modelling different fire scenarios of local heating. The forces within the secondary elements will be investigated as a preliminary study into the more complex territory of cladding behaviour.

6.3 Case 2 – Local Fire Scenarios 1

Using the same 3-dimensional model set up previously, this study will look at the effect of the central portal frame being heated while the other two frames remain at ambient temperature and provide additional support. The study will look at the effect of unprotected columns and unheated purlins. A load ratio of 0.2 has been adopted throughout. Figure 6.5 summarises the four cases analysed by VULCAN, with red coloured elements representing the heated members. The cases are:

(a) All purlins heated, columns remain cold.

(b) All purlins heated, columns heated.

(c) Half of the purlins heated, columns remain cold

(d) Half of the purlins heated, columns heated.

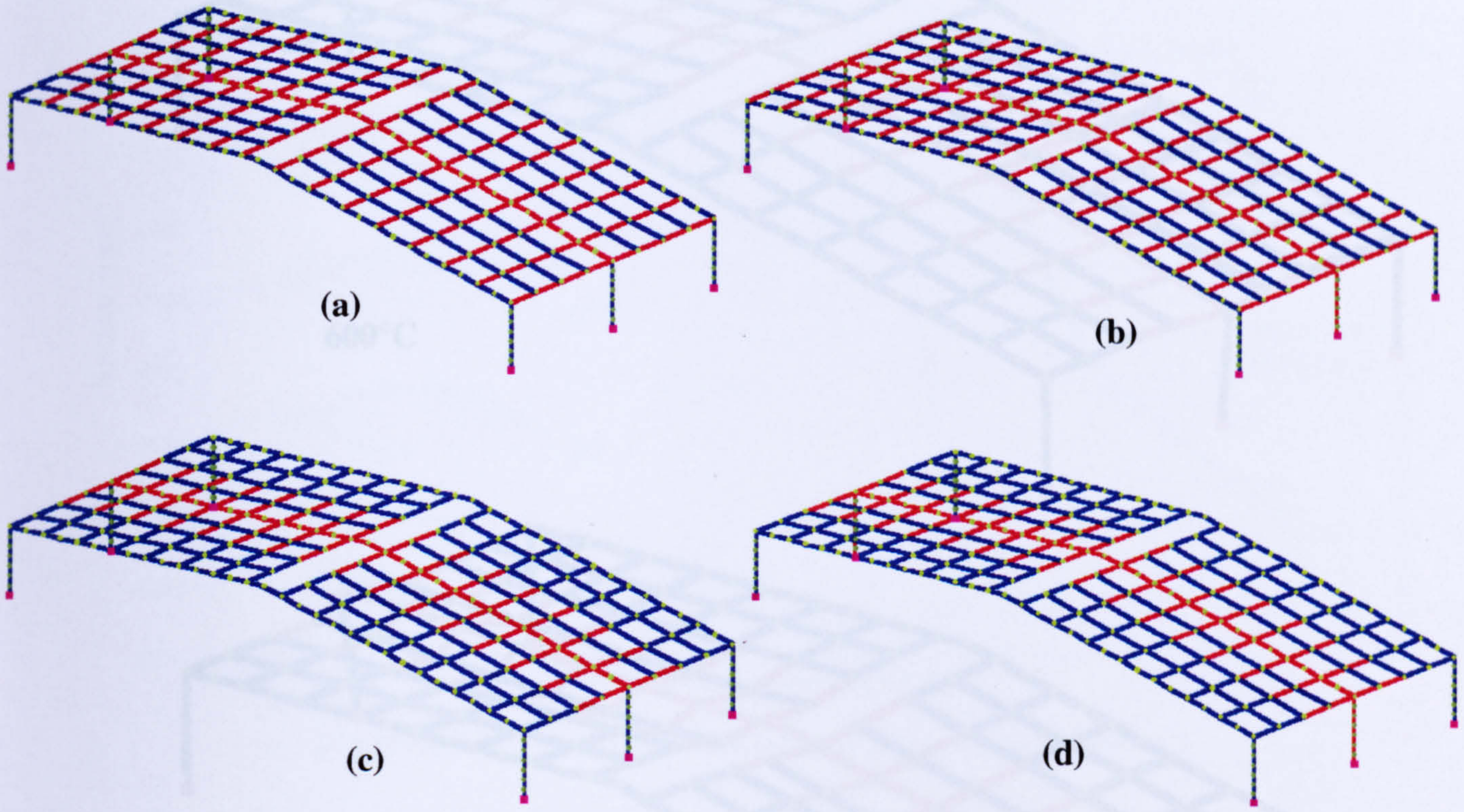

Figure 6.5 Local fire scenarios

All four cases were analysed with VULCAN and the deflected shape was generated and inspected using SHOWGRID. A visual inspection identifies any errors created during the modelling and assists in understanding the process of deformation. Figure 6.6 shows the deflected procedure predicted by the analysis for fire scenario (c), with the displacement scaled by a factor of 5.

In fact, it was found that the portal frame behaviour in each fire scenario is always dominated by expansion of the secondary elements at the initial heating stage, i.e. prior to 600°C. The rafters then start to lose their strength, followed by more rigorous deformation as temperature increases.

Although the final deformation shape at 880°C shown in Figure 6.6 does not clearly indicate a snap-through failure of the heated portal frame, the plot of vertical displacement at the apex shows the excessive vertical displacements with negligible horizontal movement. The plot is shown in Figure 6.7 along with the results from other fire scenarios, including Case 1 from Section 6.2 where the entire roof rafters were heated.

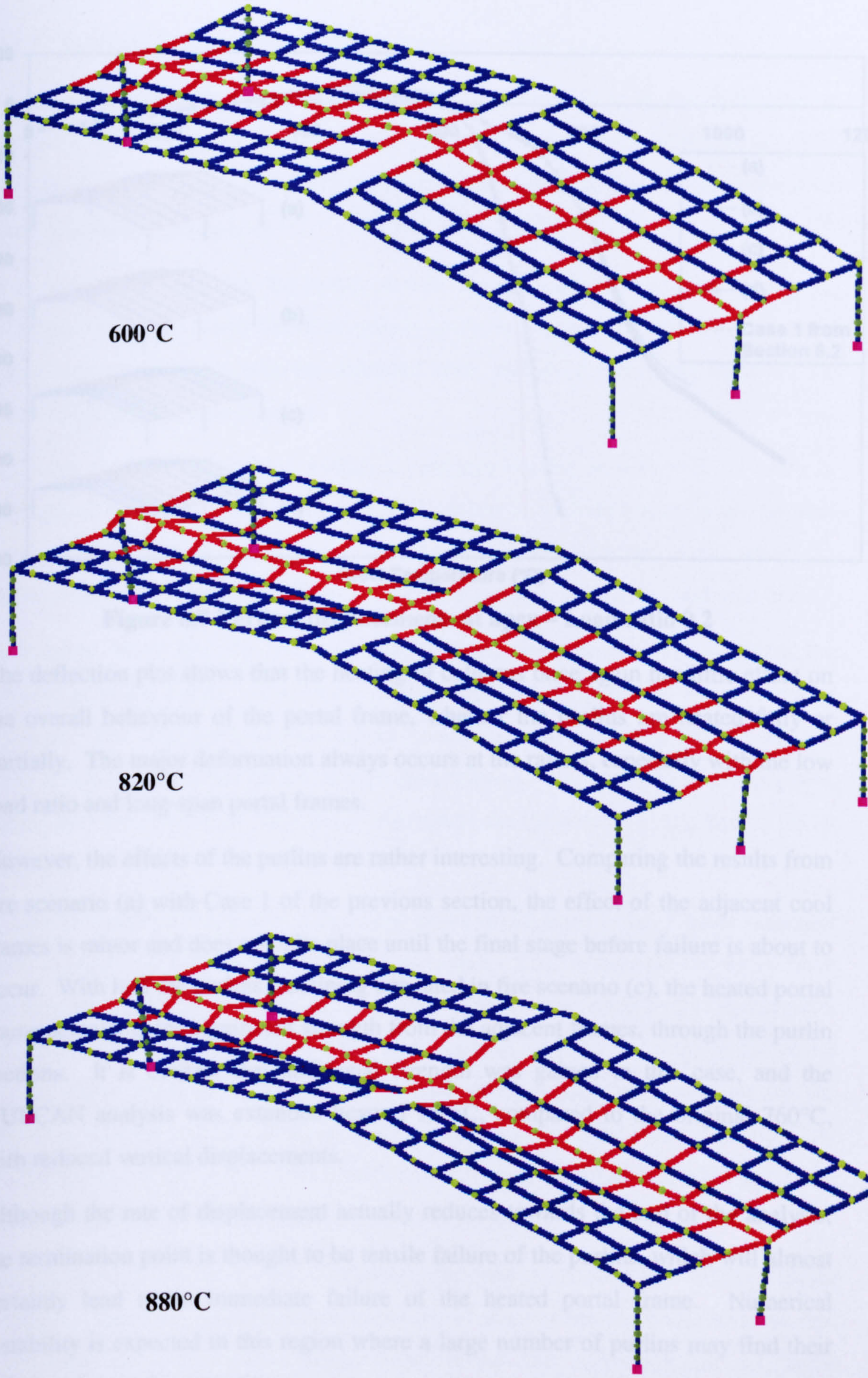

Figure 6.6 Deflected shape – fire scenario (c)

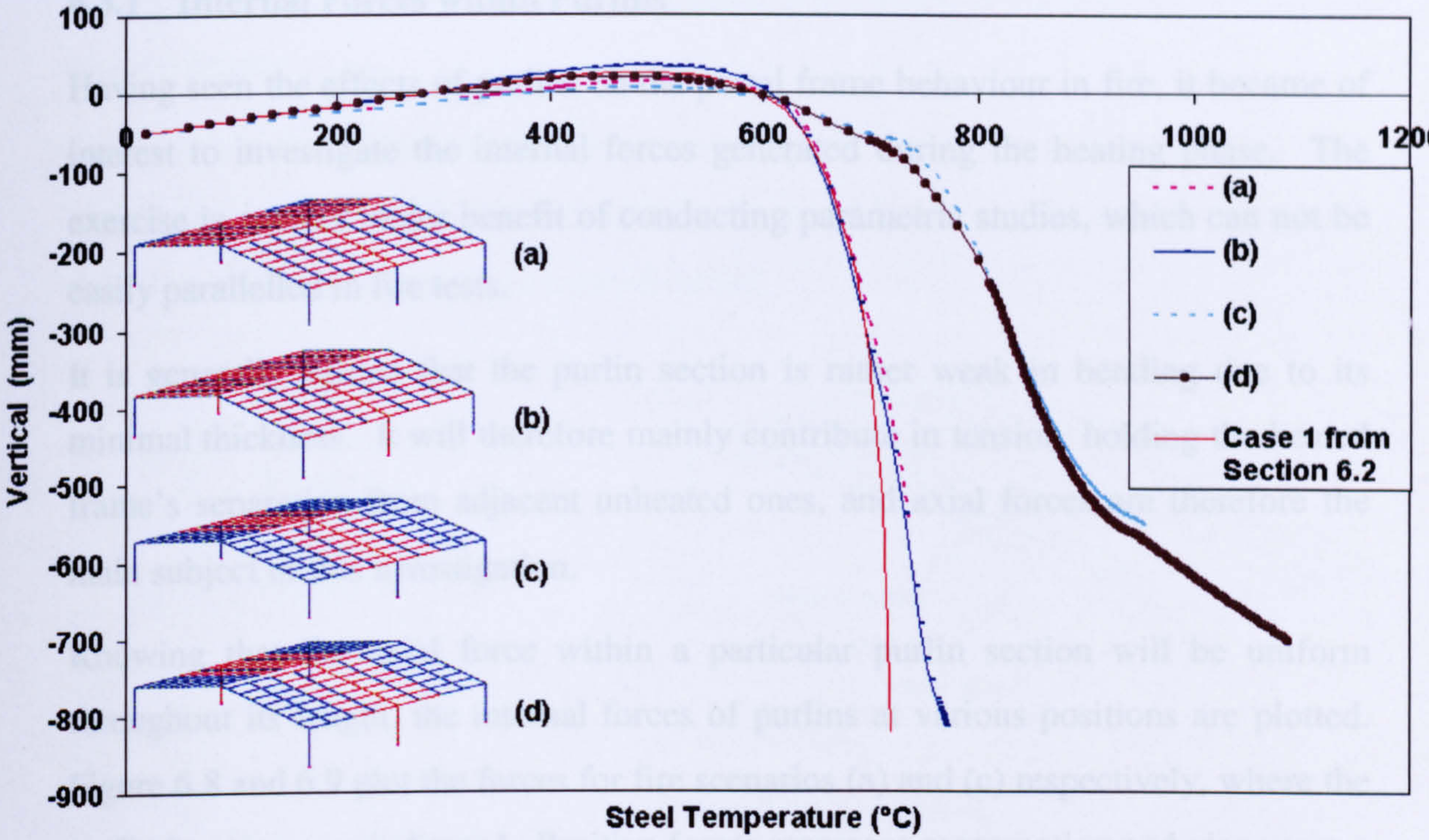

Figure 6.7 Vertical displacements at apex – Load ratio 0.2

The deflection plot shows that the heating of columns once again has little effect on the overall behaviour of the portal frame, whether the purlins are heated fully or partially. The major deformation always occurs at the rafters, especially with the low load ratio and long-span portal frames.

However, the effects of the purlins are rather interesting. Comparing the results from fire scenario (a) with Case 1 of the previous section, the effect of the adjacent cool frames is minor and does not take place until the final stage before failure is about to occur. With half the purlins remaining unheated in fire scenario (c), the heated portal frame actually gains significant strength from the adjacent frames, through the purlin sections. It is evident that additional strength was gained in this case, and the VULCAN analysis was extended beyond 950°C, compared to the original 760°C, with reduced vertical displacements.

Although the rate of displacement actually reduces towards the end of the analysis, the termination point is thought to be tensile failure of the purlins, which will almost certainly lead to an immediate failure of the heated portal frame. Numerical instability is expected in this region where a large number of purlins may find their failure points at the same time.

6.3.1 Internal Forces within Purlins

Having seen the effects of purlins on the portal frame behaviour in fire, it became of interest to investigate the internal forces generated during the heating phase. The exercise is another major benefit of conducting parametric studies, which can not be easily parallelled in fire tests.

It is generally agreed that the purlin section is rather weak in bending due to its minimal thickness. It will therefore mainly contribute in tension, holding the heated frame's separation from adjacent unheated ones, and axial forces are therefore the main subject of this investigation.

Knowing that the axial force within a particular purlin section will be uniform throughout its length, the internal forces of purlins at various positions are plotted. Figure 6.8 and 6.9 plot the forces for fire scenarios (a) and (c) respectively, where the purlin locations are indicated. Positive forces represent compression and vice versa.

Both plots show that the purlins initially resist compression forces during the expansion of the purlins. The forces peak at different temperatures for each purlin location. The compressions then reduce to near zero or even drop into the tension zone at some stage before failure at high temperatures. The variation of compression forces and their peaks are very much relevant to the movement of the heated portal frame.

It can be seen that the purlin connecting eaves of adjacent portal frames (member 261) displays the highest amount of compression. This is because the eaves have more restraint to movement compared with the apex, where a relatively high amount of upward deflection was detected due to expansion. Adding on to this is the effect of the entire mesh interaction. The purlins are provided with restraint by the members representing the cladding, from which only one-sided restraint is available for the purlins at the eaves. When sufficient deformation is gained within the purlin connecting the eaves, the compression starts to reduce.

The force path for the purlin connecting the near apex (member 205) is rather different. There are minimal forces in the initial stage of heating because it was free to expand due to the upward displacement of the apex. Compression only takes place when the rate of deflection for the portal frame decreases. Eventually when the

snap-through of the portal frame takes place, the compression reduces to zero and tension begins.

It is worth noticing that all purlins are resisting tension just before failure, although the tension force is small, and this enables the portal frame to gain additional strength from the adjacent frames as mentioned earlier.

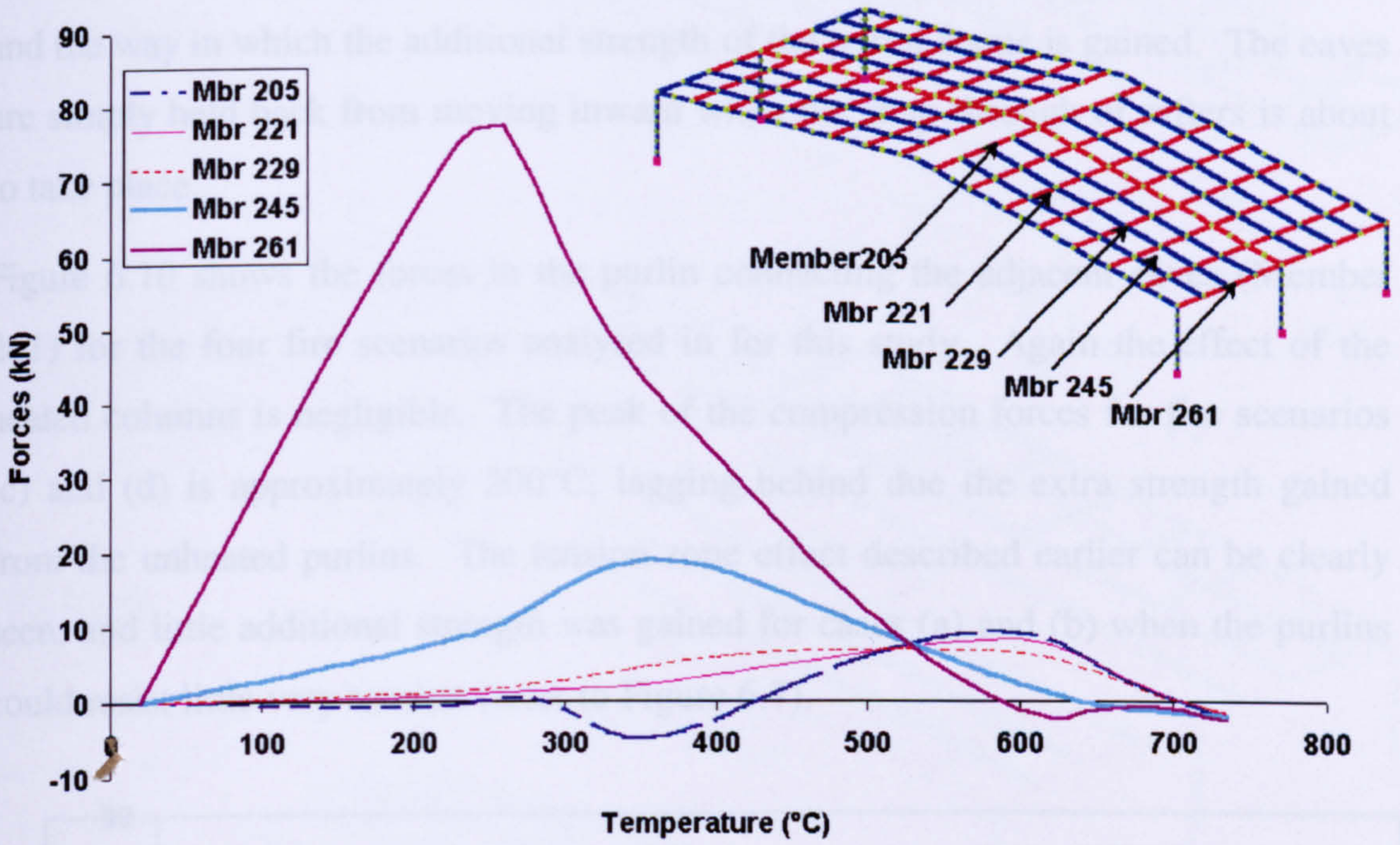

Figure 6.8 Axial forces within purlins – Fire Scenario (a)

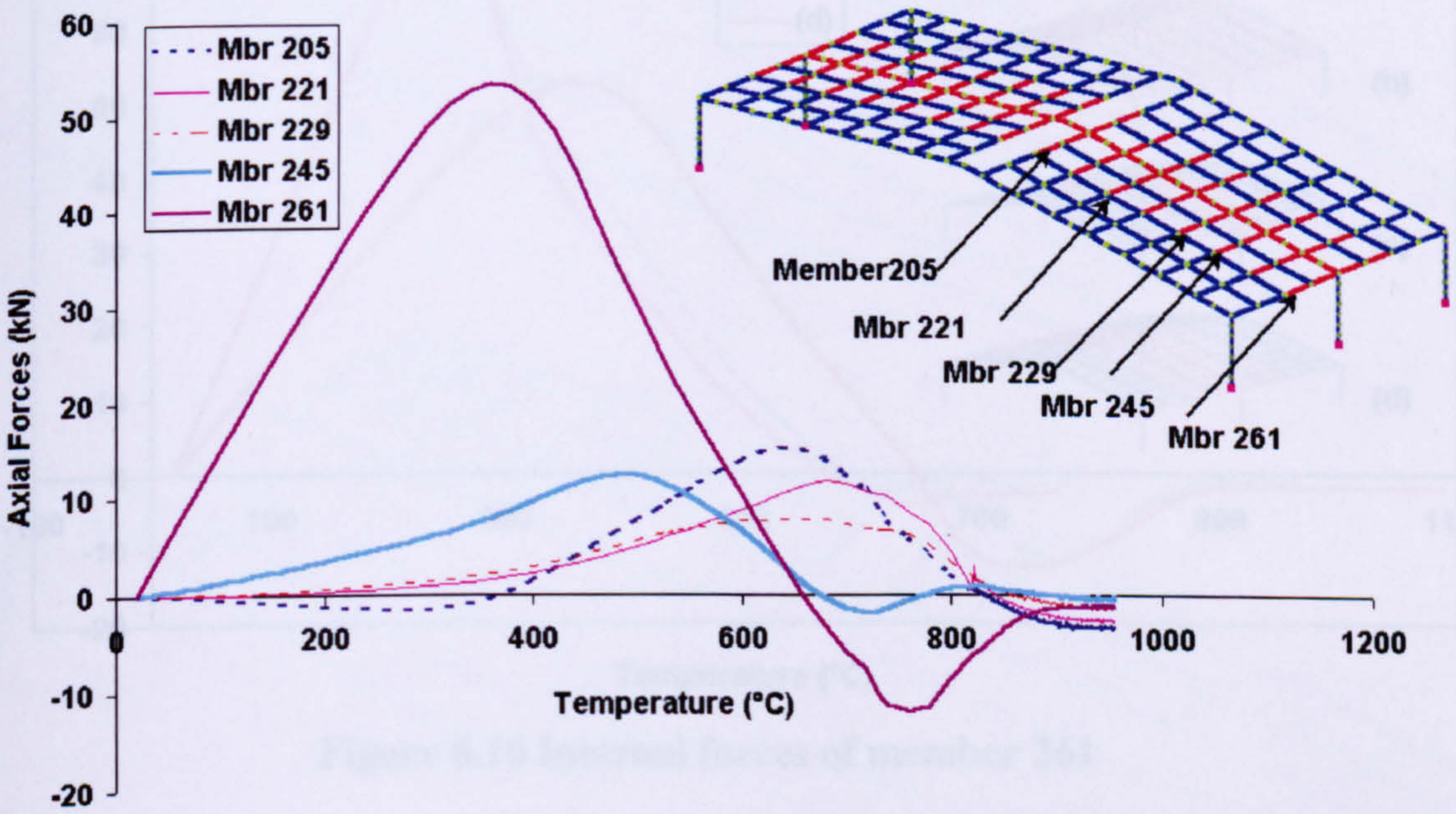

Figure 6.9 Axial forces within purlins – Fire Scenario (c)

The purlins' internal forces for the two different fire scenarios show similar patterns. The forces are higher for fire scenario (a) due to the higher amount of expansion. Interestingly the purlins connecting eaves points dip down into the tension zone at one stage in fire scenario (c) and have to resist a significant amount of tension. The tension force peak remains more or less at the same point where the analysis for fire scenario (a) terminates. This could be the main contribution of the unheated purlins and the way in which the additional strength of the portal frame is gained. The eaves are simply held back from moving inward when the snap-through of rafters is about to take place.

Figure 6.10 shows the forces in the purlin connecting the adjacent eaves (Member 261) for the four fire scenarios analysed in for this study. Again the effect of the heated columns is negligible. The peak of the compression forces for fire scenarios (c) and (d) is approximately 200°C, lagging behind due the extra strength gained from the unheated purlins. The tension zone effect described earlier can be clearly seen, and little additional strength was gained for cases (a) and (b) when the purlins could resist little very tension (refer to Figure 6.7).

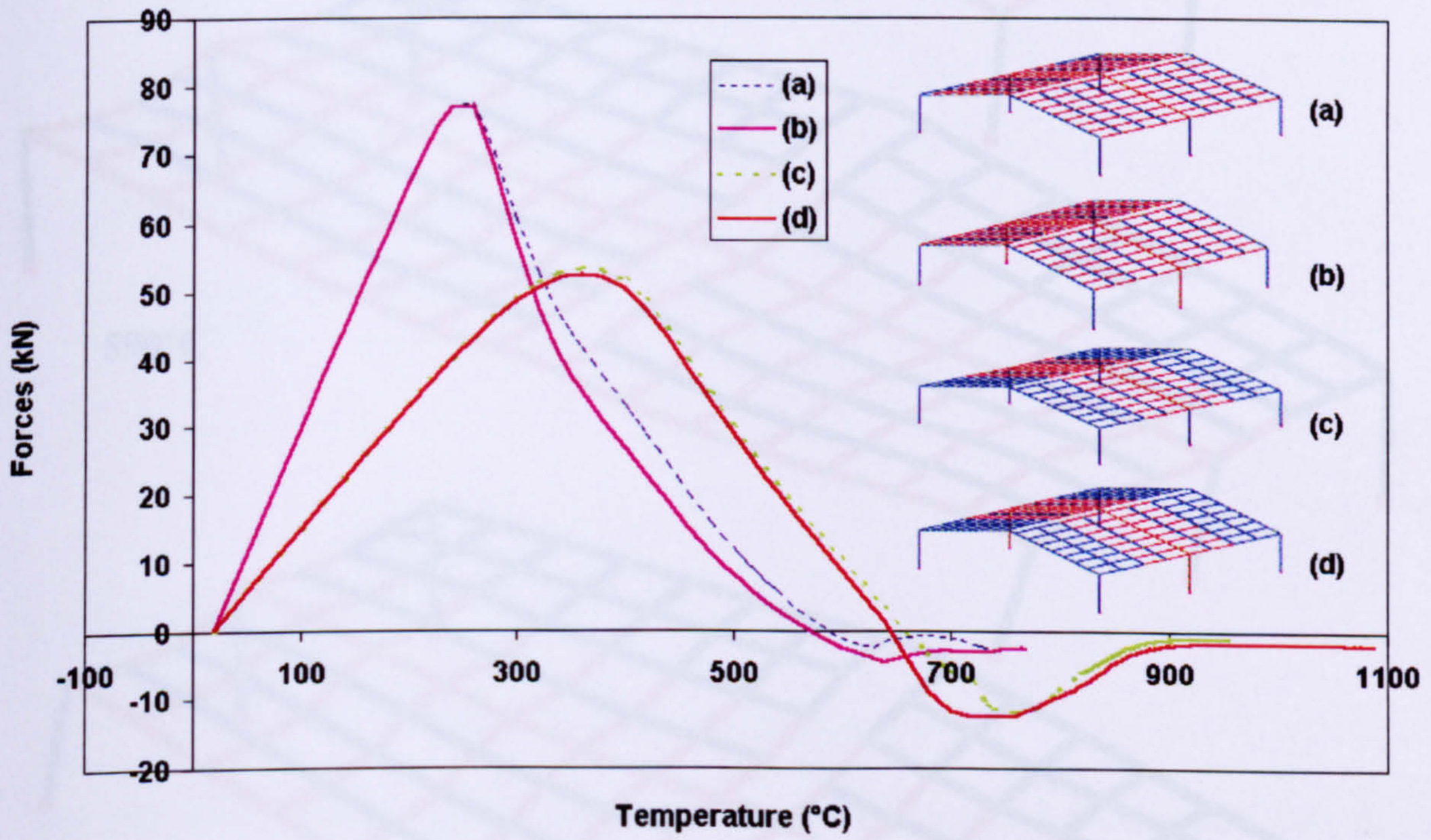

Figure 6.10 Internal forces of member 261

6.4 Case 3 – Local Fire Scenario 2

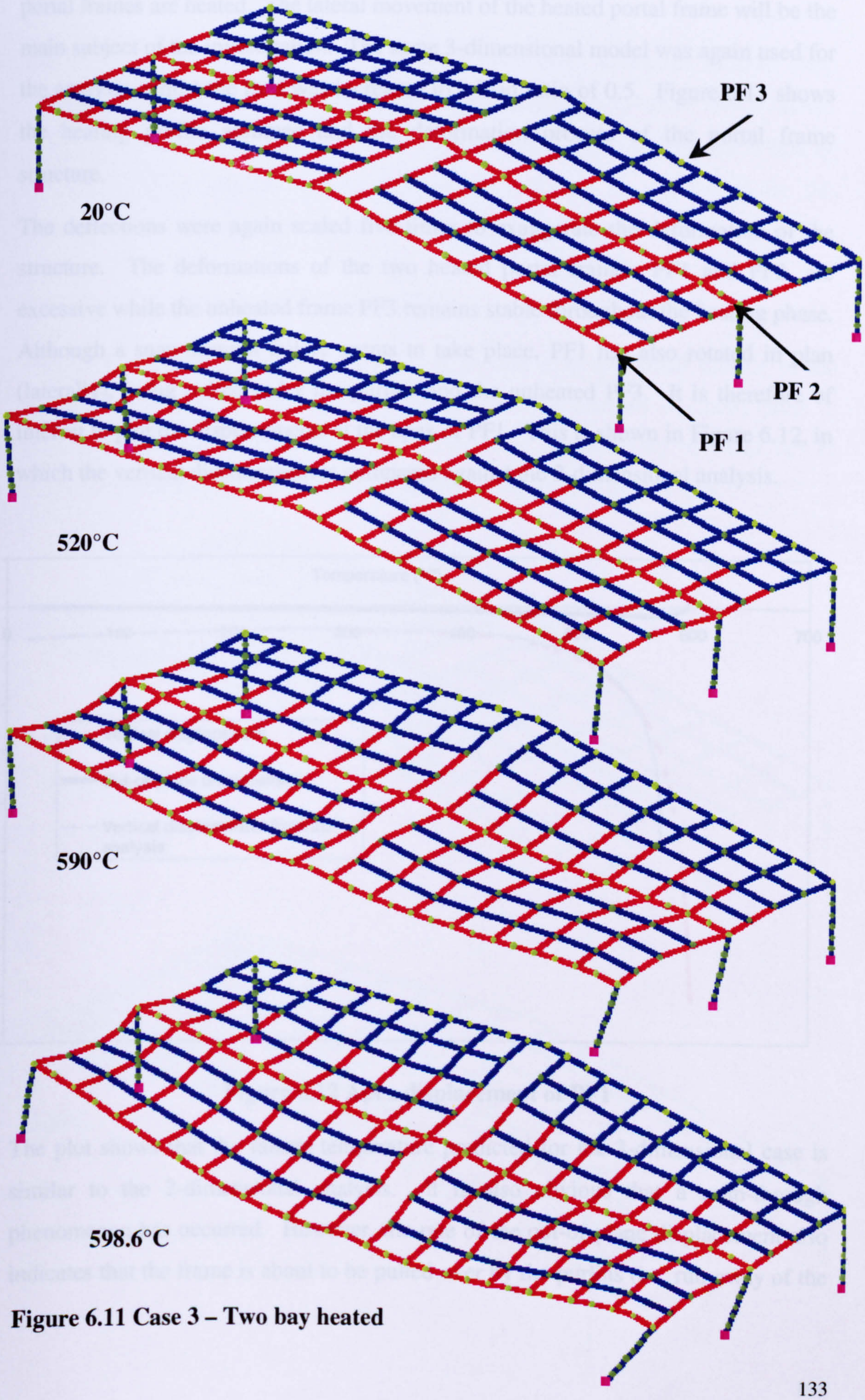

Figure 6.11 Case 3 – Two bay heated

This section describes the analysis conducted for the fire case where only two of the portal frames are heated. The lateral movement of the heated portal frame will be the main subject of the investigation. The same 3-dimensional model was again used for the analysis, whilst the load was increased to a load ratio of 0.5. Figure 6.11 shows the heating profile assumed and the deformation process of the portal frame structure.

The deflections were again scaled five times to exaggerate the deformation of the structure. The deformations of the two heated portal frames, PF1 and PF2, are excessive while the unheated frame PF3 remains stable throughout the heating phase. Although a snap-through failure seems to take place, PF1 has also rotated in plan (laterally), being pulled in by the purlins and the unheated PF3. It is therefore of interest to plot the displacements at the apex of PF1. This is shown in Figure 6.12, in which the vertical displacement is compared against the 2-dimensional analysis.

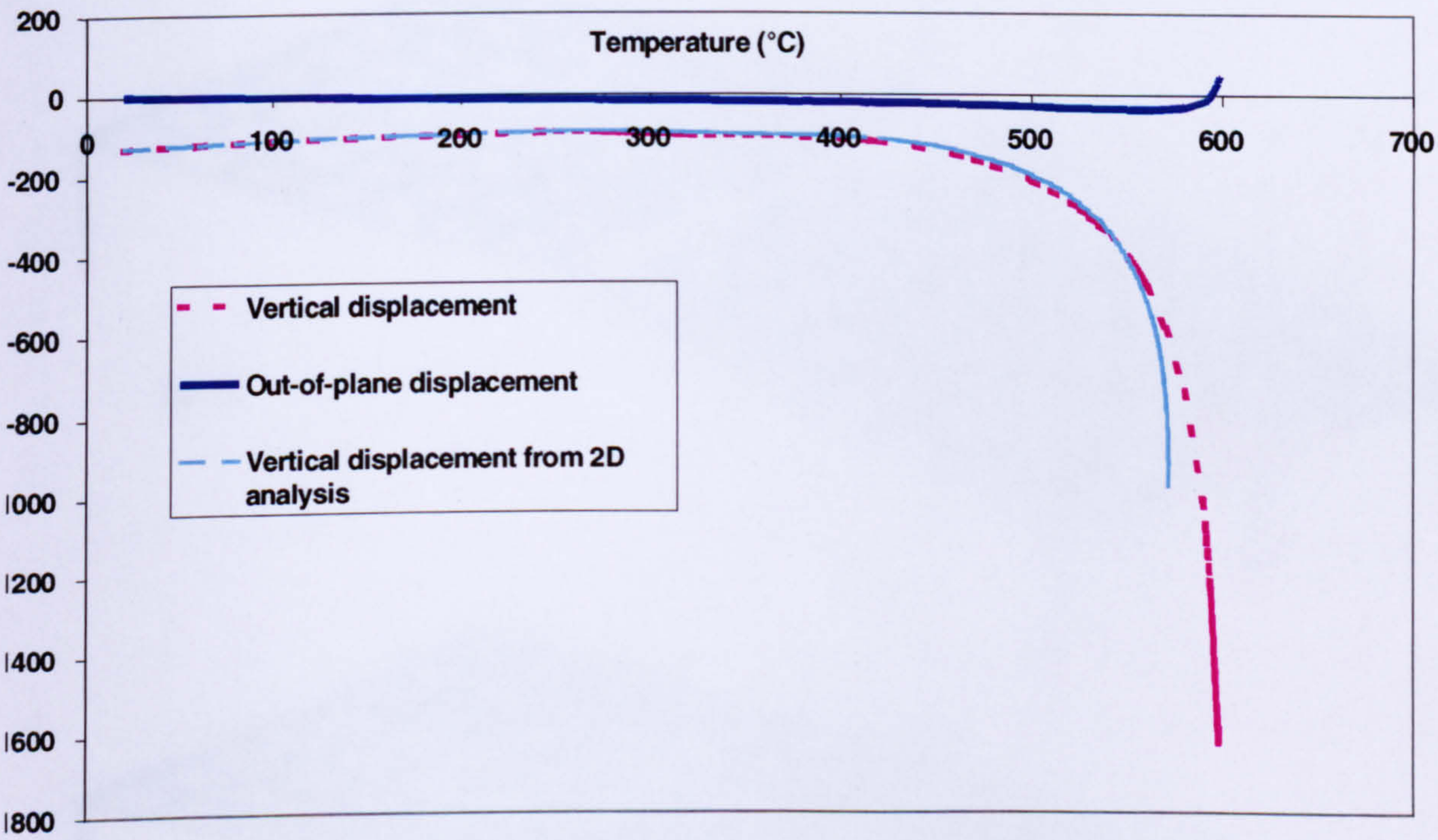

Figure 6.12 Apex displacement of PF1

The plot shows that the failure temperature predicted for the 3-dimensional case is similar to the 2-dimensional analysis. It is also obvious that a snap-through phenomenon has occurred. However, the rate of the out-of-plane displacement also indicates that the frame is about to be pulled over by the purlins (i.e. run-away of the

displacements). This is due to the rigid unheated frame at the far end. Such a phenomenon was not noticed previously.

The phenomenon could be transient or could even exist within the analysis only. One may argue that the purlins are simply not strong enough to create such a failure. In fact, the analytical assumption that the connections between purlins and rafters do not fail in fire conditions may be too onerous and may be responsible for this observation. Further research on this area is recommended.

6.5 Case 4 – Local Fire Scenario 3

The final case analysed within this study is to look at a very small portion of the portal frame structure heated due to a minor fire. The analysis is mainly done to visually inspect the deformation and to demonstrate the capability of VULCAN in the 3-dimensional analysis. Figure 6.13 shows the deformation sequence.

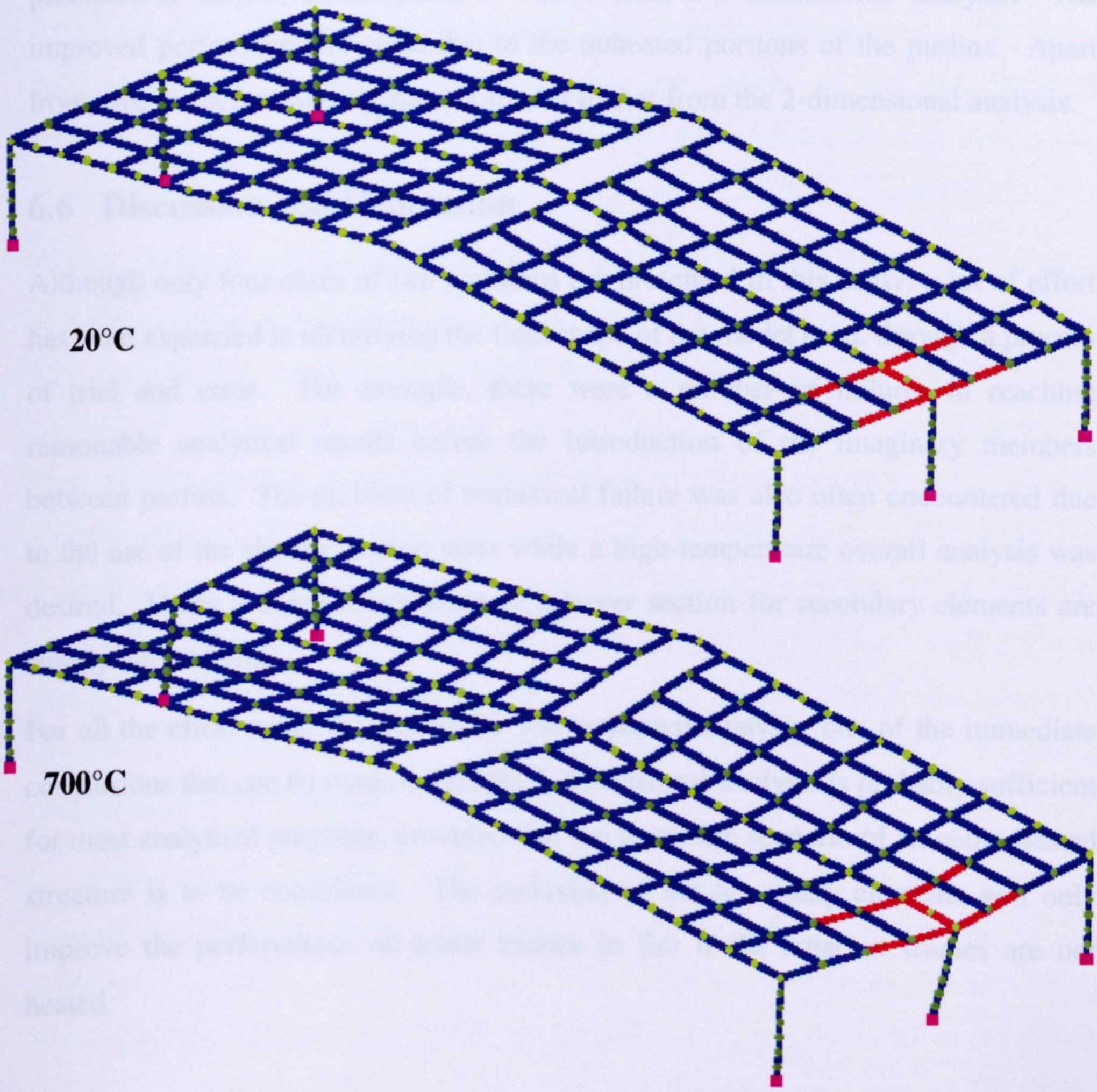

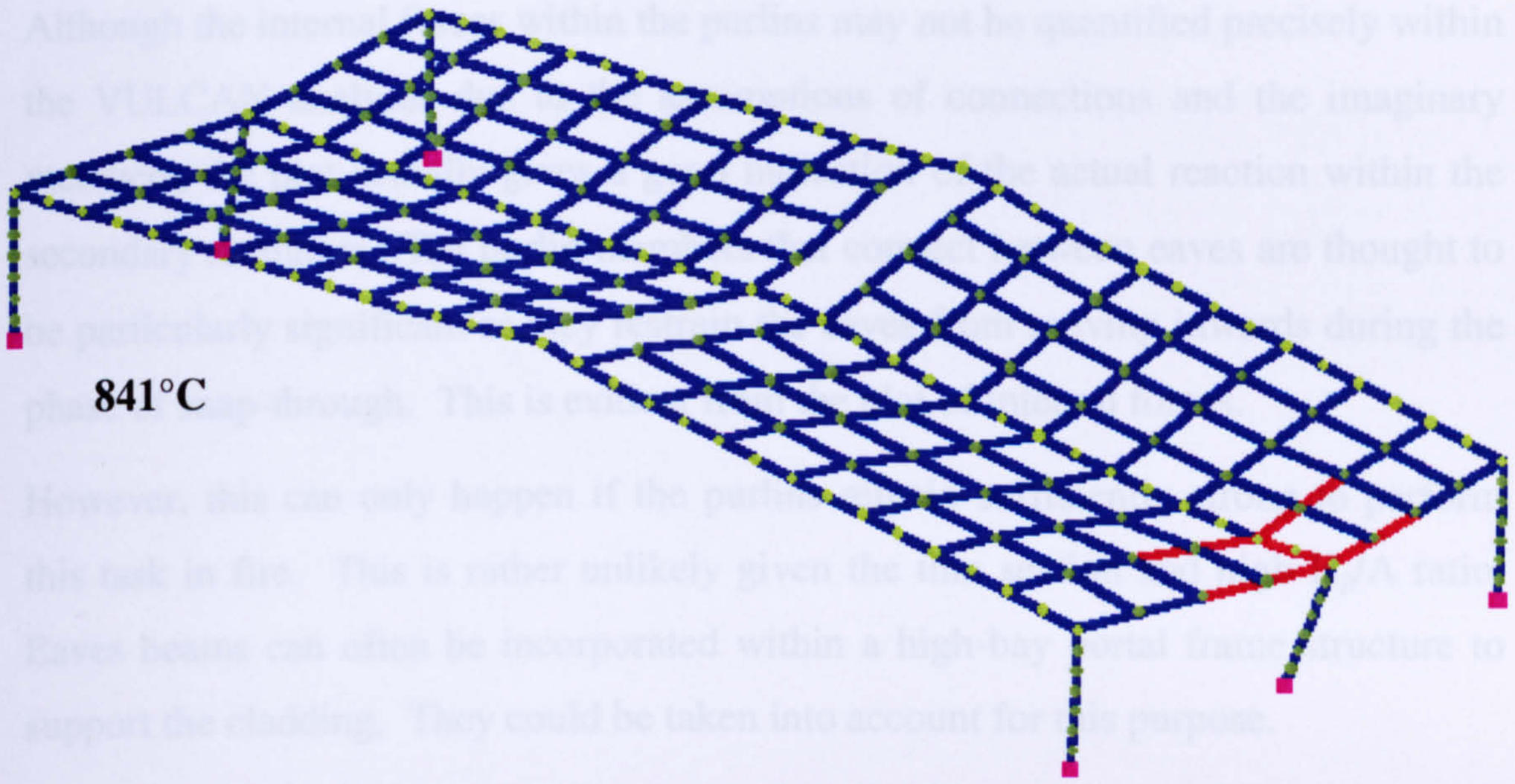

Figure 6.13 Case 4 – Corner fire

It can be seen that the deformation is actually minor. The final failure temperature is predicted to be 841°C, compared to 713°C from a 2-dimensional analysis. The improved performance is again due to the unheated portions of the purlins. Apart from this, the deformation pattern is similar to that from the 2-dimensional analysis.

6.6 Discussion and Conclusion

Although only four cases of fire scenarios are presented in this study, a lot of effort has been expended in identifying the final shape of the model used, through a process of trial and error. For example, there were a number of failures in reaching reasonable analytical results before the introduction of the imaginary members between purlins. The problem of numerical failure was also often encountered due to the use of the slender section sizes while a high-temperature overall analysis was desired. Using a lower temperature or a larger section for secondary elements are simply unjustifiable.

For all the effort made to achieve the 3-dimensional analysis, one of the immediate conclusions that can be made is that the 2-dimensional analysis is probably sufficient for most analytical purposes, provided that the worst fire scenario of an entire heated structure is to be considered. The inclusion of the secondary elements will only improve the performance of portal frames in fire if the adjacent frames are not heated.

Although the internal forces within the purlins may not be quantified precisely within the VULCAN analyses due to the assumptions of connections and the imaginary members, the plot actually gives a good indication of the actual reaction within the secondary members. The purlin members that connect between eaves are thought to be particularly significant as they restrain the eaves from moving inwards during the phase of snap-through. This is evident from the plot of internal forces.

However, this can only happen if the purlins remain sufficiently strong to perform this task in fire. This is rather unlikely given the thin section and high H_p/A ratio. Eaves beams can often be incorporated within a high-bay portal frame structure to support the cladding. They could be taken into account for this purpose.

The analyses within Section 6.3 demonstrate that the heating of columns has little effect on the overall behaviour of portal frames. It is actually a common industrial practice to fire-protect portal frame columns in boundary conditions. However, VULCAN can not predict local buckling and twisting deformations. The local deformation, if it takes place, may have some effect on the fire resisting walls/claddings that the columns support. These walls/cladding are required to stay in place for the designated period so that external spread of flame is prohibited.

Having said that a 2-dimensional analysis is probably sufficient if the worst fire scenario is under consideration, it is often assumed the worst-case scenario is a fire that heats up the entire roof, including the rafters and secondary elements. The analysis in Section 6.4, where two of the three portal frames are heated, has demonstrated that the effect of the heated frame may cause sideways overturning of the heated frame. There is little evidence that this has ever taken place in reality but it demonstrates the importance of considering various fire scenarios as potential worst cases. A more sophisticated approach might be to consider developing fires within a large portal frame warehouse where cooling and heating may happen at the same time at different locations. This could have a detrimental effect on collapse if the appropriate fire heating profile is adopted.

In conclusion, the 3-dimensional analyses conducted within the study may not represent well the true interaction behaviour of the cladding and purlins in a real fire situation. However the study has brought up several issues where further investigation would seem useful. The analyses also complete the series of parametric

studies on portal frame behaviour in fire, as proposed within the research programme.

7 Development of Simplified Estimation of Critical Temperatures for Portal Frames in Fire

Much of portal frame behaviour in fire has been illustrated and discussed in the previous chapters. The characteristic failure mode has been shown in experiments and further explored in parametric studies. The introduction of the concept of "fire hinges" at the critical temperature has been discussed. The formation of fire hinges is due to the reduced plastic moment capacity of the steel section at elevated temperature. It is recognised that the concept can be applied relatively quickly and safely to estimate the critical temperatures of portal frames in fire.

Structures of this type are not usually required by legislation to have a minimum fire resistance period. However, if a portal frame building has a separation from the adjacent building which is less than required (depending on the size of the façade), the relevant external wall of the building is required to have sufficient fire resistance to prevent fire spread across the boundary[57]. Hence the columns supporting the external wall (the vertical cladding façade) would require a fire resistance of 60 minutes and a moment-resisting foundation to resist the overturning moment generated in fire. Alternatively, the entire portal frame can be designed for a fire resistance of 60 minutes [2]. In this case, the proposed estimation method is thought to be useful to enabled a practising engineer to estimate simply the limiting temperatures of a portal frame or to check against the results generated by a sophisticated computer program.

This chapter describes the simplified approach based on Plastic Theory, which enables calculation of the failure temperatures of steel portal frames for different load cases and at different load levels, by inserting fire hinges at appropriate locations. Different fire scenarios, including both localised and completely developed fires, are considered for a range of frame geometries. Particular attention is given to pitched-roof portal frames due to the popularity of this form of construction.

The results from this simplified approach are compared against analytical results from the non-linear finite element program, VULCAN. Worked examples of the simplified calculations will be shown.

7.1 The Simplified Method

Since the mid-1950s portal frame design in the U.K. has been widely based on the principles of Plastic Theory, using a balance of internal and external work for strength calculation. Often these are designed as basic pitched-roof frames with pinned column-bases, avoiding high foundation cost, as well as the complexity of forming a rigid base connection. Detailed illustrations of this design method can be found in many standard texts[20,24,62].

The simplified approach presented here simply follows the work balance procedure. The frame eventually creates sufficient plastic hinges as loads increase to form a mechanism which may include pre-existing hinged connections. Given a compatible set of small displacements of this mechanism caused by articulation of the hinges, the work done by the external loads in displacing is balanced by the work done by the internal plastic moments in rotation of their plastic hinges. The equilibrium work balance equation can be expressed as:

$$\sum W_j \delta_j \text{ (External work done)} = \sum M_p \theta_p \text{ (Internal work done)} \tag{7.1}$$

Once a failure mechanism has been identified, the appropriate failure load can be found from equation (7.1). Finding the correct mechanism, which occurs at the minimum value of this collapse load, involves testing all possible collapse mechanisms of the portal frame.

The relationship does not change under fire conditions, and thus the work equation will still be valid. However, the external work done is clearly dependent on the loading in the fire limit state, which can be determined from codes of practice for structural fire resistant design such as the British Standard BS5950 Part 8[13]. As explained in the earlier chapters, the vertical dead load in fire is usually the dominant external load, since design imposed loading is considerably reduced by the partial safety factor for this accidental limit state.

The compatible internal work done is however induced by the forming of plastic hinges. Because of the elevated temperature, the yield stress of steel is reduced and this results in a reduction of the plastic moment capacity of the steel section. Such

hinges are regarded as "fire hinges". By inserting these fire hinges into the portal frame, the level of reduction in plastic moment capacity required in order to achieve a failure mechanism at a given fire limit state load can be found. The strength reduction factors of steel at elevated temperature are given in fire resistance codes such as BS5950 Part 8 or the draft Eurocode EC3 Part 1.2[15]. Provided that the fire hinges are assumed to form in steel members which are at the same temperatures, it is possible to calculate the reduction factors required for the collapse mechanism to form in fire. The steel temperature giving this reduction can be found, and this is the failure temperature of the portal frame. If a fire resistance time is required, then the relationship between atmosphere temperature and steel temperature can be modelled simply using the incremental approaches given in Eurocode 1 Part 2.2[63] for either exposed or passively protected steelwork. If the ISO834 [64] standard fire curve is assumed, as is conventional in fire testing of components, fire resistance times can be interpolated.

7.2 Application of the Simplified Method

Since the simplified method is based on the concept of plastic analysis, the procedure is best illustrated by some examples. This section will demonstrate the application of the simplified method described earlier to some typical portal frames. The initial cases will consider a fire which heats up the entire rafter of a simple goal-post frame and a pitched-roof frame. Further examination will consider its applicability to localised heating of frames.

The results from these worked examples will be validated in the later sections.

7.2.1 Goal-Post Portal Frame – Entire Rafter Heated

A typical goal-post portal frame with pinned bases was set up as shown in Figure 7.1. The loading has been simplified as point loads. For the given problem, there are only two possible failure mechanisms at ambient temperature. When the entire rafter is heated in fire, a similar mechanism is produced, in which fire hinges are positioned at the rafters. The shapes of the failure modes, the "sway" and the "combined" mechanisms, are shown in Figure 7.2.

In the following calculations, the internal and external work done for each mechanism will be shown, in term of the reduction factor of the strength of steel at elevated temperature, which is denoted as η.

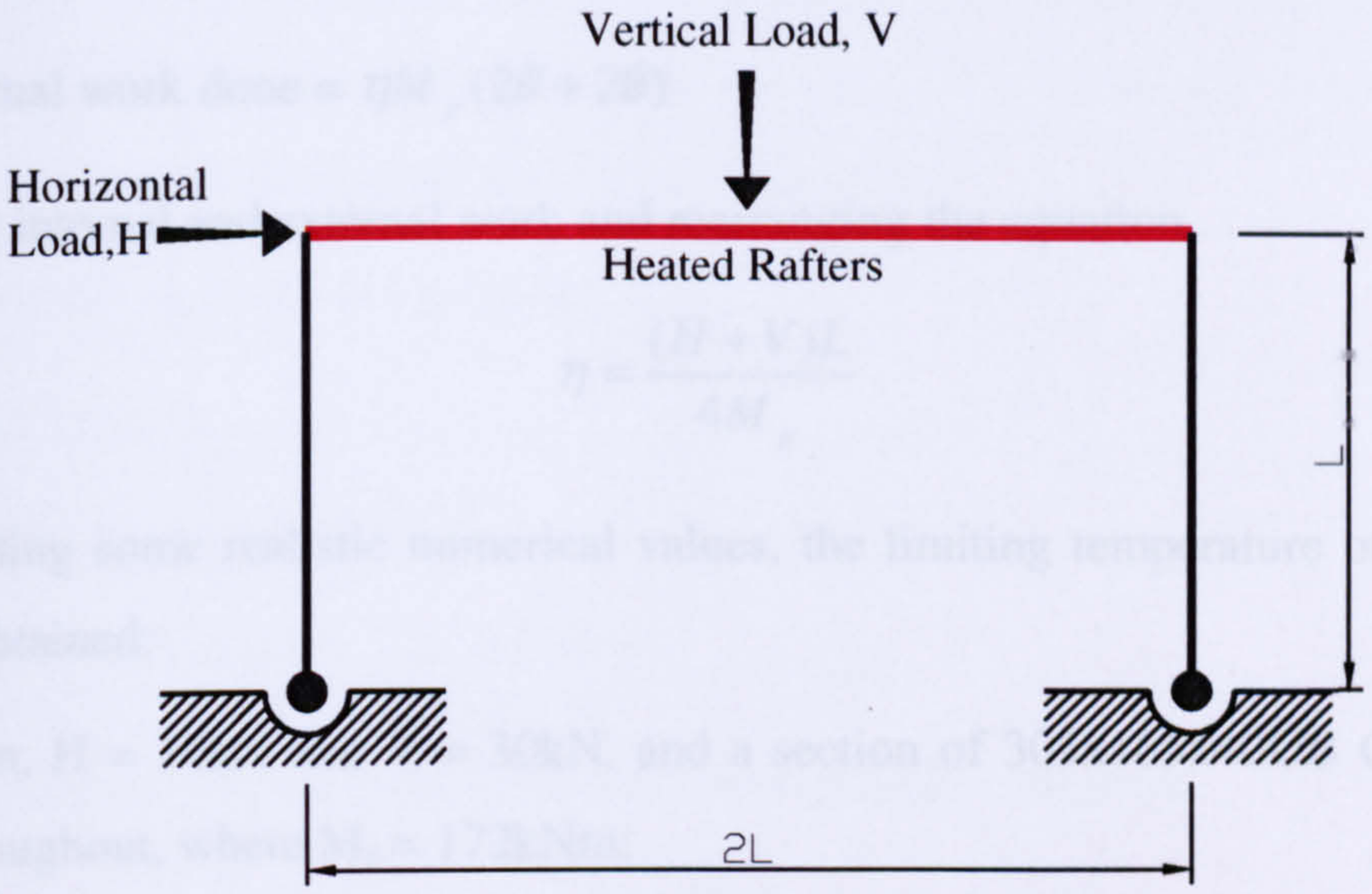

Figure 7.1 Goal-Post Portal Frame with Rafters Heated

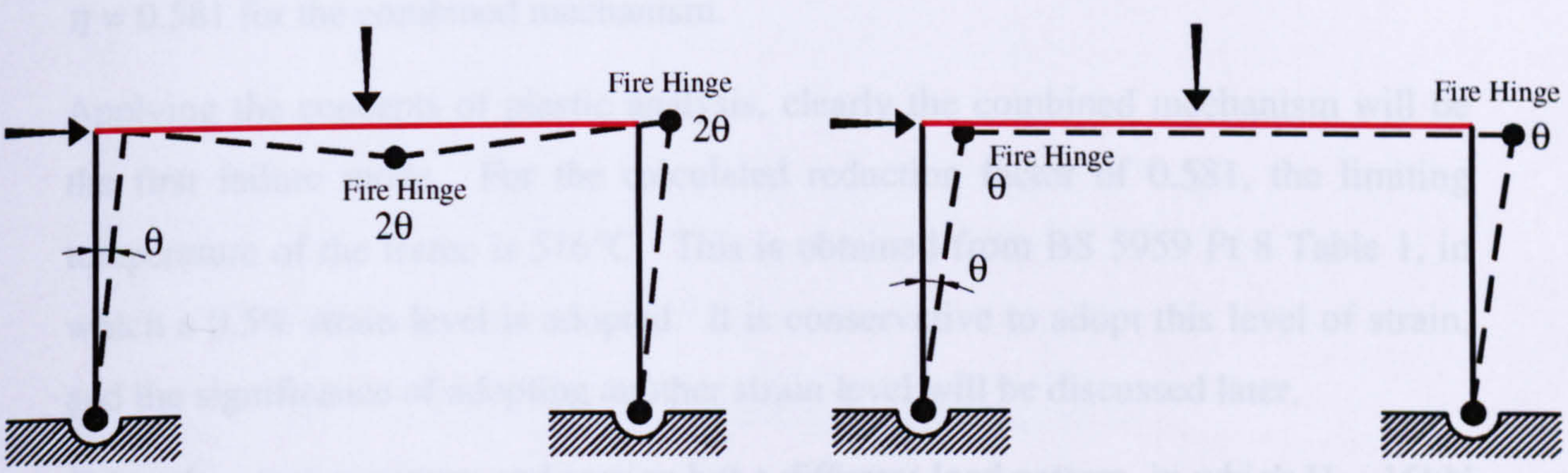

Figure 7.2 Failure Mechanisms – (Left) Combined Mechanism and (Right) Sway Mechanism

Sway Mechanism

The external work done = $HL\theta$

The internal work done = $\eta M_p(\theta+\theta)$

where M_p is the plastic resistance moment of the rafter section at ambient temperature, η is the strength reduction factor and θ is the angle of rotation in radians.

Equating the internal and external work and rearranging the equation,

$$\eta = \frac{HL}{2M_p} \tag{7.2}$$

Combined Mechanism

The external work done = $HL\theta + VL\theta$

The internal work done = $\eta M_p(2\theta + 2\theta)$

Equating internal and external work and rearranging the equation,

$$\eta = \frac{(H+V)L}{4M_p} \tag{7.3}$$

By adopting some realistic numerical values, the limiting temperature of the frame can be obtained:

If L=10m, H = 10kN and V = 30kN, and a section of 305x165x40UB Grade 43 is used throughout, where M_p = 172kNm:

$\eta = 0.291$ for the sway mechanism or

$\eta = 0.581$ for the combined mechanism.

Applying the concepts of plastic analysis, clearly the combined mechanism will be the first failure mode. For the calculated reduction factor of 0.581, the limiting temperature of the frame is 516°C. This is obtained from BS 5959 Pt 8 Table 1, in which a 0.5% strain level is adopted. It is conservative to adopt this level of strain, and the significance of adopting another strain level will be discussed later.

Using the same geometry and section but a different load pattern, in which H = 15kN and V = 10kN, results in:

$\eta = 0.436$ for the sway mechanism or

$\eta = 0.363$ for the combined mechanism.

In this case, the sway mode is the first failure mode, and this results in a critical temperature of 575°C.

7.2.2 Goal-Post Portal Frame – Localised Heating Profile

Considering a localised fire near to right-hand column of the portal frame, the right eaves region now has the highest temperature, but the other parts of the frame will

stay relatively cool. As a result, a fire hinge will form near to the right eaves. In order to create a failure mechanism the fourth hinge has to exist, and this will be a normal plastic hinge, assuming no significant loss of strength due to the localised fire. The failure once again employs the collapse mechanism shown in Figure 7.2. For the sway mechanism, one plastic hinge forms near to the left eaves and a fire hinge forms near to the right eaves. In the case of a combined mechanism, the plastic hinge will form near the mid-span of the rafter.

Using the same simplified approach:

Sway Mechanism

The external work done = $HL\theta$

The internal work done = $\eta M_p\theta + M_p\theta$

Equating internal and external work and rearranging the equation,

$$\eta = \frac{HL}{M_p} - 1 \tag{7.4}$$

Combined Mechanism

The external work done = $HL\theta + VL\theta$

The internal work done = $\eta M_p 2\theta + M_p 2\theta$

Equating internal and external work and rearranging the equation,

$$\eta = \frac{\frac{(H+V)L}{M_p} - 2}{2} \tag{7.5}$$

Using the same frame geometry as in Section 7.2.1 with H = 10kN and V = 30kN:

η = -0.419 for sway mechanism or

η = 0.163 for combined mechanism.

Since the sway mechanism produces a reduction factor of less than 0, this failure mode will not exist. The combined mechanism gives a critical temperature of 720°C.

7.2.3 Pitched-Roof Portal Frame – Entire Rafter Heated

In this section, the simplified method will be applied to determine the failure temperatures for the common form of industrial pitched-roof portal frame with pinned bases.

Under fire conditions the most common collapse mechanism for pitched-roof portal frames has been found from previous parametric studies to be a rotational failure of part of the roof section, which is also the usual failure mode under vertical roof load at ambient temperature.

Considering a widespread fire which results in heating of the whole of a portal frame the collapse mechanism is illustrated in Figure 7.3, with fire hinges forming at the apex and eaves.

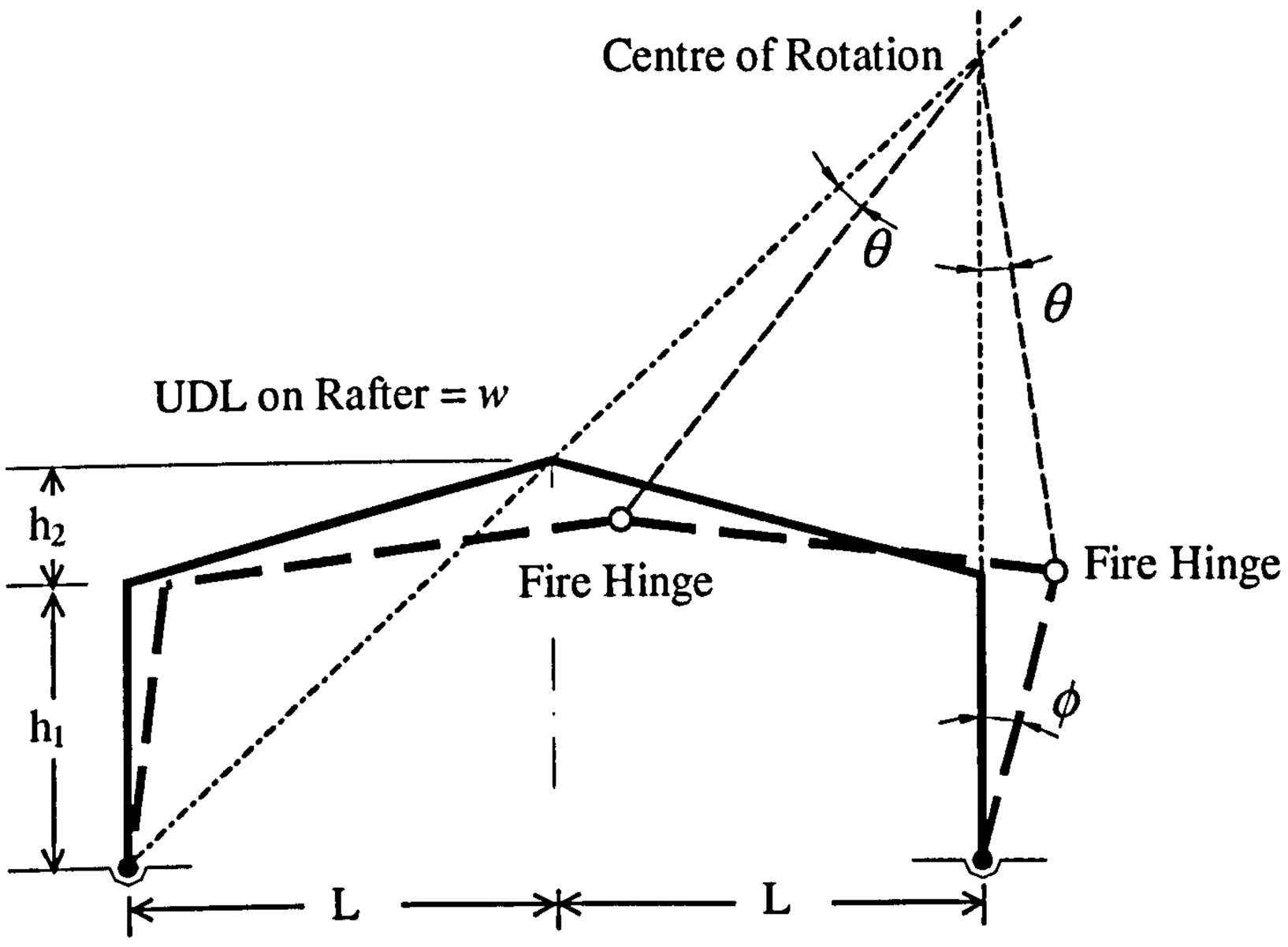

Figure 7.3 Failure mechanism and location of fire hinges – frame heated overall

The external work done = $wL^2\theta$

The internal work done = $M_p\eta(\theta + \theta + \phi + \theta)$

where M_p is the plastic resistance moment of the rafter section at ambient temperature, η is the reduction factor and $\phi = \frac{h_1 + 2h_2}{h_1}\theta$.

Equating internal and external work and rearranging the equation,

$$\eta = \frac{wL^2}{M_p\left(3+\frac{h_1+2h_2}{h_1}\right)} \tag{7.6}$$

Using a portal frame of fairly practical dimensions, (h_1 = 7m, h_2 =4m, L = 15m) and loading, designed for ambient temperature limit states with dead, imposed and wind loads, a realistic column section would be 533x210x92UB G43 and the rafter section would be 457x191x89UB G43 without haunches. This is the same portal frame previously designed for the parametric studies. An estimation of the vertical load at the fire limit state using BS5950 partial safety factors would be 2.4kN/m. Substituting these values into equation (7.6) gives η = 0.190, corresponding to a BS5950 Pt8 failure temperature, at 0.5% strain, of 697°C.

A further check was performed to calculate the critical temperatures assuming other failure modes (i.e. the sway mechanism and the panel mechanism), and it was found that the rotational mechanism is the first failure mode.

7.2.4 Pitched-Roof Portal Frame – Localised Heating Profile

Considering next a localised fire near to one of the portal frame columns, the eaves region now has the highest temperature. The failure once again employs the rotational collapse mechanism shown in Figure 7.3, with one plastic hinge forming near to the apex and a fire hinge forming in the rafter near to the heated eaves. Using the same simplified approach:

The external work done = $wL^2\theta$

The internal work done = $M_p[\theta+\eta\theta+\eta(\phi+\theta)]$

Equating the internal and external work as in the former example, the reduction factor can be shown to be

$$\eta = \frac{\left(\frac{wL^2}{M_p}\right)-2}{1+\left(\frac{h_1+2h_2}{h_1}\right)} \tag{7.7}$$

Adopting the same portal frame parameter values as for the previous case, the reduction factor value turns out to be negative. The significance of this will be discussed in later sections. If a higher load level of 6kN/m is applied with the same frame geometry, the calculated η value is 0.140 and the failure temperature is 735°C.

7.3 Validation of the Simplified Method

Although the concept behind the simplified method and its applicability are not complicated, it is necessary to prove the validity of the technique. The portal frames used in the worked examples are now set up and analysed with VULCAN so that the results can be compared. More detailed validation has been performed on the pitched-roof portal frame, including various load levels and geometries, since this form of construction is the more common.

7.3.1 Goal-Post Portal Frame – Entire Rafters Heated

The individual goal-post portal frame used in Section 7.2.1 was set up and analysed, and the results are compared against the results calculated by the simplified method. Various load combinations have been analysed, and the cases are presented in Table 7.1.

	Vertical Load (kN)	Horizontal Load (kN)	Simplified Method	Vulcan Analysis
Case 1	20	10	575°C	610°C
Case 2	30	10	516°C	555°C
Case 3	40	10	451°C	497°C
Case 4	10	15	575°C	620°C

Table 7.1 Comparison of Critical Temperatures on Goal-Post Portal Frame – Entire Rafters Heated

Among these load combinations, Case 4 experiences a sway failure mode and the others fail by the combined mechanism. It can be seen that the simplified method produces conservative results compared to VULCAN. However the critical temperatures given by BS5950 Pt8 are based on a strain level of 0.5%. When a higher level of strain is adopted (i.e. 1% by interpolation and 1.5%) the calculated

results are much closer to the VULCAN analysis. These are summarised in Table 7.2.

	Simplified Method, 0.5% Strain	Simplified Method, 1.0% Strain	Simplified Method, 1.5% Strain	Vulcan Analysis
Case 1	575°C	594°C	609°C	610°C
Case 2	516°C	540°C	561°C	555°C
Case 3	451°C	488°C	513°C	497°C
Case 4	575°C	594°C	609°C	620°C

Table 7.2

7.3.2 Goal-Post Portal Frame – Localised Heating Profile

A similar validation procedure has been conducted with the localised heating profile on one of the eaves of the goal-post portal frame. The same portal frame and load combinations were used, and the results are shown in Table 7.3.

	Simplified Method, 0.5% Strain	Simplified Method, 1.0% Strain	Simplified Method, 1.5% Strain	Vulcan Analysis
Case 1	- *	- *	- *	1055°C
Case 2	720°C	732°C	743°C	723°C
Case 3	568°C	588°C	603°C	596°C
Case 4	- *	- *	- *	°C

* Negative reduction factor obtained which does not yield critical temperature.

Table 7.3 Comparison of Critical Temperatures on Goal-Post Portal Frame – Localised Heating Profile

Once again the results of Cases 2 and 3 compare well with the VULCAN analysis. However, the calculations for Cases 1 and 4 produce negative results for the reduction factors for both the sway and combined mechanisms. This indicates that, even when the strength of the fire hinge drops to zero, this is not sufficient to produce a failure mechanism. This will be discussed in detail later in Section 7.4.

7.3.3 Pitched-Roof Portal Frame – Entire Rafters Heated

A series of VULCAN analyses were performed using the portal frame layout from the worked examples in Section 7.2.3 (span 30m,column height 7m, eaves-to-apex height 4m), applying different load levels and obtaining the failure temperatures. The load levels are presented in terms of their proportion of the failure load of the frame at ambient temperature, known as the Load Ratio. The results are compared against those calculated from the simplified approach in Table 7.4. Equation (7.6) was adopted for the simplified approach calculation.

	Load Ratio	Load (kN/m)	Simplified Method, 0.5% Strain	Simplified Method, 1.0% Strain	Simplified Method, 1.5% Strain	VULCAN Analysis
Case 5	0.1	1.21	778°C	794°C	818°C	803°C
Case 6	0.2	2.42	697°C	711°C	723°C	715°C
Case 7	0.3	3.62	642°C	656°C	669°C	664°C
Case 8	0.4	4.83	598°C	615°C	629°C	620°C
Case 9	0.5	6.04	556°C	578°C	594°C	576°C
Case 10	0.6	7.25	519°C	542°C	563°C	532°C
Case 11	0.7	8.46	476°C	507°C	530°C	489°C
Case 12	0.8	9.60	421°C	469°C	497°C	439°C

Table 7.4 Comparison of failure temperatures from VULCAN and simplified approach – Pitched-Roof Frame with Entire Rafter Heated.

Once again it can be seen that the simplified approach compares well with the finite element results. Further analyses were conducted to investigate the validity of the proposed method with various frame geometries, changing the spans and heights. The load has been maintained at a Load Ratio of 0.2. The cases and results are summarised in Table 7.5.

It can be seen that the critical temperatures of the frames of different geometries fall into the same region. This agrees with the finding from the previous parametric studies, that portal frames with the same Load Ratio fail at similar temperatures, even when the simplified approach is used. The simplified approach gives results close to the VULCAN analysis, especially when the strength reduction is based on a strain level of 1.0%.

	Span **2L** (m)	Column Height h_1 (m)	Eaves to Apex h_2 (m)	Simplified Method, 0.5% Strain	Simplified Method, 1.0% Strain	Simplified Method, 1.5% Strain	VULCAN Analysis
Case 13	20	7	4	708°C	721°C	732°C	717°C
Case 14	40	7	4	698°C	712°C	724°C	711°C
Case 15	60	7	4	697°C	711°C	723°C	700°C
Case 16	30	11	4	692°C	704°C	717°C	706°C
Case 17	30	15	4	692°C	703°C	716°C	703°C
Case 18	8	4	0.8	691°C	703°C	716°C	705°C

Table 7.5 Comparison of failure temperatures from VULCAN and simplified approach – Various Geometries.

Among all the cases in this section, the failure mechanism of the frame is the rotational mode. It was recognised that sway failure rarely dominates in fire for practical frames under realistic loading conditions. However, the simplified approach can also be applied to predict a sway failure mechanism for pitched-roof portal frames, by inserting the fire hinges near the two eaves. Consider the case where a horizontal uniformly distributed load of 2.8kN/m is applied to each column of a portal frame (similar frame geometry to that used in Table 7.4), but with no vertical load. The horizontal load is a realistic wind load determined from BS6399 [7.5] with the fire limit state load factors from BS5950 Pt8. This will force a sway failure mechanism due to lack of the zero vertical load. The results are shown in Table 7.6.

	Horizontal Load (kN/m)	Vertical Load	Simplified Method, 0.5% Strain	Simplified Method, 1.0% Strain	Simplified Method, 1.5% Strain	VULCAN Analysis
Case 19	2.8	0	753	782	766	780°C

Table 7.6 Sway Mechanism for Pitched Roof Portal Frame.

7.3.4 Pitched-Roof Portal Frame – Localised Heating Profile

The final series of validations repeat the cases taken from Table 7.4 but with a localised heating profile at one of the eaves. Equation (7.7) was applied for the calculation using the simplified approach.

	Load Ratio	Load (kN/m)	Simplified Method, 0.5% Strain	Simplified Method, 1.0% Strain	Simplified Method, 1.5% Strain	VULCAN Analysis
Case 5	0.1	1.21	Negative	Negative	Negative	1063°C
Case 6	0.2	2.42	Negative	Negative	Negative	860°C
Case 7	0.3	3.62	Negative	Negative	Negative	796°C
Case 8	0.4	4.83	Negative	Negative	Negative	749°C
Case 9	0.5	6.04	734°C	756°C	745°C	713°C
Case 10	0.6	7.25	635°C	661°C	648°C	650°C
Case 11	0.7	8.46	564°C	600°C	585°C	589°C
Case 12	0.8	9.60	502°C	549°C	527°C	526°C

Table 7.7 Comparison of failure temperatures from VULCAN and simplified approach – Pitched Roof Frame with Localised Heating Profile.

Similarly to the localised-heating cases from the goal-post portal frames, the lower load levels give negative reduction factors. The other cases compare well with the VULCAN analysis.

7.4 Discussion

It can be seen from the validation that the simplified approach generally produces results close to the VULCAN analysis. It should be noted that the failure behaviour predicted by VULCAN differs between one case and another. Figure 7.4 shows the VULCAN predictions for the two different cases of the entire rafter heated and the localised heating profile. It can be seen that the case where the entire rafter is heated has a less sudden failure profile compared to the other case. As a result VULCAN can follow the failure process up to high displacements.

The critical temperatures from VULCAN shown in all the validations within Section 7.3 are the final equilibrium points of the analysis, (i.e. Points 2 and 3 as shown in Figure 7.1). However, the simplified method is based on a small-displacement approach. This is likely to produce some discrepancies between failure temperatures obtained from the two approaches.

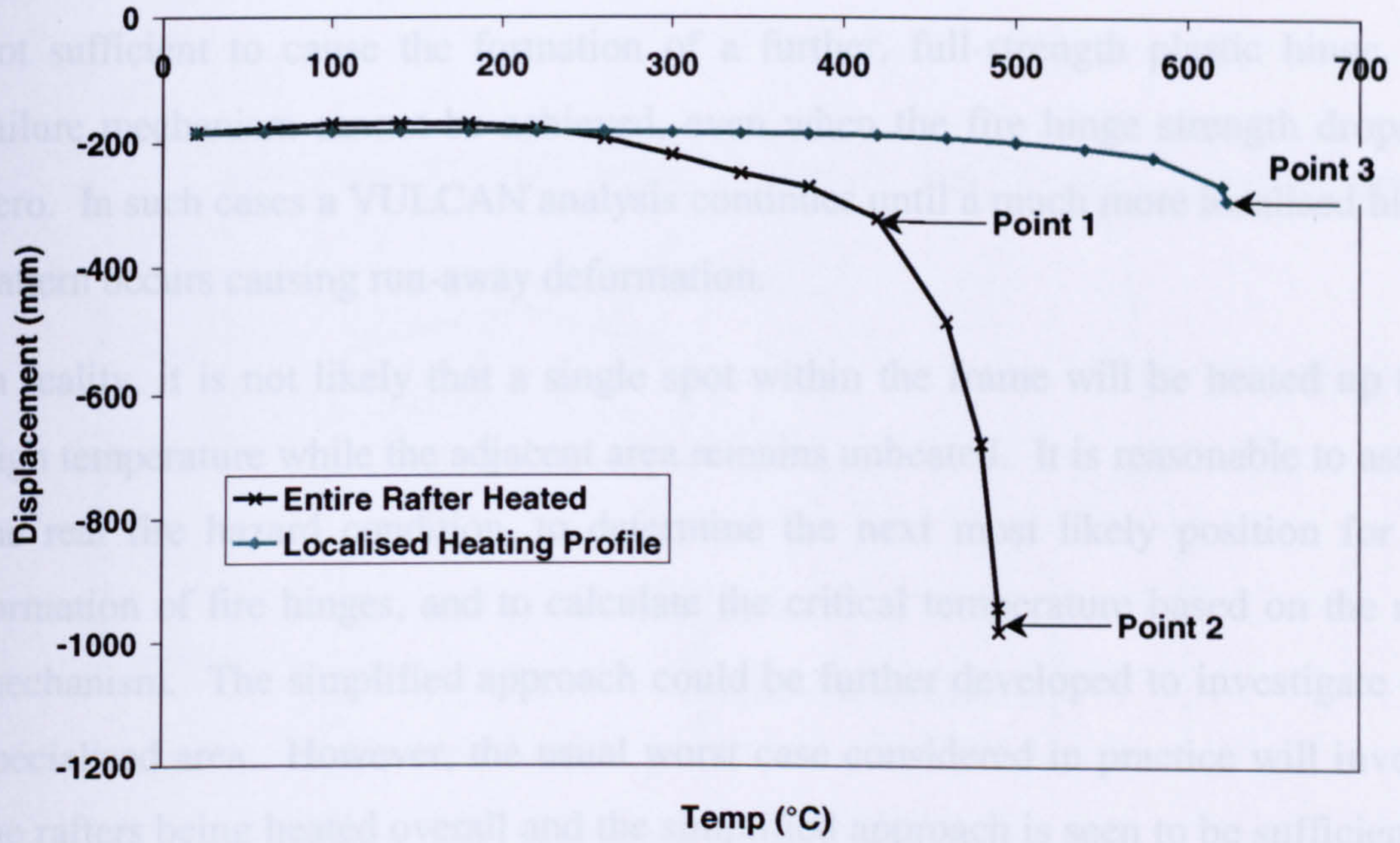

Figure 7.4 Apex Vertical Displacement – Typical Failures Predicted by VULCAN

7.4.1 Strain Level

According to BS5950 Pt8 *"any non-composite members in bending which are unprotected, or protected with fire protection materials which have demonstrated their ability to remain intact, should not exceed a strain level of 1.5%."* It can be seen from the validations that, if the reduction factors at 1.5% strain are adopted, the results are always close to, or exceed, the temperatures predicted by VULCAN. If the 0.5% strain level is considered, it always produces lower critical temperatures compared to VULCAN. Therefore, it is reasonable to treat these as the upper and lower bounds of the critical temperatures.

Since there are other uncertainties within the frame and the fire conditions, it is difficult to propose a single solution as a definitive failure temperature of the frame, and the upper and lower bounds will provide the range for further comparisons.

7.4.2 Negative Reduction Factor

In some cases, especially for portal frames with localised heating profile and a low level of loading, negative reduction factors were derived from the simplified approach. This obviously does not lead to any critical temperature. In the localised fire scenario, after the formation of one fire hinge the low level of applied loading is

not sufficient to cause the formation of a further, full-strength plastic hinge. A failure mechanism cannot be achieved, even when the fire hinge strength drops to zero. In such cases a VULCAN analysis continues until a much more localised hinge pattern occurs causing run-away deformation.

In reality, it is not likely that a single spot within the frame will be heated up to a high temperature while the adjacent area remains unheated. It is reasonable to assess the real fire hazard condition, to determine the next most likely position for the formation of fire hinges, and to calculate the critical temperature based on the new mechanism. The simplified approach could be further developed to investigate this specialised area. However, the usual worst case considered in practice will involve the rafters being heated overall and the simplified approach is seen to be sufficient to predict the critical temperatures.

7.4.3 Validity of the Concept of Fire Hinges

The typical pitched-roof frame with pinned bases requires two extra hinges to form a failure mechanism. For the rotational failure mode described to occur under fire conditions, the two hinges will form near the apex and one of the eaves, and both of these will be fire hinges in the case where the entire rafter is heated. If the concept of inserting fire hinges is valid, a different fire scenario, with only the locality of the apex and one eaves connection heated, should produce a similar failure mechanism and failure temperature identical to scenario where the entire rafter is heated.

These two heating scenarios were modelled on the same portal frame using VULCAN in order to verify this argument. The results of the analyses are shown in Figure 7.5, in which the vertical displacements at the apex are plotted. The scenario where the entire rafter is heated has a higher upward displacement before the snap-through takes place, due to its greater expansion, and thus higher internal force. However, the analyses show that both frames fail at the almost same temperature. In other words, whether or not the central part of the individual rafter member is heated has very little effect on the failure temperature.

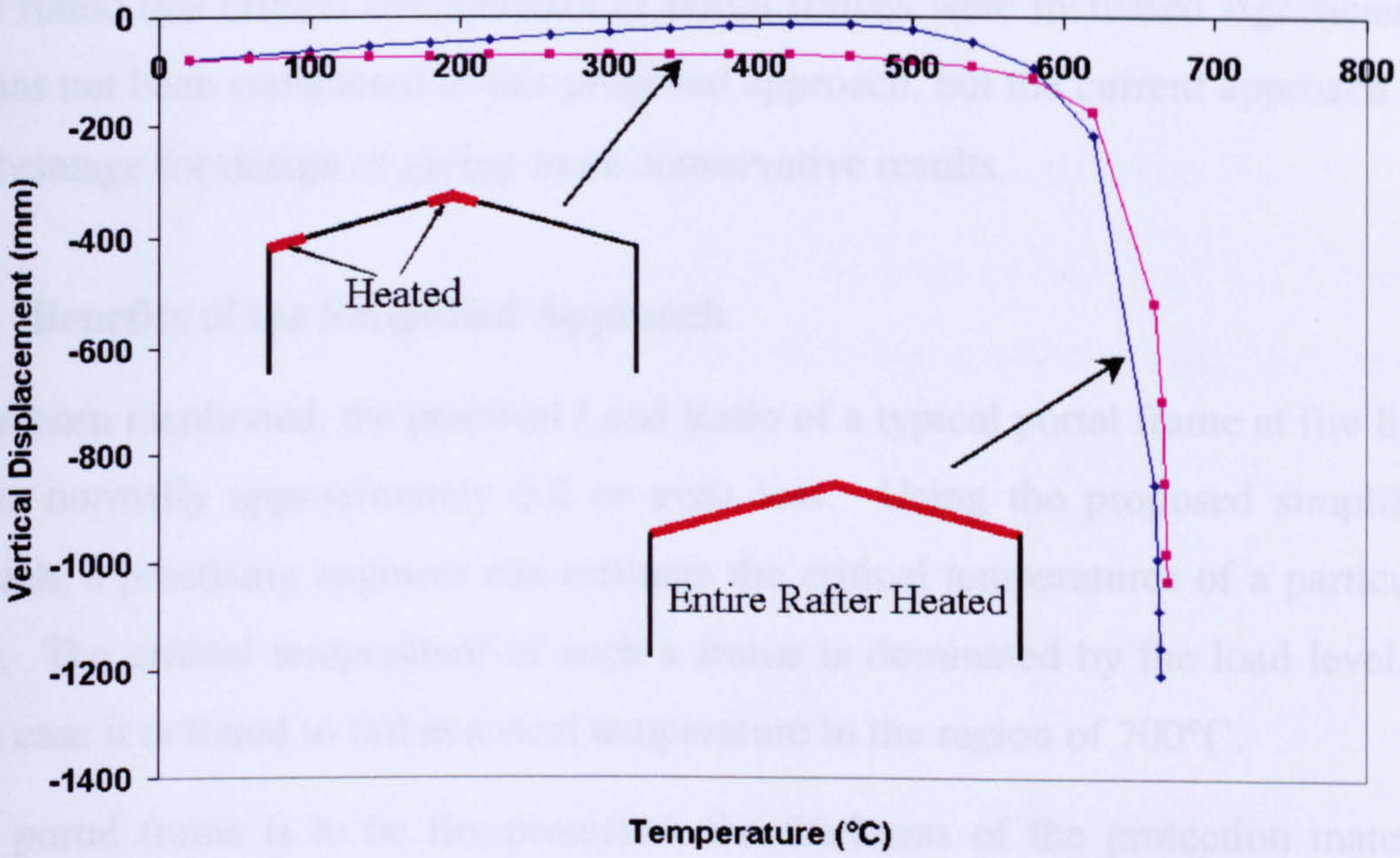

Figure 7.5 Vertical Displacement at Apex

It can be concluded that, if the portal frames are heated locally at the critical points, the failure temperature can be as low as in the worst fire case. If the critical points are protected from heating, this will create a different failure mechanism and higher critical temperature.

7.4.4 Practical Issues

While calculating the critical temperatures, the approach has ignored the use of haunches at the eaves of the portal frame. Such frames should be capable of being treated in the same way, but the position of one of the hinges is moved away from the eaves to the haunch-end, both at ambient temperature and in the fire case.

If the failure temperatures shown in Table 1 are compared with the limiting temperatures of isolated members given by Table 5 of BS5950 Pt8, it is seen that the values for "members in bending not supporting a concrete slab" form a lower bound to the critical temperatures of the portal frames in overall heating.

Although most practical portal frames are designed with pinned bases, the real base connections and foundations actually provide some degree of rotational stiffness to the column bases. Four holding-down bolts are normally used to secure such a base to the foundation, and it is believed that this provides a certain amount of restraint which enables portal frames to perform better in fire than their idealisation suggests.

VULCAN has also been used to study the effect of semi-rigid base connections, and it was found that critical temperatures of portal frames were increased significantly. This has not been considered in this proposed approach, but the current approach has the advantage for design of giving more conservative results.

7.4.5 Benefits of the Simplified Approach

As has been mentioned, the practical Load Ratio of a typical portal frame at fire limit state is normally approximately 0.2 or even less. Using the proposed simplified approach, a practising engineer can estimate the critical temperatures of a particular frame. The critical temperature of such a frame is dominated by the load level, in which case it is found to fail at a steel temperature in the region of 700°C.

If the portal frame is to be fire-protected, the thickness of the protection material would normally be based on a critical temperature of 550°C. Knowing that the critical temperature of the frame is actually around 700°C, the fire-protection thickness can be reduced significantly. However, it is the fact that the portal frame will only be required by regulation to achieve certain fire resistance when there is a boundary condition, and this requirement is usually 60 minutes[7.1]. The unprotected steel temperature will be in excess of 900°C for 60 minutes exposure using the Standard BS476 standard fire curve. Therefore, a structural fire engineering approach is not likely to enable the total elimination of the fire protection requirement.

7.5 Conclusion

An application of the normal principles of plastic analysis of portal frames has been attempted here, with the variation that fire hinges, which have a reduced plastic moment capacity, are introduced into the work-balance equation and the ultimate goal is to estimate the critical steel temperature in fire. The calculated results have been compared with VULCAN analyses, and the comparisons have shown that the proposed method gives a reasonably good estimation of the failure temperatures, particularly for the most usual and most critical fire scenario in which the frame is heated overall.

In cases where a very localised part of a portal frame is subjected to fire the approach has not predicted any failures at very low load levels. This is a relatively specialised

area, where the proposed approach could be further developed. However, for the most usual fire case it provides a practical method of estimating critical steel temperatures, and by further interpolation a method of estimating fire resistance times in terms comparable to those used in design codes for isolated members.

The significance of the simplified approach has been discussed, and the approach could potentially reduce the fire protection thickness required under the current regulatory system.

8 Discussion

The main purpose of this chapter is to present and discuss several issues in relation to the behaviour of portal frames in fire, on which some investigation has been conducted which has not been covered in the previous studies presented. These are not directly in line with the studies of portal frame behaviour in fire but concern other issues surrounding the topic. It is aimed firstly to review the main initial purpose of the research project, and then to discuss the current guidance available for designers.

One of the most significant recent developments in the use of fire engineering approaches in design of buildings is to consider the concept of performance-based design. The latest EuroCode[63.] includes the provision to assess realistic fire temperatures likely to be encountered in a real building fire. This is known as the Natural Fire Concept, and this section will discuss its implications for portal frame structures.

8.1 Initial Research Objectives

The research project was supported by the Health and Safety Laboratories (HSL), Buxton with the aim of investigating the behaviour of industrial warehouses in response to internal fires of any size. HSL was particularly interested in the structural behaviour and on how this affects the venting of smoke in the event of a fire, especially on the occasions when highly toxic smoke is produced as a result of the fire.

The research has been focused mainly on the behaviour of the main portal frames, including the setting-up of experimental model and finite element analyses. It was apparent that cladding behaviour in fire differs greatly from the main frame behaviour, especially in the context of computer modelling. The detailed behaviour of cladding cannot in fact be modelled by VULCAN, due to the beam-slab set-up of the finite element program.

The cladding is very much, if not totally, dependent on its supporting purlins, and it has been seen from the fire tests that the purlins are vulnerable in fire. The purlins can buckle and twist in the early stages of a fire and this may result in the cladding failing, or even falling off the building.

Skylights are very often installed as part of industrial warehouse structures. The skylight is normally made of PVC or a similar type of material which softens and melts at relatively low temperatures, before any significant deformation of purlins can take place.

It was evident from the parametric studies that, given the relatively low load levels at the fire limit state, portal frames do not fail before the frame temperatures reach at least 650°C (see Figure 5.22). This includes the built-in assumption of pinned column bases and could be rather conservative, even for the simple base connections commonly adopted for portal frames. In the fire tests conducted at Buxton it was quite difficult to create a collapse scenario for the portal frame model, and roof insulation had to be introduced in the final test to enable a high temperature to be reached. It is almost certain that high ventilation will be available before any structural collapse of main frames is seen. Similarly, any toxic smoke produced in a fully developed fire is unlikely to be contained within the warehouse structure throughout the fire period.

The behaviour of purlins and cladding was briefly modelled within the 3-dimensional parametric studies in Chapter 6. A mesh was created to represent the overall roof structure, but distortion and failure of cladding can not be predicted. The representation of cladding used was artificially assumed to be unheated to enable the analyses to reach high temperatures. It seems likely that further investigations into the precise behaviour of cladding will be complex because of a number of variables which are unpredictable in nature, such as the fixings and the interlock of cladding of various profiles under the influence of heating, in conjunction with applied load.

Much knowledge about portal frame behaviour was gained from the fire tests and parametric studies. The common failure mode found throughout the research was snap-through of the rafters. This has been very well predicted by the VULCAN analyses, both in 2- and 3-dimensional parametric studies. However, the analyses terminate immediately as the snap-through occurs. In the fire test conducted at Buxton, in which snap-through was seen, the frame did not deflect further because the additional loading barrels hanging from the rafters came into contact with the ground and thus released the applied load. In future research it would be of interest to track the deflection past the limit-point, although equilibrium paths then become unstable. It is logical to predict that these will re-stabilise at higher deflection, and

this needs to be investigated if the problem of masonry wall collapse is to be properly investigated.

It has been assumed in industry that catenary action generated by the sagging rafters is sufficient to pull-in the portal frame columns, resulting in collapse of the entire structure. This is the basic assumption within the SCI publication regarding portal frame behaviour in boundary conditions[9], which is commonly adopted throughout the UK. Consequently further design consideration will have to be given to such behaviour.

However, the author has had numerous discussions with researchers and has scanned incident reports for the UK, as reported in *"Fire Prevention"* magazine, dating back to 1990. There was little evidence from these searches that total collapse of an industrial portal frame, including column pull-in, is ever seen to happen. Qualitative explanations can be given, and this subject will be discussed further in the following sections.

With the studies conducted in this research programme it is possible to look into the validity of the well-known SCI document mentioned above, and to relate this back to the current UK Building Regulations requirements. The next section aims to review the document and discuss its implications.

8.2 Current Guidance Document

In order to prevent spread of flame from one building to another, it is required under the UK Building Regulations to design a fire-resisting façade for buildings which are in "boundary conditions". These are defined as cases where the spatial separation is insufficient to ensure that only low levels of radiation are received by the adjacent buildings. The fire-resisting façade has to satisfy the requirements of insulation, integrity and stability for the designated period of time.

Approved Document B: Fire Safey[57] is used to interpret the fire safety requirements of the Building Regulations 1991. For single-storey portal frame structures in boundary conditions, it refers to the SCI publication[9] for advice. The content of this SCI publication has been mentioned previously in Section 1.3.1, in which a simplified method has been described to calculate the base overturning moment in fire conditions. Engineers either have to fire-protect the entire portal frame or to

design the foundation and base connections to resist such moments. The latter solution is the more commonly adopted, and often results in much bigger foundations being designed for portal frames in boundary conditions.

The simplified method has actually been derived from a basic mathematical model which is also described in the SCI publication. The mathematical model assumed that deformation of the portal frame in fire is symmetrical about the vertical line through the apex, and takes into consideration the column movements, expansion and the reduced moment capacity of the rafters. The assumed deflected shape is shown in Figure 8.1, and this actually agrees with the deformation predicted by VULCAN in the parametric studies.

Figure 8.1 Model for calculation of overturning moment

Using the same mathematical model, a spreadsheet can be created to calculate the resulting overturning moment at the column bases. An investigation of the relationships between the column rotation, rafter temperature and resultant overturning moment has been conducted. The portal frame model designed for the 3-dimensional parametric studies has again been adopted for the investigation.

Assuming a constant rafter elongation of 2%, as suggested within the SCI guidance, the resultant base overturning moment can be plotted against the amount of column rotation at various rafter temperatures. The plot is shown in Figure 8.2 for a single-bay portal frame without consideration of wind load. It can be seen that the overturning moment reduces as the column rotates further. Similarly the overturning moment is less for a reduced rafter temperature. A similar pattern of reduction of moment can be found for all types of portal frames, including multi-bay frames and cases where additional wind load is present.

In the simplified method proposed within the SCI guidance, 1° of column rotation is recommended and a moment reduction factor of 0.065 for both fire hinges has been adopted, which is equivalent to a rafter temperature of 880°C. Reference is made to BS5950 Part 8: Table 1 – Strength reduction factors for steel complying with grades 43 and 50 of BS4360, at 1.5% strain level. Consequently these values of column rotation and rafters temperatures have been recognised throughout the industry. Obviously using different assumptions, if they can be justified, can significantly reduce the design overturning moment.

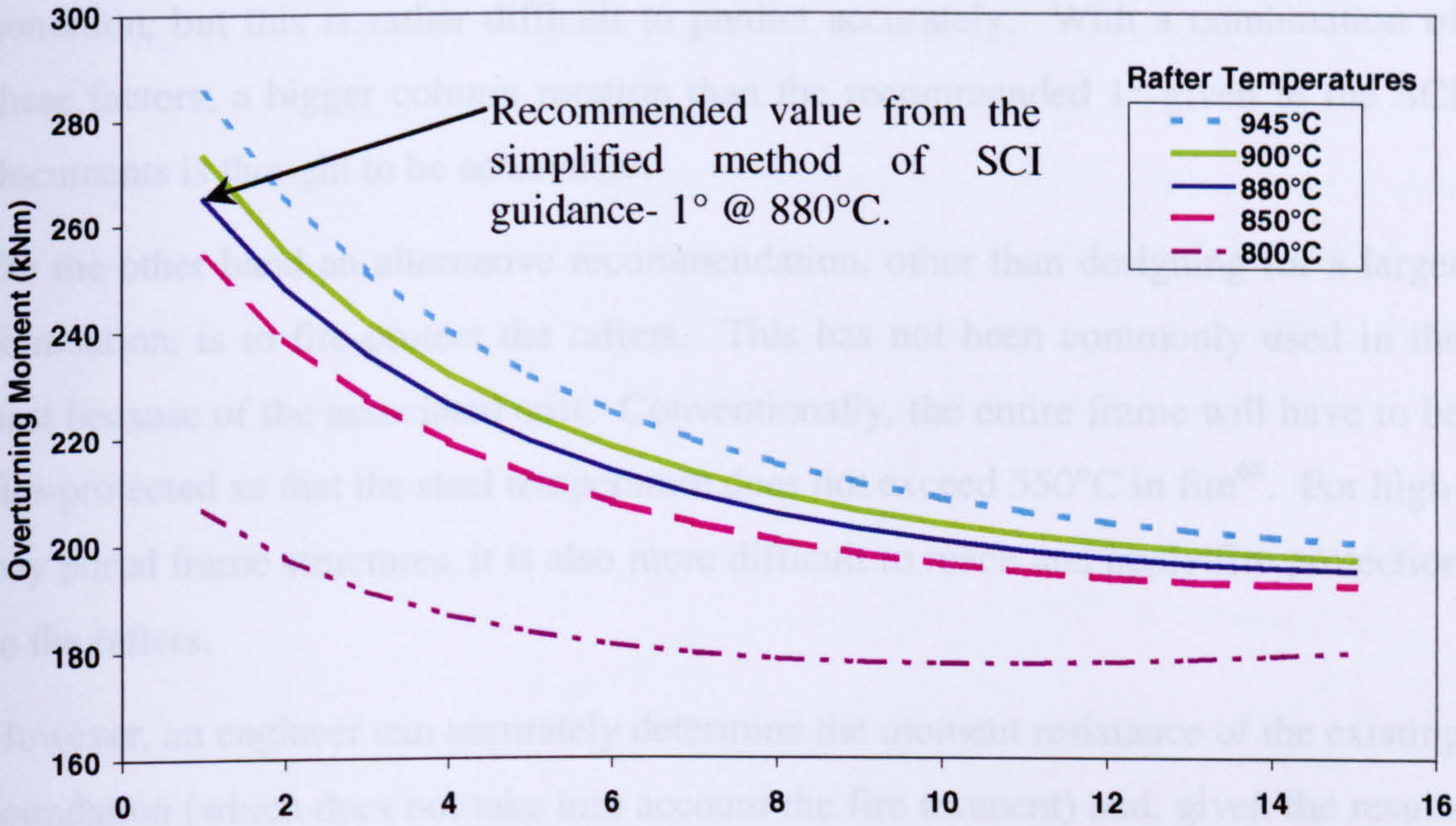

Figure 8.2 Base overturning moment vs. column rotation and rafter temperatures

8.2.1 Practicality

The graph plotted in Figure 8.2 was generated by an Excel spreadsheet which is linked to the design parameters. The plot is simple but can be extremely useful for structural or foundation engineers when designed for overturning moment under fire conditions. The latest EuroCode 3 (Annexes J and L) allows engineers to design for semi-rigid connections and to estimate the rotational stiffness and moment resistance of base connections. Structural engineers can simply design a base connection which can accommodate higher rotation (assuming the base connections do not lose much strength in fire) and hence the foundation size can be reduced to resist a lower overturning moment. Using the example given in Figure 8.2, if a column rotation of

5° can be allowed instead of the conventional assumption of 1°, the overturning moment can be reduced from 264 to 194kNm, a reduction in 26%.

Alternatively, the column rotation can be gained from the rotation of the entire foundation (if a pad foundation is used). This will have to involve determining the interaction between the soil and foundation, and careful selection of partial safety factors for soil and loading.

Further movement of columns may be possible due to their bending under the fire condition, but this is rather difficult to predict accurately. With a combination of these factors, a bigger column rotation than the recommended 1° given in the SCI documents is thought to be achievable.

On the other hand an alternative recommendation, other than designing for a larger foundation, is to fire-protect the rafters. This has not been commonly used in the past because of the associated cost. Conventionally, the entire frame will have to be fire-protected so that the steel temperature does not exceed 550°C in fire[68]. For high-bay portal frame structures, it is also more difficult to reach and apply fire protection to the rafters.

However, an engineer can accurately determine the moment resistance of the existing foundation (which does not take into account the fire moment) and, given the results from the spreadsheet shown earlier, determine the limiting temperature for overturning of the column to take place. Using the example shown in Figure 8.2, if the existing foundation can already resist an overturning moment of 180kNm, the columns can not be pulled over until the rafters reach 800°C. This can be seen as the limiting temperature for the rafters to cause failure of the columns. The thickness of fire protection can therefore be reduced accordingly from a limiting temperature of 550°C to 800°C.

If an intumescent type of protection system is adopted, this may only require a minimal thickness which can be applied in one layer, so that it can be applied to the rafters in a reduced construction time, reducing both labour and material costs.

All the discussion in this section obviously involves accommodating a significant amount of column movement so that the base overturning moment can be reduced. The approach is only suitable for the construction of external façades using steel profile cladding systems which can sustain high deflection. If masonry construction

is used for the façade, further consideration should be given to the stability of walls. This is complicated by the thermal behaviour of masonry walls and is not covered within the scope of the present research.

The proposed approaches can however be validated with VULCAN analysis if the finite element program can be improved to predict the post-snap-through phase of the portal frame deflections.

8.2.2 Internal Fire Spread

The SCI guidance on portal frames in boundary conditions addresses the issue of external spread of flame. It is thought that consideration of internal fire spread, which could be affected by portal frame behaviour, has somehow been overlooked. It is not unusual to construct a compartment wall within an industrial warehouse, to separate different ownership or types of occupancy (e.g. inclusion of an office block within a warehouse). Figure 8.3 shows some common systems for constructing compartment walls.

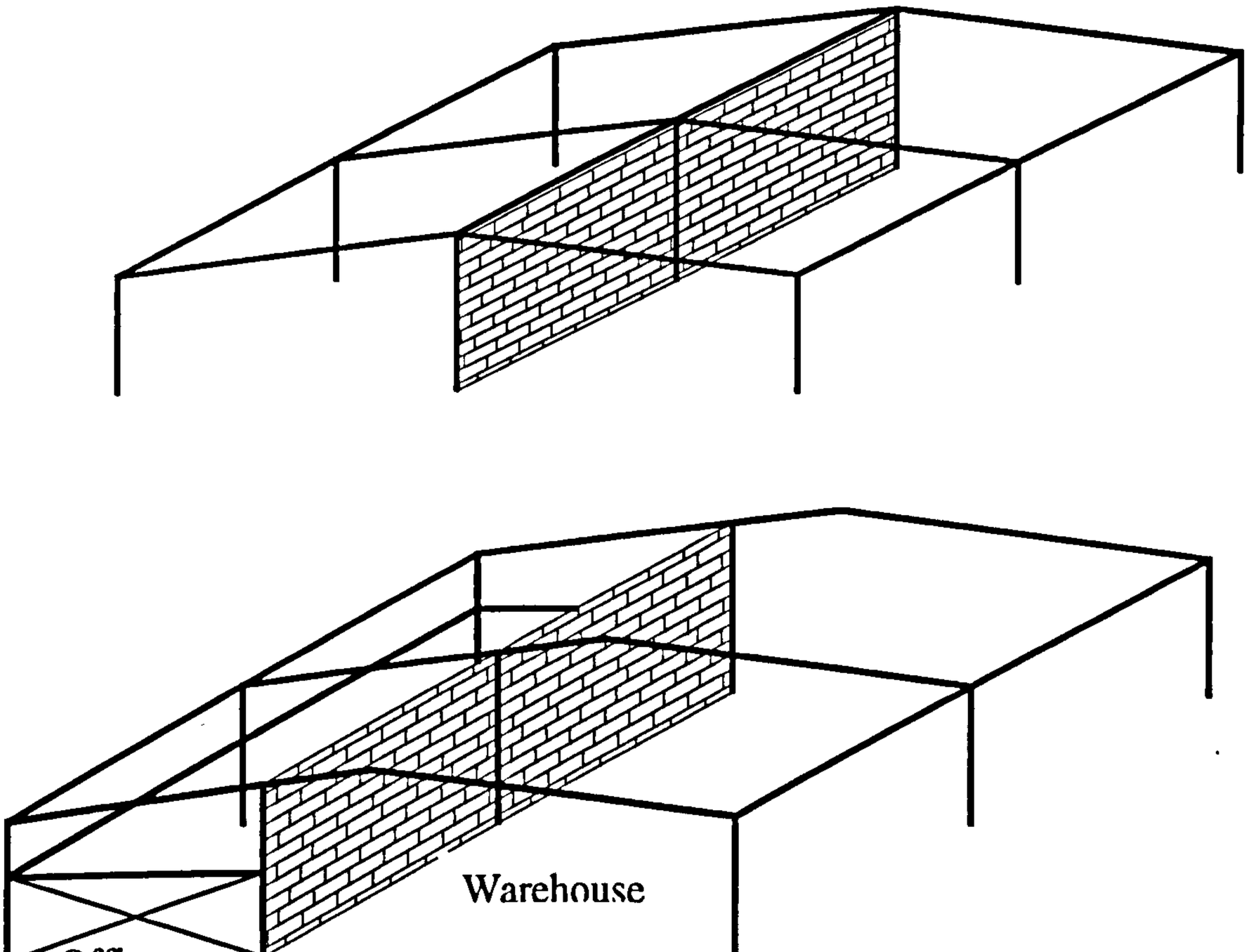

Figure 8.3 Compartment walls – separation of different ownership (top) or types of occupancy (bottom)

In these situations, the compartment walls will have to satisfy the same criteria of insulation, integrity and stability. Obviously if the rafters deflect excessively in the vertical direction in fire conditions, the stability and integrity of walls can no longer be maintained. The problem is often neglected, and simply enlarging the foundation does not provide a solution.

A simple solution is to design the compartment wall to resist an extra point load. This may not be easy when it comes to the assessing a realistic point load, and may result in an unrealistically thick wall. Movement joints around the wall-to-rafter interaction is not possible because the vertical deflection could be massive when a snap-through takes place.

Fire-protecting the rafters can be a possible solution, but again careful selection of a limiting temperature is necessary. Even with the conventional assumption of 550°C, the rafters could have deflected significantly, both upwards during expansion and downwards when they lose strength. Alternatively, it is possible to include additional vertical props at the point of wall-to-rafter interaction to carry the downward load from the rafter. Appropriate fire protection will have to be applied to the props.

It seems that there is no easy design solution. More importantly this is a crucial issue of which designers should be aware and take account.

8.3 Performance-based Design – Natural Fires

The concept of performance-based design for buildings under fire conditions has been raised frequently both in academia and the construction industry, and this is thought to be the future direction of fire engineering. Performance-based design will look at the real behaviour of structures under real fire conditions. This research has already investigated the real structural behaviour of portal frames under fire conditions, but real fire temperatures are rarely discussed.

When a prescriptive code specifies the requirement of fire resistance periods of the order of 30, 60, 90 and 120 minutes, the gas temperatures are assumed uniform and follow the furnace test temperatures which can be represented by the equation below. The simple curve is known as the Standard Fire Curve from BS 476:

$$T = 20 + 345\log(8t + 1) \qquad (8.01)$$

where,

T = Gas temperature in °C

t = Time in seconds

This Standard Fire Curve was specifically developed to represent fully-developed room fires, and this may not represent a large warehouse fire. A typical industrial warehouse will have a much higher ceiling and more free flow of internal air which will produce fire temperatures very different from those in a small room fire.

A real fire, more commonly known as a natural fire, characteristic is mainly dependent on the following factors:

- Fire load – amount and type.
- Distribution of fire load.
- Ventilation, e.g. size of windows etc.
- Geometry of the structure – size and shape.
- Thermal characteristics of the enclosure boundaries.

Other less important factors include the humidity of the atmosphere.

For an industrial warehouse, the fire load could range from medium to very high density. Ventilation is even more difficult to predict. The opening of a skylight, if it happens at an early stage, could introduce a large amount of ventilation, but additional ventilation can be brought about by failure of roof cladding, which is less easy to predict.

An approach to prediction of natural fire temperatures is available within EuroCode 1[63]. The approach is only validated for relatively small compartment (i.e. a floor area of 500m^2 or less). It assumes that flashover takes place at the start of the calculation and the entire compartment is a single temperature zone. An investigation of the natural fire temperatures within a medium-sized industrial warehouse has been conducted using the EuroCode 1 approach. Although the model is not validated for such large compartment sizes, it is thought that it could provide indications of the various influencing factors. The calculation procedure has been formulated into a spreadsheet format for ease of use.

A compartment of 30m x 60m x 9m height has been adopted, which can be approximated to the 3-dimensional model set-up for the parametric studies.

Ventilation of 10% and 20% of the floor area has been assumed in two separate cases. In terms of fire load density, the draft British Standard DD240 provides information for the storage purpose-group with a value of 1800MJ/m^2, assuming an 80% fractile. An average fire load density for this purpose-group is 1180 MJ/m^2. This is considered a rather severe fire load as it is equivalent to 100kg of wood per square metre. A reduced fire load of 900MJ/m^2 is considered in a separate calculation. This is equivalent to the fire load level of a retail area, again assuming an 80% fractile. The geometry of the structure and the material of the boundary enclosures have been kept constant. The results of the calculations are plotted in Figure 8.4.

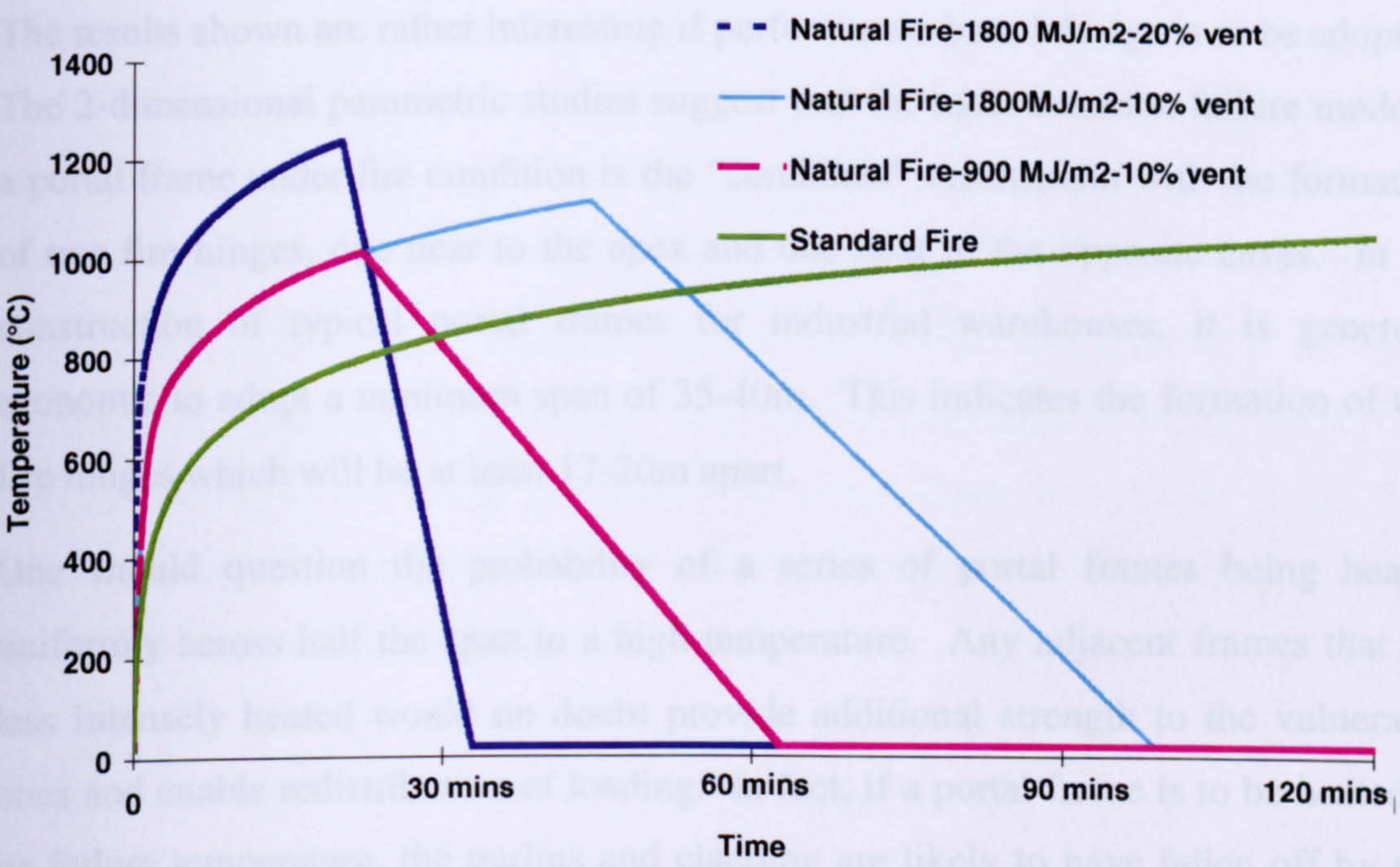

Figure 8.4 Natural fires vs. standard fire curve

It is worth mentioning that the natural fire scenario could well be very onerous because it assumes that all the fire load is consumed simultaneously as soon as sufficient ventilation is available. In reality, the fire will start locally and spread to the entire warehouse. However, with such a massive floor area within the warehouse, it is not impossible to have total burn-out in one localised area whilst the fire is starting in another. Therefore it could be misleading to rule immediately that natural fire temperatures are more severe than the standard fire curve.

In fact, the assumption of flashover within the entire warehouse is questionable. Flashover often takes place in a small enclosure, but is rarely seen in a huge space.

Flashover in a localised area within a warehouse is possible. With such intense local heating, the roof cladding would fail and introduce extra ventilation and cooling to the area. A more sophisticated natural fire model will be required for such circumstances.

Despite all these provisions, the results for the natural fire calculation give a good indication of the effects of fire load and ventilation. With larger amounts of ventilation available the fire would have grown faster and reached higher temperatures. However, such a fire will burn out sooner and cool down quicker. With the same amount of ventilation a higher fire load density simply results in a longer and hotter fire.

The results shown are rather interesting if performance-based design is to be adopted. The 2-dimensional parametric studies suggest that the most common failure mode of a portal frame under fire condition is the "combined" mechanism with the formation of two fire hinges, one near to the apex and one near to the opposite eaves. In the construction of typical portal frames for industrial warehouses, it is generally economic to adopt a minimum span of 35-40m. This indicates the formation of two fire hinges which will be at least 17-20m apart.

One should question the probability of a series of portal frames being heated uniformly across half the span to a high temperature. Any adjacent frames that are less intensely heated would no doubt provide additional strength to the vulnerable ones and enable redistribution of loading. In fact, if a portal frame is to be heated to its failure temperature, the purlins and cladding are likely to have fallen off by this stage, and the only load that the portal frame is likely to support is its self-weight.

This offers one qualitative explanation for the earlier situation where no total collapse of the portal frame structure was seen. It is the author's opinion that performance-based design, which includes a proper risk assessment, could lead to future solutions which disregard the possibility of portal frame rafters pulling over the columns under fire conditions.

8.4 Conclusion

The previous studies have purely focused on the structural behaviour of portal frames in fire. This discussion chapter offers a chance to divert attention to other areas of

consideration, and to enable the entire picture of "portal frames in fire" to be drawn. One of the most important factors identified was the ventilation available in the event of a fire.

Introduction of early ventilation to an industrial portal frame warehouse fire can lead to diluted toxic smoke being released from a chemical fire. This was one of the main initial concerns for Health and Safety Laboratories. Besides, ventilation is the key factor in allowing a faster burn-out and hence a more intense fire; this will also result in a faster rate of cooling within the fire compartment. With a large amount of ventilation available, the rate of heating of the steel frames will be reduced and delay the structural failure, if it is to take place.

Using the mathematical model described in the SCI guidance, it is found that engineers can achieve a more economical design for portal frames with boundary conditions, compared to simply following the guidance's recommendation. There is however the issue of internal compartment walls which should be noted in design.

The concept of performance-based design has been discussed with the main emphasis on natural fire calculations. This leads to consideration of risk assessment (i.e. the probability for a total collapse of the portal frame structure to occur). The main aims have been to provide some possible directions for future development of the design of portal frames in boundary conditions.

9 Conclusions

This research on portal frame behaviour in fire has been based on two main foundations: the fire tests at Buxton and parametric studies using the finite element program VULCAN. Subsequent development of the simplified calculation method and other discussions have been elaborated and built from these grounds. This chapter outlines the main conclusions drawn from the work and gives recommendations for further research.

9.1 Fire Tests

A scaled model portal frame was designed and built at Buxton, for which the designated load level was made equivalent to a typical industrial frame at the fire limit state. Three major fire tests were conducted on the scale model. Several indicative tests on isolated cladding panels were conducted prior to these tests in order to investigate test method and to establish correct use of instrumentation.

In the first two tests, the rafters were not heated to their collapse temperature. The main reasons were the relatively large amount of ventilation which kept the steel cool, and a lack of insulation to the roof sheeting. Lateral deformation was the most obvious deformation observed after these tests. Significant measures were taken in the third test, including insulating the roof of the model, in order to enable a collapse mechanism to take place as a final stage in the testing programme. The heated frame collapsed completely in this test, and a failure mechanism was formed.

Considerable understanding was gained from the post-fire investigations on the deformed structure. The secondary elements, especially the Z-purlins which are used to support the cladding, were initially thought to be weak, and deformed at an early stage of any significant fire. In the third test, however, the purlins showed some strength, in providing additional support to the heated rafters by acting in tension, and also enabling some load to be distributed to the adjacent cool frames. This effect was further demonstrated later in the three-dimensional parametric studies.

In all the fire tests, lateral deformation was observed in the rafters, in which a double curvature was formed. This was again influenced by the restraint provided by the purlins, and the curvature was markedly larger in the bottom flanges of the rafters than in the top flanges, which were more directly restrained by the attached purlins.

Thus, it seems that lateral buckling failure of rafters under fire conditions can be prevented by providing sufficient purlin restraints. Design checks can be made by assuming the purlin-spacing as the effective length for minor-axis buckling to occur, and the relative moment capacity of rafters can be calculated using the reduced strength at designated temperatures.

The other significant observation from the fire tests was the typical collapse mechanism of the portal frames. In the third test, the rotational stiffness of the column base was set at an insignificant level, so that a pinned base could safely be assumed. The collapse mode of the portal frame was found to be a combined mechanism, similar to the failure mechanism at ambient temperature. This was predicted by the VULCAN analysis, in which plastic hinges forming at high temperature could be seen clearly, as well as from the deformed structure after the test.

One of the main benefits of conducting real fire tests is that the data can be used to calibrate the numerical results from computer modelling. With the steel temperatures and displacements recorded during the tests, the numerical data was compared against VULCAN analyses. It was found that VULCAN results compared relatively well with the experimental data, especially for the third test where the uncertainty about the column base stiffnesses had been eliminated. These comparisons led to increased confidence in the use of VULCAN analysis in modelling portal frame behaviour at elevated temperature. The subsequent part of the research relies heavily on the use of VULCAN to enable the proposed parametric studies to be conducted, as well as in establishing the simple calculation method presented in Chapter 7 for the prediction of portal frame failure temperatures in fire.

9.2 Parametric Studies

Initial studies were conducted to investigate the suitability of VULCAN analysis for modelling portal frame performance in fire. A major effort was made to ensure that the program could handle sloping members, to represent the inclined rafters of typical portal frame warehouses.

The parametric studies were conducted in two separate stages, composed of two- and three-dimensional analyses. The two-dimensional numerical model is relatively

small, with less nodes and elements, and therefore a large number of analyses can be conducted relatively quickly. A variety of influencing factors could therefore be considered within the two-dimensional parametric studies, such as the load ratio, frame geometry, heating profiles, effect of horizontal load and base rotational stiffness.

With the inclusion of secondary members in the three-dimensional modelling, each model was significantly larger and each analysis was longer. The analysis can easily be subject to instability due to the very small section sizes used for the representation of purlins and cladding elements. Therefore only a limited number of analyses were conducted, and the main investigation concerned the effects of different fire scenarios.

From the two-dimensional analyses it was found that a considerable majority of the failure modes induced under fire condition involved a combined mechanism. Sway failure was only found in a series of analyses where the horizontal forces were dominant, with pinned bases assumed for the columns. The separate probabilities of the occurrence of fire and high wind, and the much lower probability of a simultaneous occurrence of both, make such a case extremely unlikely. In more usual cases the combined mechanism will occur, regardless of vertical load levels and frame geometries.

In order to mobilise the combined mechanism under fire conditions, two fire hinges (plastic hinges with reduced moment capacity due to elevated temperature) are required to form, near to the apex and eaves respectively. Once this has taken place as the portal frame continues to heat up, the snap-through phenomenon will take place and an additional fire hinge will form near to the other eaves. VULCAN analysis terminates as soon as the snap-through occurs, since the apex deflects downwards rapidly with a stiffness which becomes negative, and the solution procedure can no longer handle such a response.

The dominant factor which influences the critical temperature at which snap-through takes place is the load ratio of the rafters. Frames with various geometries were found to have similar failure temperatures under the same load levels. In fact, the limiting temperatures given in BS5950 Part 8 can be utilised as a reference for the upper and lower bound of failure temperatures for portal frames, assuming that the

entire rafter is heated up uniformly. This fire scenario was found to be the most onerous heating profile. The heating of columns seems to have negligible effect on the failure temperature. A local fire always causes the frame to fail at a higher temperature, especially for a fire which only affects the mid-section of a rafter (i.e. the quarter-point of the entire span) or the region near to the apex.

The effect of rotational stiffness at the column bases is always a debatable issue. Firstly, when a portal frame is designed to have pinned bases at ambient temperature, the actual "pinned" connection often comprises four holding down bolts securing the base plate to the concrete foundation. Such a connection detail was found to behave more as a semi-rigid connection, with significant rotational stiffness, rather than as a pinned connection. If the base connections of a portal frame remain relatively cool in fire, this will improve the failure temperature of the frame by up to 20% for cases similar to those analysed within this research, depending on load levels and the actual stiffnesses of the bases. However, it is normal practice to account for a worst-case fire scenario, which often assumes that the connections are heated. Obviously the rotational stiffness will reduce as the temperature of the connection increases. It is questionable whether the base connections will be heated to the same temperature as the rafters under any fire conditions, and logic suggests that they will actually remain much cooler. VULCAN was subsequently developed to account for the reduction of connection rotational stiffness at elevated temperature in accordance with the strength and stiffness reduction factors from EC3. This is described in Chapter 2.

While setting up the three-dimensional model for the parametric studies, the secondary roof elements were simulated with a mesh. The mesh was found to give an acceptable representation of the purlins and roof cladding. However it cannot represent any failure that is likely to occur, since local effects are not modelled within VULCAN.

The benefits of having adjacent cool frames were again demonstrated in the analyses, in which the purlins acted in tension to hold up the highly deformed rafters. The plots of internal forces within the mesh give further evidence for this argument.

However, if the worst fire scenario is assumed, in which the entire roof and all rafters are heated uniformly to high temperature, the portal frame deflections and failure

temperature are similar to the results from a two-dimensional analysis. In other words, a two-dimensional analysis is probably sufficient for fires which engulf the whole building. However, it is rather unlikely that a large portal frame warehouse will experience flashover throughout the entire compartment, and thus cause all the rafters to heat up to the same temperature. It is beyond the scope of this research to investigate such issues, but it is part of the essential risk analysis which should eventually inform performance-based design codes for such structures.

9.3 Further Investigation

A simplified method has been developed to estimate the critical temperatures of portal frames in fire, based on Plastic Theory and the insertion of fire hinges into the frame. The results from the simplified method have been compared against the two-dimensional VULCAN analysis and a good correlation was achieved. A lower-bound solution can be calculated using an appropriate strain level. However, the method sometimes does not produce an immediate result if a localised fire with low load ratio is considered, and only one fire hinge is assumed. A different failure mechanism has to be explored by inserting plastic or fire hinges at various positions. The process may have to be repeated many times before finding a true solution. The simplified method can be useful for determining the limiting temperatures of portal frames, and can lead to a reduced fire protection requirement.

An attempt has been made to review the current guidance document for portal frames in boundary conditions. The relationship between column rotation and overturning moment was explored. Using design combinations of appropriate connection details and frame limiting temperatures, the required measures to prevent total collapse of a portal frame in fire could be reduced.

The significance of a real fire which occurs in a large portal frame warehouse was also discussed. The high amount of ventilation which is usually present becomes a very important factor, having effects on both steel temperatures and the movement of toxic smoke in the event of a fire. The behaviour of the secondary elements, particularly cladding, in fire plays an important role in deciding how much ventilation can be available.

Performance-based design is becoming a global concept based on real (natural) fire temperatures and structural response under such temperatures, incorporating a certain degree of risk assessment in generating partial safety factors. A real fire analysis may be able to prove that flashover within the entire warehouse compartment is unlikely, and therefore that some frames will remain cooler and provide the additional support required to those in the immediate vicinity of the fire. With an appropriate risk assessment, it is the author's opinion that such an approach can lead to removal of the current measures required for portal frames in boundary conditions in the fire limit state.

9.4 Recommendations for Further Work

As a result of the work conducted during this project, there are several areas in which further research could lead to better understanding of the total structural response for pitched-roof portal frames in fire.

The fire tests and numerical modelling of pitched-roof portal frames were both terminated as soon as the snap-through of rafters took place. This is regarded as a major structural failure and is usually the end-point for most structural analysis. However there is a possibility that portal frame can reach a second equilibrium state after snap-through and that total collapse may not occur. If such behaviour can be proven, or even designed for, a huge saving could result from the omission of fire protection or large foundations. Further development of VULCAN to predict such behaviour is essential, so that parametric studies can be conducted for various types of frame. This may be possible by providing alternative solution procedures such as the Arc-Length Method, which are formulated to follow equilibrium paths through regions of transient instability. Further testing of portal frames to include heating of all frames to the post-snap-through phase will be beneficial for investigation and validation of such upgrades to the program.

The assumption of pinned column bases is always conservative for portal frame structures. Further understanding of the overall issue of base response characteristics can replace the current conservatism, without losing any advantages to the portal frame behaviour in fire. Such studies should include investigation of the interaction between the soil and the foundation, as well as the thermal response (i.e. the likely

maximum temperature reached) of the base connection in a warehouse fire, and the thermal degradation of the connection characteristics.

Further investigation on the behaviour of secondary members such as purlins and cladding at elevated temperature are not possible using VULCAN, unless a way can be found of accounting for local effects such as flange and web buckling. The prediction of local effects could also lead to investigation of the interaction between columns and the wall cladding. Columns are required by the Building Regulations to be protected if they are supporting the fire-resisting cladding. Local failures within columns will undoubtedly jeopardise the integrity of the cladding which they support.

Finally, it is necessary to take advantage of the global development of performance-based design, which often leads to the use of less onerous but more realistic fire conditions. Structural behaviour has to be integrated within this approach to attain the maximum benefits for an overall scheme.

9.5 Concluding Remarks

This research provides a comprehensive overview of pitched-roof portal frame behaviour in fire, for which relatively little research has previously been carried out. The research has investigated a number of factors which affect the structural response, and has suggested alternative approaches to improve its performance. Further research is necessary to provide better understanding and further benefits.

The finite element program VULCAN has proved to be a powerful tool for modelling structural response at elevated temperatures. Such tools enable deeper investigations than are possible using prescriptive or codified methods, and reduce the need for conducting physical experiments. Further use of the program can undoubtedly provide a valuable contribution to future research on the performance of structures in fire, and in the development of more rational design processes.

Reference

1. Fire Prevention No.180, "Roofing Fire Leads to Multi-million warehouse loss", (June 1985).
2. Fire Prevention No.181, "Toxic Chemicals Involved in Huge Warehouse Blaze", (July/August 1985).
3. Fire Prevention No.182, "Huge Loss in Computer Warehouse Blaze", (September 1985).
4. Fire Prevention 252, "Serious Fires in Warehouses and Storage Premises during 1991", "FPA case book of fires – Warehouse (page 46-54)", (September 1992).
5. Fire Prevention 265, "Casebook of Fires (page 34-40)", (December 1993).
6. Fire Prevention 279, "Warehouse (page 40-45)", (May 1995).
7. Fire Prevention 296, "Warehouse Blaze Destroys 15 House", (January/February 1997).
8. Department of the Environment and Welsh Office, "The Building Regulations 1991, Approved Document B : Fire Safety", (1992).
9. Newman, G.M., "Fire and steel construction: The Behaviour of Steel Portal Frames in Boundary Conditions", The Steel Construction Institute, (1990).
10. Eurofer, "Steel and Fire Safety – A global approach", (1990).
11. British Standards Institution, "DD 240: Part 1, Code of Practise for the Application of Fire Safety Engineering Principles to Fire Safety in Buildings", (1997).
12. O'meagher, A.J.; Bennetts, I.D.; Dayawansa, P.H. & Thomas, I.R., "Design of 8Single Storey Industrial Buildings for Fire Resistnaces", Journal of the Australian Institute of Steel Construction, Vol 26, Number 2, May 1992.
13. British Standards Institution, "BS5950: Structural Use of Steelwork in Building, Part 8: Code of Practice for Fire Resistant Design", BSI, (1990).
14. British Standards Institution, "BS5950: Structural Use of Steelwork in Building, Part 1: Code of Practice for Design in Simple and Continuous Construction", BSI, (1992).

15. EuroCode 3, "Design of Steel Structures: Part 1.2 : General rules, Structural fire design", (1995).

16. Ramberg,W. & Osgood W., "Description of Stress-Strain Curves by Three Parameters", National Advisory Committee for Aeronautics, Technical Note 902, (1942)

17. Kirby, B.R., and Preston, R.R., "High Temperature Properties of Hot-rolled Structural Steel for use in Fire Engineering Design Studies", Fire Safety Journal, 13, (1988), pp27-37.

18. Witterveen, J.; Twilt, L. & Bijlaard, F.S.K, "Theoretical and Experimental Analysis of Steel Structures at Elevated Temperatures", IABSE, 10th Congress, Tokyo, Final Report, Zurich.

19. Najjar, S.R., "Three-Dimensional Anaysis of Steel Frames and Subframe in Fire", PhD Thesis, University of Sheffield, (1994)

20. Horne, M.R. & Morris, L.J., "Plastic Design of Low-rise Frames", Granada Publishing Limited, (1981)

21. Morris, L.J. & Plum, D.R., "Structural Steelwork Design to BS 5950", Longman Scientific & Technical, (1988).

22. Nethercot, D.A., "Limit States Design of Structural Steelwork", Chapman & Hall, (1991).

23. Hockey, S.M.; Camp, P.I. & Deaves, D.M., "Behaviour of Warehouse Roofs in Fire Situations PhaseI", WS Atkins Safety and Reliability, (1996).

24. Heyman, J., "Plastic Design of Structures, Vols. 1 & 2", Cambridge University Press, (1969).

25. The Steel Construction Institute, "Steel Designers' Manual", Blackwell Science, Fifth edition, (1994)

26. Hibbit, Karlsson and Sorensen Inc., "ABAQUS Finite Element Analysis Programme", (1988).

27. Hibbitt, Karlsson and Sorensen, Inc., "ABAQUS manual. - Theory manual. - Version 4.8.", (1989).

28. El-Zanaty, M.H.; Murrray D.W. & Bjorhovde, R., "Inelastic Behaviour of Multistorey Steel Frames", PhD Thesis, Department of Civil Engineering, University of Alberta, (1980).

29. El-Rimawi, J.A., "The Behaviour of Flexural Members under Fire Conditions", PhD Thesis, University of Sheffield, (1989).

30. Saab, H.A., "Non-Linear Finite Element Analysis of Steel Frames in Fire Conditions", PhD Thesis, (1990).

31. Bailey, C.G., "Simulation of the Structural Behaviour of Steel-framed Buildings in Fire", PhD Thesis, University of Sheffield, (1995).

32. Shepherd, P., "The performance in Fire of Restrained Columns in Steel-Frame Construction", PhD Thesis, University of Sheffield, (1999).

33. Huang, Z., Burgess, I.W. & Plank, R.J., "Layered slab elements in the modelling of composite frame behaviour in fire", Second International Conference on Concrete Under Severe Conditions, Tromsö, (1998), pp785-794.

34. Huang, Z., Burgess, I.W. & Plank, R.J., "Non-linear analysis of reinforced concrete slabs subject to fire", A.C.I. Structural J., **96 (1)**, (1999), pp127-135.

35. Huang, Z., Burgess, I.W. and Plank, R.J., 'The Influence of Shear Connectors on the Behaviour of Composite Steel-Framed Buildings in Fire', J. Construct. Steel Research, 51 (3), (1999) pp219-237.

36. Huang, Z., Burgess, I.W. and Plank, R.J., 'Effective Stiffness Modelling of Composite Concrete Slabs in Fire', Research Report DCSE/99/F/1, University of Sheffield, (1999).

37. Allam, A.M., Green, M.G., Burgess, I.W. & Plank, R.J., "Fire engineering design of steel framed structures - Integration of design and research", Second World Conference on Structural Steel Design, San Sebastian, *J. Const. Steel Research*, 46 (1-3), (1998), Paper No. 170.

38. Fahad, M.K., Allam, A.M., Liu, T.C.H., Burgess, I.W. and Plank, R.J., 'Effects of Restraint on the Behaviour of Steel Frames in Fire', Paper 64, Eurosteel 99, Prague.

39. Cai, J, Burgess, I.W. & Plank, R.J., "VULCAN Formulation for Asymmetric Cross-section Beams", Research Report DCSE/99/F/2, University of Sheffield, (1999).

40. Al Jabri, K., Lennon, T., Burgess, I.W. & Plank, R.J., "The behaviour of steel and composite beam-column connections in fire", Second World Conference on Structural Steel Design, San Sebastian, *J. Const. Steel Research*, **46 (1-3)**, (1998), Paper No. 180.

41. Al Jabri, K., Burgess, I.W., Lennon, T. & Plank, R.J., "The Performance of Frame Connections in Fire", Acta Polytechnica-Eurosteel '99, Vol. 39, No. 5, pp 65-76, (1999).

42. Bathe, K., "Finite Element Procedures in Engineering Analysis", Prentice-Hall Inc., (1982).

43. Shepherd, P., "Appendix B ShowGrid Graphical Interface", PhD Thesis, University of Sheffield, (1999)

44. Leston-Jones, L.C, "The Influence of Semi-Rigid Connections on the Performance of Steel Framed Structures in Fire", PhD Thesis, University of Sheffield, (1997)

45. Leston-Jones, L.C., Burgess, I.W., Lennon, T, Plank, R.J., "Elevated-temperature Moment-Rotation Tests on Steelwork Connections", Proc Instn Civ. Engrs Structs & Bldgs, **122**, (1997) pp 410-419.

46. Al-Jabri, K, "The Behaviour of Steel and Composite Beam-to-column Connections in Fire", PhD Thesis, University of Sheffield, (2000)

47. Lawson, R.M., "Behaviour of Steel Beam-to-column connections in fire.", The Structural Engineer, 1990, **68** (14), pp. 263-271

48. Lawson, R.M., "Enhancement of Fire Resistance of Beams by Beam to Column Connections", Technical Report, SCI Publication 086, (1990)

49. Crisfield, M.A., "Iterative Solution Procedures for Linear and Non-linear Structural Analysis", Transport and Road Research Laboratory Report 900, (1979)

50. Crisfield, M.A., "A Fast Incremental/Iterative Solution Procedure that Handles 'Snap-Through'", Computer & Structures, **13**, (1981), pp55-62

51. Crisfield, M.A., "Variable Step Length for Non-linear Structural Analysis", Transport and Road Research Laboratory Report 1049, (1979)

52. Wickstrom, U., "TASEF-2 – A Computer Program for Temperature Analysis of Structures, Exposed to Fire", Report No. 79-2, Department of Structural Mechanics, Lund Institute of Technology, (1989)

53. Becker, J, Bizri, H. and Bresler, B., "FIRES-T – A Computer Program for the Fire Response of Structures-Thermal", Report No. UCB FRG 71-1, Fire Research Group, Structural Mechanics Department of Civil Engineering, University of California, Berkeley, (1974)

54. Franssen J-M, Cadorin J-F, "Competitive steel buildings through natural fire safety concept: Part 2 – Work Group 1: Natural Fire Models", Profil Arbed Centre de Recherches, (March 1999)

55. Twilt, L., Van Oerle, J.," Competitive steel buildings through natural fire safety concept: Part 3 – Work Group 3: Fire Characteristics for Use in a Natural Fire Design of Building Structures" Profil Arbed Centre de Recherches, (March 1999)

56. Fontana, M., Fetz, C., "Competitive steel buildings through natural fire safety concept: Part 4 – Work Group 4: Statistic", Profil Arbed Centre de Recherches, (March 1999)

57. The Building Regulations 1991, Approved Document B, "Fire Safety", Department of the Environment, Transport and the Regions, (2000).

58. Wald, F., "Column Bases", Czech Technical University, (1995).

59. Wald, F. and Jaspart, J., "Stiffness Design of Column Bases", Journal of Constructional Steel Research, 46: 1-3, Paper 135, (1998).

60. Ermopoulos, J. and Stamatopoulos N., "Mathematical Modelling of Column Base Plate Connections", Journal of Constructional Steel Research, Vol 36 No. 2, pp 79-100, (1996).

61. Jaspart, J. and Vandegans, D., "Application of the Component Method to Column Bases", Journal of Constructional Steel Research 48, pp 89-106, (1998).

62. Horne, M.R., "Plastic Theory of Structures", Pergamon Press Ltd., (1979).

63. Eurocode 1: "Basis of Design and Actions on Structures. Part 2.2: Actions on Structures Exposed to Fire", CEN, Brussels,(1993).

64. ISO 834, "Fire Resistance Tests - Elements of Building Construction", International Organisation for Standardisation, (1985).

65. British Standard Institute, "BS 6399: Loading for Buildings, Part 2: Code of Practice for Wind Loads", BSI , (1997).

66. Wong, S.Y., Burgess, I., Plank R. and Atkinson, G., "The Response of Industrial Portal Frame Structures to Fire", Acta Polytechnica, Vol. 39, No.5 (1999), pp169-181.

67. Wong, S.Y., Burgess, I. and Plank R., "Simplified Estimation of Critical Temperatures of Portal frames in Fire", Paper 09.03, Steel Structures of the 2000's, (2000).

68. Association of Specialist Fire Protection Contractors and Manufacturers Limited (ASFPCM); "Fire Protection for Structural Steel in Buildings"; 2nd Edition – Revised; (1992)